



National Library of Canada

Cataloguing Branch
Canadian Theses Division

Ottawa, Canada
K1A 0N4

Bibliothèque nationale du Canada

Direction du catalogage
Division des thèses canadiennes

NOTICE

The quality of this microfiche is heavily dependent upon the quality of the original thesis submitted for microfilming. Every effort has been made to ensure the highest quality of reproduction possible.

If pages are missing, contact the university which granted the degree.

Some pages may have indistinct print especially if the original pages were typed with a poor typewriter ribbon or if the university sent us a poor photocopy.

Previously copyrighted materials (journal articles, published tests, etc.) are not filmed.

Reproduction in full or in part of this film is governed by the Canadian Copyright Act, R.S.C. 1970, c. C-30. Please read the authorization forms which accompany this thesis.

**THIS DISSERTATION
HAS BEEN MICROFILMED
EXACTLY AS RECEIVED**

AVIS

La qualité de cette microfiche dépend grandement de la qualité de la thèse soumise au microfilmage. Nous avons tout fait pour assurer une qualité supérieure de reproduction.

S'il manque des pages, veuillez communiquer avec l'université qui a conféré le grade.

La qualité d'impression de certaines pages peut laisser à désirer, surtout si les pages originales ont été dactylographiées à l'aide d'un ruban usé ou si l'université nous a fait parvenir une photocopie de mauvaise qualité.

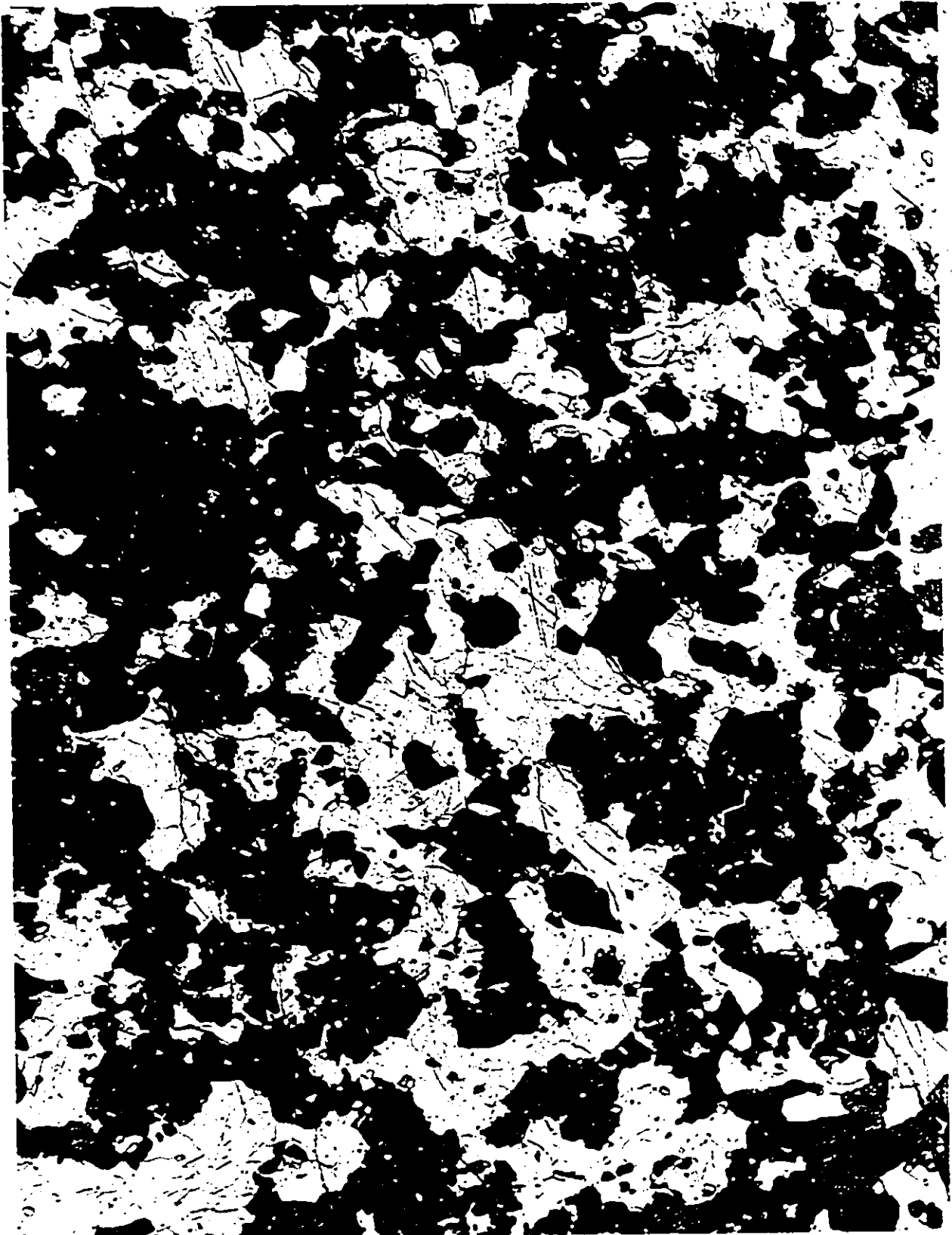
Les documents qui font déjà l'objet d'un droit d'auteur (articles de revue, examens publiés, etc.) ne sont pas microfilmés.

La reproduction, même partielle, de ce microfilm est soumise à la Loi canadienne sur le droit d'auteur, SRC 1970, c. C-30. Veuillez prendre connaissance des formules d'autorisation qui accompagnent cette thèse.

**LA THÈSE A ÉTÉ
MICROFILMÉE TELLE QUE
NOUS L'AVONS REÇUE**



UNIVERSITÉ D'OTTAWA
UNIVERSITY OF OTTAWA



FRONTISPIECE

Photomicrograph of a mafic charnockite (J-35) from the Adirondack Mts., N.Y.

(x17)

Plane polarized light

White: plagioclase (andesine)

Dark green: amphibole (ferrohastingsite)

Bluish green and granular: clinopyroxene (ferrosalite)

" " " prismatic (lower right corner): orthopyroxene (eulite)

Dark beige: garnet (almandine)

Brown (centre left): biotite

Black: Fe-Ti oxides and Fe sulphides

BACK PAGE

Photomicrograph in partially polarized light

SPATIAL DISTRIBUTION OF CRYSTALS AND PHASE EQUILIBRIA
IN
CHARNOCKITIC GRANULITES FROM THE ADIRONDACK MOUNTAINS, NEW YORK

by
Lo-Sun Jen

A thesis
Submitted in partial fulfillment of the requirements
for the degree of
DOCTOR OF PHILOSOPHY
in geology
to the
School of Graduate Studies
University of Ottawa

May 1975

Abstract

Twelve specimens of charnockitic granulites from the Adirondack Mountains in New York were investigated in detail with an aim to increasing our understanding of chemical processes that take place during high-grade metamorphism. Data were obtained on the chemical composition of the rocks, the spatial distribution of the contained crystals, the distribution of Mg and Fe^{2+} between non-equivalent sites in some of the ferromagnesian minerals, the distribution of Mg, Fe^{2+} , and Mn among coexisting orthopyroxene, clinopyroxene, amphibole, and garnet, and the composition of coexisting magnetite and ilmenite.

The spatial distribution of orthopyroxene, clinopyroxene, amphibole and feldspar was investigated by measuring the frequency of the different kinds of contacts between like and unlike crystals, and by comparing the results with those expected for a random mingling of the crystals. The results show that some aspects of the distributions are random, while others represent a departure from randomness towards a distribution which favours the occurrence of contacts between unlike grains. These results are interpreted in relation to a rearrangement of matter during metamorphism to bring about a reduction in interfacial free energy.

By use of Mössbauer spectroscopy, the distribution of Mg and Fe^{2+} in the M_1 and M_2 sites of orthopyroxene was determined for four crystals of different Fe/Mg ratio. The resulting distribution agrees very closely with that obtained experimentally by Saxena and Ghose (1971) at 700°C .

The distribution of Mg, Fe^{2+} , and Mn among orthopyroxene, clinopyroxene, amphibole, and garnet, produces the following sequence of decreasing affinity for Fe and Mn:

Fe: garnet orthopyroxene amphibole clinopyroxene

Mn: garnet orthopyroxene clinopyroxene amphibole

Moreover, for any mineral pair, the distribution points define exactly or very nearly a linear or curvilinear pattern, which may be taken to indicate that exchange equilibrium was very closely established during metamorphism.

The distribution of Mg and Fe^{2+} between orthopyroxene and clinopyroxene is examined from a thermodynamic viewpoint. Data from the present study provide needed information on the iron-rich end of the 'exchange isotherm', and when combined with the magnesium-rich data from India produce a well defined isotherm. A good 'fit' to these data points can be obtained by assuming that both mineral phases are simple mixtures (Guggenheim, 1967), with small departures from ideal behaviour.

The composition of coexisting magnetite and ilmenite, when compared with the experimental data of Buddington and Lindsley (1964) indicate a temperature of less than 600°C and an oxygen fugacity less than 10^{-18} atm. Reaction and re-equilibration are thought to have taken place, to some extent during cooling of the rocks.

The rocks evidently represent a suite of cogenetic mafic igneous rocks of calc-alkaline type, that was metamorphosed at about 735°C. Metamorphic pressures are more difficult to estimate, but a confining pressure of 6 Kbs and a water vapour pressure of about 4.8 Kbs are not in conflict with experimental results on phase equilibrium studies.

TABLE OF CONTENTS

PART 1

GEOLOGY AND PETROGRAPHY

	PAGE
I INTRODUCTION	1
Statement of Problem	1
General Statement	1
General Geology	4
Field Sampling	6
Laboratory Work	7
Acknowledgements	12
II MINERALOGY, PETROGRAPHY AND BULK-ROCK CHEMICAL ANALYSES	15
Feldspars	15
Orthopyroxene	19
Clinopyroxene	20
Amphibole	20
Garnet	21
Biotite	22
Quartz	22
Opagues	22
Apatite	23
Carbonate	23
Zircon	23

PART 2

THE SPATIAL DISTRIBUTION OF CRYSTALS IN ROCKS

	PAGE
III GENERAL PRINCIPLES	24
Definitions	24
Background and Methods	24
Spatial Distribution as a Function of Inter- facial Free Energy	30
Effect of Chemical Reactions on Spatial Distribution	32
Procedure	33
Models for Spatial Distribution of Minerals in Rocks	35
(i) <u>Spatial distribution of crystals of a particular phase</u>	39
(ii) <u>Association of unlike phases</u>	39
IV SPATIAL DISTRIBUTION OF CRYSTALS IN CHARNOCKITIC GRANULITES FROM THE ADIRONDACK MOUNTAINS	42
General Statement	42
Homogeneity	42
Spatial Distribution - The Overall Pattern	45
Spatial Distribution of Pyroxenes, Amphibole and Feldspar	46
Interpretation	48

PART 3
ION EXCHANGE EQUILIBRIA

	PAGE
V CHEMICAL COMPOSITION OF COEXISTING FERRO-MAGNESIAN MINERALS	55
General Statement	55
Chemical Composition of Pyroxenes, Amphibole, Garnet, Biotite, Magnetite, and Ilmenite	55
VI INTRACRYSTALLINE ION EXCHANGE	63
The Mössbauer Effect	63
Crystal Structure of Orthopyroxene, Clinopyroxene and Garnet	65
The Mössbauer Experiment	66
Interpretation	69
VII INTERCRYSTALLINE ION EXCHANGE EQUILIBRIUM: ORTHOPYROXENE-CLINOPYROXENE-AMPHIBOLE-GARNET	
(I) ORTHOPYROXENE-CLINOPYROXENE	82
Distribution of Mg and Fe ²⁺ Between Coexisting Orthopyroxene and Clinopyroxene	82
<u>Model 1. Ideal Solutions</u>	83
<u>Model 2. Non-ideal Solutions</u>	88
Distribution of Mn Between Coexisting Orthopyroxene and Clinopyroxene	98
(II) DISTRIBUTION OF Mg, Fe ²⁺ , AND Mn BETWEEN COEXISTING ORTHOPYROXENE AND ALMANDINE	99

	PAGE
(III) DISTRIBUTION OF Mg, Fe ²⁺ , AND Mn BETWEEN COEXISTING CLINOPYROXENE AND ALMANDINE	101
(IV) DISTRIBUTION OF Mg, Fe ²⁺ , AND Mn BETWEEN COEXISTING ORTHOPYROXENE AND AMPHIBOLE	105
(V) DISTRIBUTION OF Mg, Fe ²⁺ , AND Mn BETWEEN COEXISTING CLINOPYROXENE AND AMPHIBOLE	109
(VI) DISTRIBUTION OF Mg, Fe ²⁺ , AND Mn BETWEEN COEXISTING ALMANDINE AND AMPHIBOLE	113
SUMMARY	119
VIII DISTRIBUTION OF IRON AND TITANIUM BETWEEN COEXISTING MAGNETITE AND ILMENITE	122
General Consideration	122
Phase Equilibrium	122

PART 4

PHASE EQUILIBRIUM AND PETROGENESIS

IX PHASE EQUILIBRIUM, METAMORPHIC GRADE, AND ORIGIN	131
Phase Equilibrium	131
Metamorphic Grade	138
<u>Position of the studied charnockitic granulites in the metamorphic zones of the Adirondacks</u>	141
<u>Temperature, pressure and partial pressure of water during metamorphism</u>	145
Origin	152
REFERENCES	157

	PAGE
APPENDIX I A Fortran IV Computer Program to Perform Calculations from Chemical Analyses of Pyroxenes, Garnets, Amphiboles and Micas	184
APPENDIX II A Fortran IV Computer Program for Analysis of Grain Transitions (Randomness Test) based on Chi Square Test	205
APPENDIX III A Sample Calculation of Test for Randomness of Crystals in a Rock . .	210
APPENDIX IV Observed and Expected Transition Matrices for Charnockitic Granulites from the Adirondack Mts., New York .	213
APPENDIX V Transition Series for Charnockitic Granulites from the Adirondack Mts., New York	220
APPENDIX VI Mass-balance of Chemical Reactions 36 to 40	243
PLATES	245

LIST OF FIGURES

	PAGE
1. Qtz-K feld-Plag modal compositional plot of twelve charnockitic granulites from the Adirondack Mtns., N.Y.	3
2. Sample location map with geology	8
3. A two-dimensional analogue of randomness model in the form of a random mosaic	38
4. A sketch to show the point-sample and line-transect methods of spatial distribution measurements of crystals in thin-sections	44
5. The orthopyroxene crystal structure	67
6. Mössbauer spectrum of J-35 orthopyroxene measured at room temperature and pressure	70
7. Mössbauer spectrum of J-35 clinopyroxene measured at room temperature and pressure	70
8. Mössbauer spectrum of J-80 orthopyroxene measured at room temperature and pressure	71
9. Mössbauer spectrum of J-80 clinopyroxene measured at room temperature and pressure	71
10. Mössbauer spectrum of J-80 almandine garnet measured at room temperature and pressure	72
11. Mössbauer spectrum of J-35 orthopyroxene measured at T=77°K, P=1 atm	72
12. Mössbauer spectrum of J-80 orthopyroxene measured at T=77°K, P=1 atm	73

	PAGE
13. Mössbauer spectrum of J-80 clinopyroxene measured at T=77°K, P=1 atm	73
14. Mössbauer spectrum of J-105B orthopyroxene measured at T=77°K, P=1 atm	74
15. Mössbauer spectrum of J-105Bclinopyroxene measured at T=77°K, P=1 atm	74
16. Mössbauer spectrum of J-106 orthopyroxene measured at T=77°K, P=1 atm	75
17. Mössbauer spectrum of J-106 clinopyroxene measured at T=77°K, P=1 atm	75
18. Distribution isotherms for the distribution of Fe ²⁺ and Mg between M ₁ and M ₂ sites in orthopyroxene	81
19. Distribution of Mg and Fe ²⁺ between coexisting orthopyroxene and clinopyroxene from the charnockitic granulites	85
20. Distribution of Mg and Fe ²⁺ between coexisting orthopyroxene and clinopyroxene from the charnockitic granulites in terms of a $\left(\frac{X}{1-X}\right)_{\text{Mg}}^{\text{opx}}$ vs $\left(\frac{X}{1-X}\right)_{\text{Mg}}^{\text{cpx}}$ plot	86
21. Distribution of Mg and Fe ²⁺ between coexisting orthopyroxenes and clinopyroxenes from the charnockitic granulites	91
22. Activity-composition diagram for orthopyroxenes from the charnockitic granulites	95

	PAGE
23. Activity-composition diagram for clinopyroxenes from the charnockitic granulites	95
24. Mg-Fe ²⁺ distribution diagram for the Adirondack, Madras, Quairading, and Broken Hill pyroxenes	96
25. Coexisting orthopyroxene and clinopyroxene in the Ca-Mg-Fe system	97
26. Distribution of Mn between coexisting orthopyroxene and clinopyroxene from the charnockitic granulites	100
27. Distribution of Mg and Fe ²⁺ between coexisting orthopyroxene and almandine garnet from the charnockitic granulites. Data from some Indian, Swedish and Ugandan charnockites and related granulites are included	102
28. Distribution of Mg and Fe ²⁺ between coexisting orthopyroxene and almandine garnet from the charnockitic granulites in terms of a $\left(\frac{X}{1-X}\right)_{Mg}^{opx}$ vs $\left(\frac{X}{1-X}\right)_{Mg}^{gar}$ plot. Some Indian, Swedish and Ugandan charnockites and related granulites are also plotted	103
29. Distribution of Mn between coexisting orthopyroxene and almandine garnet from the charnockitic granulites	104
30. Distribution of Mg and Fe ²⁺ between coexisting clinopyroxene and almandine garnet from the charnockitic granulites	106

31.	Distribution of Mg and Fe ²⁺ between coexisting clinopyroxene and almandine garnet from the charnockitic granulites in terms of a $\left(\frac{X}{1-X}\right)_{Mg}^{cpx}$ vs $\left(\frac{X}{1-X}\right)_{Mg}^{gar}$ plot	107
32.	Distribution of Mn between coexisting clinopyroxene and almandine garnet from the charnockitic granulites	108
33.	Distribution of Mg and Fe ²⁺ between coexisting orthopyroxene and amphibole from the charnockitic granulites	110
34.	Distribution of Mg and Fe ²⁺ between coexisting orthopyroxene and amphibole from the charnockitic granulites in terms of a $\left(\frac{X}{1-X}\right)_{Mg}^{opx}$ vs $\left(\frac{X}{1-X}\right)_{Mg}^{amph}$ plot	111
35.	Distribution of Mn between coexisting orthopyroxene and amphibole from the charnockitic granulites	112
36.	Distribution of Mg and Fe ²⁺ between coexisting clinopyroxene and amphibole from the charnockitic granulites	114
37.	Distribution of Mg and Fe ²⁺ between coexisting clinopyroxene and amphibole from the charnockitic granulites in terms of a $\left(\frac{X}{1-X}\right)_{Mg}^{cpx}$ vs $\left(\frac{X}{1-X}\right)_{Mg}^{amph}$ plot	115

	PAGE
38. Distribution of Mn between coexisting clinopyroxene and amphibole from the charnockitic granulites	116
39. Distribution of Mg and Fe^{2+} between coexisting amphibole and almandine garnet from the charnockitic granulites	117
40. Distribution of Mg and Fe^{2+} between coexisting amphibole and almandine garnet from the charnockitic granulites in terms of a $\left(\frac{X}{1-X}\right)_{Mg}^{amph}$ vs $\left(\frac{X}{1-X}\right)_{Mg}^{gar}$ plot	118
41. Distribution of Mn between coexisting amphibole and almandine garnet from the charnockitic granulites	120
42. Compositional relationships of ilmenite solid solutions (Ilm ss), magnetite solid solutions (Mt ss) and their pure end member molecules in the system $TiO_2-FeO-Fe_2O_3$	123
43. Exchange of iron and titanium ions between coexisting ilmenite solid solutions (Ilm ss) and magnetite solid solutions (Mt ss)	125
44. Shift and relation of the ilmenite-magnetite tie line in response to a change in temperature and fugacity of oxygen	126

	PAGE
45. Phase diagram showing compositional tie lines of coexisting ilmenite solid solutions (Ilm ss) and magnetite solid solutions (Mt ss) from the charnockitic granulites together with some published results from igneous and metamorphic rocks	128
46. Composition of coexisting ilmenite solid solutions and magnetite solid solutions as determined experimentally by Buddington and Lindsley (1964) at varying temperature and fugacity of oxygen. Data from present study and other sources are included	129
47. Orthogonal AFM plot showing the phase relations among coexisting clinopyroxene, almandine garnet, and amphibole in the analyzed charnockitic granulites along with the bulk rock compositions	133
48. Orthogonal AFM plot showing the phase relations among coexisting orthopyroxene, clinopyroxene, and amphibole in the analyzed charnockitic granulites along with the bulk rock compositions	134
49. Orthogonal AFM plot showing the phase relations among coexisting orthopyroxene, clinopyroxene, and almandine garnet in the analyzed charnockitic granulites along with the bulk rock compositions	135

50.	Orthogonal AFM plot showing the phase relations among coexisting orthopyroxene, clinopyroxene, almandine, and amphibole in the analyzed charnockitic granulites along with the bulk rock compositions. A fifth phase, biotite, is also shown (rock J-105B). All iron in this mineral is assumed to be ferrous iron. Except for J-105B, these rocks do not contain K-feldspar	136
51.	Schematic Schreinemakers bundle in a P_{H_2O} -T field showing univariant reaction curves for reactions 36 to 40. The supposed relative positions of mineral assemblages 2, 3, 4, and 5 are indicated	139
52.	P-T field of the charnockitic granulites studied in terms of breakdown and chemical reactions of phases	147
53.	Variation diagram showing a Mg-ΣFe-Alk trend and a calc-alkali trend in the charnockitic granulites from the Adirondack Mtns., N.Y.	154

LIST OF TABLES

	PAGE
1. Mineral assemblages and modal analysis of charnockitic granulites from the Adirondack Mts., N.Y.	16
2. Bulk rock chemical compositions of eleven charnockitic granulites from the Adirondack Mts., N.Y.	17
3. Plagioclase compositions in terms of % An of the twelve charnockitic granulites from the Adirondack Mts., N.Y.	19
4. Summary of spatial distribution of orthopyroxenes, clinopyroxenes, amphiboles and feldspars in charnockitic granulites from the Adirondack Mts., N.Y.	49
4a. Type and frequency of spatial distribution of feldspar (F), amphibole (A), orthopyroxene (H) and clinopyroxene (C) in the charnockitic granulites from the Adirondack Mts., N.Y.	50a
5. Chemical compositions of orthopyroxenes from charnockitic granulites from the Adirondack Mts., N.Y. together with recalculated analyses	57
6. Chemical compositions of clinopyroxenes from charnockitic granulites from the Adirondack Mts., N.Y. together with recalculated analyses	58

	PAGE
7. Chemical compositions of amphiboles from charnockitic granulites from the Adirondack Mts., N.Y. together with recalculated analyses	59
8. Chemical compositions of garnets from charnockitic granulites from the Adirondack Mts., N.Y. together with recalculated analyses	60
9. Electron microprobe analysis of J-105B biotite from charnockitic granulites from the Adirondack Mts., N.Y. together with calculated formula	61
10. Electron microprobe analyses of coexisting magnetite (Mt) and ilmenite (Ilm) solid solutions	62
11. Site occupancy (Fe^{2+}) numbers for four orthopyroxenes from charnockitic granulites from the Adirondack Mts., N.Y.	79
12. Mole fractions of Mg and Fe^{2+} for coexisting orthopyroxene and clinopyroxene from mafic charnockitic granulites from the Adirondack Mts., and from Madras, India	84
13. Distribution coefficients for the coexisting orthopyroxene and clinopyroxene from the Madras area, and the Adirondack Mts., N.Y.	87
14. Activity coefficients of the Adirondack and Madras orthopyroxene (γ^{opx}) and clinopyroxene (γ^{cpx})	92

15. Activity data of the Adirondack and Madras
orthopyroxene (a^{opx}) and clinopyroxene (a^{cpx}).

94



PART 1

GEOLOGY AND PETROGRAPHY

I INTRODUCTION

Statement of Problem

This thesis presents the results of a study of the spatial distribution of crystals, and a study of phase equilibrium in some charnockitic granulites from the Adirondack Mountains in New York. These studies were undertaken in an attempt to increase our understanding of the processes that take place during the crystallization of high-grade metamorphic rocks. The spatial distribution of crystals in a rock may give information on nucleation sites and the role of interfacial free energy in metamorphic crystallization, and data on the association of minerals and their chemical composition may provide information on the equilibrium characteristics of complex silicate and oxide systems containing minerals of variable composition.

General Statement

The term charnockite was proposed by Holland (1893, p162) for a hypersthene-bearing granite found near Madras, India. Later, Holland (1900, p125, 128) described a charnockite series which consists of acid, intermediate, basic and ultrabasic orthopyroxene-bearing plutonic and metamorphic rocks. More recently Subramanian (1959, p328) attempted to redefine charnockite as a hypersthene-bearing

rock with or without garnet, characterized by greenish-blue feldspars and greyish-blue quartz, the dominant feldspar being a microperthite. This has restricted the term charnockite to the acid charnockites of Holland (1900).

The rock suite under investigation has close similarities to intermediate and basic charnockites from India and other parts of the world. In the present thesis the terms charnockite and charnockitic granulites will be used in a broad sense intended by Holland (1900). Two samples, J-50 and J-99, without orthopyroxene, are also included because of close association and similarity in chemical composition to the other charnockitic rocks. More specific terms will be used locally, and these follow the nomenclature used by Philpotts (1966, p13) and de Waard (1969, p78) as shown in Fig. 1.

The modal proportion of quartz, K feldspar and plagioclase in some rocks that will be described in detail below are shown in Fig. 1. Most of these fall in the field of norite and anorthosite, two in the field of jotunite and two in farsundite. In addition, the rocks contain 10-50 per cent ferromagnesian minerals. Thus the rocks of the present study belong to the intermediate and basic divisions of the charnockite series.

Since the original work of Holland, charnockites from the type area near Madras have been studied extensively by Howie (1955), Pichamuthu (1953), Howie and Subramaniam


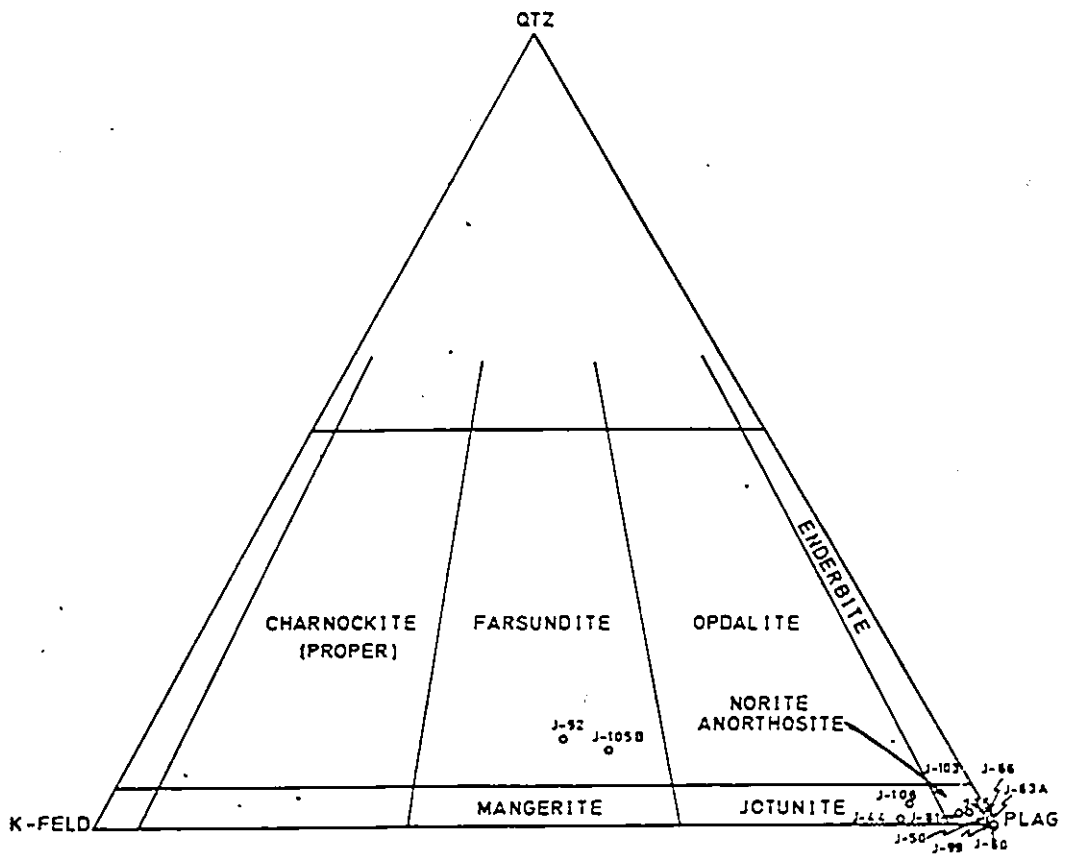


Figure 1. Qtz-K feld-Plag modal compositional plot of twelve charnockitic granulites from the Adirondack Mts., N.Y.



(1957), Subramaniam (1962) and Sen and Sahu (1970). According to Subramaniam (1962) these rocks resulted from the emplacement of a charnockitic magma into a sequence of meta-sediments and mafic granulites.

The best known group of charnockites in North America occurs in the Adirondack Highlands, within the Grenville Province of the Canadian Shield. The field relation and petrology of these rocks have been described in detail by Buddington (1939, 1952, 1963, 1965, 1966, 1969) and de Waard (1964, 1965a, 1965b, 1967, 1969). The present study provides additional information on these interesting rocks particularly on the chemical composition of the minerals and on the spatial distribution of the contained crystals.

General Geology

The Precambrian rocks of the Adirondack Mountains form part of the Grenville Province of the Canadian Shield and comprise igneous and metamorphic rocks of various compositions (Buddington, 1939). According to Stockwell (1972, p2), the most recent orogeny in this part of the Shield (the Grenvillian Orogeny) occurred about 1,000 m.y. ago.

The nature and sequence of intrusion and deformations in the Adirondack area were described by Buddington (1952, p39) and are summarized in the following paragraphs.

Following the deposition of a sequence of limestones, sandstones, shales, etc. (the Grenville Series), three major orogenic events took place in the Adirondack region. During the earliest event the Grenville Series was folded, and anorthosite, olivine diabase or gabbro, and the quartz syenitic and charnockitic series were emplaced in sequence, as is indicated by the presence of intrusive contacts.

During the second period of orogeny, deformation and metamorphism occurred on a regional scale. Garnet crystallized in many of the rocks that were affected by this metamorphism. At this time, the quartz syenitic and charnockitic series were invaded by dikes of hypersthene diabase.

The third and last period of orogenic deformation and metamorphism was marked by the emplacement of various granitic rocks, particularly granite and subordinate alaskite, microcline granite and soda-granite.

Unmetamorphosed basaltic dikes marked the end of the history of intrusions and deformations in the area.

Successive metamorphism and deformation has produced in the Adirondack region a variety of medium to high grade metamorphic and plutonic rocks. Nearly all of these rocks have been affected to some extent by deformation and metamorphism, and may be described as being gneisses and granulites. The charnockitic granulites of the present study are

largely orthogneisses (Buddington, personal communication, 1969) and are closely associated with anorthosites, olivine gabbros, migmatites, and hornblende- and pyroxene-bearing granitic and syenitic gneisses. They occur as small plutons, dike-like bodies and as layered rocks of possible sedimentary or volcanic origin. All of these are situated in and around the main anorthosite massif of the central and eastern Adirondack Mountains (de Waard, 1969, p221, and also Fig. 2). Most of these rocks are homogeneous but in some, a small scale layering is discernible. A foliation, marked by the preferred orientation of crystals is probably present in all of these rocks, but is not conspicuous. The rocks are fine to medium-grained, i.e. mean grain size normally is 0.2 to 1.5 mm.

Small apophyses into anorthosite have been observed, indicating that some of the charnockitic granulites may be of magmatic origin.

Field Sampling

Valuable information regarding the charnockite localities in the Adirondacks was kindly provided by Professor A.F. Buddington of Princeton University. An area measuring 30 miles by 20 miles, situated immediately west of Lake Champlain, was chosen as the sample area for the present

study (Fig. 2). A few mineral and bulk rock chemical analyses from this area were previously reported by Buddington (1952). These data together with some information from him through personal communications have greatly assisted the writer in locating favourable sites for obtaining samples. Altogether, one hundred and twenty rock samples were collected during a period of 15 days early in August and in October, 1969. The locations of those rocks that were selected for detailed study are shown in Fig. 2.

Laboratory Work

One hundred standard-size thin-sections were examined and 12 rocks containing different mineral assemblages, and little alteration were chosen for further study. These rock samples are J-35, J-44, J-50, J-63A, J-66, J-80, J-81, J-92, J-99, J-103, J-105B, and J-106.

Each of the above mentioned rock samples, except J-92, was first crushed into small fragments (less than two inches in diameter) in a chipmunk crusher. Several representative fragments were hand-picked and ground to fine powders (<200 mesh) by use of a porcelain mortar and pestle: this material was used for bulk-rock chemical analysis. The remaining fragments were passed through a disc grinder several times, and the resulting powders then sieved with Cu-wire metal sieves. About 100 to 150 grams of this material, between 170 and 230 mesh, was used for mineral separation.

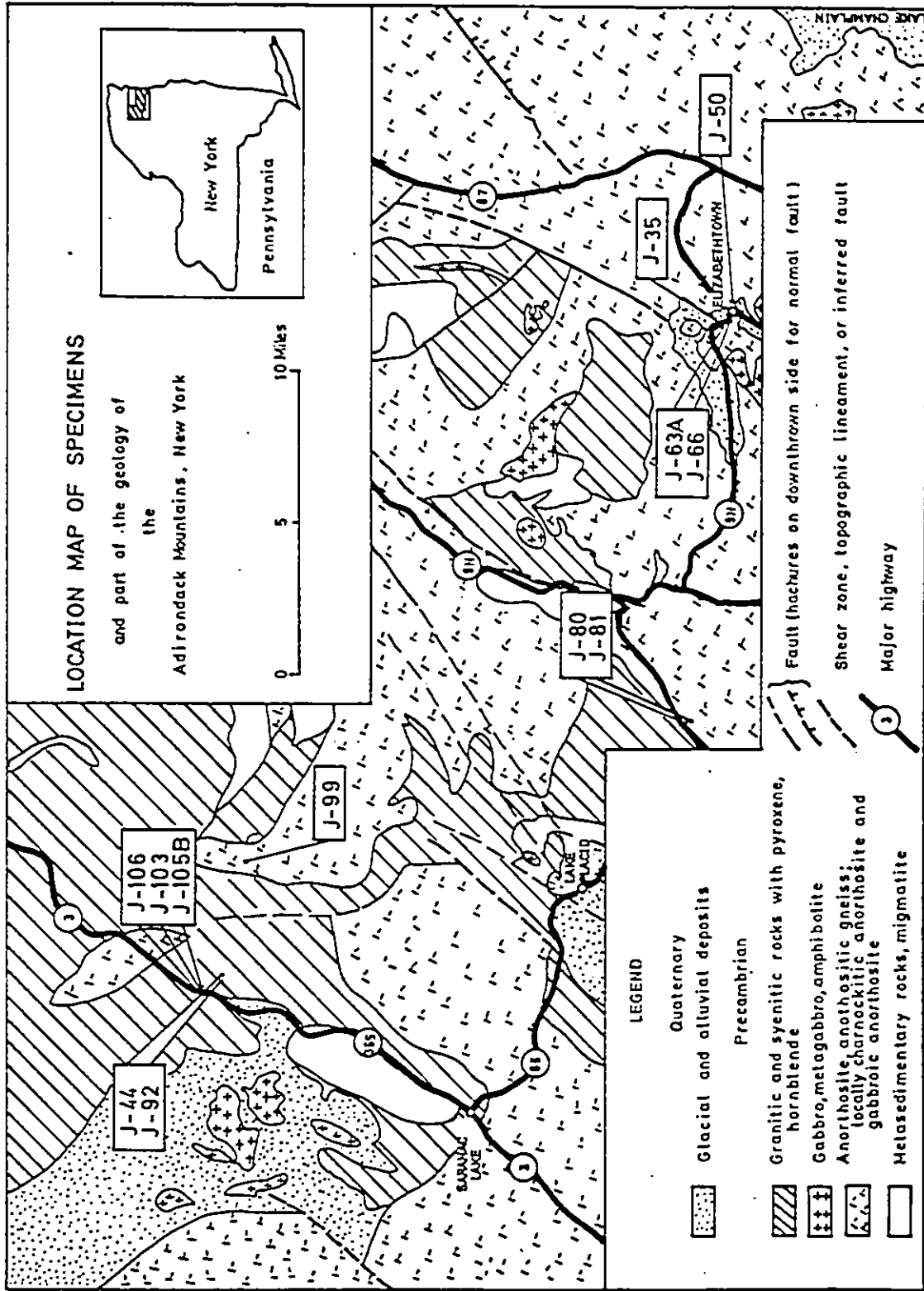


Figure 2. Sample location map with geology After Geological Map of New York, 1961, Adirondack Sheet (J. G. Broughton et al)

These powders were first washed and rinsed with distilled water and acetone. The samples were then dried in an electric oven at temperatures of about 105°C. After cooling, the powders were spread on a piece of clean paper and the strongly magnetic minerals together with iron contamination were removed with a hand magnet.

Pyroxenes, amphiboles and garnets in the eleven rocks chosen for detailed chemical study were separated and purified to >99%, with many >99.9% pure, using combinations of the Frantz isodynamic separator and various dilutions of heavy liquids, mainly methylene iodide and Clerici solution (thallium malonate-formate).

The mineral and rock samples (approximately 100 mg of each) were taken into solution employing the perchloric acid method. They were then analyzed for total Fe, MgO, CaO, Na₂O, K₂O and MnO by means of atomic absorption spectrometry in the Geochemical Laboratory, Department of Geology, University of Ottawa. A Techtron model AA4 atomic absorption spectrophotometer was used following a procedure similar to that described by Kretz (1970).

FeO was analyzed by a rapid wet chemical method that was developed by the writer (Jen, 1973). Fe₂O₃ was then calculated from the determined FeO and total Fe as Fe₂O₃ obtained by atomic absorption, using the equation

$$\text{wt\% Fe}_2\text{O}_3 = \text{wt\% total Fe as Fe}_2\text{O}_3 - 1.1 \text{ wt\% FeO}$$

SiO₂, Al₂O₃ and TiO₂ in the silicate minerals, and total Fe and TiO₂ in magnetites and ilmenites were analyzed by use of an electron microprobe, located at Carleton University. SiO₂, Al₂O₃ and TiO₂ in the rocks were determined, through Dr. I. Ermanovics at the Geological Survey of Canada; SiO₂ and TiO₂ were determined colorimetrically and Al₂O₃ by use of a Perkin-Elmer model 303 atomic absorption spectrophotometer.

The USGS BCR-1 basalt standard was used as a check on accuracy for all the wet chemical analyses. An analyzed ilmenite standard and a NASA pyroxene standard were used in the probe analysis. The computer program by Rucklidge and Gasparri (1969) was used for the probe data reduction.

Analyses, excepting the probe analyses were measured in duplicate. In the probe analysis, 2 to 4 measurements were made per mineral grain, and 2 to 5 mineral grains of the same mineral were analyzed per rock section (polished-thin section). For each measurement spot, counts were recorded for 5 time intervals of 10 seconds each.

The precision of the analyses, expressed in terms of standard deviation (s) and percentage relative deviation (c) were determined by analyzing standard USGS BCR-1 ten times, and NASA pyroxene standard (LUD) fifteen times. Standard and relative deviations were calculated by use of the equations

$$s = \sqrt{\frac{\sum (x-\bar{x})^2}{n}}$$

$$c = 100s/\bar{x} \quad (\text{Ahrens and Taylor, 1961, p116})$$

where x = determination or measurement per sample
 \bar{x} = sample mean
 n = number of sample measurements

Results are shown in the following table, which also provides indication of the accuracy that was achieved.

Analytical precision and accuracy

USGS BCR-1 by AA (FeO by titration) NASA Pyroxene by Electron Microprobe

NASA Pyroxene	(Furnished by N.D. MacRae, 1971)	\bar{x}	s	c
SiO ₂	51.61	50.59	0.96	1.90
Al ₂ O ₃	5.92	5.90	0.16	2.71
TiO ₂	0.27	0.21	0.046	21.90
BCR-1	(Flanagan, 1967*, 1973)			
Fe ₂ O ₃	3.20*	3.17	0.18	5.67
FeO	9.08*	9.10	0.16	1.75
MgO	3.46	3.58	0.14	3.91
MnO	0.18	0.19	0.01	5.26
CaO	6.92	6.81	0.40	5.87
Na ₂ O	3.27	3.47	0.19	5.47
K ₂ O	1.70	1.70	0.06	3.52

Formula calculations and ionic ratios for the minerals were obtained by use of a Fortran IV computer program (Appendix I) using an IBM 360/65 computer installed at the Computing Centre, University of Ottawa.

Methods used to obtain information on cation distribution within crystals (the Mössbauer experiment) and on the spatial distribution of crystals will be described in subsequent chapters.

Acknowledgements

The writer is grateful to Dr. Ralph Kretz for his continued interest, encouragement and guidance during the course of this research and for his critical reading of the manuscript. Drs. F.P. Agterberg and Donald D. Hogarth have also offered many valuable discussions and suggestions regarding the statistical analysis and the mineralogical aspects of the thesis, respectively. Dr. William K. Fyson made some valuable editorial comments.

Dr. Michael Townsend of the Mines Branch, Department of Energy, Mines and Resources, Ottawa, generously provided the facilities of his Mössbauer laboratory. The Mössbauer experiments and spectral fitting were performed by Messrs. Jacques Gosselin, Robert Tremblay and Donald Carson, who also participated in many discussions pertaining to the results.

The writer also wishes to thank Dr. Edgar Froese of the Geological Survey of Canada for critically reading the manuscript. His valuable discussions regarding chemical reactions, petrogenesis, and the pyroxene equilibria were

appreciated. Drs. Donald H. Lindsley of the State University of New York at Stony Brook, and A.R. Philpotts of the University of Connecticut have critically reviewed the entire thesis which has been greatly improved through their comments and suggestions.

Thanks must also be extended to Drs. Ingo Ermanovics and A.G. Plant of the Geological Survey of Canada for their assistance in obtaining some chemical analyses and electron microprobe analysis of a biotite sample respectively. The analysis of minerals by electron microprobe was done by Mr. Paul Mainwaring under the supervision of Dr. David Watkinson of the Department of Geology, Carleton University.

Dr. S.K. Saxena of the City University of New York kindly provided a computer run on the least square solution of an equation for co-existing pyroxenes based on a simple mixture solution model. Mass balance of five chemical reactions by Dr. T.M. Gordon of the Geological Survey of Canada was also appreciated.

The writer is particularly indebted to Dr. A.F. Buddington of Princeton University, who kindly provided advice concerning the collection of rock samples. Also appreciated are the many valuable discussions and encouragement he offered during the initial phases of the study.

Thanks are also extended to Mrs. Diane Garrett for her helpful suggestions pertaining to analytical aspects of

the laboratory work and development of a rapid ferrous iron analytical technique. Mr. Edward Hearn prepared the photomicrographs.

National Research Council of Canada research grants awarded to Dr. Ralph Kretz and financial support from the Department of Geology, University of Ottawa have made this research possible.

II MINERALOGY, PETROGRAPHY AND BULK-ROCK
CHEMICAL ANALYSES

The mineral assemblages and modal analyses of the twelve charnockitic granulites that were selected for detailed study are shown in Table 1. Bulk-rock chemical analyses of eleven of these rocks are shown in Table 2. These data will be discussed in a later chapter.

A brief description of the minerals present in the rocks is given in the following sections. Chemical analyses of orthopyroxene, clinopyroxene, amphibole, garnet, magnetite, and ilmenite will be presented in Part 3 of this thesis, which deals with exchange equilibrium.

Feldspars

The feldspars are fine to medium grained and granoblastic. K-feldspar is commonly perthitic and locally may be microperthitic. Potash feldspar, some showing microcline twinning, occurs in trace amounts in only a few samples. The perthitic feldspars are mostly blebby and rod perthite. String perthite and mesoperthite have also been observed. Plagioclase commonly occurs as two types, well twinned and clear crystals as well as antiperthitic crystals. They may be optically positive or negative. $2V_x$ determined for J-35 plagioclase is $2V_x=83.5^\circ$ and for J-66 $2V_x=85^\circ$. Grain shapes vary from xenoblastic to hypidioblastic, and are more hypidioblastic than K-feldspars. Compositions of plagioclase

Table 1 Mineral Assemblages and Modal Analysis of
Charnockitic Granulites from the Adirondack Mountains, N.Y. (in %)

Mineral	J-35	J-44	J-50	J-63a	J-66	J-80	J-81	J-92	J-99	J-103	J-105b	J-106	AV
Plagioclase	45.4	45.1	59.1	50.8	48.6	22.8	30.0	36.9	43.1	51.7	33.6	51.8	43.3
Perthitic Feldspar	-	7.6	-	-	-	-	1.1	35.7	-	1.5	25.3	5.0	6.4
Antiperthitic Feldspar	Trace	21.6	7.2	Trace	-	1.0	2.0	2.8	-	15.1	1.5	3.5	4.6
Microcline	-	-	0.4	-	-	-	-	-	-	Trace	-	Or 1.2	Trace
Orthopyroxene	3.7	7.8	-	2.2	5.3	23.6	15.8	6.2	-	10.3	9.2	10.8	7.9
Clinopyroxene	17.9	6.2	15.3	15.7	15.6	13.5	20.0	1.9	28.2	9.0	3.4	8.7	13.0
Amphibole	7.1	7.9	4.8	0.1	2.7	8.3	-	4.0	11.1	4.5	2.5	9.6	5.2
Biotite	0.3	Trace	-	Trace	Trace	0.1	Trace	0.3	0.4	Trace	1.4	Trace	0.2
Garnet	13.2	-	9.1	20.9	15.8	8.5	16.0	Trace	7.8	-	8.3	-	8.3
Quartz	0.6	0.5	0.5	0.4	0.7	-	0.5	9.2	0.1	1.0	6.5	1.6	1.8
Myrmekite	-	Trace	-	-	-	-	-	Trace	-	-	Trace	-	Trace
Opakes**	10.5	2.0	3.2 ^v	6.8	8.1	14.2	8.5	1.3	6.8*	4.8	3.3	5.0	6.2
Apatite	1.2	0.9	0.2	2.8	2.6	8.0	5.9	1.1	2.4	1.8	2.4	2.8	2.7
Zircon	Trace	0.4	-	-	Trace	-	-	<0.1	-	Trace	0.3	-	Trace
Calcite	Trace	Trace	0.1	0.4	0.4	-	0.2	0.5	0.1	0.2	2.3	Trace	0.4
Total	99.9	100.0	99.9	100.1	99.8	100.0	100.0	100.0	100.0	99.9	100.0	100.0	100.0

Trace - <0.1%
+ - Myrmekite with unmeasurable mixed quartz and feldspar
** - Opakes consist of magnetite, ilmenite, pyrrhotite and pyrite
* - No magnetite; v no pyrrhotite; magnetite grains in J-50 and J-105b are too tiny to be focused by electron beam of microprobe
Av. No. of point counts = 2500

Table 2 Bulk rock chemical compositions of eleven charnockitic granulites from the Adirondack Mts., N.Y.

BULK ROCKS
CHARNOCKITIC GRANULITES

SP.No. Oxides	J-35	J-44	J-50	J-63A	J-66	J-80	J-81	J-99	J-103	J-105B	J-106	AV.
SiO ₂	40.80	60.55	49.50	47.70	45.50	41.05	42.10	46.40	53.00	57.50	53.30	48.86
Al ₂ O ₃	13.20	12.85	19.20	14.50	14.40	8.70	11.80	14.20	13.60	13.40	13.30	13.56
TiO ₂	5.35	1.35	2.60	3.65	4.25	4.75	4.65	3.75	2.85	2.30	2.80	3.48
Fe ₂ O ₃	1.80	1.46	1.77	2.05	2.05	5.24	2.81	1.66	1.38	1.84	2.10	2.20
FeO	19.16	8.81	9.31	14.38	17.18	21.49	19.53	14.09	11.62	10.03	11.09	14.24
MgO	3.21	1.26	2.58	3.59	3.43	5.20	5.27	3.63	2.35	2.03	2.33	3.17
MnO	0.32	0.21	0.13	0.24	0.27	0.36	0.35	0.25	0.26	0.18	0.23	0.25
CaO	12.31	4.76	10.47	8.90	7.62	10.47	10.20	11.02	7.08	4.16	6.74	8.52
Na ₂ O	2.49	3.69	2.76	2.98	2.97	1.72	1.99	3.01	4.06	3.72	3.86	3.02
K ₂ O	0.68	4.93	1.05	1.28	0.69	0.46	0.71	0.96	2.97	3.77	2.98	1.86
Total	99.32	99.87	99.37	99.27	98.36	99.44	99.41	98.97	99.17	98.93	98.73	99.16
Atomic or ionic %												
Fe ²⁺ +Fe ³⁺	68.64	47.91	54.05	58.57	64.22	67.26	62.97	58.14	52.29	50.15	52.46	63.08
Mg	19.67	11.40	24.61	24.47	21.71	26.12	28.43	25.34	17.91	16.67	18.13	24.62
Na+K	11.69	40.69	21.34	16.96	14.07	6.62	8.60	16.52	29.80	33.18	29.41	12.30
Ca	82.24	43.15	77.07	72.02	71.12	85.10	82.14	76.99	56.55	42.58	56.15	78.95
Na	15.05	30.23	18.37	21.82	25.08	12.69	14.49	19.04	29.35	34.42	29.12	15.79
K	2.71	26.62	4.56	6.16	3.80	2.21	3.37	3.97	14.10	23.00	14.73	5.26

range from An_{23} (oligoclase) to An_{42} (calcic andesine). Table 3 shows the compositions of plagioclases in the 12 rocks studied as determined by the maximum extinction angle method (synthesized by Wynne-Edwards, 1959, unpublished). Plagioclases may show wavy extinction and vague zoning (normal zoning: core-rim= An_5). Some myrmekitic texture has been observed in samples J-105B and J-44.

Orthopyroxene

Orthopyroxene crystals are fine grained, granoblastic to short prismatic granoblastic in shape, commonly hypidioblastic. Pleochroism varies from pale green or pale grey to light pink. Prismatic cleavage is often well developed. The crystals are optically biaxial (-), and are closely associated with clinopyroxene and biotite where they occur, less frequently with garnet, amphibole and opaques. The orthopyroxene grains occur as two types, (1) with well-defined grain boundaries, and (2) with vaguely defined grain boundaries with clinopyroxene. Occasionally they may show exsolution lamellae of clinopyroxene in some of the rocks (J-44, J-92, J-103). Commonly they are inclusion-free. However, apatite and opaques may be included in very small amounts and biotite may occur as an alteration product along cleavages. For J-35, $2V_x = 60.5^\circ$.

Table 3 Plagioclase compositions in terms of %An content of the twelve charnockitic granulites from the Adirondack Mountains, N.Y.

Sp. No.	J-35	J-44	J-50	J-63A	J-66	J-80	J-81	J-92	J-99	J-103	J-105B	J-106
%An	An ₃₂	An ₂₃	An ₄₂	An ₃₂	An ₃₂	An ₂₉	An ₃₂	An ₂₈	An ₃₅	An ₂₆	An ₂₈	An ₂₈

Clinopyroxene

Clinopyroxene crystals are fine to medium grained pale green to greenish in colour. Most grains are granoblastic; very few grains show prismatic habit probably due to the orientation of the thin sections (perpendicular or at an angle to the foliation). Xenoblastic to hypidioblastic in shape, most grains show moderate to strong birefringence. Some grains may be partially or entirely surrounded by amphibole, but with no reaction rim. The clinopyroxene grains are commonly closely associated with amphibole, orthopyroxene, garnet, opaques and biotite. Apatite and opaques are common inclusions. All crystals are optically biaxial (+). Grains show slight pinkish pleochroism in J-99. Multiple twinning occurs in J-103. Minor amounts of fine exsolution lamellae of a second clinopyroxene (less calcic?) occur in some grains of a few samples (J-103, J-105B and J-106). For clinopyroxene J-35, $2V_z=58^\circ$, and $c\alpha z=41^\circ$.

Amphibole

Amphibole crystals are fine to medium grained, granoblastic to short prismatic, pale brownish green, and xenoblastic to hypidioblastic. Apatite and opaques are common inclusions. The amphibole grains may show myrmekitic texture with quartz (e.g. locally in J-66). $2V$ determined for J-35 amphibole is $2V_x=74.5^\circ$. The optic angle is consistent with an intermediate member of the hornblende series

which is determined by the chemical analyses. A generalized pleochroism is

X = light yellow-green to light greenish yellow

Y = dark green to dark to light brownish green

or greenish brown to brownish red

Z = dark green, brownish green to light reddish brown

Absorption: $X < Y > Z$

Locally some porphyroblastic grains have been observed in some rocks. Smaller grains often are inclusion-free or contain fewer inclusions than the larger grains. Some large grains are poikiloblastic.

Garnet

Garnet crystals are pinkish in colour and are fine grained in all rocks except J-105B. The garnet grains are xenoblastic to idiomorphic in shape and may be inclusion-free to poikiloblastic, with opaques, quartz, clinopyroxene, feldspars and apatite as inclusions. They may show corrosive or embayment texture with quartz and plagioclase (J-66, J-105B), may be myrmekitic with quartz (symplektite) (J-99), and may also be clustered as in most of the rocks as well as random under the microscope.

Biotite

Biotite crystals are reddish brown to reddish in colour; they are very fine grained, xenoblastic to hypidioblastic, and are associated with pyroxenes, amphibole, opaques and garnet. The biotites occur as traces of poorly defined grains along cleavages of orthopyroxene in some rocks (e.g. J-80). They appear to be a disappearing phase (relic primary phase) in some rocks but appearing phase (secondary) in the others as an alteration product. Generally, they are inclusion-free.

Quartz

Quartz crystals are fine to very fine grained and xenoblastic. They may be associated with all minerals but appear to occur commonly as inclusions in amphibole and garnet (e.g. J-105B) probably as a reaction product. They show undulose extinction, and are usually inclusion-free.

Opaques

Opaque minerals are fine grained and often appear as aggregates of crystals. By use of an ore microscope, four different types of opaque phases were identified in the charnockitic granulites, but in the less mafic (intermediate) rocks, only two to three types of opaque phases are present. These opaque phases are magnetite, ilmenite, pyrite, and pyrrhotite. The iron oxides are of major concern

in the present study. Most rocks contain magnetite except J-50 and J-105B, and all rocks contain ilmenite. Ore microscopic study has also revealed that ilmenite is the major iron oxide and magnetite commonly occurs as very fine-grained crystals in and/or closely associated with ilmenite. Magnetite or titanomagnetite lamellae are sometimes also present within ilmenite crystals.

Apatite

Apatite is very fine grained and commonly idiomorphic. It occurs commonly as inclusion in all minerals except quartz and zircon.

Carbonate

Carbonate is fine-grained and xenoblastic to hypidioblastic. It is closely associated with clinopyroxene (J-66), amphibole, biotite and quartz (J-105B) probably as an alteration product.

Zircon

Zircon is very fine grained, usually occurs as idiomorphic prismatic crystals, and is inclusion-free. It is commonly associated with mafic minerals especially pyroxenes.



PART 2

SPATIAL DISTRIBUTION OF CRYSTALS
IN ROCKS



III GENERAL PRINCIPLES

Definitions

Like phase: A like-phase contact is a contact between two crystals of the same mineral

Unlike phase: An unlike-phase contact is a contact between two crystals of different minerals

Transition: A sequence of two crystals along a linear traverse, for example AA AB BA where A and B are minerals

Transition matrix: A matrix composed of all the different kinds of transitions observed in a rock or defined by a particular model

Transition series: A series of transition matrices derived from a particular transition matrix. For example from a matrix for minerals A, B, and C, another could be derived by considering minerals B and C together denoting them as Q, giving an AQ matrix

Background and Methods

Although studies on spatial distributions in the field of ecology (e.g. Gleason, 1920; Neyman, 1939; Clark and Evans, 1954; Moore, 1954; Pielou, 1959) and in metallurgy (e.g. Smith, 1948, 1952; Gurland, 1967) have been underway

for some time, comprehensive studies of spatial distributions of crystals in rock began little more than a decade ago.

Harker (1939) and others had long ago presented some information on the distribution of minerals in small volumes of rock, as seen in thin-section, but Ramberg (1952, p220-229), DeVore (1956, 1959), Laffitte (1957,p328), Rogers and Bogy (1958) and Lafeber (1963, 1966) were among the first to examine the subject in greater detail or to consider the subject in terms of interfacial energy. Ramberg, DeVore, and Laffitte suggested that recrystallization may produce a rearrangement of the minerals so as to reduce the total interfacial free energy of the rock.

Rogers and Bogy (1958) and Mahan and Rogers (1968) observed and recorded the kind and frequency of crystal contacts in some granitic and metamorphic rocks. Observations were made along linear traverses across thin-section of the rocks. They found more K-feldspar to K-feldspar contacts in metamorphic rocks than in granitic rocks, and attributed the tendency for K-feldspar crystals to be separated from each other (in granitic rocks) to magmatic crystallization.

Lafeber (1963) used two methods for the analysis of randomness in the distribution of crystals in some granitic rocks. The line sampling method, is similar to that used by Rogers and Bogy (1958) and records all grain

boundaries encountered along a group of parallel lines through a rock. Allowance is made for grains or grain boundaries that are intersected more than once. The area sampling method involves counting all the grains and boundaries in a selected area of a thin-section. He realized that the first method may be biased in favour of minerals that occur as coarser grains, while the second method is difficult to use unless a drawing is made of the rock section.

Agterberg (1967) described a method which may be used to characterize the spatial distribution of minerals in crystalline rocks. The method, which makes use of power spectrum analysis, was applied to two specimens of gabbro from the Muskox Intrusion, and appears to be especially useful in detecting faint layering or other types of periodicity in the arrangement of minerals in rocks.

Vistelius (1966) considered the problem of the origin of the Mt. Belaya granodiorite by examining the distribution of minerals within samples of the rock body. His method of obtaining data is similar to the line-sampling method described above, and his observations were presented in matrix form (transition matrix). Vistelius considered the sequence of crystals recorded along a line through the rocks in terms of the theory of Markov chains; and he concluded from his study that the observed patterns of crystals in the Mt. Belaya granodiorite are consistent with patterns

expected to be produced by magmatic crystallization. In a recent study (1972, p518-519) he defined ideal granites as those in which the sequence of crystal contacts have simple markovian properties, and suggested that metasomatism will produce grain contact sequences which are Markov chains of the second and higher orders. This was supported by Romanova (1972, p517) in a study of the effect of greisenization on the grain sequence in granitic rocks.

Kretz in 1969 (p39-65) carried out tests for homogeneity and randomness in the spatial distribution of crystals in a metamorphic rock and described various methods that may be used for minerals present in major and minor amounts. An area of a thin-section of a pyroxene-scapolite-sphene granulite from Quebec was tested for homogeneity by dividing the area into quarters and determining the mineral proportions in each quarter. The line sampling (line-transect) method, similar to that used by Vistelius (1966) was applied to a homogeneous portion of the thin-section. This study showed that pyroxene and scapolite are evidently distributed at random; and led to the conclusion that the nucleation sites for the minerals were randomly determined and were independent of other crystals in the neighbourhood.

From the study of a suite of gneisses from Shetland and Siberia, Flinn (1969) concluded that the minerals are not randomly distributed but are arranged so that grain contacts between unlike phases occur more frequently than

expected on the basis of randomness. He suggested that interfacial energy between unlike crystals is less than that between like crystals, and that interfacial energy has been responsible for the observed distribution.

R. Kretz and his students have found many such distributions; the results have not been published.

In the present study the method of Vistelius is applied to a suite of rocks from the Adirondacks. This will be referred to as the "line transect method". According to this method, the sequence of crystals encountered along a linear traverse through a rock is considered in relation to the theory of Markov chains. In a random arrangement of crystals, the probability of encountering a crystal of mineral A will depend only on the frequency of occurrence of crystals of A in the traverse as a whole, and will be independent of the nature of the preceding crystal, whether A or some other mineral. Thus in an aggregate of crystals of A and B:

$$p(A/B) = p(A)$$

$$p(A/A) = p(A)$$

where $p(A/B)$ is the probability of moving from a crystal of B to one of A, and $p(A/A)$ is the probability of moving from a crystal of A to another of A. Also, $p(A)$ is the probability of encountering A in the whole traverse, for example if, altogether, the traverse passed over 400 crystals of A and 600 of B, $p(A)$ would be $400/1000=0.4$. The above is the model

of randomness that will be employed in the present study. A two-dimensional picture of this model was illustrated by Kretz (1969).

Two kinds of departure from the random model are immediately apparent. Firstly, if $p(A/A) > p(A)$, a tendency toward clustering of A, beyond that expected in a random distribution, would be anticipated, and secondly, if $p(A/B) > p(A)$, crystals of A and B would be inferred to be more strongly associated than in a random distribution.

The chi square test may be used to decide if the random model is accepted or rejected.

The rocks of the present study appear to be homogeneous in hand specimens. In the majority of the thin-sections, grain apparent diameters vary between 0.2 and 1.5 mm, excluding some very fine-grained inclusions. In sample J-92, which is somewhat coarser, grain size ranges from 0.2 to 3 mm.

A standard thin-section was cut from each of the rocks, in a random direction. Modal analyses and mineral assemblages of the rocks are shown in Table 1. The phases considered are total feldspar (F=plagioclase ± K-feldspar), orthopyroxene (H), clinopyroxene (C), amphibole (A), garnet (G), opaque minerals (D=ilmenite ± magnetite ± pyrite ± pyrrhotite), and all other minor phases (O=biotite ± quartz ± apatite ± zircon ± calcite).

The present study will concentrate on the spatial distribution of total feldspar, the two pyroxenes and amphibole. The distribution of garnet and opaque minerals will not be considered in detail, for grain boundaries between two garnet crystals and two crystals of opaque minerals could not be seen under the polarizing microscope and were not recorded. Also, the distribution of biotite, quartz, apatite, zircon and calcite will not be considered.

Measurements were carried out with a Zeiss research microscope equipped with a moving stage. The number of transitions measured ranged from 500 to 987, averaging 768.5 measurements per thin-section. Analysis of grain transitions based on chi square test was performed by a Fortran IV computer program (Appendix II) using an IBM 360/65 computer at the Computing Centre, University of Ottawa.

Spatial Distribution as a Function of Interfacial Free Energy

The role of interfacial free energy (f) in aggregates of crystals has been discussed by Smith (1948), DeVore (1956, 1959), Kretz (1966b), Swalin (1962, p180-213), Gurland (1968), Spry (1969, p25-29) and Flinn (1969). Smith (1948, p18-21), Sinnott (1958, p272-273) and Swalin (1962, p213) report that in annealed metals, the interface between like phases (i.e. two crystals of the same metal) have a higher interfacial free energy than those between unlike

phases, and DeVore (1959, p216-217) and Flinn (1969) suggested that this may also be true for silicates. Thus a rock in which the crystals are randomly distributed may tend to recrystallize to increase the proportion of unlike grain contacts and decrease the proportion of like grain contacts, thereby decreasing its total interfacial free energy.

The specific interfacial free energy for an interface between phases α and β is the Helmholtz free energy associated with unit area of interface and was defined by Johnson (1959) as follows:

$$f = \frac{F^S}{\Omega} = \frac{F - F^\alpha - F^\beta}{\Omega} \quad (1)$$

where F is the total Helmholtz free energy of a system that contains phase α , phase β , and an α - β interface.

F^α is the bulk Helmholtz free energy of phase α .

F^β is the bulk Helmholtz free energy of phase β .

F^S is the total interfacial free energy.

Ω is the interfacial area.

Similarly, interfacial free energy may be defined as the Gibb's free energy (G) associated with interface:

$$f = \frac{G^S}{\Omega} = \frac{G - G^\alpha - G^\beta}{\Omega} \quad (2)$$

Thus

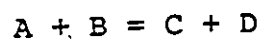
$$F^S = \sum (f^{\alpha\alpha} \Omega^{\alpha\alpha}) + \sum (f^{\beta\beta} \Omega^{\beta\beta}) + \sum (f^{\alpha\beta} \Omega^{\alpha\beta}) \quad (3)$$

Notice that the total interfacial free energy in unit volume of rock may decrease by decreasing one or all of the terms in Ω , i.e. by increasing grain size. Also, it may decrease by decreasing $(\Omega^{\alpha\alpha} + \Omega^{\beta\beta})$ and increasing $\Omega^{\alpha\beta}$, by the same amount, provided $2f^{\alpha\beta} < (f^{\alpha\alpha} + f^{\beta\beta})$ or by decreasing $\Omega^{\alpha\beta}$, and increasing $(\Omega^{\alpha\alpha} + \Omega^{\beta\beta})$ by the same amount, provided $2f^{\alpha\beta} > (f^{\alpha\alpha} + f^{\beta\beta})$. This latter decrease in energy, although small in magnitude could be achieved by a rearrangement of crystals in the rock, or by the initial nucleation and growth of crystals, during metamorphism, at sites which would produce, preferentially, interfaces of relatively low energy.

Other factors that are likely to affect the spatial distribution of crystals in rocks insofar as they affect interfacial free energy are: temperature, pressure, composition, partial pressure of vapour phase and compressional or shear stress. While the effects of temperature (Bonie and Derge, 1956; Smith, 1948) and composition (DeVore, 1955, 1956, 1959; Johnson, 1959) are small, the roles of the other factors are relatively unknown. However, their effects on the relatively dry and high grade rocks studied are unlikely to be large.

Effect of Chemical Reactions on Spatial Distribution

Metamorphic crystallization of rocks is brought about by one or more chemical reactions, leading to the formation of new phases. Consider for example a reaction



where A, B, C, and D are minerals. If the reaction between crystals A and B has gone to completion, crystals of the stable products, C and D, may show tendency to occur close to each other in the rock. At univariant equilibrium one may find all four minerals closely associated in a rock. Therefore, the position occupied by crystals of one mineral may depend on the distribution of crystals of other minerals, and this dependence may show up, even if weakly developed, by a statistical study of the kind and frequency of grain contacts found in the rock. Thus mineral associations may appear for reasons other than those involving interfacial free energy.

Procedure

The mineral assemblage of a rock is a list of all the minerals present, and the first order transition ideally records the frequency of transitions or grain contacts for all of these minerals. The data may be expressed in matrix form (a transition matrix) and may be discussed in relation to the theory of Markov chains (Anderson and Goodman, 1957, p89-99; Agterberg, 1966, p764-765; Kretz, 1969, p58-59; Vistelius, 1966, p48-50). From this first order transition matrix a series of other transition matrices may be obtained through a procedure of combining two or more 'phases' at a time. This procedure is similar to the combining or lumping of states by Kemeny and Snell (1960, p123-125). The group of matrices will be referred to, in short, as a 'transition series'.

In the following the term 'order' is employed to designate one of a group of transition matrices derived from an original transition matrix. It bears no relation to 'powering', which is commonly used in the study of stochastic processes (e.g. Anderson and Goodman, 1957, p89-110; Parzen, 1962, p191-192; Vistelius, 1966, p48-50).

The first order transition matrix need not contain all the minerals of a rock, and one may lump together several minerals that occur in small amounts, thus arriving at a number of 'phases' in the first order transition matrix that will be less than the number of minerals in the rock. The set of transition matrices derived therefrom will be called the 2nd order transition matrix, the 3rd order transition matrix, and so on.

Several types of spatial distribution studies may be carried out, namely:

1. The spatial distribution of all mineral phases - the gross pattern.
2. The spatial distribution of all major phases in the rock.
3. The spatial distribution of minor phases in the rock.
4. The preferred associations of two unlike phases.
5. The preferred associations of three or more different kinds of phases, here called a 'complex'.

6. The clustering of crystals of a phase.
7. The spatial distribution of units consisting of two unlike crystals in the rock.
8. The spatial distribution of complexes.

For the distribution of minor phases the nearest-neighbour method (Clark and Evans, 1954; Kretz, 1966a, 1969) and the random-point method (Moore, 1954; Kendall and Moran, 1963; Kretz, 1969) would be more appropriate than the line-transect method (Vistelius, 1966; Kretz, 1969) used in the present study.

The present study will focus on types 4, 6 and 7 above with brief consideration of 1 and 2.

Models for Spatial Distribution of Minerals in Rocks

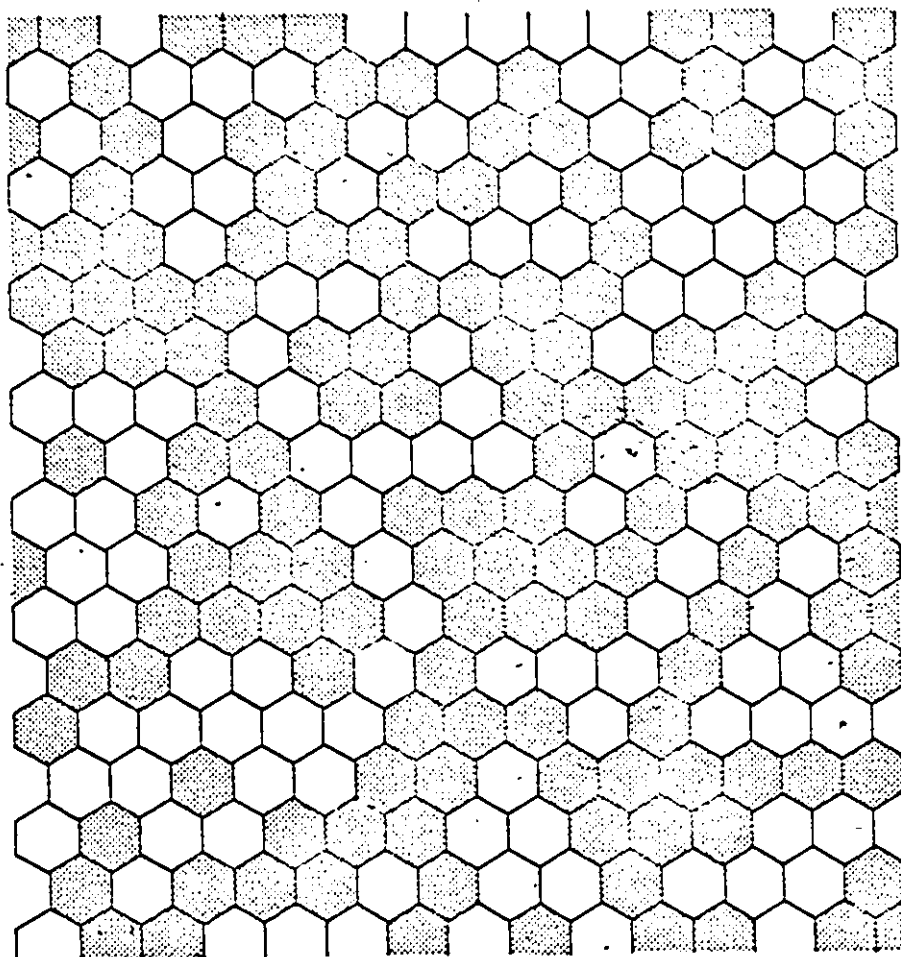
In a rock composed of several minerals, a nearly infinite number of possibilities exist for the arrangement of crystals in the rock, provided that the volume is sufficiently large to contain several thousands of crystals. In a consideration of this problem, a random distribution of crystals would appear to offer a convenient point of departure. Although a random distribution of points in space may be readily characterized, and utilized in the study of 'minor' minerals in a rock (Kretz, 1969) no adequate definition appears to exist for the distribution of many small volumes (crystals) in space. The best one can do at present is to

construct a model in which all the small volumes have the same size and shape. These can then be arranged in a random sequence, thus building up a 'rock' in which the crystals are randomly distributed. A two-dimensional analogue of such a model is shown in Fig. 3. Notice that a certain amount of clustering of crystals is an integral part of a random distribution. Notice also that the distribution may be described in terms of like and unlike contacts. A traverse across this model would produce a random sequence of crystals and crystal transitions, in agreement with the 'line-transect method' of testing for randomness.

A regular distribution may be defined as a distribution in which the crystals are more uniformly or widely distributed than in a random distribution. In terms of the simple model of Fig. 3, this would result in a larger number of unlike contacts, i.e. a greater tendency for unlike crystals to be associated with each other. In a traverse through such a distribution, the probability of encountering a crystal of a particular mineral would depend on the nature of the preceding crystal, and the 'chain' of observations would possess Markovian properties.

In a rock composed of several minerals, a great variation is possible, such that some may be apparently random while others are non-random. For example in a rock composed of minerals A, B, C, and D, A and B may be associated more frequently than expected, i.e. A and B form a two-

Figure 3. A two-dimensional analogue of randomness model
in the form of a random mosaic (After Kretz, 1969)



phase association while C and D may be distributed randomly. Should A, B, and C be associated, i.e. form a complex, the distribution may nevertheless be dealt with in terms of a number of two-phase associations. Additional variation may be introduced by the possibility that a particular two-phase association may itself be regular or randomly distributed in the rock volume.

A clustered distribution is here defined as an aggregation of crystals of the same phase, beyond that found in a random distribution (Fig. 3). It also possesses Markovian properties. Several possibilities arise, for example, clusters of crystals of mineral A may be regularly associated with those of another mineral B, thus producing many A-A contacts and many A-B contacts. The clusters themselves may or may not be randomly distributed. The case in which clusters are dispersed will not be considered since it would require an entirely different method of assessing the degree of dispersion (Gruener, 1965; Gurland, 1968, p281).

The present study attempts to obtain information on the distribution of crystals in rocks by use of the line-transect method and with the help of the above models. After observing and recording all crystal-crystal transitions, the number of all kinds of transitions expected (based on the model of randomness) are compared with the number observed by use of the chi square test. If the calculated or measured chi square exceeds the chi square at the 95% level of signifi-

cance and with the appropriate degrees of freedom (the expected chi square) the model of randomness is rejected.

Initially, two questions may be added: (i) How are crystals of a particular mineral (e.g. A) distributed, and (ii) is there any preferred association between any two minerals (e.g. A and B).

(i) Spatial distribution of crystals of a particular phase

The spatial distribution of crystals of phase A in a rock composed of A and other minerals (B, C, D), where these are designated O, is evaluated as follows. If the measured chi square is less than the expected chi square the distribution of crystals of A is considered to be random (R), regardless if the observed transitions of AA are greater than, equal to, or less than the expected values (the probability of the observed transitions of AA for these three cases is the same* - Agterberg, 1973, personal communication). If the measured chi square is greater than the expected value, the distribution of A is considered to be non-random. If the number of AA transitions is less than expected, A is anti-clustered (AC), and if the number of AA transitions is greater than expected, A is clustered (C). Distributions of crystals of B, C and D may be determined in the same way.

(ii) Association of unlike phases

The association of two unlike phases (e.g. A and B) in a rock composed of A, B and O = (C + D) is evaluated as

* Two equal probabilities, both 0.5, are for the cases (1) greater than, and (2) less than.

follows. If the measured chi square is less than the expected value, regardless if the measured transitions of AB are greater, equal, or less than expected, the distribution of A and B in the rock is taken to be random. If the measured chi square is greater than expected, the distribution of A and B is not random. Now, if the number of AB transitions is less than expected, the distribution with regard to A and B is referred to as anti-regular (ARg), and if the number of AB transitions is greater than expected, i.e. A and B are preferentially associated, the distribution with regard to A and B is referred to as regular (Rg). Distributions of AC, AD, BC, BD and CD in the rock may be determined in the same way.

The above may be summarized as follows:

(i) Distribution of a particular phase
(A-O Type)

- | | | | |
|----|---------------------------|---|---------------------|
| 1. | $\sum X_m^2 < X^2_{0.95}$ | T < E or T > E
(e.g. $T_{AA} < E_{AA}$) | Random (R) |
| 2. | $\sum X_m^2 > X^2_{0.95}$ | T < E
(e.g. $T_{AA} < E_{AA}$) | Anti-clustered (AC) |
| 3. | $\sum X_m^2 > X^2_{0.95}$ | T > E
(e.g. $T_{AA} > E_{AA}$) | Clustered (C) |

(ii) Association of unlike phases
(A-B-O Type)

4. $\sum x_m^2 < x_{0.95}^2$

T < E or T > E

Random (R)

(e.g. $T_{AB} < E_{AB}$)

5. $\sum x_m^2 > x_{0.95}^2$

T < E

Anti-Regular (ARg)

(e.g. $T_{AB} < E_{AB}$)

6. $\sum x_m^2 > x_{0.95}^2$

T > E

Regular (Rg)

(e.g. $T_{AB} > E_{AB}$)

where T = observed transition

E = expected transition

A, B = minerals of interest

O = all other minerals, considered collectively

x_m^2 = 'measured' chi square

$x_{0.95}^2$ = chi square at the 95% confidence level

IV SPATIAL DISTRIBUTION OF CRYSTALS IN CHARNOCKITIC GRANULITES FROM THE ADIRONDACK MOUNTAINS

General Statement

In the rocks of the present study, crystals are nearly equidimensional, retrograde effects are minimal, and grain contacts are clearly defined. However, contacts between grains of garnet and opaque minerals could not be recognized, and the distribution of these minerals was therefore not studied in detail. All minor phases are grouped as 'others'.

The following sections deal first with the question of homogeneity, and then with details in the distribution of pyroxenes, amphibole and feldspar.

Homogeneity

Since all of the eleven specimens studied appear to be homogeneous in hand specimens and under the microscope, tests for homogeneity were carried out on only five samples. These samples, which were chosen at random are J-35, J-44, J-50, J-92 and J-106. Standard-size thin-sections were cut for each rock in a random plane where foliation is lacking and perpendicular to the foliation where it is present. The point-sample method described by Kretz (1969, p45-47) was used to test for homogeneity. The crystal density method (Kretz, 1969, p41-42) was used on J-35 and J-44 to check the results.

Using the point-sample method, a rectangular area measuring 15mm x 20mm on each thin section was divided into four quarters, and the mineral proportion in each quarter were determined by the point-count method. The points were distributed as shown in Fig. 4. The chi square test was then used to determine if the variation found may or may not be attributed to chance, i.e. whether or not the model of homogeneity may be accepted. For the homogeneity test, 252 to 337 points and an average of 307 points were counted per thin-section. Results for the distribution of feldspar(F), orthopyroxene(H), clinopyroxene(C), amphibole(A), garnet(G), opaque minerals(D) and remaining minerals(O), in these rocks are as follows:

J-35 Homogeneous, since $\Sigma \chi_m^2 = 5.04 < \chi_{0.95}^2 (v=12) = 21.03$

J-44 " " $\Sigma \chi_m^2 = 16.38 < \chi_{0.95}^2 (v=12) = 21.03$

J-50 Not homogeneous, since $\Sigma \chi_m^2 = 27.79 > \chi_{0.95}^2 (v=15) = 25.00$

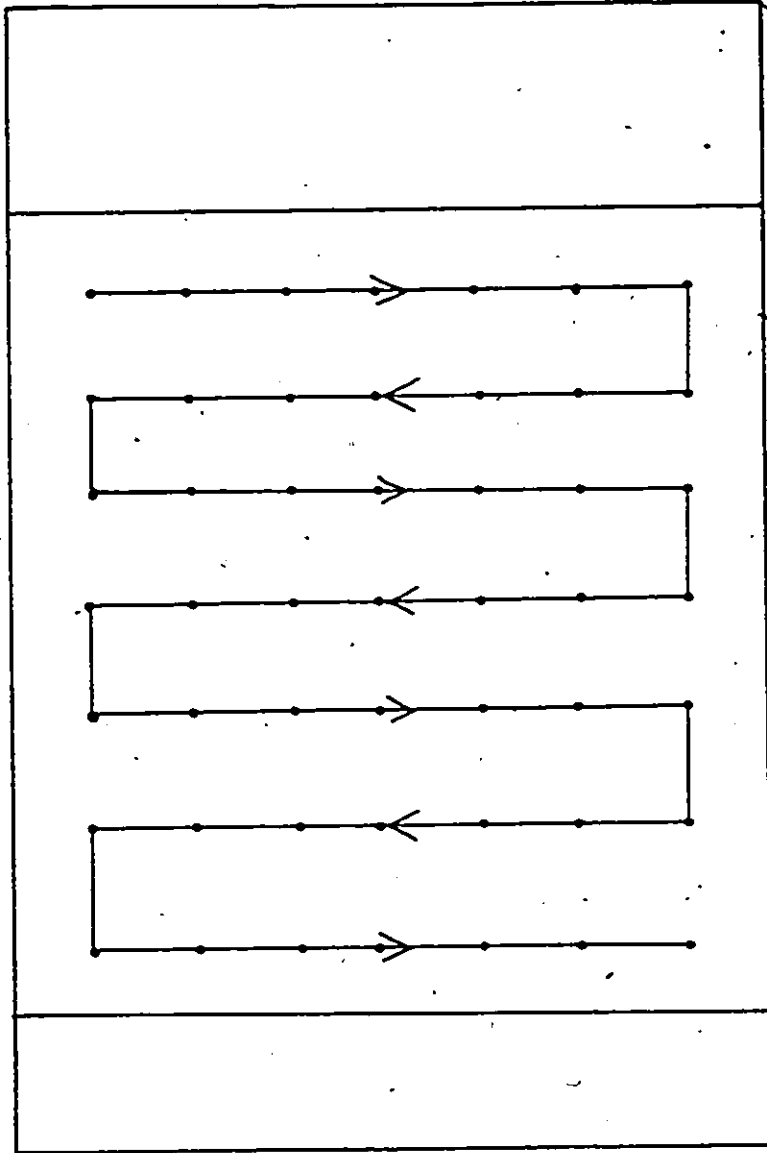
J-92 Homogeneous, since $\Sigma \chi_m^2 = 12.13 < \chi_{0.95}^2 (v=9) = 16.92$

J-106 " " $\Sigma \chi_m^2 = 16.28 < \chi_{0.95}^2 (v=15) = 25.00$

where χ_m^2 is the calculated chi square and v is the number of degrees of freedom.

Evidently sample J-50 is nearly homogeneous, or slightly heterogeneous, since χ_m^2 is very close to $\chi_{0.95}^2$. The results show that the rocks examined and probably the others as well are homogeneous or very nearly so with respect to all the minerals for which measurements were obtained.

Figure 4. A sketch to show the point-sample and line-transect methods of spatial distribution measurements of crystals in thin-sections. The point-sample method locates grains under a point system whereas the line-transect method measures the grain contacts along parallel lines.



Spatial Distribution - The Overall Pattern

Tests for randomness in the distribution of crystals in the set of samples described above were carried out by use of the line-transect method (Kretz, 1969, p58-61). All crystal-crystal contacts that were encountered along a linear traverse of the kind shown in Fig. 4 were recorded, and an average of 770 such measurements were made per thin-section. An example is given in Appendix III and the data are shown in Appendix IV. The frequency of the different kind of contacts was then compared to the frequencies that would be expected if the crystals were randomly distributed, by use of the chi square test, giving the following results

J-35	Not random,	since	$\Sigma \chi_m^2 = 62.36 > \chi_{0.95}^2 (v=25) = 37.65$
J-44	"	"	" $\Sigma \chi_m^2 = 133.83 > \chi_{0.95}^2 (v=25) = 37.65$
J-50	"	"	" $\Sigma \chi_m^2 = 118.84 > \chi_{0.95}^2 (v=36) = 51.00$
J-92	"	"	" $\Sigma \chi_m^2 = 60.83 > \chi_{0.95}^2 (v=25) = 37.65$
J-106	"	"	" $\Sigma \chi_m^2 = 44.18 > \chi_{0.95}^2 (v=25) = 37.65$

The above results indicate that with reference to all the minerals that were considered, none of the rocks has passed the particular test for randomness that was adopted.

The above information refers only to the 1st order transition matrix. The transition series must be considered before the distribution of crystals in a rock can be char-

acterized in detail. These aspects of the spatial distribution of crystals in rocks are now considered.

Spatial Distribution of Pyroxenes,
Amphibole and Feldspar

The 1st order observed and expected transition matrices together with the condensed transition series of the eleven rocks under investigation are shown in Appendices IV and V. χ^2 values were taken from Owen (1962). The spatial distribution of crystals in each of the rocks is represented by two transition series. Transition series I is composed of multiphase and two-phase transitions in matrix form, whereas transition series II consists mainly of two-phase transitions, also in matrix form.

These data show that in rocks containing garnet (G) and opaque minerals (D) the low-order transitions (1st, 2nd and 3rd orders) invariably show non-random distributions. By successively eliminating garnet and opaque minerals, as shown by series I, it is found that garnet and opaques consistently cause other minerals to appear to depart from a random distribution. A similar effect, produced by feldspar and pyroxenes was noticed in some rocks (e.g. samples J-44, J-50, J-66 and J-99 of transition series I, Appendix V). A careful examination of the results has revealed that minerals that are not distributed at random may affect the distribution of other minerals in the direction of departing from randomness, as shown in Appendices IV and V.

In view of a more recently developed chi square test (Anderson and Goodman, 1957, p97-101; Krumbein, 1967, p8) and the possibility that it may take the place of the conventional chi square test when class expectations are small (Fisher, 1950, p24; Kullback, 1959, p119), chi square values for two by two transition matrices of some of the present samples were recalculated using this newer method. The new chi square test gives a set of statistics of the form

$$\chi^2_{(m-1)^2} = 2 \sum_{ij}^m n_{ij} \log_e (\hat{P}_{ij} / \hat{P}_j) \quad (4)$$

where n_{ij} is the component value of the ij -th cell in the transition matrix,

\hat{P}_{ij} is the transition probability in the same cell,

\hat{P}_j is the marginal probability for the column of the matrix,

m is the number of states

$(m-1)^2$ is the degrees of freedom.

Using equation (4), it is found that when the expected number of transitions between two crystals in a matrix is less than 3 or 4, the chi square value obtained by the new method differs considerably from that of the conventional chi square test (by more than 2 orders of magnitude). However, when expected transitions are greater than 3 or 4, results by the two chi square methods are similar.

The spatial distributions of pyroxenes, amphibole and feldspar in the examined charnockitic granulites may be summarized from the data given in Appendices IV and V in the form of a table (Table 4). It is evident from Table 4 that crystals of pyroxenes, amphibole and feldspar are generally distributed in a random, anti-regular or regular manner, and feldspar is commonly clustered. Crystals of clinopyroxene are anti-clustered in two rocks; crystals of orthopyroxene are clustered in one rock, and crystals of feldspar in seven. The observed patterns of spatial distribution are more complex than was expected when the study was initiated. An interpretation of the data will now be presented.

Interpretation

The data of the present study, as presented in Appendices IV and V, show that all the 1st order transition matrices of the rocks studied indicate a gross pattern of non-random distribution. Although this implies the existence of some regular and/or clustered crystals, the 1st order transition is certainly not sensitive enough to detect details in the spatial distribution pattern. Detailed information can be obtained by studying the transition series.

As noted above,⁶ grain boundaries between two garnet crystals and between two crystals of opaque minerals are not readily detectable by use of the petrographic microscope.

Table 4 Summary of spatial distribution of orthopyroxenes (H), clinopyroxenes (C), amphiboles (A) and feldspars (F) in charnockitic granulites from the Adirondack Mts., N.Y.

Spatial Distribution Sp.No.	Random	-Regular	Anti-regular	Cluster	Anti-cluster
J-35	H ¹ , A ¹ , F ¹ FH, HA ¹	FC ¹ , FA, HC ¹	CA ¹		C
J-44	H, A ¹ , C ¹ HC ¹ , HA ¹ , CA ¹		FH, FC, FA	F	
J-50	H ¹ , A, C ¹ HC ¹ , HA ¹ , CA ^s		FH ^s , FC, FA	F	
J-63A	H ¹ , C HC		FH, FC	F ^s	
J-66	H, C, F ^s FH, FC ^s	HC			
J-80	H, A, C HA ^s , CA	HC	FH, FC, FA ^s ,	F	
J-81	C	HC ^s	FH, FC	H, F	
J-92	H ¹ , A ¹ , C ¹ HC ¹ , HA ¹ , CA ¹		FH, FC ^s , FA ¹	F	
J-99	A, F, CA	FA	FC ^s		C
J-103	H, A ¹ , C ¹ HC, HA ¹ , CA ¹	FA ^s	FH, FC	F	
J-106	H, A ¹ , C ^s , F FH, FC, FA, HC, HA ¹ , CA				

Superscripts s = similar values of chi squares and/or observed and expected transitions
 1 = very low values of observed and expected transitions
 e.g. less than 4 or 5

Determination of whether such minerals are clustered or not is impossible without the aid of other techniques such as ore microscopy. Like transitions of such minerals, as a result, are always zero while the expected frequencies are always greater than zero. Therefore, the presence of such minerals in a matrix would invariably increase the total chi square of the matrix and cause the spatial distribution of all the minerals to appear to depart from randomness. Since the amount of garnet and opaque minerals is small, the above effect is assumed to be negligibly small.

From Table-4 it is obvious that the majority of the spatial distributions are of the random type, while the anti-clustered type is the least common. An order in terms of decreasing frequency of occurrence may be established as follows:

$$R > ARg > C > Rg > AC$$

where R = random, ARg = anti-regular, Rg = regular, C = clustered, and AC = anti-clustered.

Furthermore Table 4 indicates that while transitions or contacts between like phases of amphibole (A), clinopyroxene (C), and orthopyroxene (H) occur as frequently as expected, transitions between crystals of feldspar (F) occur more frequently than expected. This is clearly shown in Table 4a. This table also shows that transitions between unlike phases H and C in about half of the rocks occur more frequently than expected, and transitions between H and F

Table 4a. Type and frequency of spatial distribution of feldspar (F), amphibole (A), orthopyroxene (H) and clinopyroxene (C) in the charnockitic granulites from the Adirondack Mts., N.Y.

	Number of Rock Specimens			Interpretation
	<u>Fewer than expected</u> Anti-cluster	<u>As many as expected</u> Random	<u>More than expected</u> Cluster	
HH	0	9	1	-
CC	2	9	0	-
AA	0	8	0	-
FF	0	4	7	f ^{FF} small
	Anti-regular	Random	Regular	
HC	0	6	4	f ^{HC} small
HA	0	7	0	-
HF	7	3	0	f ^{HF} large
CA	1	7	0	-
CF	8	1	1	f ^{CF} large
AF	4	1	3	-

where f is the interfacial free energy

and, between C and F in most of the rocks occur less frequently than expected. These results suggest to the writer that during metamorphism crystals of feldspar, amphibole and pyroxenes took up positions in the rock such that grain boundaries of like crystals of feldspar (which are mostly plagioclase) and unlike crystals of pyroxenes increased in proportion while those of unlike crystals of orthopyroxene and feldspar and, clinopyroxene and feldspar decreased in proportion, thereby reducing the interfacial free energy of the rock as a whole. This interpretation is based on the fundamental concept of interfacial free energy and on the assumption that such energy may play a part in determining the distribution of crystals in multi-phase systems. Although in metals, interfacial free energy between unlike crystals is generally lower than between like crystals (Bonie and Derge, 1956; Sinnott, 1958; Smith, 1948, 1952; Swalin, 1962; Gurland, 1968), no experimental information is available for silicates, and these may behave differently.

The results of the present study suggest that the interfacial free energy of grain contacts vary with type of phases. In the case of AA, HH and CC, although the interfacial free energies f_{AA} , f_{HH} and f_{CC} may not all be the same, they are generally higher than that of f_{AH} , f_{AC} and f_{HC} whereas in the case of FF or HC, the interfacial free energy f_{FF} would be less than f_{FA} , f_{FH} , f_{FC} , and that f_{HC} less than f_{HA} , f_{CA} , f_{CF} and f_{AF} . The following scheme may be derived from Table 4a:

$$(f^{CF}, f^{HF}) > (f^{HA}, f^{CA}, f^{AF}) > f^{HC}$$

$$(f^{HH}, f^{CC}, f^{AA}) > f^{FF}$$

and possibly

$$(f^{HH}, f^{CC}, f^{AA}) > (f^{FA}, f^{FH}, f^{FC}) > f^{FF}$$

Alternatively, the following relationships may be established in a rock with regard to the types of spatial distribution:

(1) For like crystals of feldspar

$$(\Sigma f)^{AC} > (\Sigma f)^R > (\Sigma f)^C$$

(2) For unlike crystals of feldspar, amphibole and pyroxenes

$$(\Sigma f)^{ARg} > (\Sigma f)^R > (\Sigma f)^Rg$$

We may define the condition for equilibrium in a system as follows:

$$\Delta F^{total} = \Delta F + \Delta(\Sigma f) + \Delta F_s = 0 \quad (5)$$

$$\Delta G^{total} = \Delta G + \Delta(\Sigma f) + \Delta F_s = 0 \quad (6)$$

where ΔF and ΔG are Helmholtz and Gibb's free energy change respectively, $\Delta(\Sigma f)$ is the interfacial free energy change and ΔF_s the strain energy change of solids. Thus defined, Σf and F_s of the solids cannot be ignored. However, under high temperature, pressure, and very low shear stress conditions as in high grade metamorphism, the strain energy of solids (Bikerman, 1959, p1658) may be negligible. This leaves two important terms ΔF (or ΔG) and $\Delta(\Sigma f)$.

Surface or interfacial free energy is usually a small portion of the total free energy of the system.

"From the data of Jura and Gurland (1952, p6033-6044) the surface free energy of MgO is 1000 ergs/cm² at 298°K, as determined by the heat of solution difference between fine and coarse particles. For an area of 3.48x10⁷cm²/mole, for the fine particles, the surface free energy results in an additional energy of 0.831 Kcal/mole and additional entropy of 70 cal deg⁻¹mole⁻¹. These values when compared to the heat of formation of MgO of 145.76 Kcal/mole and entropy of 1.952 Kcal deg⁻¹mole⁻¹ at 298°K, are small contributions to the total free energy" (DeVore, 1959, p212-213). However, such small values of surface or interfacial free energy could nevertheless play a dominant role during nucleation, crystal growth, exsolution, replacement, and diffusion transfer - processes that largely involve surfaces and interfacial phenomena (DeVore, 1959) and therefore should not be ignored when total equilibrium in a system is considered.

Now, if different types of spatial distributions occur in a system, for example clustered and random, or random and regular, the system is not in total equilibrium even when ΔG or $\Delta F=0$, since $\Delta(\Sigma f) \neq 0$.

Results of the present study have demonstrated that all three major types of spatial distribution may occur in a rock. Since this occurs frequently, although in most of the rocks there are two instead of all three types, such

mixing of different kinds of spatial distribution is evidently the rule rather than the exception. This implies that ideal cases of random, regular or clustered distribution of crystals in natural rocks is rare, and that in these rocks total interfacial free energy is rarely minimized.

Plutonic and high grade regional metamorphic rocks that crystallize slowly, and in the absence of shear stress may be expected to reduce their interfacial free energy and acquire particular distribution of crystals. Low grade metamorphic rocks, which may be subjected to high stress, might be expected to show more variation. Extreme clustering might be produced for example by breaking up a large crystal into a number of small crystals, due to the application of shear stress. In rocks that depart from equilibrium with regard to bulk free energy, the probability of encountering clustered distribution of phases might also be greater.

It is difficult to determine if the observed distribution of minerals was formed while the mineral-forming reaction took place, as the result of preferred nucleation and growth, or whether they are largely a consequence of readjustments and rearrangements that took place during the subsequent annealing of the rocks. The selection of a nucleation site may itself be dependent on interfacial free energy, and some two-phase association may be the result of the preferred nucleation of one phase on another.

Regardless of the mechanism involved, it appears that some

of the study rocks represent a lower energy level (with regard to interfacial free energy) than others. Another, entirely different interpretation of the results is possible. This supposes that the present crystal distribution is a consequence of the particular mineral-forming chemical reaction that took place. For instance a two-phase association involving minerals A and B may have formed in a rock because A and B are both products of a particular reaction. However, since crystals of feldspar, garnet, and opaque minerals were not distinguished under the microscope, evaluation of this aspect would be rather premature.

PART 3

ION EXCHANGE EQUILIBRIA

V CHEMICAL COMPOSITION OF COEXISTING
FERROMAGNESIAN MINERALS

General Statement

In order to understand the chemical processes that take place during the crystallization of multi-phase high-grade metamorphic rocks such as the charnockitic granulites of the present study, information on the equilibrium characteristics of the rocks must be determined. Such information may be obtained by careful study of the chemical composition of the constituent mineral phases.

In Part 3 of this thesis, the chemical composition of the phases orthopyroxene, clinopyroxene, amphibole, garnet, biotite, magnetite, and ilmenite are presented. These data are then used for the detailed consideration of ion exchange equilibrium between coexisting phases. In Part 4, the overall phase equilibrium and petrogenesis of the study rocks are examined.

Chemical Composition of Pyroxenes, Amphibole,
Garnet, Biotite, Magnetite, and Ilmenite

Chemical analyses of orthopyroxene, clinopyroxene, amphibole, garnet, and one biotite from the rocks that were selected for detailed study are shown in Tables 5 to 9 respectively. The orthopyroxenes vary between ferrohypersthene and orthoferrosilite and are mostly eulite in

composition (cf. Deer et al., 1962, V2, p19-22). The clinopyroxenes are mainly ferrosalite (cf. Deer et al., 1962, V2, p52-53). The amphiboles vary in composition between hornblende and ferrohastingsite and are mostly hastingsite (cf. Deer et al., 1962, V2, p278-291). Since H₂O was not determined, the amphibole formulae have been calculated on the basis of 23 oxygen ions. The garnets are all iron-rich almandines (cf. Deer et al., 1962, V1, p86-87) and the biotite appears to be a high TiO₂ and low Al₂O₃ and CaO variety (cf. Deer et al., 1962, V3, p58-60). Since H₂O was not analyzed, the biotite formula has been calculated on the basis of 22 oxygen ions. Chemical composition (major elements only) of magnetites and ilmenites are shown in Table 10. These iron oxides are mainly present as ilmenite and magnetite solid solutions.

Table 5 Chemical compositions of Orthopyroxene from charnockitic granulites from the Adirondack Mts., N.Y. together with calculated formulae.

		ORTHOPIYROXENES										
SP	NO	J-35	J-44	J-66	J-80	J-81	J-103	J-105B	J-106	AV		
OXIDES		48.92	46.50	48.14	46.80	47.75	47.82	46.56	47.13	47.45		
SiO ₂		0.67	0.44	0.64	0.91	0.89	0.57	0.51	0.67	0.66		
Al ₂ O ₃		0.09	0.11	0.00	0.06	0.12	0.10	0.08	0.09	0.08		
TiO ₂		0.43	0.92	3.25	1.35	0.24	0.80	2.30	2.10	1.51		
Fe ₂ O ₃		36.00	42.05	33.44	33.89	33.87	39.70	39.37	38.36	37.09		
FeO		11.53	6.57	14.71	13.81	14.59	9.41	9.21	9.23	11.13		
MgO		0.49	1.16	0.32	0.49	0.38	1.04	0.90	0.99	0.72		
MnO		1.53	1.58	1.03	1.15	1.54	1.69	1.70	1.70	1.49		
CaO		0.06	0.05	0.07	0.03	0.06	0.07	0.07	0.07	0.06		
H ₂ O		0.04	0.03	0.05	0.01	0.03	0.08	0.06	0.09	0.05		
K ₂ O		99.76	99.41	101.65	98.50	99.47	101.28	100.76	100.43	100.24		

$Pa = (X_{Fe^{2+}}) \times 100 = 63.7$ 78.2 56.1 57.3 56.6 70.3 70.6 70.0

Number of ions on the basis of 6 oxygens

	J-35	J-44	J-66	J-80	J-81	J-103	J-105B	J-106
Si	1.969	1.955	1.895	1.900	1.915	1.942	1.912	1.929
(Al) T	0.031	0.022	0.030	0.044	0.042	0.027	0.025	0.032
(Ti) T	0.0	0.004	0.0	0.002	0.004	0.003	0.003	0.003
(Fe ³⁺) T	0.0	0.019	0.076	0.041	0.007	0.025	0.061	0.036
(Al) O	0.001	0.0	0.0	0.0	0.0	0.0	0.0	0.0
(Ti) O	0.003	0.0	0.0	0.0	0.0	0.0	0.0	0.0
(Fe ³⁺) O	0.013	0.010	0.021	0.0	0.0	0.0	0.011	0.029
Fe ²⁺	1.212	1.479	1.101	1.153	1.136	1.348	1.352	1.313
Mg	0.692	0.442	0.863	0.838	0.872	0.570	0.564	0.563
Mn	0.017	0.041	0.011	0.017	0.013	0.036	0.031	0.034
Ca	0.066	0.071	0.043	0.050	0.066	0.074	0.075	0.075
Na	0.005	0.004	0.005	0.002	0.005	0.006	0.006	0.006
X	0.002	0.002	0.003	0.001	0.002	0.004	0.003	0.005
X _{Mg}	0.363	0.218	0.439	0.421	0.434	0.297	0.294	0.300
X _{Fe}	0.637	0.782	0.561	0.579	0.566	0.703	0.706	0.700

Superscripts
 T = tetrahedral
 O = octahedral

Table 6 Chemical composition of clinopyroxenes from charnockitic granulites from the Adirondack Mts., N.Y. together with calculated formulae

CLINOPYROXENES

SP.No.	J-35	J-44	J-50	J-63A	J-66	J-80	J-81	J-99	J-103	J-105B	J-106	AV.
Oxides												
SiO ₂	48.35	48.71	48.38	49.76	51.57	46.88	47.58	51.27	49.04	51.45	49.02	49.27
Al ₂ O ₃	1.64	1.23	2.55	2.09	2.20	2.03	2.11	1.31	1.60	1.80	1.63	1.84
TiO ₂	0.10	0.19	0.27	0.13	0.14	0.19	0.23	0.17	0.17	0.19	0.17	0.18
Fe ₂ O ₃	1.02	2.53	3.59	2.60	2.15	3.86	2.38	1.04	1.56	1.39	2.47	2.24
FeO	16.62	22.40	12.07	13.88	13.25	13.33	13.56	15.95	18.54	18.88	18.76	16.11
MgO	8.85	5.38	10.49	10.94	10.67	10.49	10.47	9.57	7.53	7.66	7.57	9.06
MnO	0.22	0.60	0.13	0.16	0.15	0.25	0.21	0.24	0.49	0.50	0.48	0.31
CaO	22.54	16.76	20.01	17.85	17.55	22.54	19.89	18.57	19.79	16.00	19.39	19.17
Na ₂ O	0.55	0.57	0.52	0.74	0.72	0.63	0.62	0.40	0.67	0.61	0.54	0.60
K ₂ O	0.06	0.03	0.06	0.05	0.07	0.02	0.08	0.04	0.17	0.09	0.13	0.07
Total	99.95	98.40	98.07	98.20	98.47	100.22	97.13	98.56	99.56	98.57	100.16	98.85

Numbers of ions on the basis of 6 oxygens

	J-35	J-44	J-50	J-63A	J-66	J-80	J-81	J-99	J-103	J-105B	J-106
Si	1.897	1.968	1.891	1.935	1.979	1.829	1.891	1.992	1.935	2.013	1.926
(Al) ^T	0.076	0.032	0.110	0.065	0.021	0.093	0.099	0.008	0.065	0.0	0.074
(Ti) ^T	0.003	0.0	0.0	0.0	0.0	0.006	0.007	0.0	0.0	0.0	0.0
(Fe ³⁺) ^T	0.024	0.0	0.0	0.0	0.0	0.072	0.004	0.0	0.0	0.0	0.0
(Al) ^O	0.0	0.026	0.008	0.031	0.079	0.0	0.0	0.052	0.010	0.083	0.001
(Ti) ^O	0.0	0.006	0.008	0.004	0.004	0.0	0.0	0.005	0.005	0.006	0.005
(Fe ³⁺) ^O	0.006	0.077	0.106	0.076	0.062	0.042	0.067	0.030	0.046	0.041	0.073
Fe ²⁺	0.545	0.757	0.395	0.452	0.425	0.435	0.451	0.518	0.612	0.618	0.616
Mg	0.518	0.324	0.611	0.634	0.610	0.610	0.620	0.554	0.443	0.447	0.443
Mn	0.007	0.021	0.004	0.005	0.005	0.008	0.007	0.008	0.016	0.017	0.016
Ca	0.948	0.726	0.838	0.744	0.722	0.942	0.847	0.773	0.831	0.671	0.816
Na	0.042	0.045	0.039	0.056	0.054	0.048	0.048	0.030	0.051	0.046	0.041
K	0.003	0.002	0.003	0.003	0.003	0.001	0.004	0.002	0.009	0.005	0.007
X _{Mg}	0.487	0.300	0.608	0.584	0.589	0.584	0.579	0.517	0.420	0.420	0.418
X _{Fe}	0.513	0.700	0.392	0.416	0.411	0.416	0.421	0.483	0.580	0.580	0.582

Superscripts T = tetrahedral
O = octahedral

Table 7 Chemical compositions of amphiboles from charnockitic granulites from the Adirondack Mts., N.Y. together with calculated formulae.

AMPHIBOLES

SP.No.	J-35	J-44	J-50	J-80	J-99	J-103	J-105B	J-106	Av.
Oxides									
SiO ₂	38.09	39.86	39.96	38.46	41.07	39.11	39.60	39.25	39.55
Al ₂ O ₃	12.14	11.34	11.53	11.31	11.28	11.40	11.23	11.18	11.30
TiO ₂	2.12	2.69	2.70	2.43	2.30	2.32	2.44	2.50	2.44
Fe ₂ O ₃	2.63	3.51	5.61	4.53	3.39	4.62	4.16	3.65	4.01
FeO	18.23	22.15	14.65	15.38	18.36	20.30	20.26	20.21	18.69
MgO	7.04	4.23	8.61	8.08	6.93	5.93	6.29	6.02	6.64
MnO	0.12	0.32	0.07	0.12	0.13	0.26	0.21	0.23	0.18
CaO	13.80	9.44	11.08	13.80	10.07	9.56	9.76	10.93	11.06
Na ₂ O	1.50	1.81	1.15	1.44	1.52	1.82	1.77	1.79	1.60
K ₂ O	1.86	1.74	2.04	1.67	1.99	1.88	1.83	1.84	1.86
Total*	97.53	97.14	97.40	97.22	97.04	97.20	97.55	97.60	97.33

Numbers of ions on the basis of 23 oxygens

	J-35	J-44	J-50	J-80	J-99	J-103	J-105B	J-106
Si	6.103	6.285	6.122	5.979	6.352	6.147	6.185	6.148
(Al) T	1.897	1.715	1.878	2.021	1.648	1.853	1.815	1.852
(Al) O	0.154	0.383	0.204	0.052	0.409	0.260	0.253	0.212
Ti	0.249	0.319	0.311	0.284	0.268	0.274	0.287	0.294
Fe ³⁺	0.309	0.417	0.647	0.530	0.395	0.546	0.489	0.430
Fe ²⁺	2.381	2.921	1.877	2.000	2.375	2.669	2.646	2.647
Mg	1.638	0.994	1.966	1.872	1.597	1.389	1.464	1.405
Mn	0.016	0.043	0.009	0.016	0.017	0.035	0.028	0.031
Ca	2.309	1.595	1.819	2.299	1.669	1.610	1.633	1.834
Na	0.454	0.553	0.342	0.434	0.456	0.555	0.536	0.544
K	0.371	0.350	0.359	0.331	0.393	0.377	0.365	0.368
X _{Mg}	0.408	0.254	0.512	0.484	0.402	0.342	0.356	0.347
X _{Fe}	0.592	0.746	0.488	0.516	0.598	0.658	0.644	0.653

* Volatiles not determined

Superscripts T = tetrahedral
O = octahedral

Table 8 Chemical compositions of garnets from charnockitic granulites from the Adirondack Mts., N.Y. together with calculated formulae.

Oxide	J-35	J-50	J-63A	J-66	J-80	J-81	J-99	J-105B	AV
SiO ₂	38.39	38.40	36.87	38.90	36.21	36.22	38.36	37.58	37.62
Al ₂ O ₃	20.70	20.68	20.71	19.85	20.71	21.67	20.58	22.18	20.89
TiO ₂	0.05	0.06	0.02	0.00	0.04	0.08	0.06	0.09	0.05
Fe ₂ O ₃	0.29	1.06	0.99	1.91	1.35	0.28	0.12	0.34	0.79
FeO	29.89	28.28	30.10	29.79	28.67	25.51	29.79	29.72	29.47
MgO	2.43	4.06	3.32	3.14	3.01	2.94	2.37	2.12	2.92
MnO	1.19	0.72	0.85	0.97	1.41	1.13	1.28	1.52	1.13
CaO	7.67	6.21	5.77	6.31	7.13	7.62	6.28	5.82	6.60
Na ₂ O	0.03	0.02	0.08	0.05	0.01	0.08	0.04	0.08	0.05
K ₂ O	0.04	0.02	0.03	0.04	0.01	0.07	0.05	0.04	0.04
Total	100.68	99.51	98.74	100.96	98.55	99.60	98.93	99.49	99.56

GARNETS

Numbers of ions on the basis of 24 oxygens

	J-35	J-50	J-63A	J-66	J-80	J-81	J-99	J-105B
Si	6.074	6.077	5.954	6.130	5.874	5.815	6.151	5.991
(Al) T	0.0	0.0	0.047	0.0	0.126	0.186	0.0	0.009
(Al) O	3.861	3.858	3.896	3.688	3.835	3.916	3.891	4.160
Ti	0.006	0.007	0.002	0.0	0.005	0.010	0.007	0.011
Fe ³⁺	0.035	0.126	0.120	0.227	0.165	0.034	0.015	0.041
Fe ²⁺	3.955	3.743	4.065	3.926	3.890	3.962	3.995	3.963
Mn	0.159	0.097	0.116	0.130	0.194	0.154	0.174	0.205
Mg	0.573	0.958	0.799	0.737	0.728	0.704	0.566	0.504
Ca	1.300	1.053	0.998	1.065	1.239	1.311	1.079	0.994
Na	0.009	0.006	0.025	0.015	0.001	0.025	0.012	0.025
K	0.008	0.004	0.006	0.008	0.002	0.014	0.010	0.008
X _{Hg}	0.427	0.204	0.164	0.158	0.158	0.151	0.124	0.113
X _{Fe}	0.873	0.796	0.836	0.842	0.842	0.849	0.876	0.887

Superscripts
 T = tetrahedral
 O = octahedral

Table 9. Electron microprobe analysis of J-105B
biotite from charnockitic granulite from the Adirondack Mts.,
N.Y. together with calculated formula

Oxide	Wt %	Ion	Number of ions on the basis of 22 oxygens	
SiO ₂	36.21	Si	5.661	} Z = 7.95
Al ₂ O ₃	12.43	Al	2.291	
TiO ₂	4.36	Ti	0.513	} XY = 5.76
Total Fe as FeO	21.76	Fe ²⁺	2.845	
MgO	10.32	Mg	2.404	
MnO	0.00	Mn	0.000	} WW = 1.93
CaO	0.03	Ca	0.005	
Na ₂ O	0.10	Na	0.030	
K ₂ O	9.50	K	1.895	
Total	94.71			

Table 10

Electron microprobe analyses of coexisting magnetite (Mt) and ilmenite (Ilm) solid solutions.
 With S=0.59, C=1.17 for Ilm as FeO and S=0.99, C=2.01 for TiO₂.

Sp. No.	J-35		J-44		J-50		J-53A		J-66		J-80		J-81		J-99		J-103		J-103B		J-106	
	Mt	Ilm	Mt	Ilm	Ilm	Mt	Mt	Ilm	Mt	Ilm	Mt	Ilm	Mt	Ilm	Mt	Ilm	Mt	Ilm	Mt	Ilm	Mt	Ilm
Oxides																						
Fe as FeO	96.64	50.90	91.31	49.59	51.74	92.90	50.72	91.97	48.91	91.95	44.44	91.21	50.07	47.16	91.84	49.26	47.15	92.42	47.72			
TiO ₂	0.05	50.35	0.96	49.00	47.00	0.56	48.22	0.58	50.53	0.19	46.98	0.73	50.58	52.42	0.23	59.01	53.76	1.00	51.55			
Total	96.69	101.25	92.27	98.59	98.74	93.46	98.94	92.55	99.44	92.14	91.42	91.94	100.65	99.58	92.07	101.27	100.91	93.42	99.27			

VI INTRACRYSTALLINE ION EXCHANGE

The Mössbauer Effect

The Mössbauer effect is the recoil-free emission and resonant absorption of nuclear γ -rays in the crystals. The theory and principles of the Mössbauer effect and its applications are readily available in the literature regarding the solid state, e.g. Wertheim (1964). The complex theoretical aspects will not be described in this thesis. In brief, however, there are three important hyperfine parameters in the Mössbauer effect. These are:

- (1) Isomer or chemical shift (I.S.) - the electric monopole interaction between nuclear charge and electron density at the nucleus.
- (2) Quadrupole splitting (Q.S.) - interaction between electric quadrupole moment and electric field gradient tensor at the nuclear site.
- (3) Magnetic hyperfine splitting (M.H.S.) - interaction between magnetic dipole moment and local magnetic field at the nuclear site.

The importance of Mössbauer-effect studies in mineralogy, crystal chemistry and petrology is that from the study of the hyperfine parameters, produced by the transition metal ions in crystals (in the present study, Fe) information is obtained on several important crystal chemical

factors. These are (1) magnitude and symmetry of the crystal fields at the lattice site, (2) number of non-equivalent sites occupied by the isotope (^{57}Fe), (3) the site population, (4) oxidation state and (5) ordering of the isotopes in complex crystal structures. Studies of this kind have been carried out by Alff and Wertheim (1961), Annersten (1974), Bancroft et al. (1967, a, b, c, 1968), Burns (1970, p115), de Coster et al. (1963), Dowty and Lindsley (1973), Dowty et al. (1972), Dundon and Walter (1967), Evans et al. (1967), Finger et al. (1972), Gay et al. (1970), Ghose (1965a, b), Ghose and Hafner (1967, 1968), Ghose et al. (1972), Hafner (1968), Hafner and Virgo (1970), Hogarth et al. (1970), Kalvius and Hafner (1968), Nicholson and Burns (1964), Virgo and Hafner (1968, 1969, 1970), Saxena and Ghose (1970, 1971), and Zverev et al. (1971).

A practical aspect of the Mössbauer spectroscopy is the quantitative estimate of the $\text{Fe}^{2+}/\text{Fe}^{3+}$ ratio in crystals, and when combined with chemical analyses, one may determine the number of ferrous and ferric ions in the different co-ordination sites in the crystal structure. Such information may not otherwise be determined by X-ray methods including the X-ray diffraction techniques (Bancroft et al., 1967b; Ghose 1965b) or by conventional chemical analysis. Furthermore even the more accurate wet chemical methods cannot avoid some oxidation of Fe^{2+} or reduction of Fe^{3+} , whereas the Mössbauer technique does not pose such problems. This is the most accurate method of determining

the $\text{Fe}^{2+}/\text{Fe}^{3+}$ ratio in lattice sites in solid materials, provided that concentrations of the chemical species are high enough for detection (Bancroft et al., 1967c, p2223; Hogarth et al., 1970, p720). The technique may also be used to check the FeO and Fe_2O_3 determined by wet chemical analyses as to the correctness of the ratio or proportion. Or, quite rapidly and precisely, it may be employed to determine FeO and Fe_2O_3 (Fe^{2+} and Fe^{3+}) in silicate minerals, in conjunction with the electron microprobe.

The present study will make use of the Mössbauer technique to determine (1) the oxidation state of iron, in orthopyroxene, clinopyroxene, and garnet; and (2) the site populations of Fe^{2+} and Mg in the lattice sites of orthopyroxenes in the charnockitic granulites from the Adirondack Mountains.

Crystal Structure of Orthopyroxene, Clinopyroxene and Garnet

The crystal structure of an orthopyroxene with 50% Fe^{2+} (i.e. $\text{Fe}^{2+}/\text{Fe}^{2+} + \text{Mg} = 0.5$) was described by Ghose (1965a). It consists of infinite chains of SiO_4 tetrahedra, linked by bands of Mg and Fe cations, extending along the c-axis. There are two octahedral sites which are designated M_1 and M_2 . M_1 site cations are surrounded by six oxygen ions each linked to one silicon atom. Cations in the M_2 sites are surrounded by four oxygen ions each linked to one silicon atom, and two bridging oxygen atoms each shared by two silicon atoms. The symmetry of M_1 sites is approximately

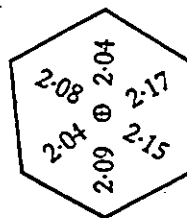
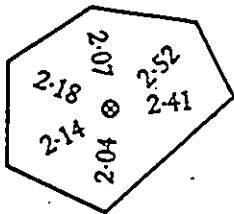
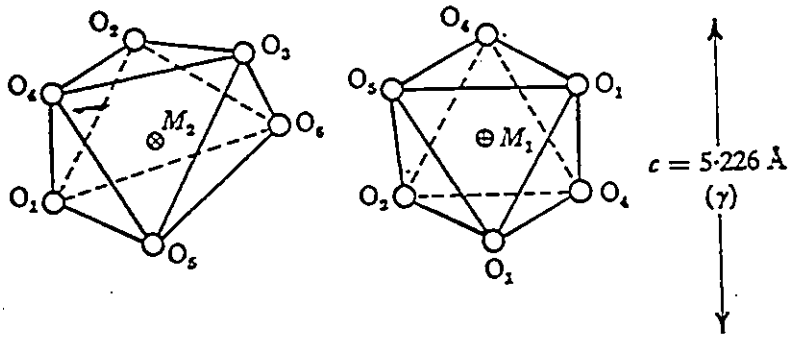
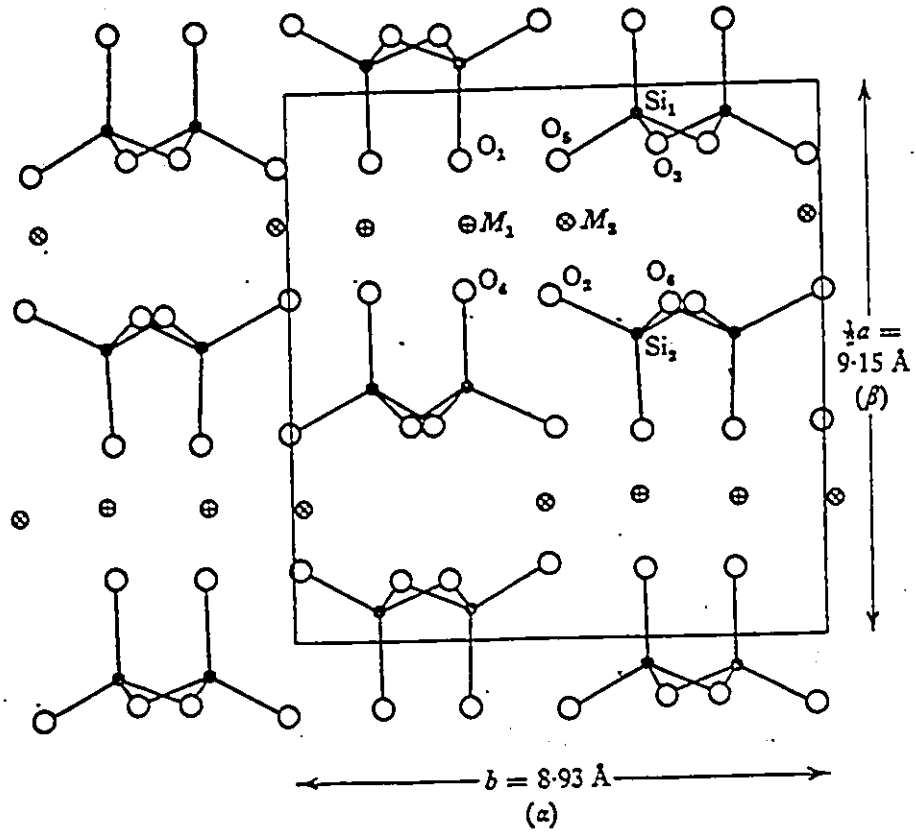
octahedral while the M_2 site is considerably distorted from octahedral (Fig. 5). The crystal structure of clinopyroxene is similar to that of the orthopyroxene, except that the cations in the M_2 sites (the distorted octahedrons), chiefly Ca^{2+} with some Fe^{2+} and Na, are eight co-ordinated with oxygen. The M_1 site is octahedral and is occupied by Fe^{2+} and Mg. The M_1 octahedron in clinopyroxene is more distorted than in orthopyroxene, and the neighbouring M_2 polyhedron is irregular (Warren and Bragg, 1929, p168; Deer et al., 1966, p102-103; Bancroft et al., 1967c, p2227; Ghose and Hafner, 1968, pGH-20).

The structure of garnet consists of independent SiO_4 tetrahedra linked by a trivalent cation in octahedral co-ordination and divalent cations in eight-fold co-ordination (Abrahams and Geller, 1958; Gibbs and Smith, 1965; Deer et al., 1966; Bancroft et al., 1967c). Thus the Fe^{2+} , Mg^{2+} , Ca^{2+} , and Mn ions in garnet are eight-fold co-ordinated whereas Fe^{3+} , and Al are six-fold co-ordinated. In the ferrimagnetic garnets such as andradite and some synthetic rare-earth iron garnets, however, considerable amount of Fe^{3+} may be present in the octahedral site (Nicholson and Burns, 1964 pA1568).

The Mössbauer Experiment

Eight mineral samples, including four orthopyroxenes (J-35, J-80, J-105B and J-106, representing two major mineral

Figure 5. The orthopyroxene crystal structure (after Burns, 1970). The figure shows the structure projected onto (001). Oxygen co-ordination polyhedra ((100) projections) and metal-oxygen distances in each site are indicated (O); $\oplus M_1$; $\otimes M_2$; \bullet silicon; \circ oxygen. Atomic co-ordinates and cell parameters from Ghose (1965).



assemblages of the present charnockitic granulites), three clinopyroxenes (J-80, J-105B and J-106) and one garnet (J-80) were purified (>99% purity), and polycrystalline powders (100-150 μ) were prepared into the form of thin discs, each approximately 30 mm in diameter and about $\frac{1}{2}$ mm in thickness. Approximately 80 to 100 mg of sample were used in each preparation. Sample powders were simply glued on to a cellophane sheet by using a commercial acrylic spray. The conventional method of adding leucite or other type of matrix was not used.

The Mössbauer resonance experiment was performed in 1972 by scientists of the Mines Branch, Department of Energy, Mines and Resources, Ottawa. A model S3 Mössbauer spectrometer of the constant acceleration type was used, in conjunction with an NS-600 512-channel multichannel analyzer. ^{57}Co embedded in a copper matrix was used as the source for the required 14.4 keV gamma rays, and stainless steel and iron foil were used as standards. Spectral measurements of samples J-35 and J-80 ortho- and clinopyroxenes together with the J-80 garnet were measured at room temperature and pressure. J-35, J-80, J-105B and J-106 orthopyroxenes and the J-80, J-105B, J-106 clinopyroxenes were measured at 77°K and atmospheric pressure, by holding the absorbers at the liquid nitrogen temperature. All absorption spectra were analyzed and fitted into Lorentzian lines by the aid of a CDC 6400 computer.

Mössbauer absorption spectra of pyroxenes, taken at room temperature, are shown in Figs. 6 to 10. None of these spectra show resolution of Fe^{2+} at the non-equivalent M_1 and M_2 sites, whereas those measured at 77°K give complete resolution of the peaks, as shown in Figs. 11 to 17. The spectra obtained at 77°K enable precise evaluation of the hyperfine parameters and area underneath the peaks produced by iron. Thus pertinent information may be obtained on the magnitude and symmetry of the crystal fields at the lattice sites, the number of non-equivalent sites, site populations, oxidation states and ordering of Fe-Mg within the crystals. Since no further improvement on spectral resolution was obtained at temperatures lower than 77°K (down to 1.7°K) as has been demonstrated by Virgo and Hafner (1968, p269), the Mössbauer spectra are generally best obtained at temperature close to 77°K (Ghose and Hafner, 1968, p4-5; Virgo and Hafner, 1968, p256-259, 1969, p72). Detailed considerations of the Mg- Fe^{2+} distribution and oxidation state of iron in pyroxenes and garnet will therefore be based entirely on the spectral data obtained at 77°K.

Interpretation

A typical Mössbauer spectrum of garnet is a simple two-line spectrum (Nicholson and Burns, 1964, pA1508; Bancroft et al., 1967c, p2234). The Mössbauer spectrum of the analyzed almandine garnet (J-80, Fig. 10) shows such a

Figure 6. Mössbauer spectrum of J-35 orthopyroxene measured at room temperature and pressure.

Figure 7. Mössbauer spectrum of J-35 clinopyroxene measured at room temperature and pressure.

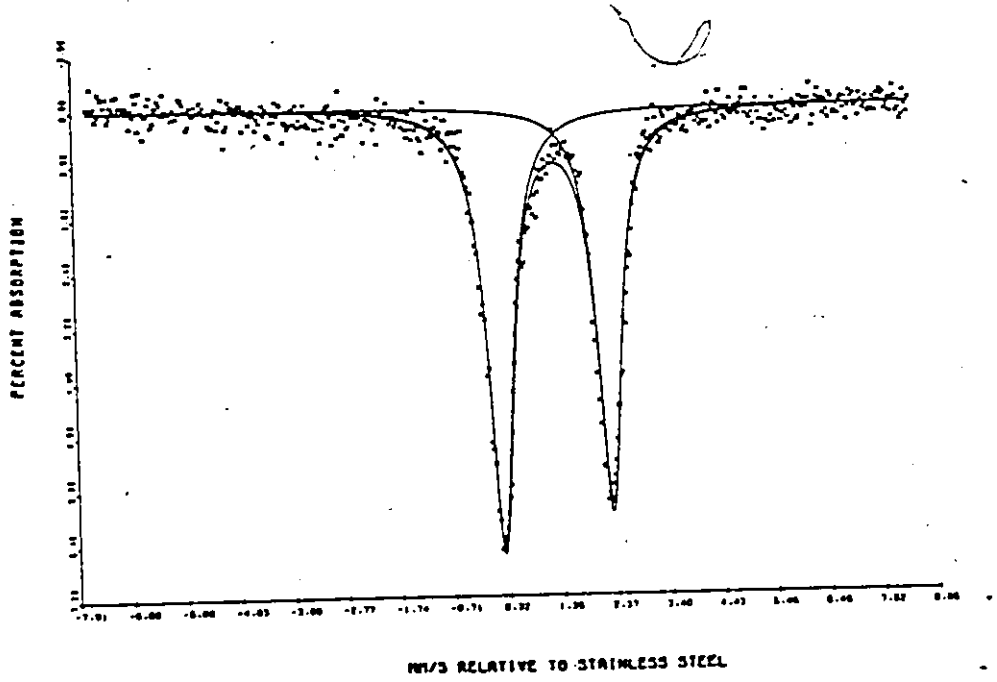
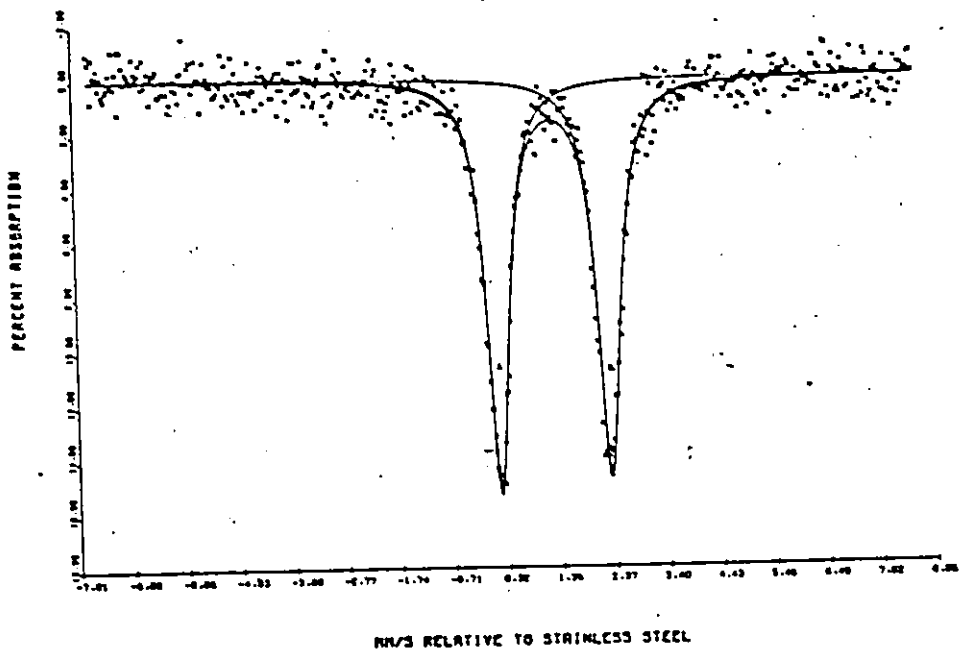


Figure 8. Mössbauer spectrum of J-80 orthopyroxene measured at room temperature and pressure.

Figure 9. Mössbauer spectrum of J-80 clinopyroxene measured at room temperature and pressure.

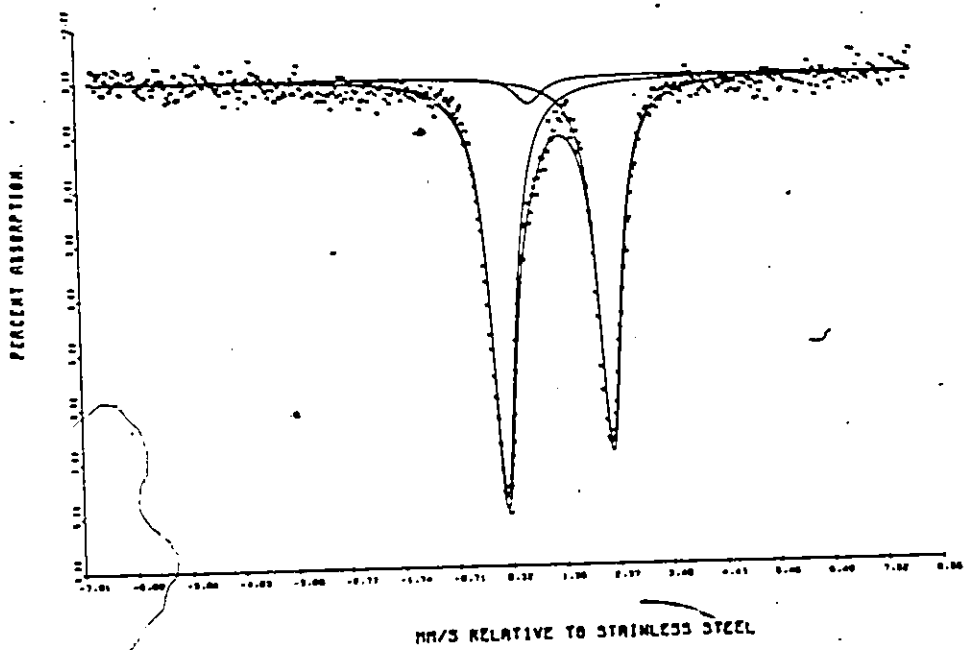
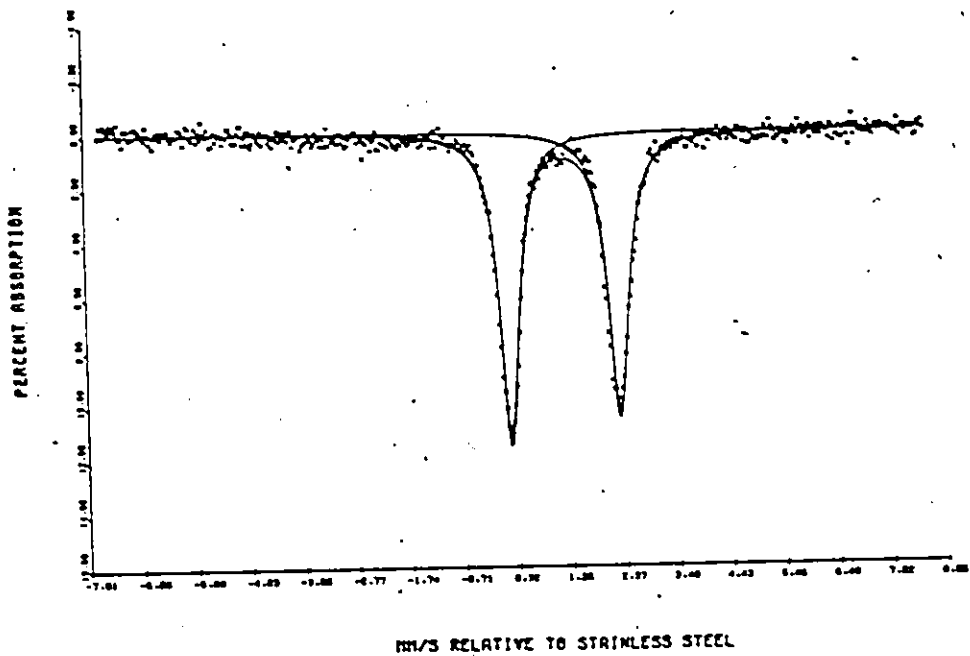


Figure 10. Mössbauer spectrum of J-80 almandine garnet measured at room temperature and pressure.




Figure 11. Mössbauer spectrum of J-35 orthopyroxene measured at $T=77^{\circ}\text{K}$, $P=1$ atm.

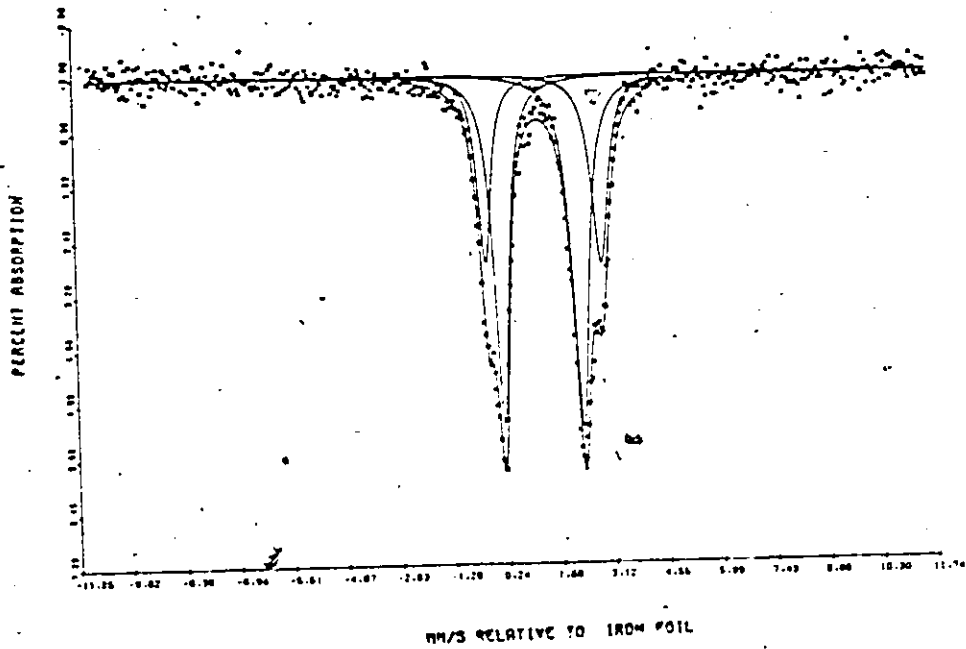
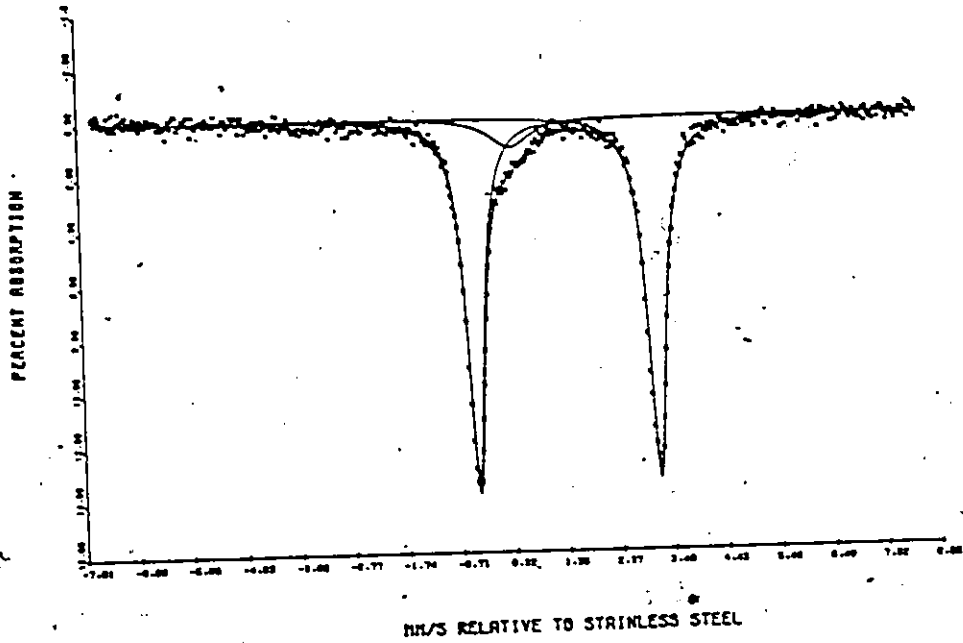


Figure 12. Mössbauer spectrum of J-80 orthopyroxene measured at $T=77^{\circ}\text{K}$, $P=1$ atm.

Figure 13. Mössbauer spectrum of J-80 clinopyroxene measured at $T=77^{\circ}\text{K}$, $P=1$ atm.

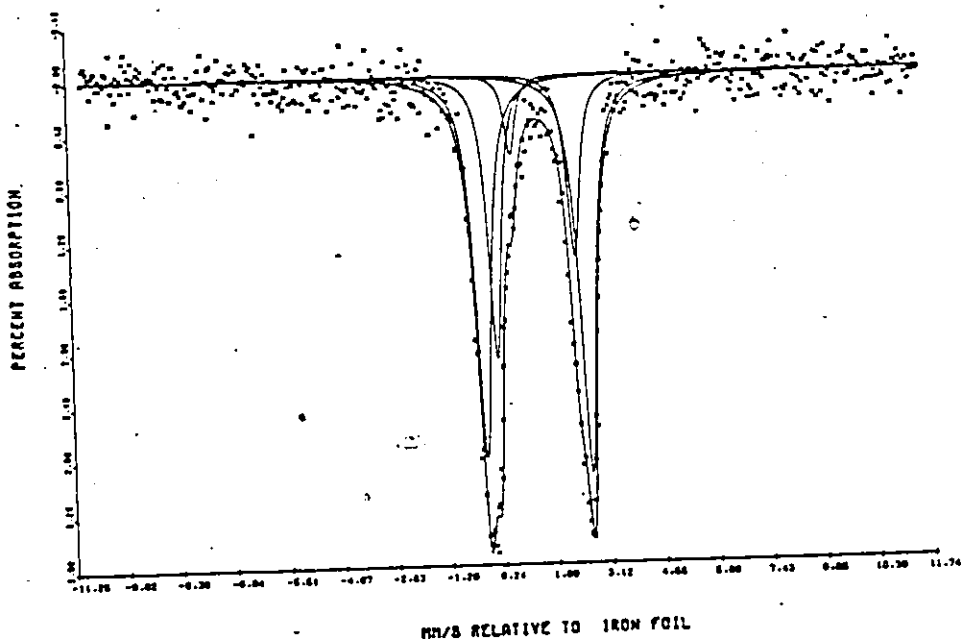
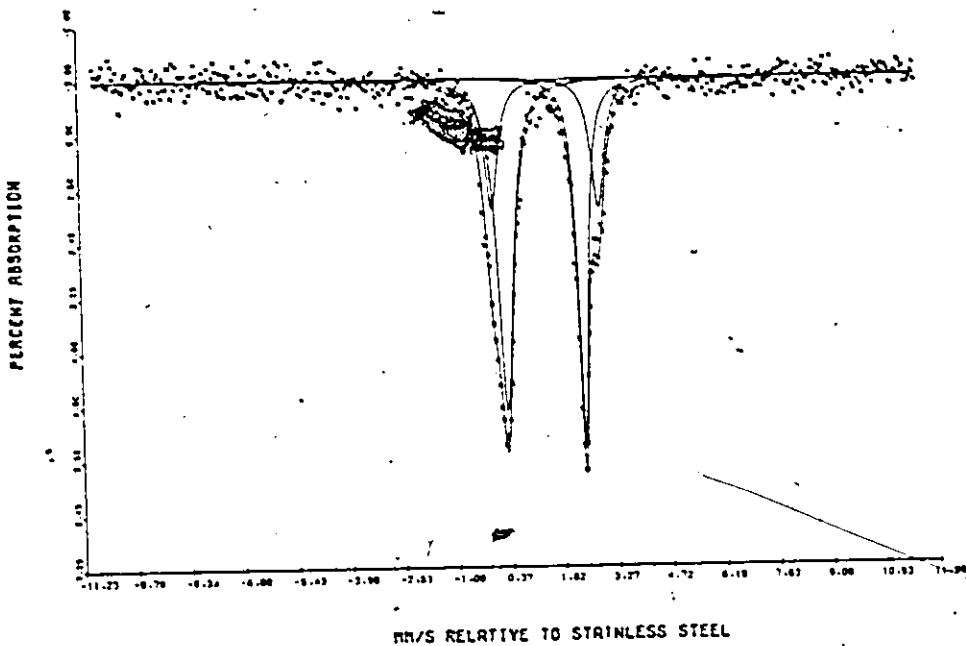


Figure 14. Mössbauer spectrum of J-105B orthopyroxene
measured at $T=77^{\circ}\text{K}$, $P=1$ atm.



Figure 15. Mössbauer spectrum of J-105B clinopyroxene
measured at $T=77^{\circ}\text{K}$, $P=1$ atm.

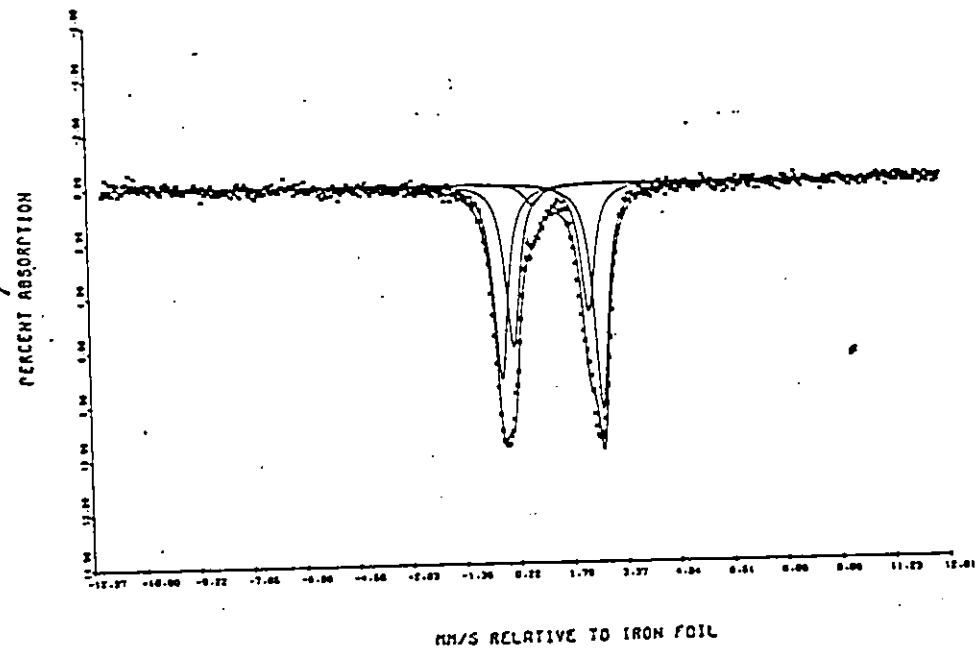
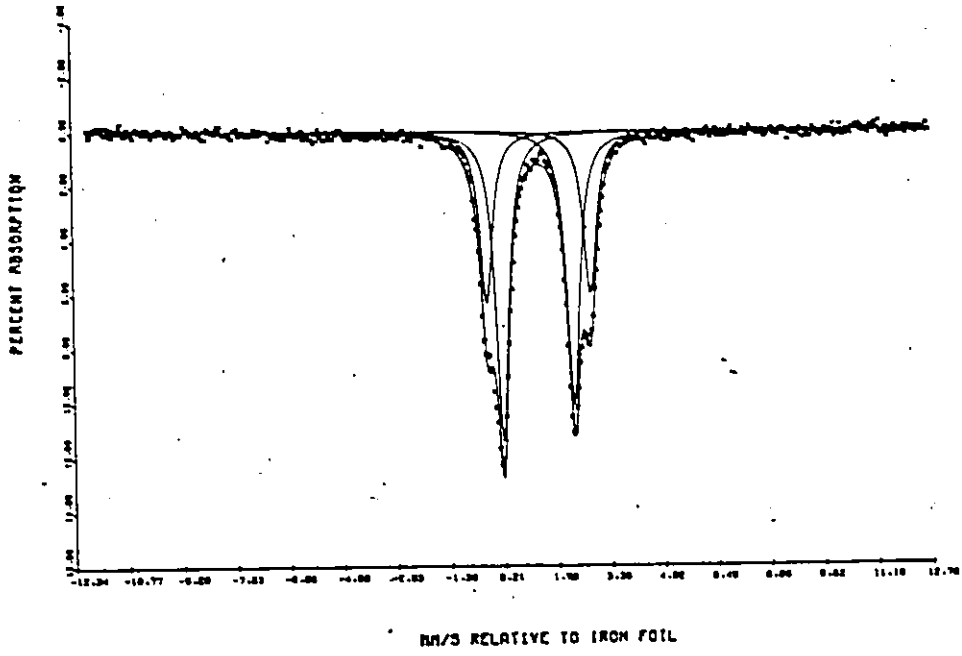
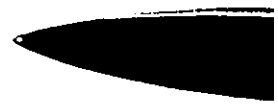
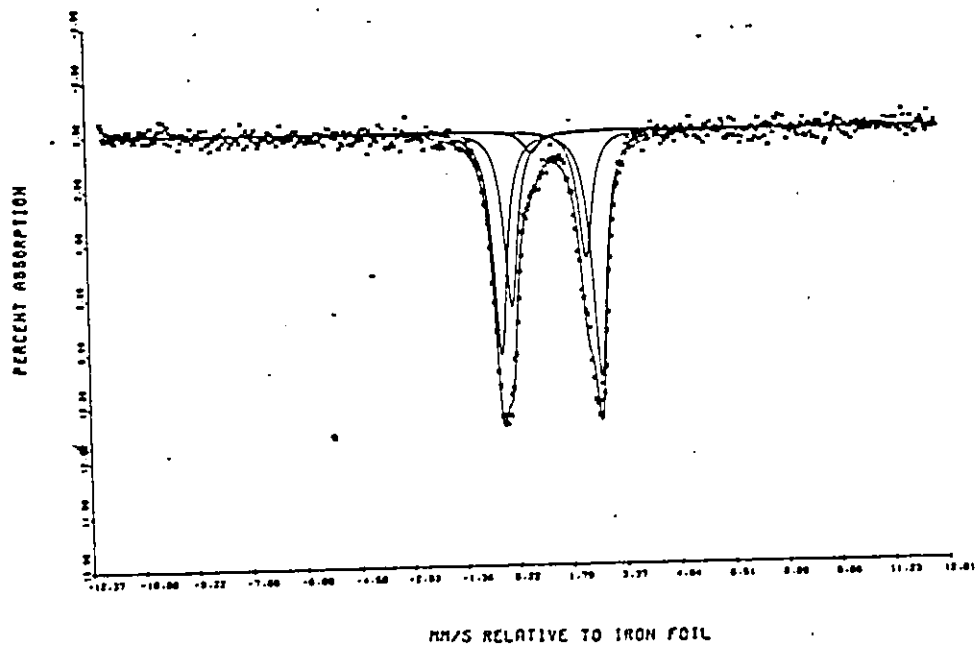
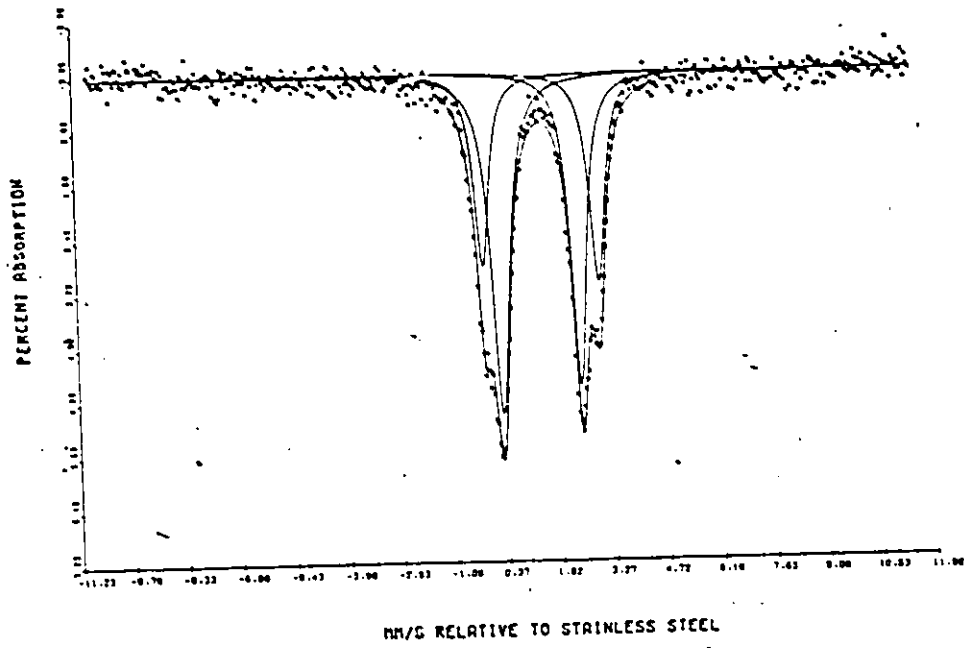


Figure 16. Mössbauer spectrum of J-106 orthopyroxene measured at $T=77^{\circ}\text{K}$, $P=1$ atm.

Figure 17. Mössbauer spectrum of J-106 clinopyroxene measured at $T=77^{\circ}\text{K}$, $P=1$ atm.



typical absorption doublet. This gives an isomer shift of 1.39 mm/sec and a very large quadrupole splitting of 3.51 mm/sec, which, from the Q.S. strongly indicates the presence of iron in the ferrous state, and, from the I.S. its presence in eight-fold co-ordination. Little Fe^{3+} is present, and is indicated by the small peak. These data, combined with chemical analyses have shown that the sample is evidently the most Fe^{2+} -rich garnet so far investigated by Mössbauer spectroscopy. All of the Fe^{2+} ions are in eight-fold co-ordination, all of the Mg will presumably also occupy that site.

With reference to the pyroxenes, there are lower velocity peaks, A_1 and A_2 , and higher velocity peaks, B_2 and B_1 . For example, in Fig. 12, the lower velocity peaks A_1 and A_2 have peak positions, in terms of velocities, at -0.060 and 0.299 mm/sec relative to stainless steel, whereas the higher velocity peaks B_2 and B_1 are 2.402 and 2.854 mm/sec respectively. The inner two peaks, A_2 and B_2 , represent Fe^{2+} at the M_2 site; the outer two peaks A_1 and B_1 represent Fe^{2+} at the M_1 site (Bancroft et al., 1967a, b, c, 1968; Evans et al., 1967; Dundon and Walter, 1967; Ghose and Hafner, 1968; Virgo and Hafner, 1968, 1969). The inner two peaks are invariably more intense, indicating that the Fe^{2+} ions are concentrated in the M_2 site in the orthopyroxene structure.

These results, as shown in Figs. 11, 12, 14, 16, are similar to those found by Ghose (1965a, p81) and Bancroft et al. (1967a, p1223). However, the present orthopyroxenes are eulite in composition, and some complexities due to the high Fe^{2+} content will be discussed in a later chapter.

The assignment of relative intensities in clinopyroxene is the reverse of that of the orthopyroxene. The outer two peaks, representing Fe^{2+} in the M_1 site, are invariably more intense (Bancroft et al., 1967c, p2227). The present clinopyroxene spectra determined at low T (Figs. 13, 15 and 17) are consistent with these expectations. A small peak, having a velocity of 0.641 mm/sec relative to iron foil, is shown in Fig. 13, which contains the spectrum of J-80 clinopyroxene. This peak (the C peak, as distinct from the A and B peaks, indicates the presence of more than 5 per cent of the total iron in the ferric state. Small amounts of Fe^{3+} are also present in J-105B and J-106 clinopyroxenes (Figs. 15 and 17). These results are in agreement with the chemical analyses.

The site occupancy numbers (or factors) $X_{\text{Fe}}^{M_1}$ and $X_{\text{Fe}}^{M_2}$ for M_1 and M_2 sites respectively in the pyroxenes are the mole fraction $\text{Fe}^{2+}/(\text{Fe}^{2+}+\text{Mg})$ at each site and may be calculated by use of the following equations:

$$X_{Fe}^{M_1} = (A_1 + B_1) / (A_1 + A_2 + B_2 + B_1) \times 2Fe^{2+} / (Fe^{2+} + Mg) \quad (7)$$

$$X_{Fe}^{M_2} = (A_2 + B_2) / (A_1 + A_2 + B_2 + B_1) \times 2Fe^{2+} / (Fe^{2+} + Mg) \quad (8)$$

where A_1 , A_2 are areas underneath peaks A_1 and A_2 respectively,
 B_1 , B_2 " " " " " B_1 and B_2 "

Substituting $I \times \Gamma$ (where I is the intensity, Γ is the half-width of a Mössbauer resonance peak) for area, equations (7) and (8) become identical with the equations given by Saxena and Ghose (1971, p539). Virgo and Hafner (1970, p206) have used the intensity alone instead of the products of intensity and halfwidth, or area underneath peak. This procedure yields somewhat different results. Since the data of the present study will be compared with the experimental data of Saxena and Ghose (1971), the area method was used, in conjunction with the intensity-halfwidth-product method, to compute the site occupancy numbers for each site. Calculations of the site populations of Fe^{2+} and Mg in each site in the pyroxenes are based on the site occupancy numbers so calculated, and are given in Table 11.

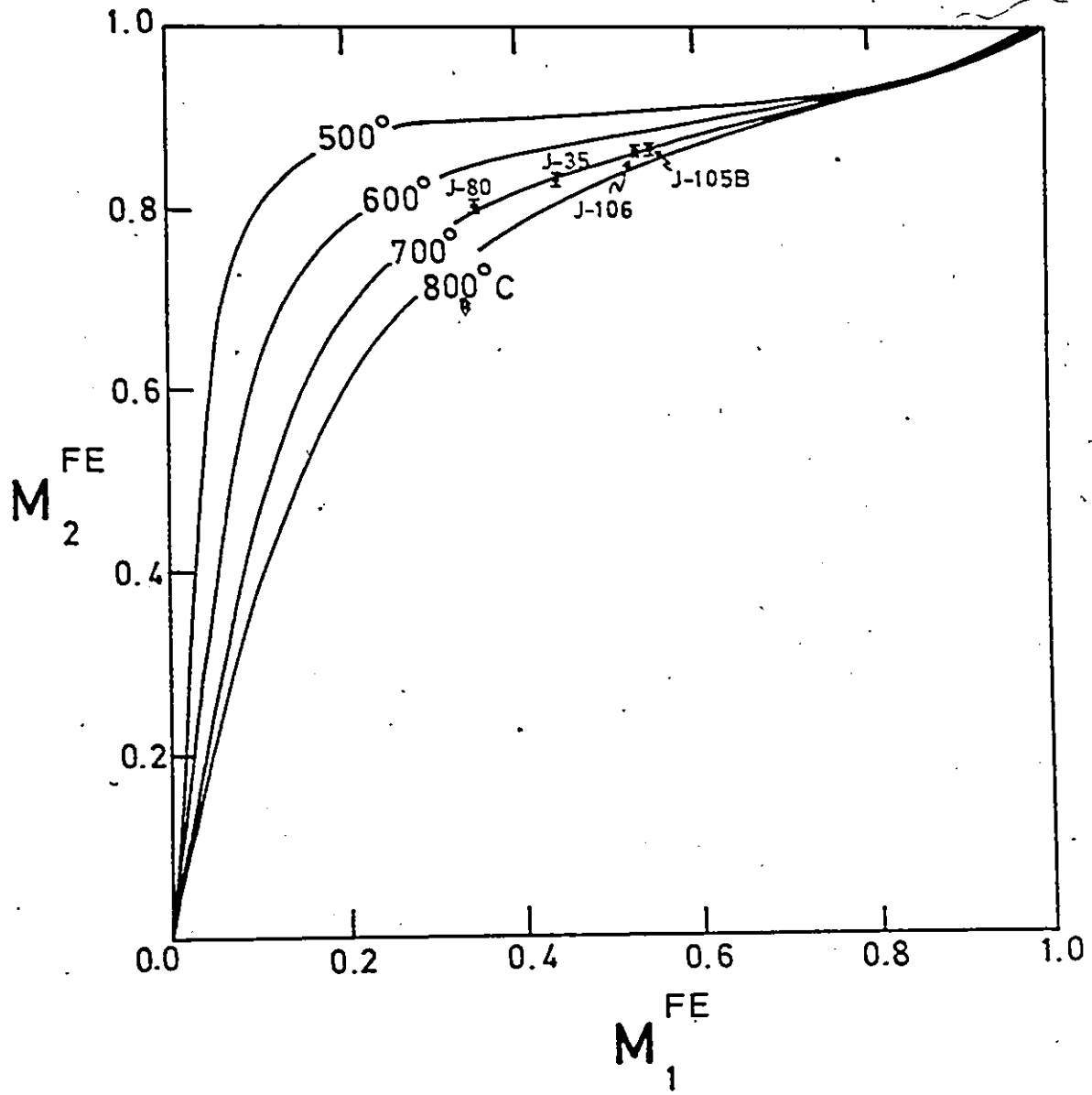
From the heating experiments of Virgo and Hafner (1969, 1970) and, Saxena and Ghose (1971), distribution isotherms for the distribution of Fe^{2+} and Mg between M_1 and M_2 sites in orthopyroxenes were obtained. These isotherms, as shown in Fig. 18 may provide information on the temperature of equilibration of naturally crystallized orthopyroxenes.

Table 11 Site occupancy (Fe^{2+}) numbers for four orthopyroxenes from charnockitic granulites from the Adirondack Mts., N.Y.

Sp.No.	J-35	J-80	J-105B	J-106
Site				
M ₁	0.442±0.004	0.349±0.007	0.544±0.007	0.529±0.003
M ₂	0.832±0.004	0.809±0.007	0.868±0.007	0.871±0.003

The data points for the distribution of Fe^{2+} and Mg in orthopyroxene of the present study fall very close to the 700°C isotherm of Saxena and Ghose (1971, p535), as shown in Fig. 18. Since ordering reactions could be induced in orthopyroxenes at temperature as low as 480°C by Virgo and Hafner (1969, 1970) it is surprising that the slowly-cooled orthopyroxenes of the present study did not achieve a greater degree of ordering. However since the nature and strength of the kinetic barriers to ordering are not yet perfectly understood (Mueller, 1962, 1967, 1969, 1970) it is possible that the ordering reaction was for some reason retarded in nature, and that the presently-found cation distribution represents a frozen-in ion exchange equilibrium. If so, the equilibrium temperature can be taken as $700^{\circ} \pm 25^{\circ}\text{C}$. It is possible, of course, that the temperature of crystallization or the peak of metamorphism was higher than this, say 800°C, and that some ordering took place in all four crystals, causing the data points in Fig. 18 to shift toward the 700°C isotherms.

Figure 18. Distribution isotherms for the distribution of Fe^{2+} and Mg between M_1 and M_2 sites in orthopyroxene, according to Saxena and Ghose (1971). Data points for 4 orthopyroxenes from the present study are shown. $M_2^{\text{Fe}} = \text{Fe}/(\text{Fe} + \text{Mg})$ atomic ratio in M_2 sites and $M_1^{\text{Fe}} = \text{Fe}/(\text{Fe} + \text{Mg})$ atomic ratio in M_1 sites.

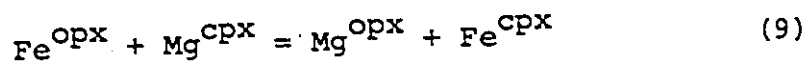


VII INTERCRYSTALLINE ION EXCHANGE EQUILIBRIUM:
ORTHOPYROXENE-CLINOPYROXENE-AMPHIBOLE-GARNET

(I) ORTHOPYROXENE-CLINOPYROXENE

Distribution of Mg and Fe²⁺ Between Coexisting
Orthopyroxene and Clinopyroxene.

The general Mg-Fe²⁺ exchange reaction between coexisting orthopyroxene (opx) and clinopyroxene (cpx) has been considered by numerous authors, notably Kretz (1961, 1963), Mueller (1960), Bartholome (1962), Saxena (1968), and Perchuk (1968). In this treatment, the distribution of Mg and Fe²⁺ within the crystals is disregarded. The reaction may be written as follows (with Fe²⁺ written as Fe):



The equilibrium constant for this reaction is:

$$K(9) = \frac{a_{\text{Mg}}^{\text{opx}} a_{\text{Fe}}^{\text{cpx}}}{a_{\text{Fe}}^{\text{opx}} a_{\text{Mg}}^{\text{cpx}}} = \frac{x_{\text{Mg}}^{\text{opx}} (1-x_{\text{Mg}}^{\text{cpx}})}{(1-x_{\text{Mg}}^{\text{opx}}) x_{\text{Mg}}^{\text{cpx}}} \cdot \frac{\gamma_{\text{Mg}}^{\text{opx}} \gamma_{\text{Fe}}^{\text{cpx}}}{\gamma_{\text{Fe}}^{\text{opx}} \gamma_{\text{Mg}}^{\text{cpx}}} \quad (10)$$

Substituting K_D for the expression that contains the X terms, and K_Y for the expression that contains the γ terms, equation (10) becomes

$$K(9) = K_D \cdot K_Y = \exp \frac{-\Delta G^\circ(9)}{RT} \quad (11)$$

Here a is activity, γ is activity coefficient, X is the mole fraction or atomic fraction, $X_{\text{Mg}} = \text{Mg}/\text{Mg} + \text{Fe}^{2+}$, $\Delta G^\circ(9)$ is the standard molar free energy change for reaction (9),

R is the gas constant, T is the absolute temperature, and K_D is the distribution coefficient. If the coexisting phases are ideal solid solutions of Mg and Fe^{2+} end members, $a = X$, $K_Y = 1$ and K_D becomes identical to $K(9)$.

Theoretically, K and K_D depend on T and P; T appears to dominate. If both pyroxene phases behave as ideal solutions, K_D is independent of composition (Ramberg and DeVore, 1951; Kretz, 1959, 1961, 1963, 1964). Some studies have shown that K_D for natural mineral pairs may also depend on composition (Davidson, 1968; Saxena and Ghose, 1971; Fleet, 1974; Maxey and Vogel, 1974).

Model 1. Ideal Solutions

The Mg/Mg + Fe ratios for coexisting orthopyroxene and clinopyroxene in charnockitic granulites from the Adirondack Mts. (present study) and from Madras, India (Howie, 1955) are listed in Table 12. These data are plotted in Figs. 19 and 20. K_D for all of these mineral pairs does not vary greatly, as shown in Table 13; the average value is 0.57. The data from India are included for comparison and to provide a greater range in Mg/Fe ratio in the mineral pairs. Notice (Fig. 19) that, in the central part of the diagram, the data points from the two sources nearly coincide, suggesting that the metamorphic condition in the Madras area may have been similar to those in the Adirondacks, and that the Madras data may therefore provide a continuation of the distribution curve obtained from the present study.

Table 12. Mole fractions of Mg (X_{Mg}) and Fe^{2+} (X_{Fe}) for coexisting orthopyroxene and clinopyroxene from mafic charnockitic granulites from the Adirondack Mts., (present study), and from Madras, India (Howie, 1955)

		Orthopyroxene (opx)		Clinopyroxene (cpx)	
		X_{Mg}	X_{Fe}	X_{Mg}	X_{Fe}
Adirondacks	J-35	0.363	0.637	0.487	0.513
	J-44	0.218	0.782	0.300	0.700
	J-66	0.439	0.561	0.589	0.411
	J-80	0.421	0.579	0.584	0.416
	J-81	0.434	0.566	0.579	0.421
	J-103	0.297	0.703	0.420	0.580
	J-105B	0.294	0.706	0.420	0.580
	J-106	0.300	0.700	0.418	0.582
Madras	3709	0.758	0.242	0.850	0.150
	4645	0.736	0.264	0.845	0.155
	2270	0.617	0.383	0.752	0.248
	2941	0.544	0.456	0.680	0.320
	4642A	0.430	0.570	0.570	0.430

Figure 19. Distribution of Mg and Fe²⁺ between coexisting orthopyroxene and clinopyroxene from the charnockitic granulites.

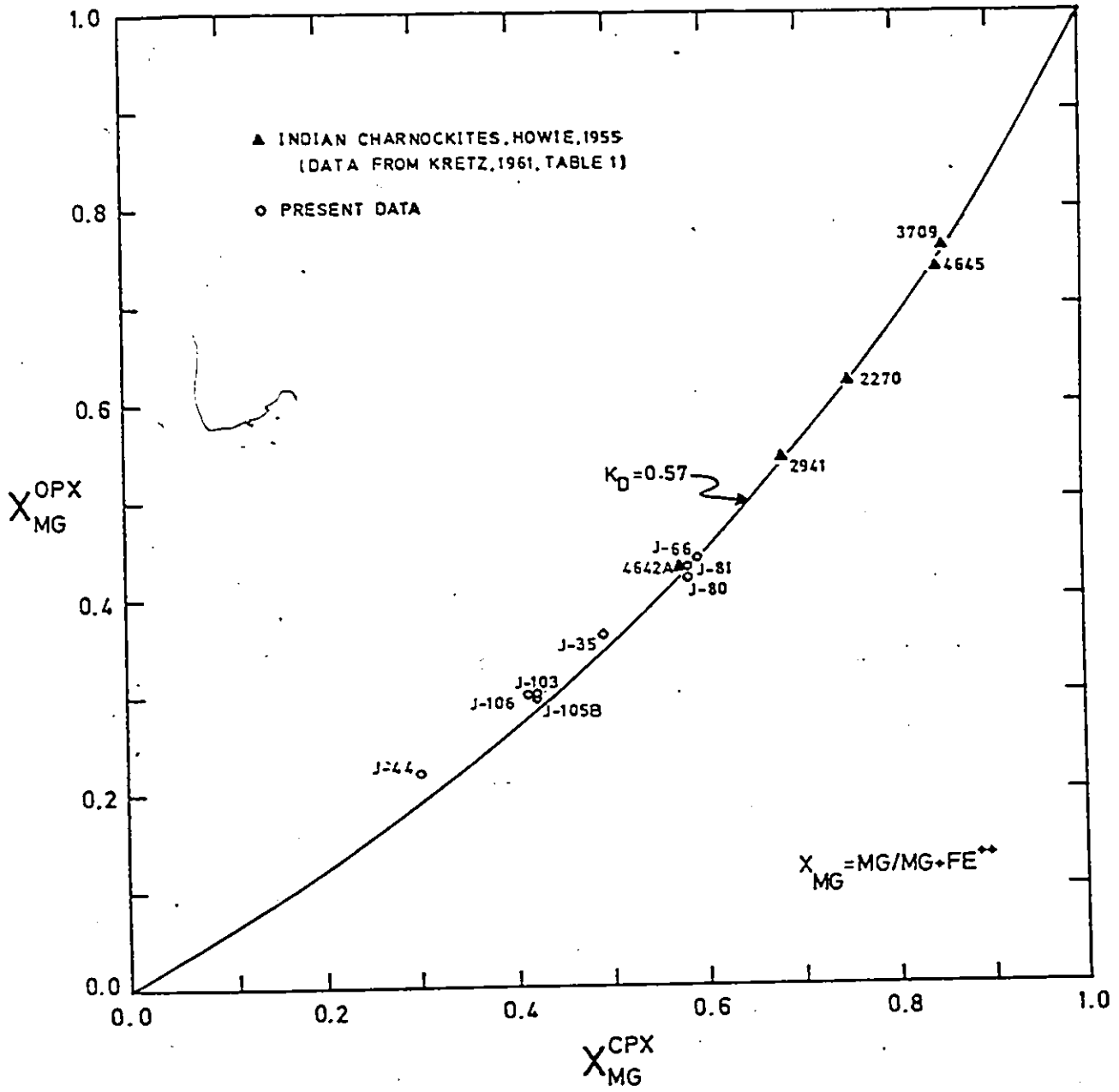


Figure 20. Distribution of Mg and Fe²⁺ between coexisting orthopyroxene and clinopyroxene from the $\left(\frac{x}{1-x}\right)_{\text{opx}}$ charnockitic granulites, in terms of a $\left(\frac{x}{1-x}\right)_{\text{Mg}}$ vs $\left(\frac{x}{1-x}\right)_{\text{cpx}}$ plot.

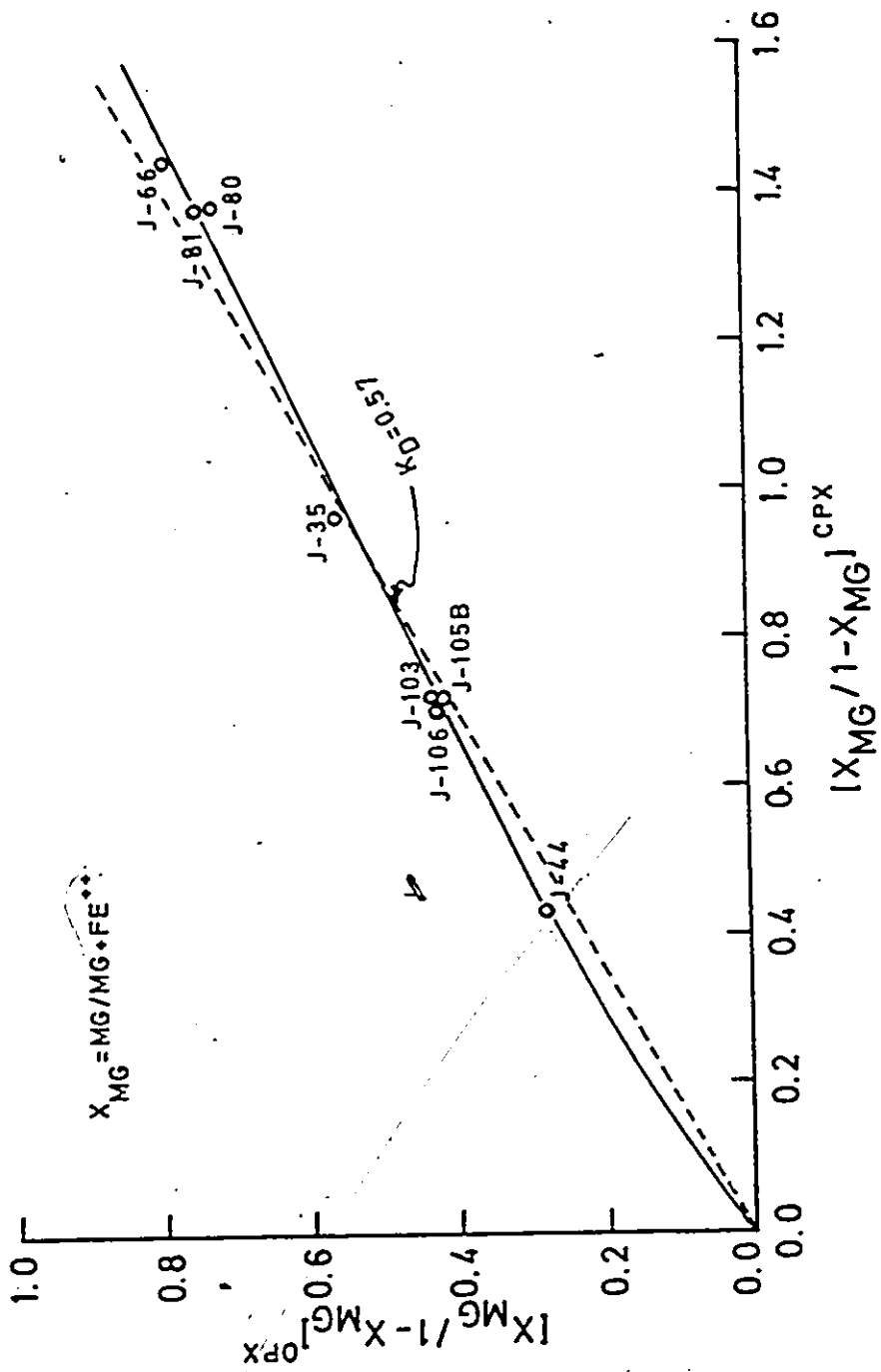


Table 13. Distribution coefficients for the coexisting orthopyroxene and clinopyroxene from the Madras Area (India), and the Adirondack Mts., N.Y.

<u>Adirondack pyroxenes</u>	<u>K_D</u>
J-35	0.60
J-44	0.65
J-66	0.55
J-80	0.52
J-81	0.56
J-103	0.58
J-105B	0.58
J-106	0.60
<u>Madras pyroxenes</u>	
3709	0.55
4645	0.51
2270	0.53
2941	0.56
4642A	0.57
<u>Average</u>	0.57

The two-ideal-solution model presumes that both minerals behave as ideal solutions. This model will be considered briefly even though orthopyroxene is obviously not an ideal solution, for it is partly ordered, as discussed in the preceding chapter. It is possible that a mineral may possess near-ideal behaviour in the sense that 'macroscopic' activity of a component is equal to its mole fraction, even though internally it is partly ordered.

In the two-ideal-solution model, K_D is constant at a given T and P, and is independent of composition. Notice (Fig. 19) that this model provides a fairly good 'fit' to the data, particularly in the Mg-rich composition range.

It is interesting to note that Lindsley et al. (1974) recently carried out an experimental determination of $K_D(\text{Mg})$ for coexisting augite and hypersthene at 810°C and obtained a value of 0.690. A variation in K_D could not be detected by the experimental methods employed. Since the experimental K_D is considerably greater than 0.57 obtained for the Madras and Adirondack rocks, the crystallization temperature for these rocks was evidently lower than 810°C .

Model 2. Non-ideal Solutions

We shall now adapt a model which assumes both minerals to be simple mixtures rather than ideal mixtures.

Equation (10) may be written as

$$\ln K = \ln K_D + \ln \gamma_{Mg}^{opx} - \ln \gamma_{Fe}^{opx} + \ln \gamma_{Fe}^{cpx} - \ln \gamma_{Mg}^{cpx} \quad (12)$$

where K and K_D are the equilibrium constant and distribution coefficient respectively for the non-ideal-solutions model.

The simple mixture solution model (Guggenheim, 1967) has been applied to minerals by Mueller (1964), Muan, Nafziger and Roeder (1964), Kitayama (1970), Kitayama and Katsura (1968), Williams (1971), and Froese and Gordon (1974). We shall presume that both orthopyroxene and clinopyroxene are simple solutions; consequently the activity coefficients will be as follow

$$\ln \gamma_{Mg}^{opx} = \alpha^{opx} (1 - X_{Mg}^{opx})^2 \quad (13)$$

$$\ln \gamma_{Fe}^{opx} = \alpha^{opx} (X_{Mg}^{opx})^2 \quad (14)$$

$$\ln \gamma_{Mg}^{cpx} = \alpha^{cpx} (1 - X_{Mg}^{cpx})^2 \quad (15)$$

$$\ln \gamma_{Fe}^{cpx} = \alpha^{cpx} (X_{Mg}^{cpx})^2 \quad (16)$$

In the above expressions, γ 's are the activity coefficients and α 's are the natural logarithms of the activity coefficients at infinite dilution. For the two components of a given binary solution, the α values for the two components are the same.

Substituting equations (13) to (16) into equation (12) the following equation is obtained

$$\ln K = \ln K_D - \alpha^{\text{cpx}} (1 - 2X_{\text{Mg}}^{\text{cpx}}) + \alpha^{\text{opx}} (1 - 2X_{\text{Mg}}^{\text{opx}}) \quad (17)$$

or

$$\ln X_{\text{Mg}}^{\text{opx}} - \ln(1 - X_{\text{Mg}}^{\text{opx}}) + \alpha^{\text{opx}} (1 - 2X_{\text{Mg}}^{\text{opx}}) = \ln K + \ln X_{\text{Mg}}^{\text{cpx}} - \ln(1 - X_{\text{Mg}}^{\text{cpx}}) + \alpha^{\text{cpx}} (1 - 2X_{\text{Mg}}^{\text{cpx}}) \quad (18)$$

Equation (17) was previously derived by Mueller (1964) and was later used by Saxena (1969, 1970, 1971, 1973) and Froese and Gordon (1974).

S.K. Saxena has kindly solved equation (17) for the data of Table 12 using a least square method. The results are: $K = 0.684$, $\alpha^{\text{opx}} = 0.670$, $\alpha^{\text{cpx}} = 0.816$. These values may be inserted into equation (18) to plot the distribution curve shown in Fig. 21. This curve provides an improved 'fit' to the data points for the natural mineral pairs. The activity coefficients of the thirteen pairs of pyroxenes may now be calculated using equations (13) and (15). The results are shown in Table 14. These values indicate a positive deviation from ideality ($\gamma > 1.0$), in agreement with the result of Saxena (1969a, b, 1971) and Saxena and Ghose (1971) and contrary to those of Olsen and Bunch (1970) and Blander (1972).

The results of the above analysis may be compared with those obtained by Froese and Gordon (1974) for the Quairading pyroxenes (Davidson, 1968) as follows:

Figure 21. Distribution of Mg and Fe²⁺ between coexisting orthopyroxene and clinopyroxene from the charnockitic granulites.

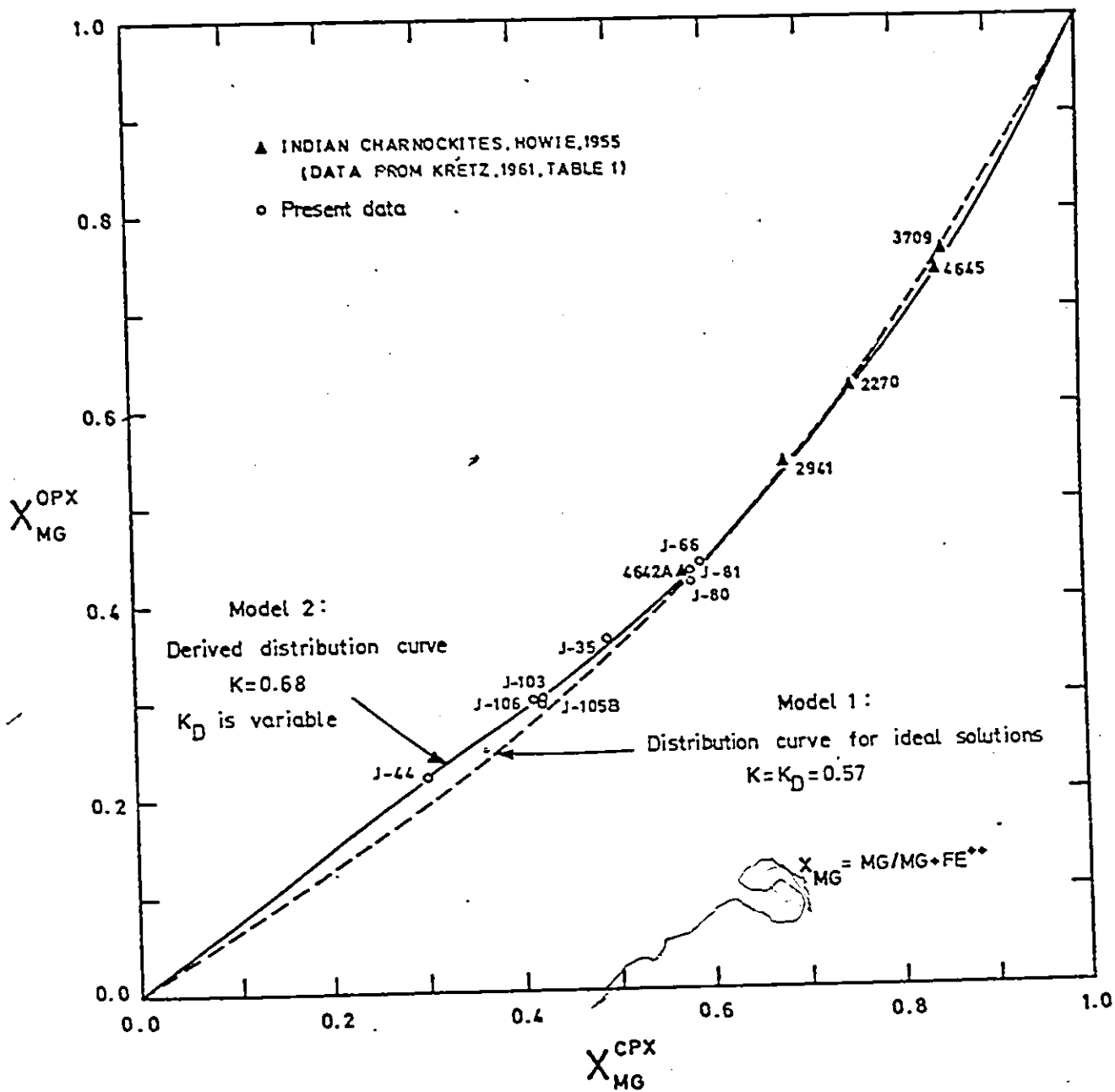


Table 14. Activity coefficients of the Adirondack and Madras orthopyroxene (γ^{opx}) and clinopyroxene (γ^{cpx})

	Orthopyroxene		Clinopyroxene	
	$\gamma_{\text{Mg}}^{\text{opx}}$	$\gamma_{\text{Fe}}^{\text{opx}}$	$\gamma_{\text{Mg}}^{\text{cpx}}$	$\gamma_{\text{Fe}}^{\text{cpx}}$
Adirondack Pyroxenes				
J-35	1.313	1.092	1.240	1.213
J-44	1.517	1.032	1.491	1.076
J-66	1.235	1.139	1.148	1.328
J-80	1.252	1.126	1.152	1.321
J-81	1.240	1.135	1.155	1.315
J-103	1.392	1.061	1.316	1.155
J-105B	1.403	1.060	1.316	1.155
J-106	1.391	1.062	1.319	1.154
Madras Pyroxenes				
3709	1.040	1.477	1.019	1.804
4645	1.047	1.438	1.020	1.790
2270	1.103	1.291	1.052	1.586
2941	1.150	1.226	1.086	1.458
4642A	1.243	1.132	1.162	1.302

<u>Present study</u>	<u>Froese and Gordon</u>
α_{opx} 0.670	0.447
α_{cpx} 0.816	0.625
K 0.684	0.662

From the data of Tables 12 and 14, the activities for the thirteen pairs of pyroxenes may be calculated. The results are shown in Table 15. Activity-composition diagrams for orthopyroxene and clinopyroxene may also be constructed and are shown in Figs. 22 and 23.

The two-simple-solutions model for coexisting orthopyroxene and clinopyroxene is evidently superior to the two-ideal-solutions model, for it provides a better 'fit' to the data of the present study, as well as data from other sources (Fig. 24). However different combinations of various kinds of solutions would presumably produce models that would 'fit' the data equally well. Obviously, experimental studies are now needed to provide further information in activity-composition relation in the pyroxene minerals.

A comparison with data on pyroxenes from other well known charnockitic areas in the world is shown in Fig. 24.

In order to illustrate the observed variation in calcium content in the pyroxenes of the present study, the Ca Mg Σ Fe ratios have been calculated and plotted together with other data in Fig. 25. A vertical spread in the clino-

Table 15. Activity data of the Adirondack and Madras orthopyroxene (a^{opx}) and clinopyroxene (a^{cpx})

	Orthopyroxene		Clinopyroxene	
	$a^{\text{opx}}_{\text{Mg}}$	$a^{\text{opx}}_{\text{Fe}}$	$a^{\text{cpx}}_{\text{Mg}}$	$a^{\text{cpx}}_{\text{Fe}}$
Adirondack Pyroxenes				
J-35	0.477	0.696	0.604	0.622
J-44	0.331	0.807	0.447	0.753
J-66	0.542	0.639	0.676	0.546
J-80	0.527	0.652	0.673	0.550
J-81	0.538	0.642	0.669	0.554
J-103	0.413	0.746	0.553	0.670
J-105B	0.412	0.748	0.553	0.670
J-106	0.417	0.743	0.551	0.672
Madras Pyroxenes				
3709	0.788	0.357	0.866	0.271
4645	0.771	0.380	0.862	0.278
2270	0.681	0.494	0.791	0.393
2941	0.626	0.559	0.738	0.467
4642A	0.535	0.645	0.662	0.560




Figure 22. Activity-composition diagram for orthopyroxenes from the charnockitic granulites, using a simple solution model.




Figure 23. Activity-composition diagram for clinopyroxenes from the charnockitic granulites, using a simple solution model.

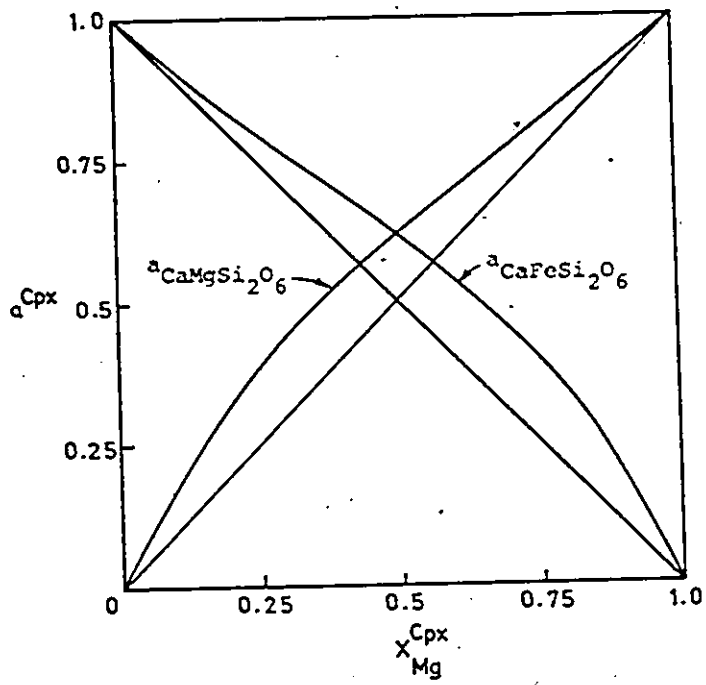
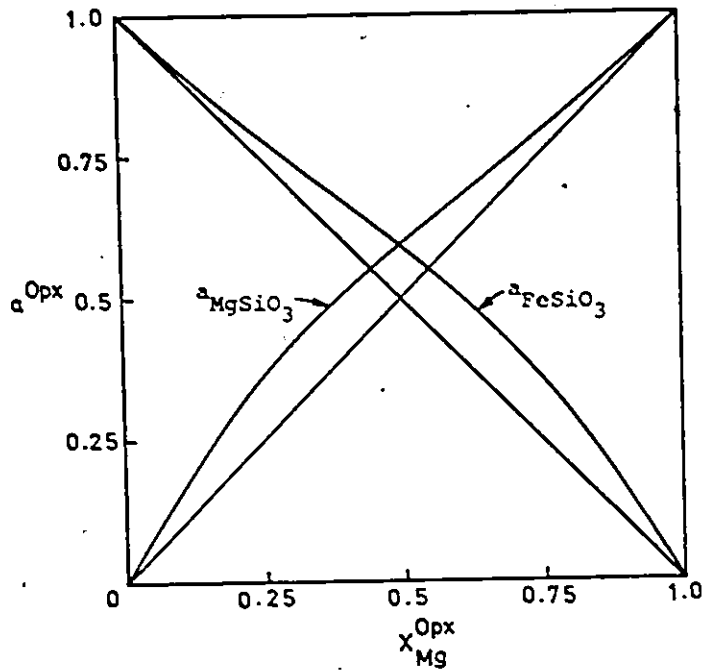


Figure 24. Mg-Fe²⁺ distribution diagram for the Adirondack pyroxenes (open circles), Madras pyroxenes (solid triangles, from Howie, 1955; Kretz, 1961), Quairading pyroxenes (dots, from Davidson, 1968) and high grade pyroxenes from Broken Hill (open circles with crosses, from Binns, 1962). Equilibrium constant is the same as in Fig. 21.

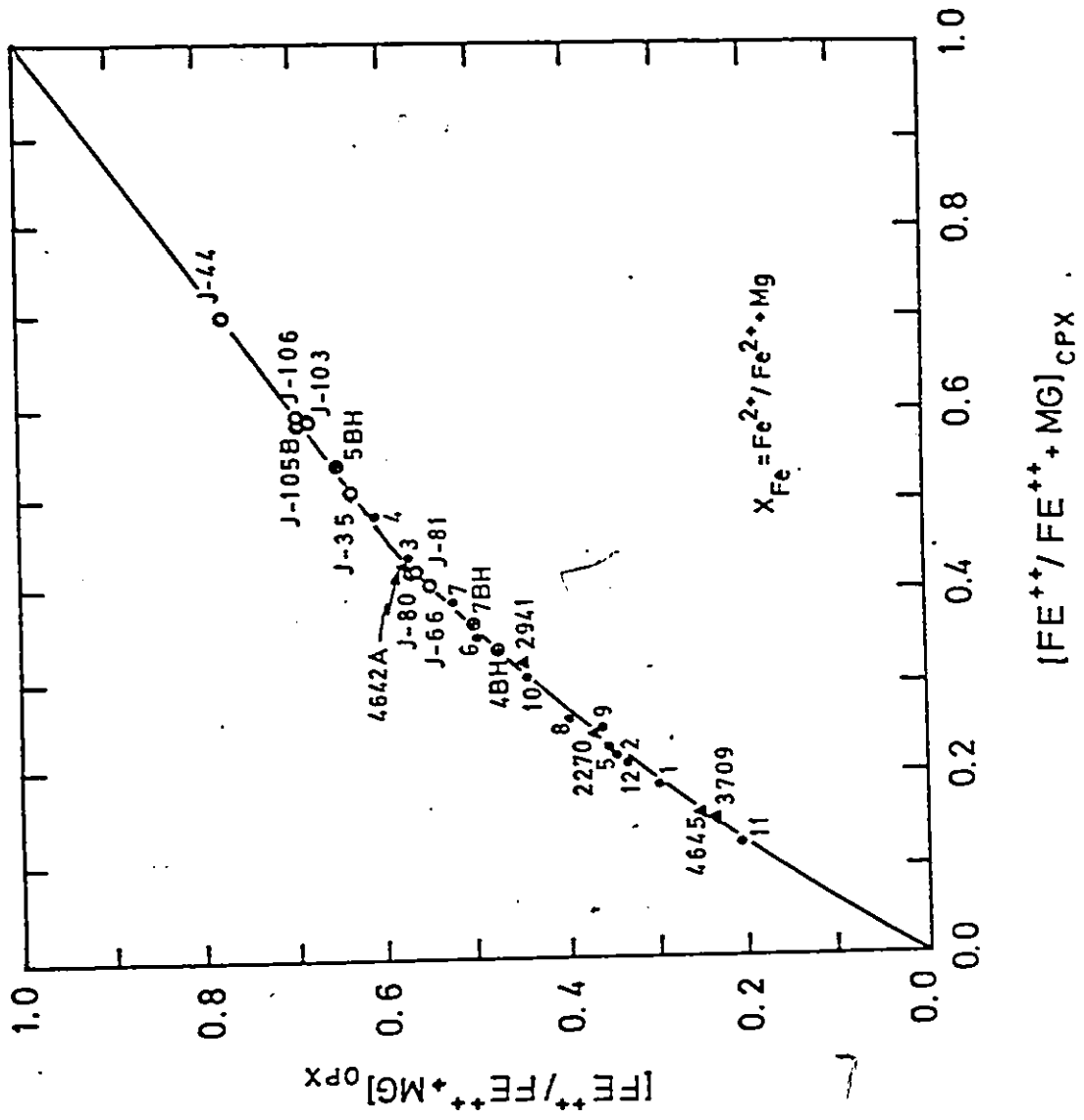
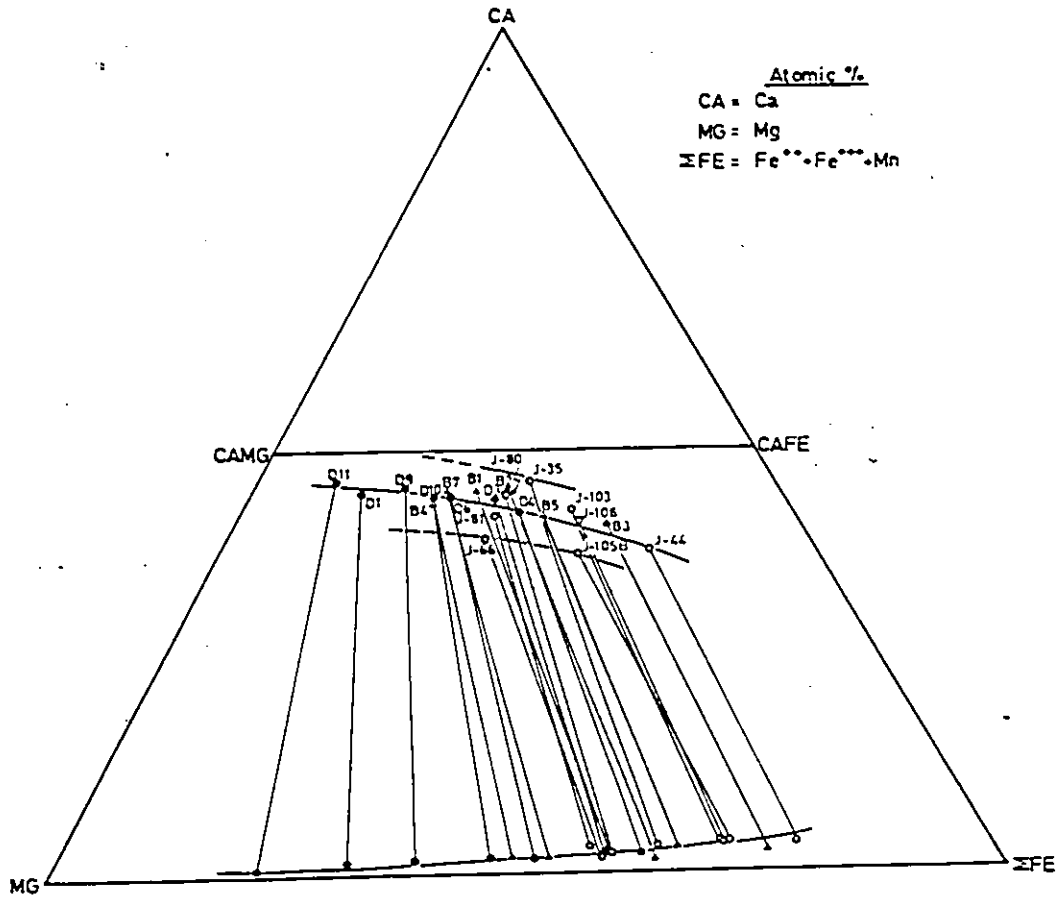


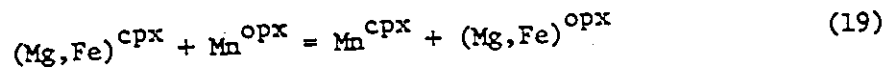
Figure 25. Coexisting orthopyroxene and clinopyroxene in the Ca-Mg-Fe system. Dots - Quairading pyroxenes (Davidson, 1968); solid triangles - lower grade Broken Hill pyroxenes (Binns, 1962); open triangles - higher grade Broken Hill pyroxenes (Binns, 1962); open circles - present data. The Kondapalli and Madras charnockites (Leelanandam, 1967) occupy the field covered by D11 to J-35.



pyroxene points has been interpreted by Davidson (1968) as resulting from differences in metamorphic grade. The charnockitic granulites of the present study were evidently equilibrated at a nearly uniform temperature and the vertical spread in these data points may be due to other factors such as analytical error, exsolution, or the effects of Al and Ti on the distribution of Ca between the minerals.

Distribution of Manganese Between Coexisting Orthopyroxene and Clinopyroxene

The general intercrystalline Mn - (Mg + Fe²⁺) exchange equilibrium between coexisting orthopyroxene and clinopyroxene may be treated in terms of a Mn-Mg exchange and a Mn-Fe exchange reaction or both of these may be combined as follows:



$$K(19) = \frac{a_{Mn}^{cpx} a_{Mg,Fe}^{opx}}{a_{Mg,Fe}^{cpx} a_{Mn}^{opx}} = \frac{X_{Mn}^{cpx} X_{Mg,Fe}^{opx}}{X_{Mg,Fe}^{cpx} X_{Mn}^{opx}} \cdot \frac{Y_{Mn}^{cpx} Y_{Mg,Fe}^{opx}}{Y_{Mg,Fe}^{cpx} Y_{Mn}^{opx}} \\ = \exp \frac{-\Delta G^{\circ}(19)}{RT} \quad (20)$$

where $X_{Mn} = Mn^{2+} / Mn^{2+} + Fe^{2+} + Mg$, and $a_{Mg,Fe}$ is an undefined activity, depending on the Mg/Fe ratio in the mineral (Kretz, 1961). Since X_{Mn}^{opx} and X_{Mn}^{cpx} are small, the distribution coefficient may be written as:

$$K_D(\text{Mn})^{\text{cpx/opx}} = \frac{X_{\text{Mn}}^{\text{cpx}}(1-X_{\text{Mn}}^{\text{opx}})}{(1-X_{\text{Mn}}^{\text{cpx}})X_{\text{Mn}}^{\text{opx}}} = \frac{X_{\text{Mn}}^{\text{cpx}}}{X_{\text{Mn}}^{\text{opx}}} \quad (21)$$

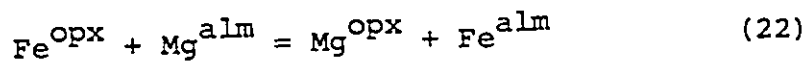
The distribution of Mn between pyroxene minerals of the present study is shown in Fig. 26; the mean distribution coefficient is 1.15:

$$K_D(\text{Mn})^{\text{opx/cpx}} = \frac{X_{\text{Mn}}^{\text{opx}}}{X_{\text{Mn}}^{\text{cpx}}} = 1.15$$

This diagram demonstrates that K_D (the expression containing the four activity coefficients in equation (20)) is independent of X_{Mn} and that equilibrium with respect to Mn-(Mg and Fe) exchange has been closely approached.

(II) DISTRIBUTION OF Mg, Fe²⁺, AND Mn BETWEEN COEXISTING ORTHOPYROXENE AND ALMANDINE

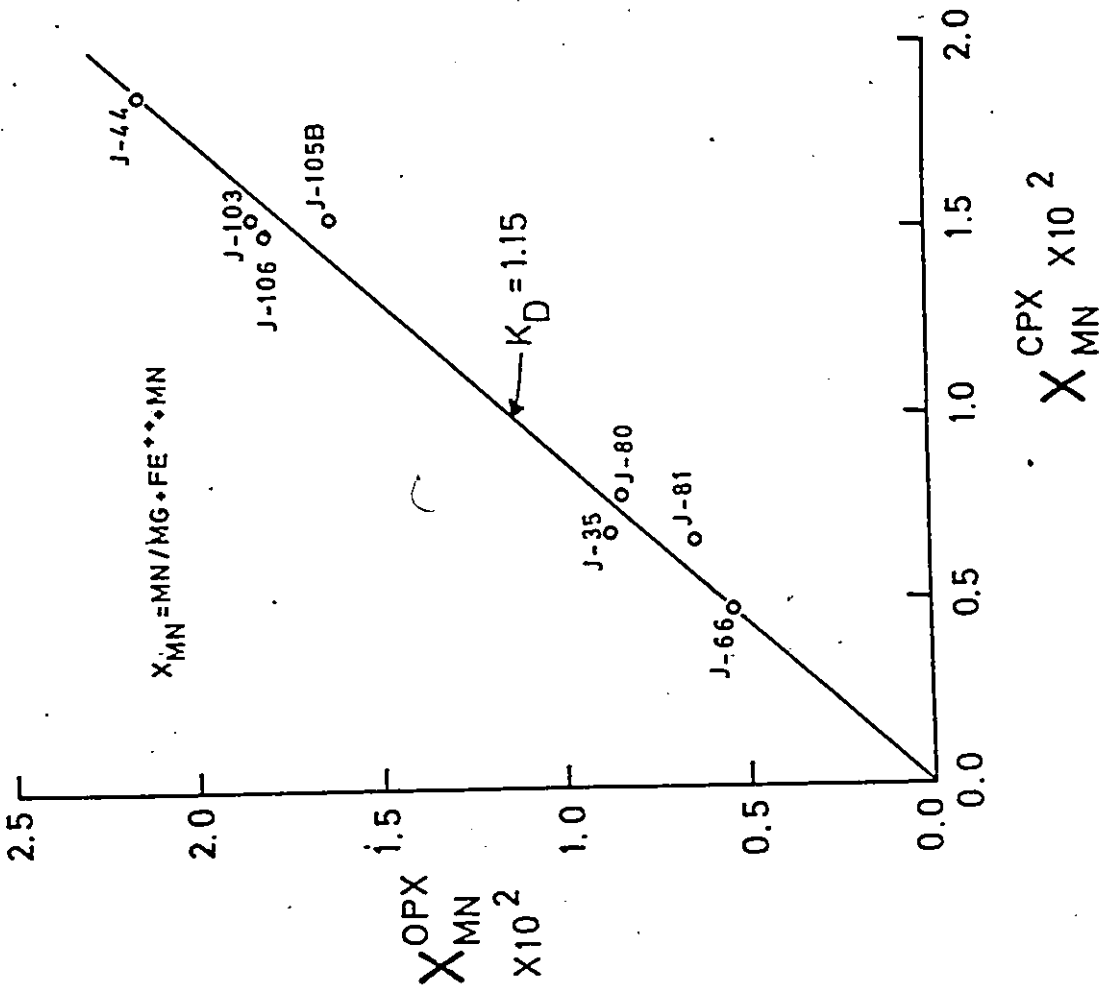
The Mg-Fe²⁺ exchange reaction for coexisting orthopyroxenes (opx) and almandine garnets (alm) (or (gar)) may be written as:



Assuming almandine (alm) is an ideal solid solution of Mg and Fe²⁺, then

$$K(22) = \frac{a_{\text{Mg}}^{\text{opx}} X_{\text{Fe}}^{\text{alm}}}{a_{\text{Fe}}^{\text{opx}} X_{\text{Mg}}^{\text{alm}}} = \exp \frac{-\Delta G^\circ(22)}{RT} \quad (23)$$

Figure 26. Distribution of Mn between coexisting orthopyroxene and clinopyroxene from the charnockitic granulites.



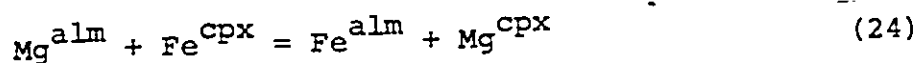
The distribution of Mg and Fe²⁺ between coexisting orthopyroxene and almandine in the rocks of the present study (and in a few additional rocks) is shown in Figs. 27 and 28. $K_D(\text{Mg})^{\text{opx}/\text{alm}}$ is nearly constant, with an average of 3.95. If almandine is assumed to be an ideal solution, an estimate of the equilibrium constant (K(22)) may be obtained by use of the activities for orthopyroxene that were derived previously. This yields a value of $K(22) = 4.59$. Departure from ideal mixing in one or both of the coexisting orthopyroxene and almandine is clearly shown in Fig. 28.

The distribution of Mn between orthopyroxene and almandine is shown in Fig. 29. Although the data points are somewhat scattered, most lie near a curve which follows the equation

$$K_D(\text{Mn}) = \frac{x_{\text{Mn}}^{\text{opx}}}{x_{\text{Mn}}^{\text{alm}}} = 0.21$$

(III) DISTRIBUTION OF Mg, Fe²⁺, AND Mn BETWEEN COEXISTING CLINOPYROXENE AND ALMANDINE

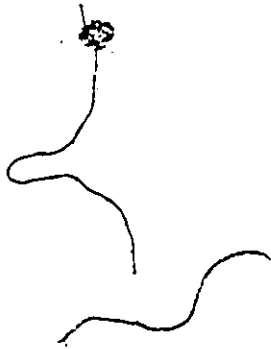
The Mg-Fe²⁺ exchange equilibrium for clinopyroxene and almandine may be expressed by the following exchange reaction:



Assuming almandine (alm) is an ideal mixture of Mg and Fe²⁺ end members, then:

$$K(24) = \frac{a_{\text{Mg}}^{\text{cpx}} x_{\text{Fe}}^{\text{alm}}}{a_{\text{Fe}}^{\text{cpx}} x_{\text{Mg}}^{\text{alm}}} = \exp \frac{-\Delta G^\circ(24)}{RT} \quad (25)$$

Figure 27. Distribution of Mg and Fe²⁺ between coexisting orthopyroxene and almandine garnet from the charnockitic granulites. Data from some Indian, Swedish and Ugandan charnockites and related granulites are included.



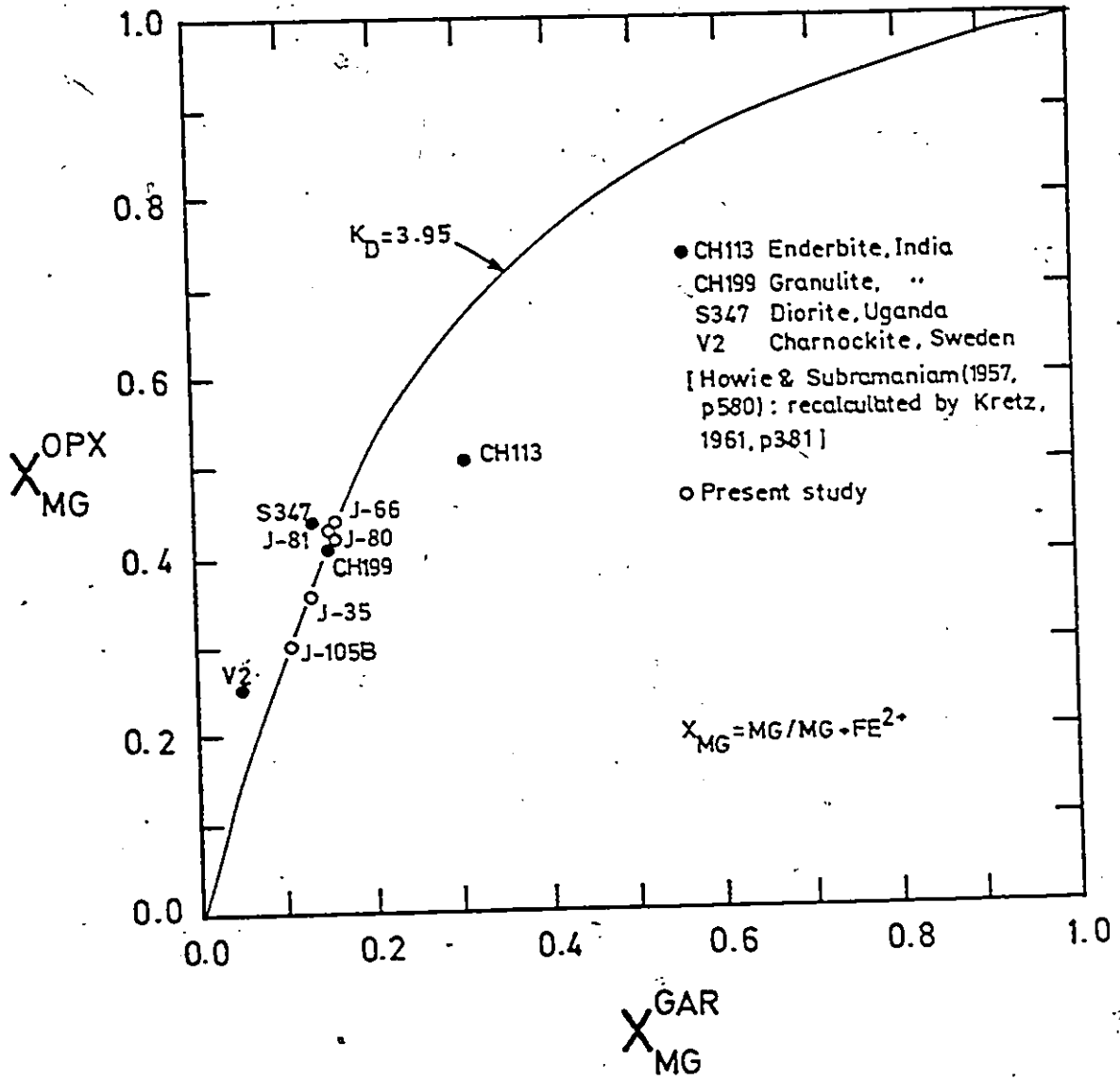


Figure 28. Distribution of Mg and Fe²⁺ between coexisting orthopyroxene and almandine garnet from the charnockitic granulites, in terms of a $(\frac{X}{1-X})_{\text{opx}}$ vs $(\frac{X}{1-X})_{\text{gar}}$ plot. Some Indian, Swedish and Ugandan charnockites and related granulites are also plotted. Source of data as in Fig. 27.

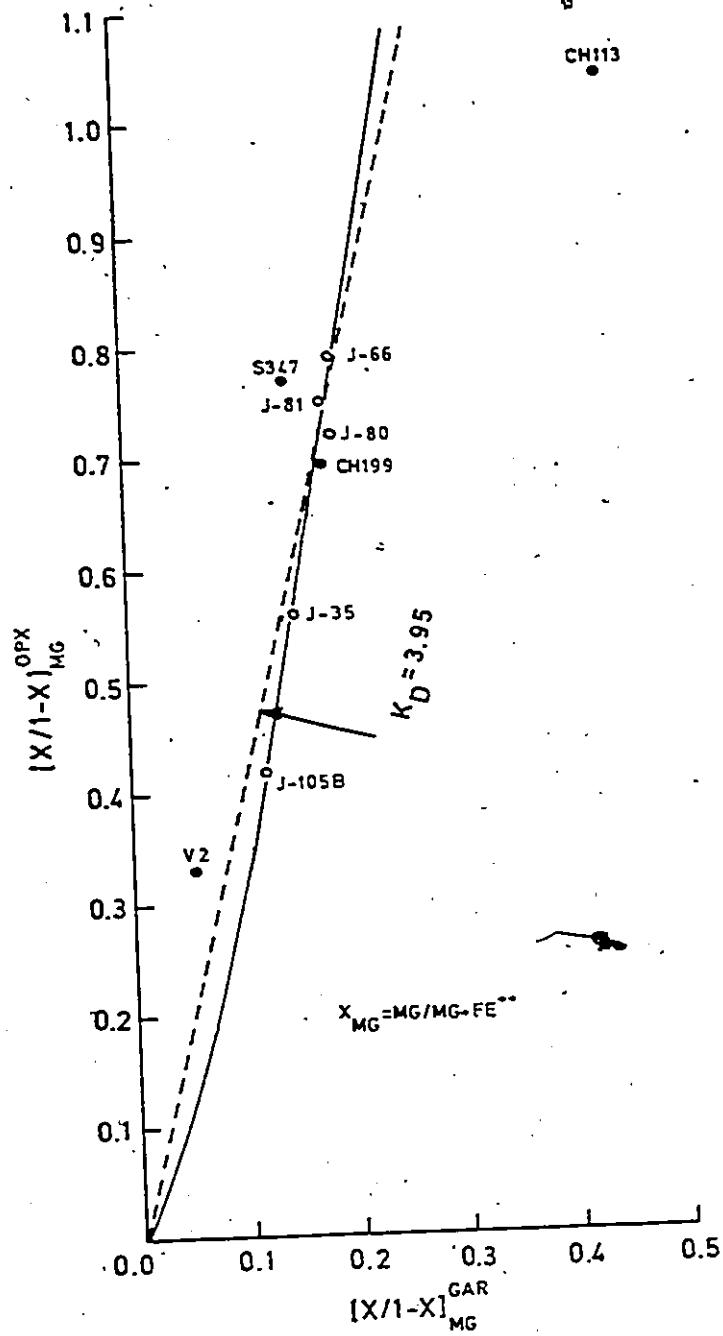
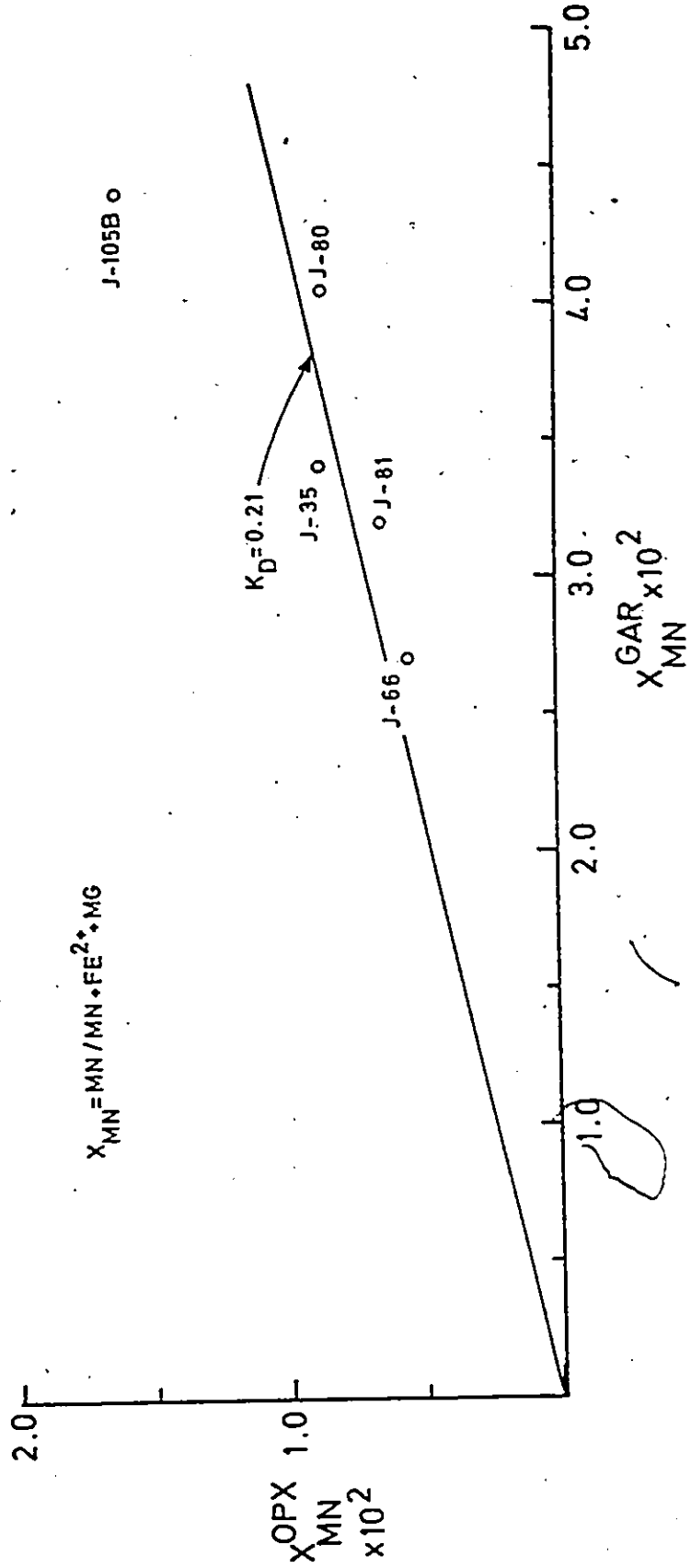


Figure 29. Distribution of Mn between coexisting orthopyroxene and almandine garnet from the charnockitic granulites.



L

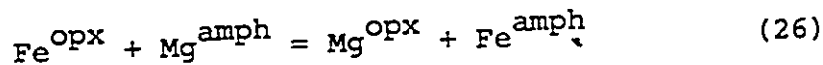
The distribution of Mg and Fe²⁺ between these two phases is shown in Figs. 30 and 31. For all mineral pairs except J-50, $K_D(\text{Mg})^{\text{cpx/alm}}$ is nearly constant with an average value of 6.95. An estimate of K(24) may be obtained by use of the activities for clinopyroxene that were derived previously. This yields a value of $K(24) = 6.62$.

The distribution of Mn between clinopyroxene and almandine is shown in Fig. 32. All the distribution points save J-105B fall near the curve $K_D(\text{Mn}) = 0.20$.

Two aberrant distributions have appeared, namely Mg-Fe in sample J-50 and Mn-(Mg,Fe) in sample J-105B. These may be attributed to analytical error (other than lack of precision) or alternatively, to departure from exchange equilibrium.

(IV) DISTRIBUTION OF Mg, Fe²⁺, AND Mn BETWEEN COEXISTING ORTHOPYROXENE AND AMPHIBOLE

The Mg-Fe²⁺ exchange reaction between coexisting orthopyroxene (opx) and amphibole (amph) may be expressed as follows:



Assuming that the amphiboles are ideal solutions of the Mg and Fe²⁺ end members:

$$K(26) = \frac{a_{\text{Mg}}^{\text{opx}} x_{\text{Fe}}^{\text{amph}}}{a_{\text{Fe}}^{\text{opx}} x_{\text{Mg}}^{\text{amph}}} = \exp \frac{-\Delta G^\circ(26)}{RT} \quad (27)$$

Figure 30. Distribution of Mg and Fe²⁺ between coexisting clinopyroxene and almandine garnet from the charnockitic granulites.

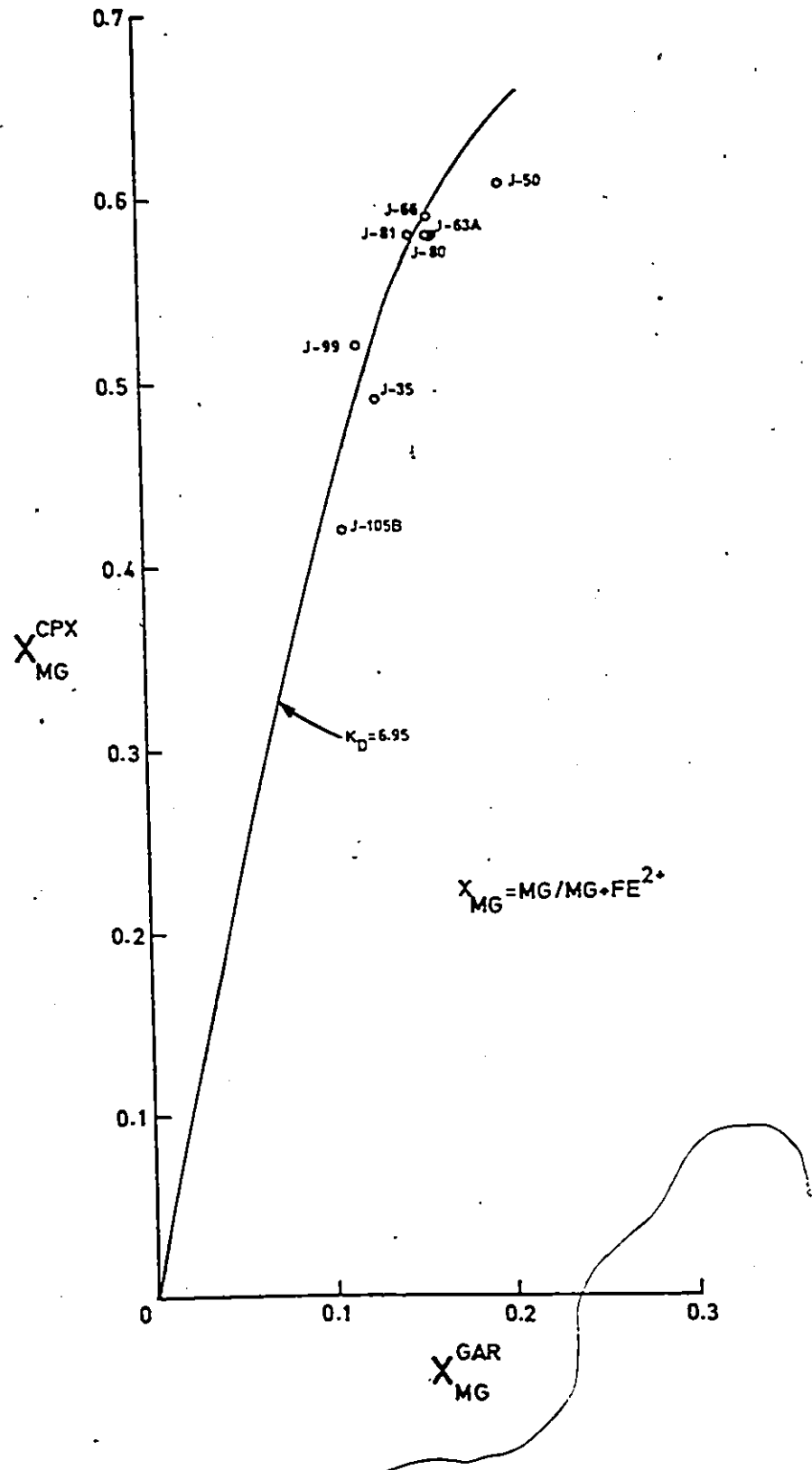


Figure 31. Distribution of Mg and Fe²⁺ between coexisting clinopyroxene and almandine garnet from the charnockitic granulites, in terms of a $\left(\frac{X}{1-X}\right)_{\text{cpx}}$ vs $\left(\frac{X}{1-X}\right)_{\text{gar}}$ Mg plot.



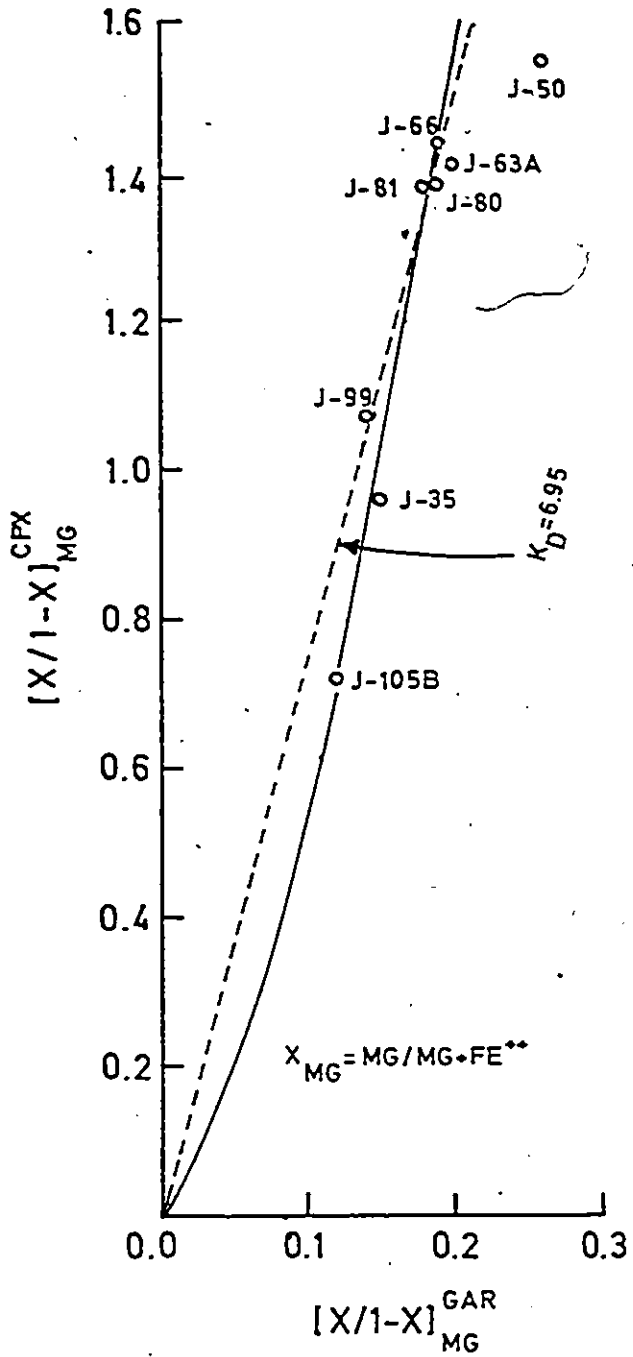
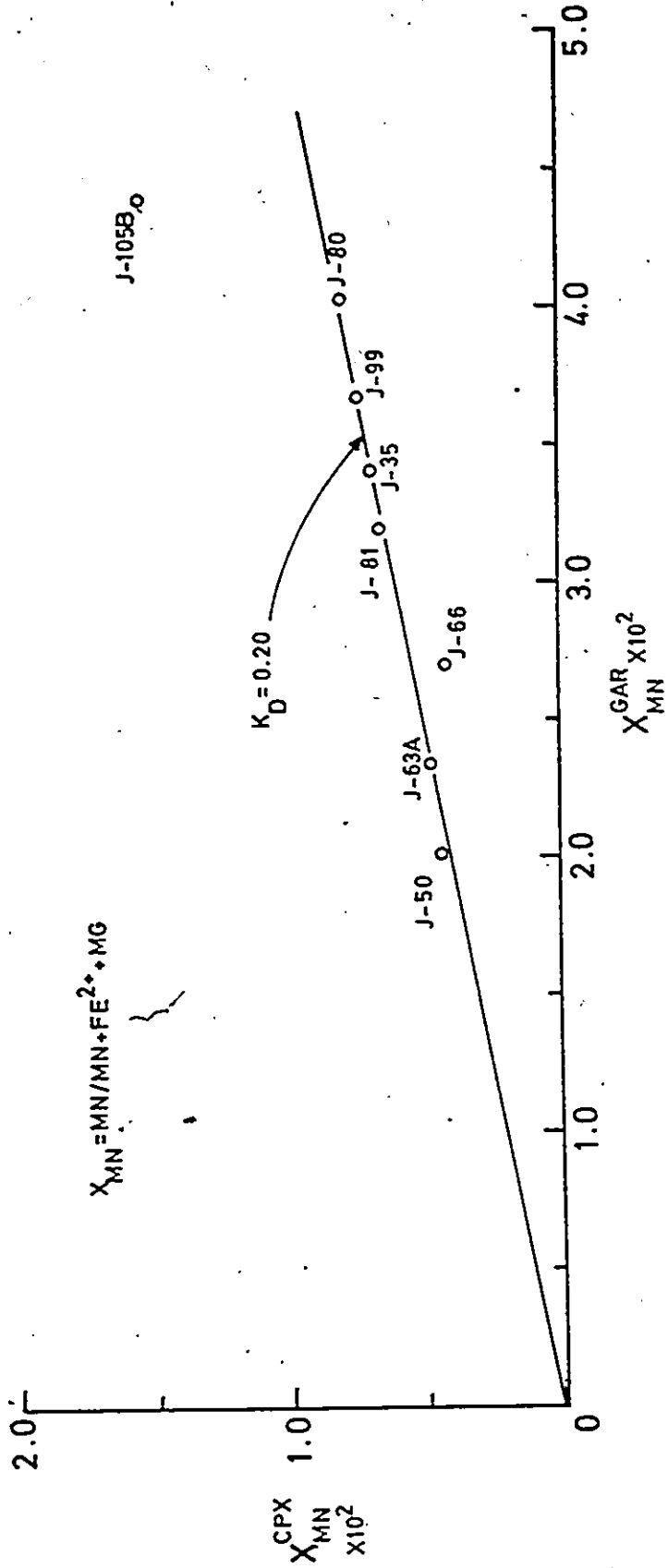


Figure 32. Distribution of Mn between coexisting clinopyroxene and almandine garnet from the charnockitic granulites.

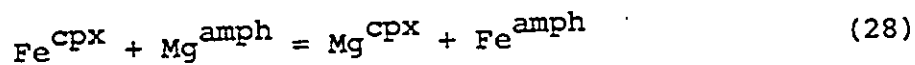


Data from the present study and from other charnockitic areas are shown in Figs. 33 and 34. The distribution coefficient is remarkably constant, at $K_D = 0.81$. An estimate of the equilibrium constant, from equation (27) and activities for orthopyroxene derived previously is $K(26) = 1.03$. However, the very uniform value of K_D , suggests that both orthopyroxene and amphibole depart from ideal behaviour, in such a way that the expression containing the four activity coefficients remains independent of composition.

The distribution of Mn between orthopyroxene and amphibole is shown in Fig. 35. The Mn-(Mg,Fe) distribution coefficient in all specimens is very nearly 2.18.

(V) DISTRIBUTION OF Mg, Fe²⁺, AND Mn BETWEEN COEXISTING CLINOPYROXENE AND AMPHIBOLE

The clinopyroxene-amphibole exchange equilibrium may be evaluated in terms of the reaction



Assuming amphiboles are ideal mixtures:

$$K(28) = K_D(\text{Mg}) = \frac{a_{\text{Mg}}^{\text{cpx}} x_{\text{Fe}}^{\text{amph}}}{a_{\text{Fe}}^{\text{cpx}} x_{\text{Mg}}^{\text{amph}}} = \exp \frac{-\Delta G^\circ(28)}{RT} \quad (29)$$

Figure 33. Distribution of Mg and Fe²⁺ between coexisting orthopyroxene and amphibole from the charnockitic granulites.

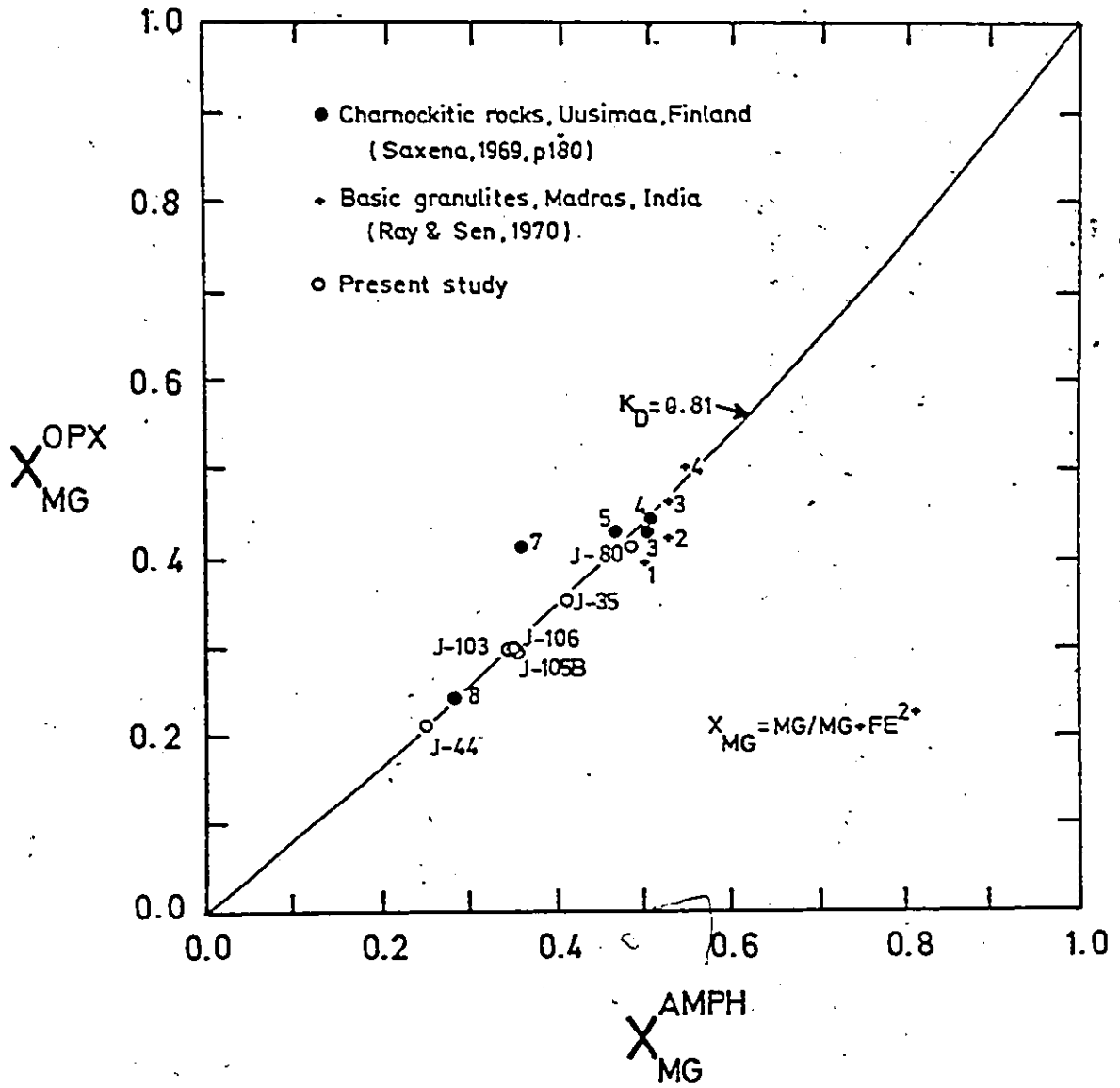
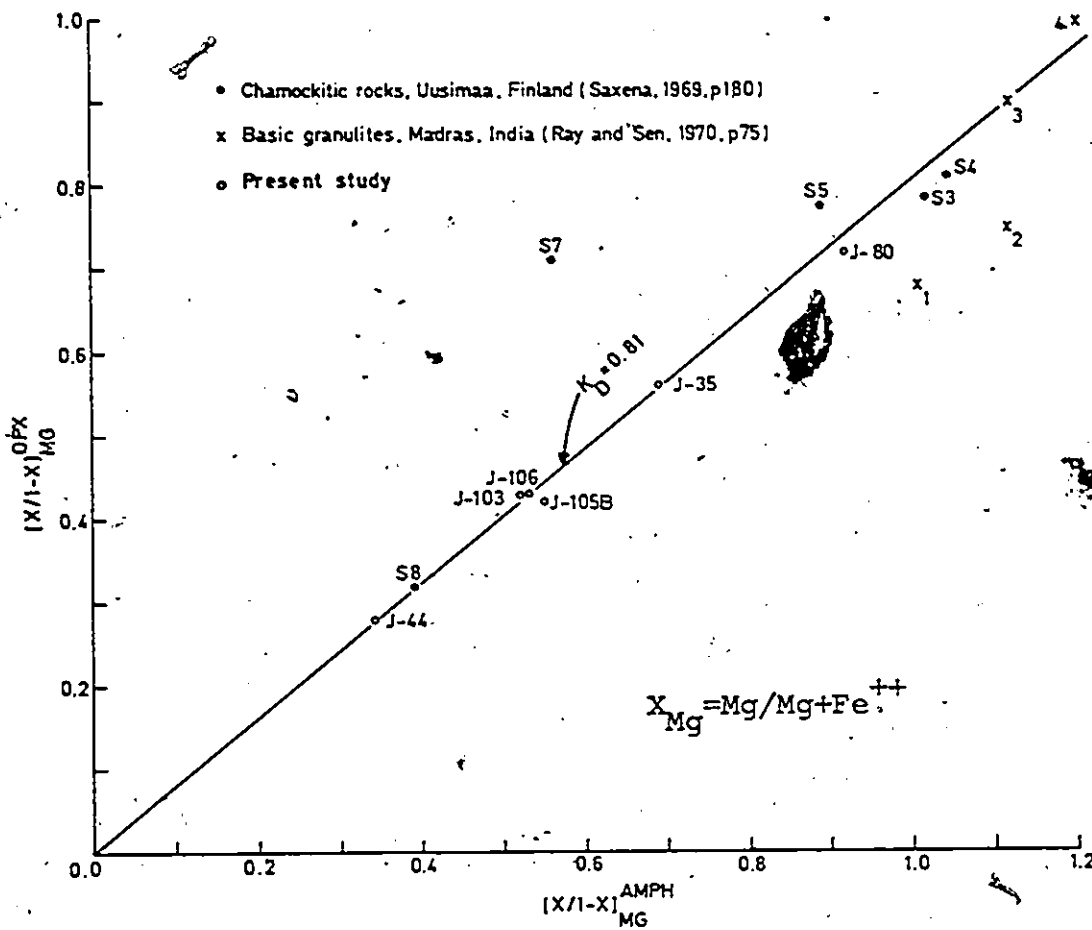


Figure 34. Distribution of Mg and Fe²⁺ between coexisting orthopyroxene and amphibole from the charnockitic granulites, in terms of a $\left(\frac{X}{1-X}\right)_{\text{opx}}$ vs $\left(\frac{X}{1-X}\right)_{\text{amph}}$ plot.





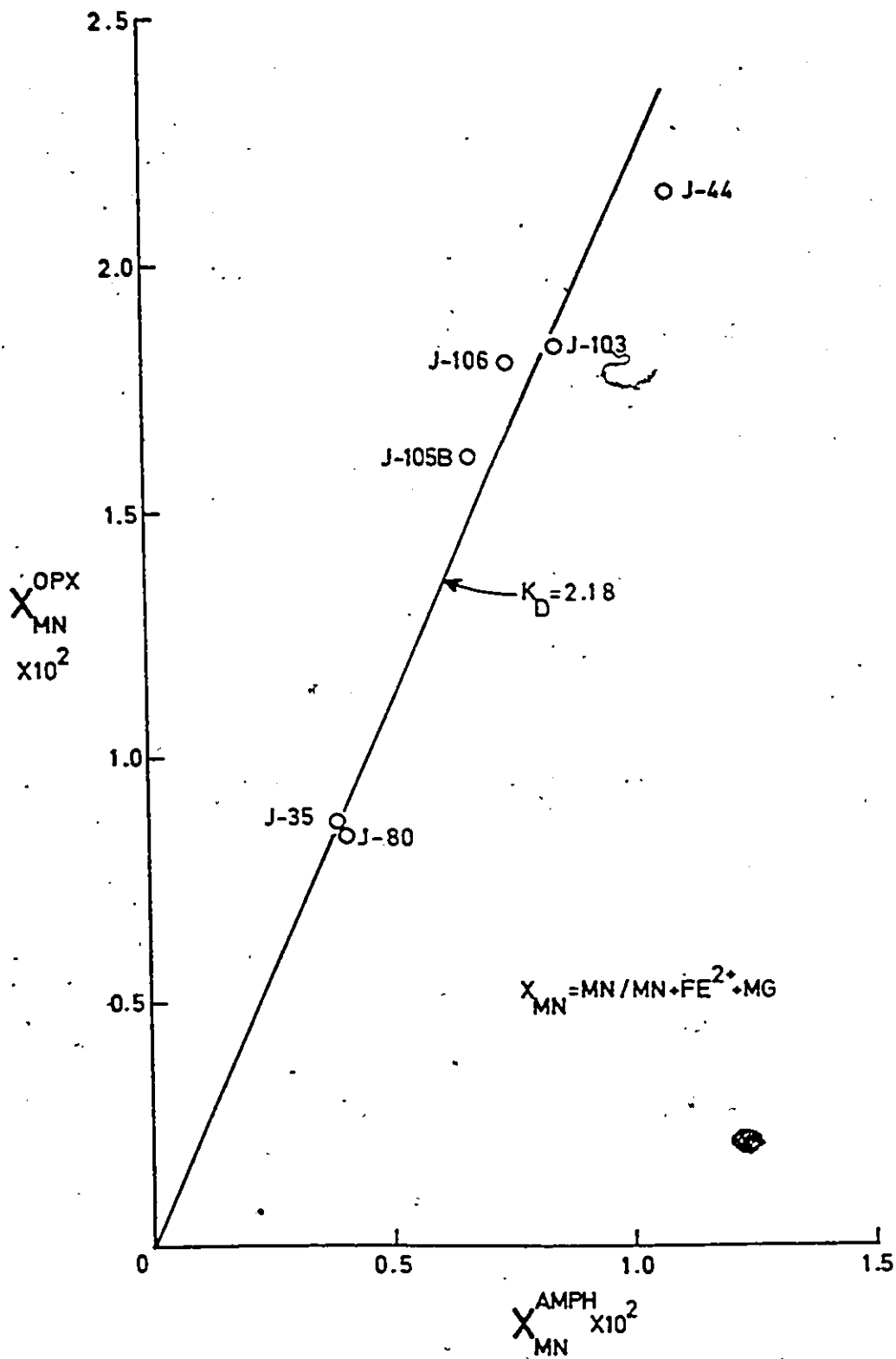


Figure 35. Distribution of Mn between coexisting orthopyroxene and amphibole from the charnockitic granulites.

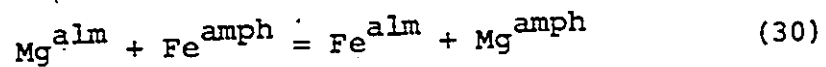




The distribution of Mg and Fe²⁺ in eight pairs of coexisting clinopyroxene and amphibole is shown in Figs. 36 and 37, which contain, in addition, some data from charnockitic rocks in Finland. The distribution coefficient is nearly constant at 1.40. An estimate of K(28), employing activities for clinopyroxene reported earlier in this chapter is 1.51. The distribution of Mn is shown in Fig. 38. The distribution coefficient for Mn-(Mg,Fe²⁺) exchange is remarkably constant, as shown in Fig. 38, with a mean value of 1.80.

(VI) DISTRIBUTION OF Mg, Fe²⁺, AND Mn BETWEEN COEXISTING ALMANDINE AND AMPHIBOLE

The distribution of Mg and Fe²⁺ between almandine and amphibole, may be evaluated by considering the reaction:



$$K(30) = \frac{a_{\text{Fe}}^{\text{alm}} a_{\text{Mg}}^{\text{amph}}}{a_{\text{Mg}}^{\text{alm}} a_{\text{Fe}}^{\text{amph}}} = \exp \frac{-\Delta G^{\circ}(30)}{RT} \quad (31)$$

The distribution of Fe²⁺ and Mg in five pairs of coexisting almandine and amphibole is shown in Figs. 39 and 40. The distribution coefficient is nearly constant, at 4.54.

Figure 36. Distribution of Mg and Fe²⁺ between coexisting clinopyroxene and amphibole from the charnockitic granulites.

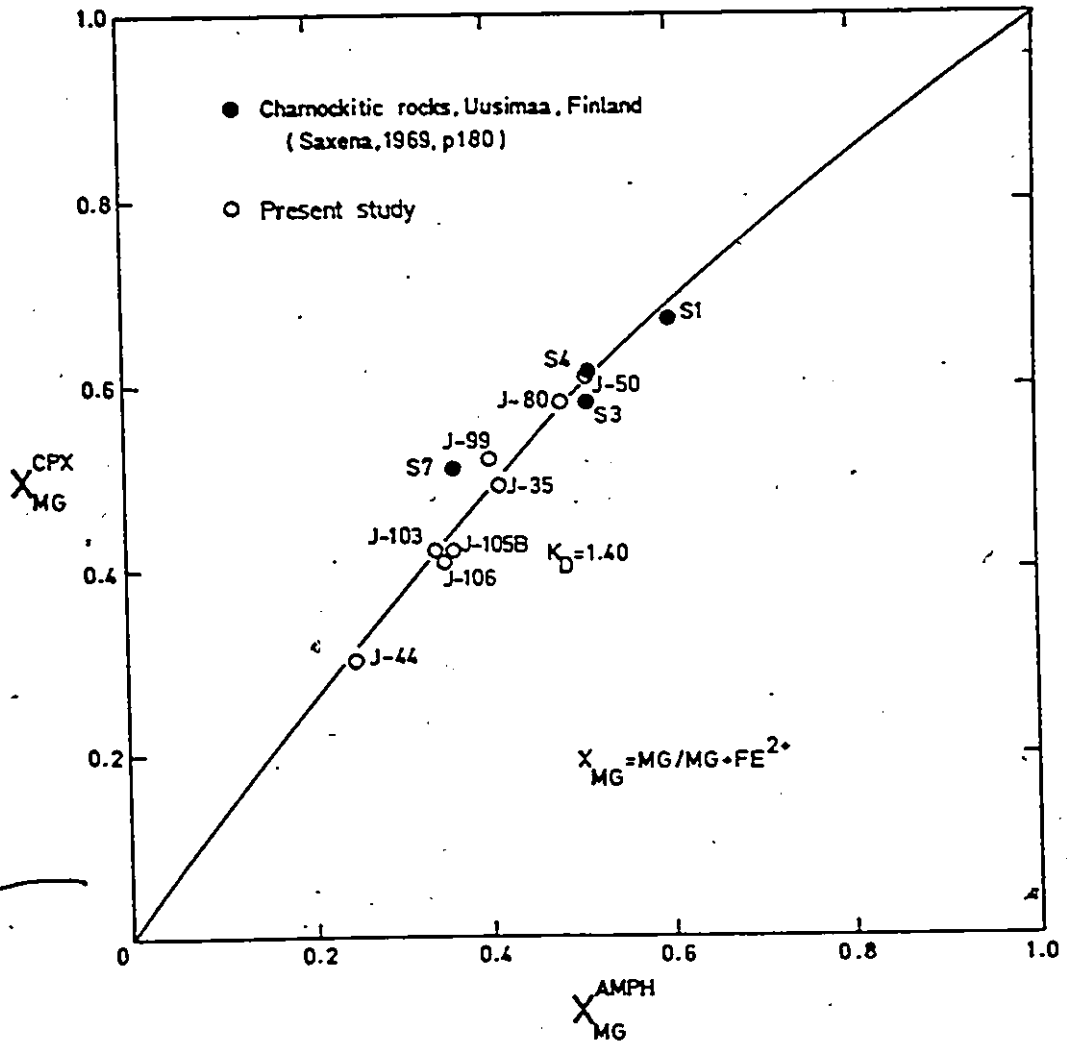


Figure 37. Distribution of Mg and Fe²⁺ between coexisting clinopyroxene and amphibole from the charnockitic granulites, in terms of a $\left(\frac{X}{1-X}\right)_{\text{cpx}}$ vs $\left(\frac{X}{1-X}\right)_{\text{amph}}$ Mg plot.

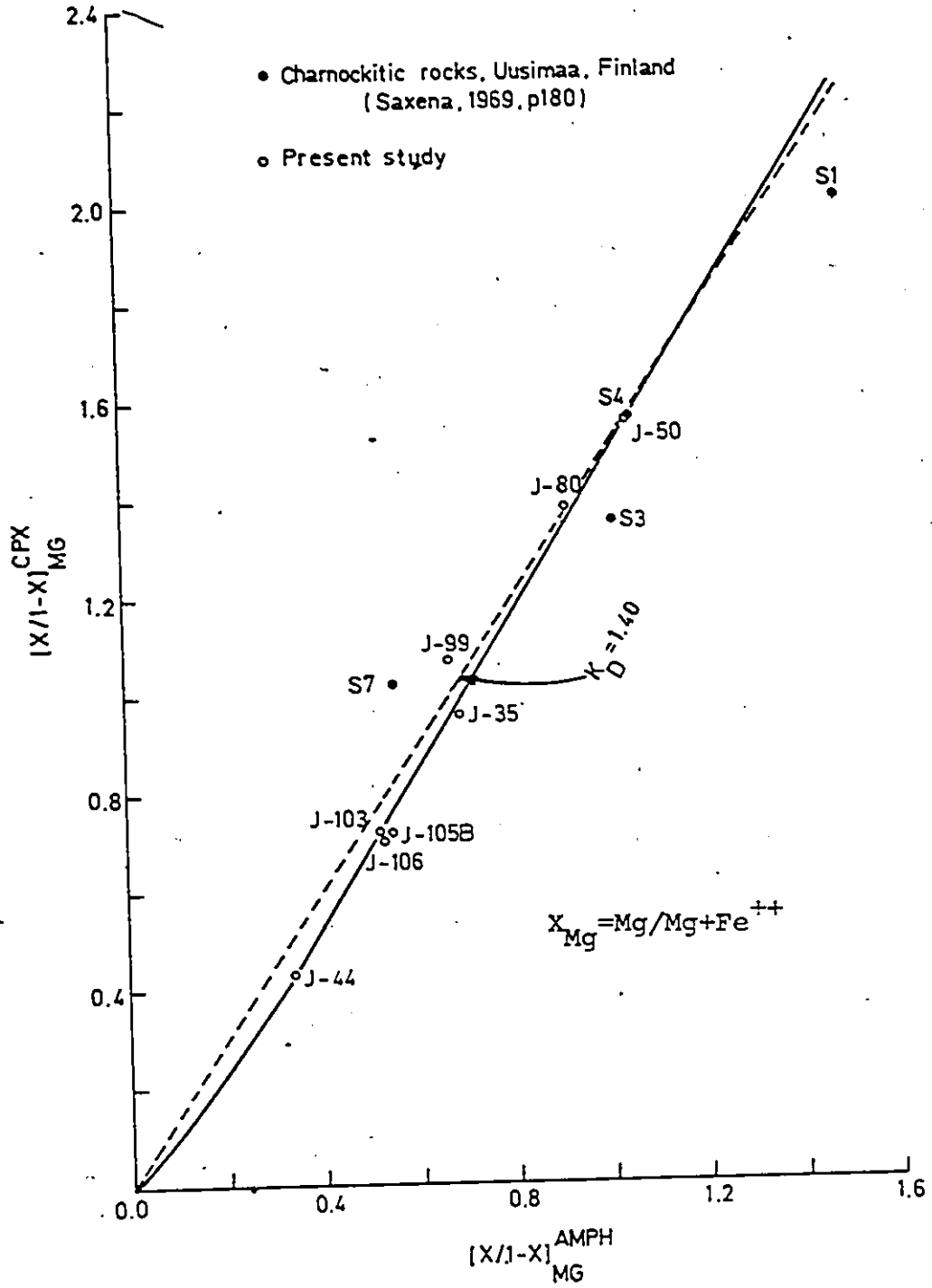
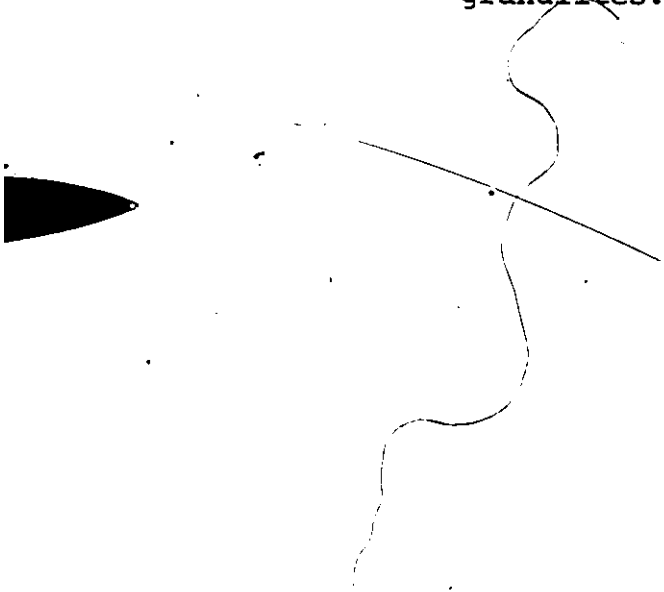


Figure 38. Distribution of Mn between coexisting clinopyroxene and amphibole from the charnockitic granulites.



89

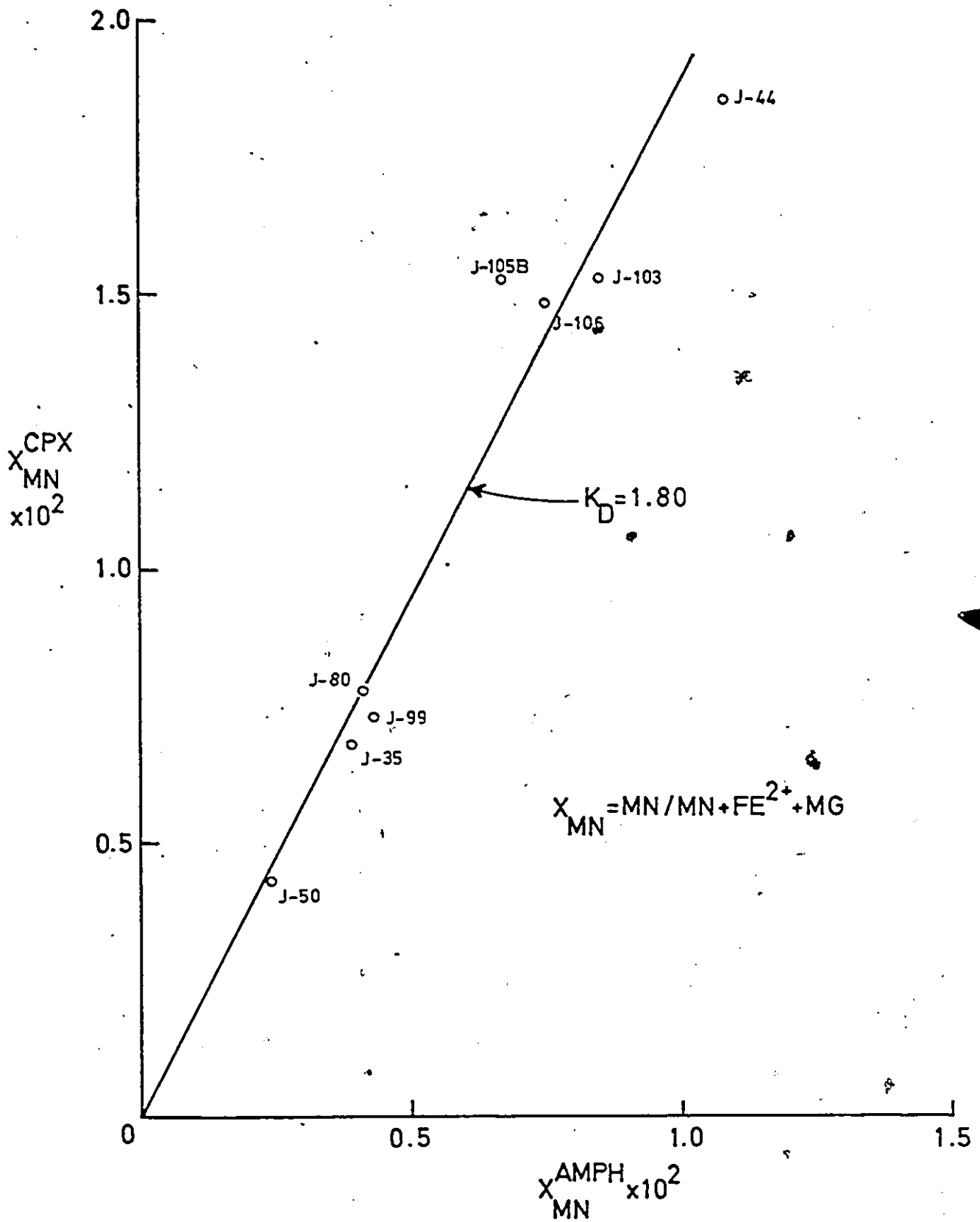


Figure 39. Distribution of Mg and Fe²⁺ between coexisting amphibole and almandine garnet from the charnockitic granulites.

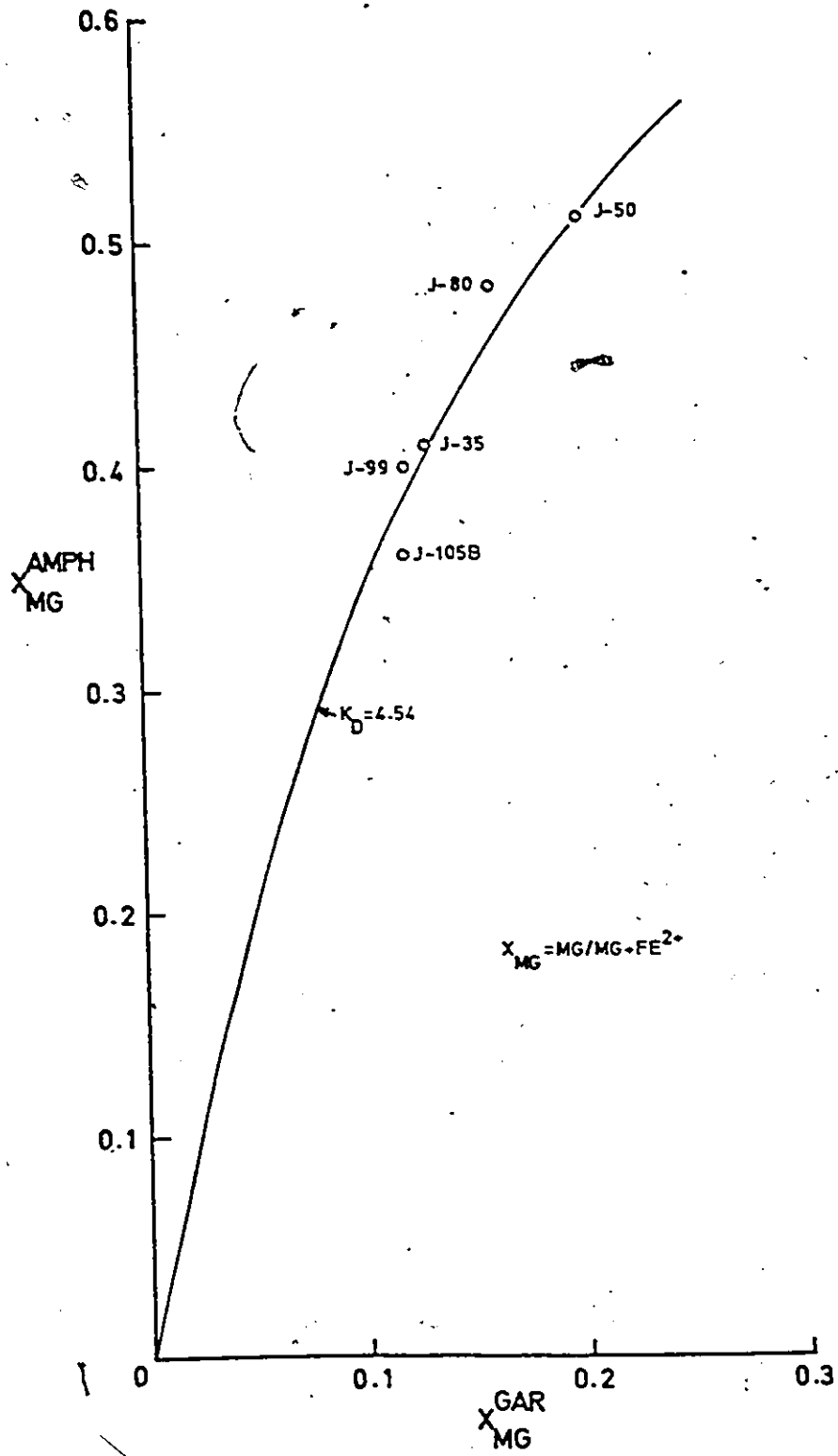
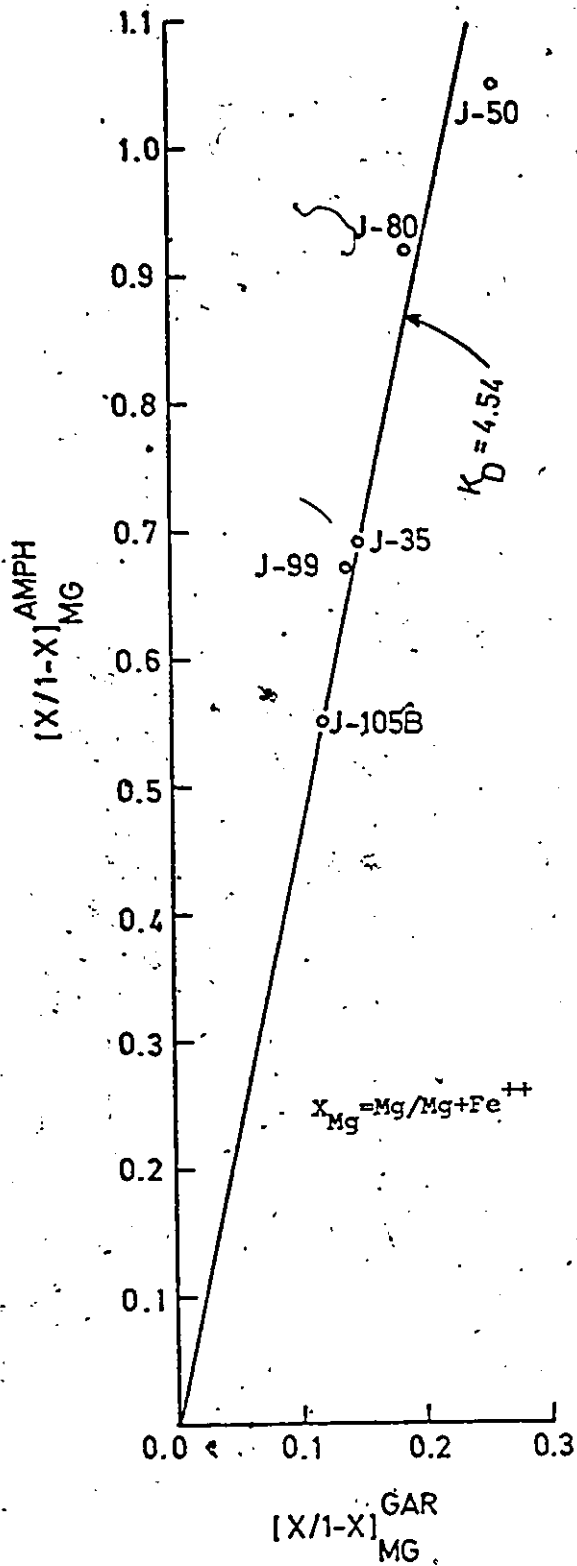


Figure 40. Distribution of Mg and Fe²⁺ between coexisting amphibole and almandine garnet from the charnockitic granulites, in terms of a $\left(\frac{X}{1-X}\right)_{\text{amph}}$ vs $\left(\frac{X}{1-X}\right)_{\text{gar}}$ plot.



The distribution of Mn between the two minerals is shown in Fig. 41. The Mn-(Mg,Fe²⁺) distribution coefficient is nearly constant, with a mean value of 8.54.

Summary

The above results show that the elements Mg, Fe²⁺, and Mn are systematically distributed among orthopyroxene, clinopyroxene, amphibole, and garnet within the charnockitic granulites of the present study. The stepwise decrease in the affinity a mineral possesses for an element is as follows:

Mg	clinopyroxene	amphibole	orthopyroxene	almandine
Fe ²⁺	almandine	orthopyroxene	amphibole	clinopyroxene
Mn	almandine	orthopyroxene	clinopyroxene	amphibole

Moreover, with very few exceptions, the concentration of an element in one mineral bears a functional relationship with that in a coexisting mineral. The existence of these relationships and their nature are consistent with expectations based on the principle of thermodynamic equilibrium, and are taken as indication that exchange equilibrium was established and preserved in the rocks of the study area.

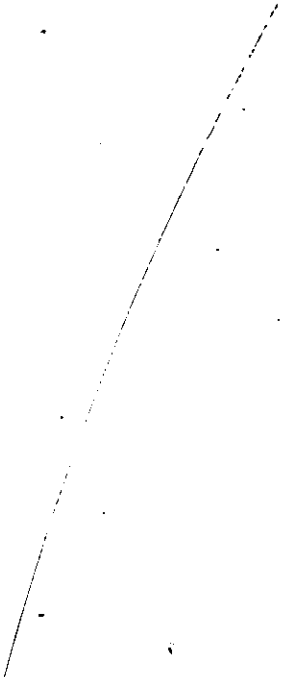

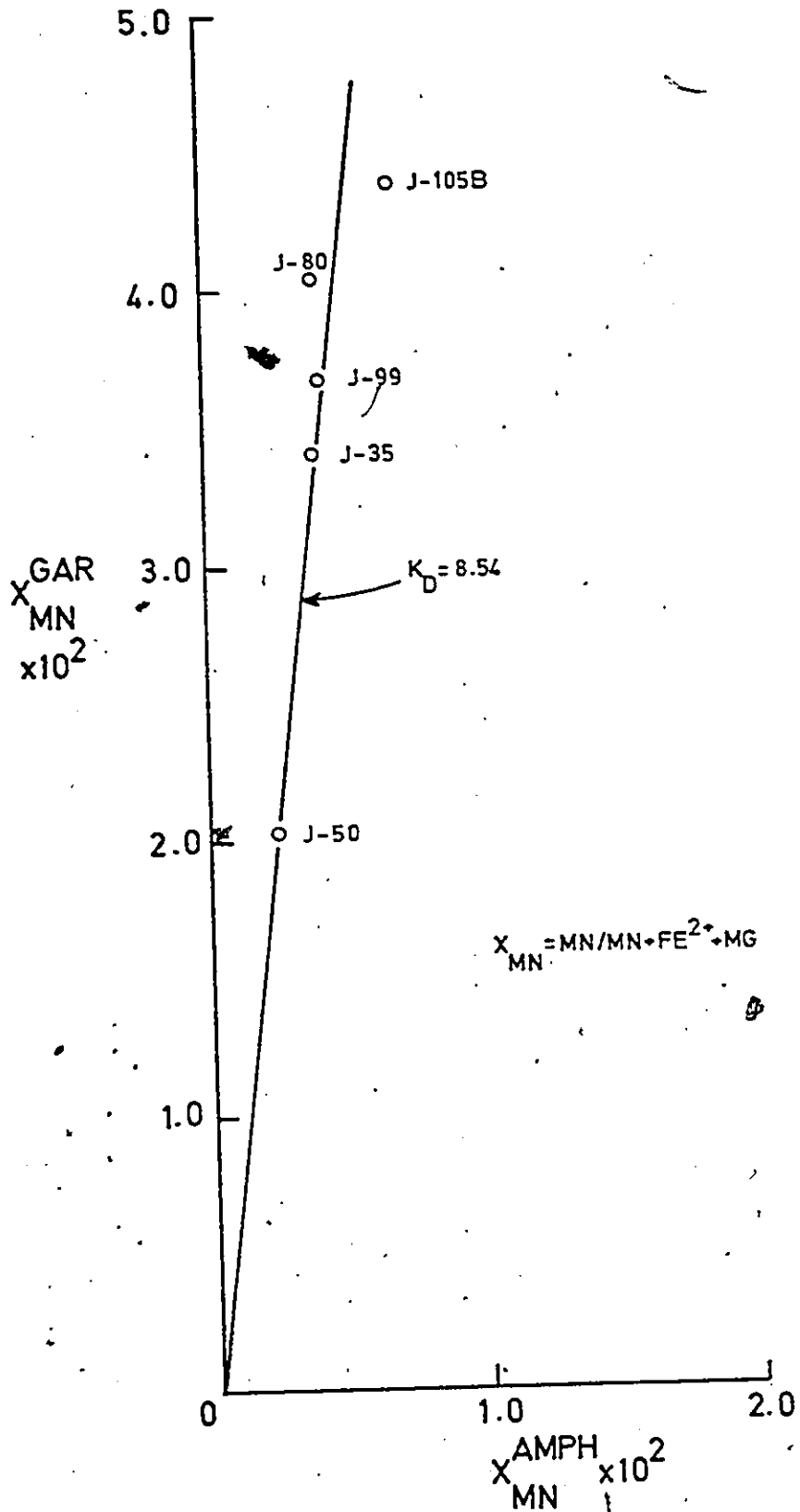


Figure 41. Distribution of Mn between coexisting amphibole and almandine garnet from the charnockitic granulites.





The nature of the distribution patterns are capable of providing some information on the properties of the mineral-solid solutions, notably the relationships between activity and concentration within them. For example, some activity-concentration relationships may be deduced for orthopyroxene and clinopyroxene, based on the distribution of Mg and Fe between them, and these indicate some departure from the ideal mixture model of solid solutions. More precise characterization of the nature of activity-concentration relationships [§] must come from direct experimental methods.

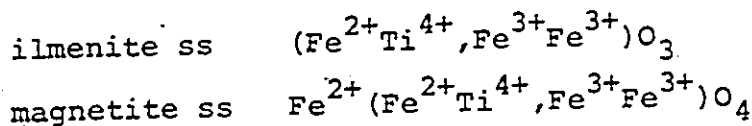
VIII DISTRIBUTION OF IRON AND TITANIUM BETWEEN
COEXISTING MAGNETITE AND ILMENITE

General Consideration

Ilmenite and magnetite are the chief iron oxides in the charnockitic granulites of the present study. Electron microprobe analyses (Table 10) shows that these minerals are solid solutions of iron and titanium oxides. Assuming that the ilmenite solid solution lies on the FeTiO_3 - Fe_2O_3 join and that the magnetite solid solution lies on the Fe_2TiO_4 - Fe_3O_4 join, the composition of the ilmenite solid solution (Ilm ss) may be expressed by the formula $(\text{FeTiO}_3, \text{Fe}_2\text{O}_3)$, and magnetite solid solution (Mt ss), as an inverse spinel, by $[\text{Fe}^{2+}(\text{Fe}^{2+}\text{Ti}^{4+})\text{O}_4, \text{Fe}^{3+}(\text{Fe}^{2+}\text{Fe}^{3+})\text{O}_4]$. These minerals may then be regarded as binary solid solutions, as shown in Fig. 42.

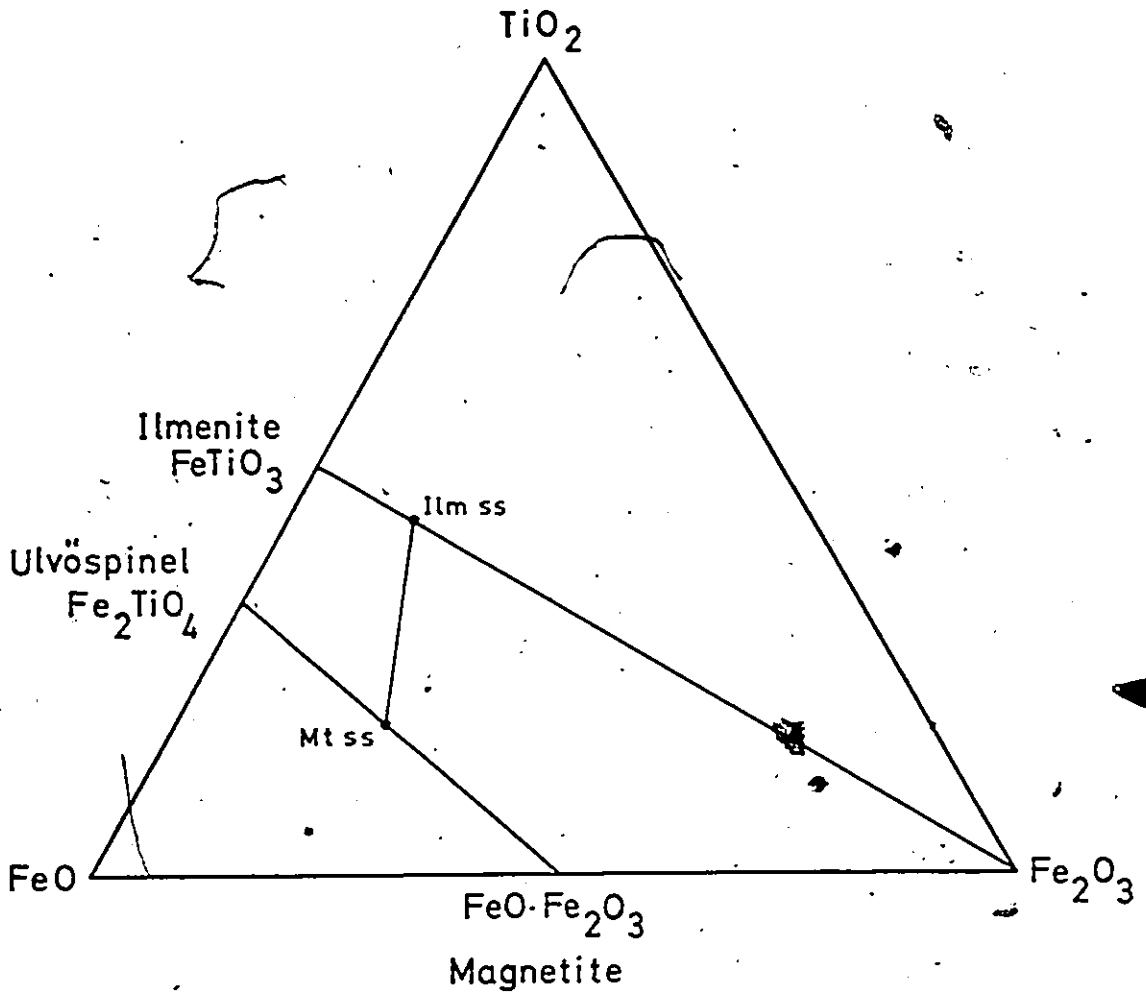
Phase Equilibrium

The formulas for ilmenite ss and magnetite ss, as written above, may be expressed in an alternate form, as follows:

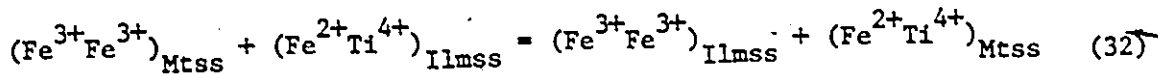


Consequently, equilibrium between coexisting ilmenite ss and magnetite ss, in relation to the 'slope' of the tie

Figure 42. Compositional relationships of ilmenite solid solutions (Ilm ss), magnetite solid solutions (Mt^{ss}) and their pure end member molecules in the system $\text{TiO}_2\text{-FeO-Fe}_2\text{O}_3$.



line in Fig. 42, may be regarded as an exchange reaction, involving species $Fe^{2+} Ti^{4+}$ and $Fe^{3+} Fe^{3+}$, as shown in Fig. 43. The reaction is as follows:



At equilibrium

$$\mu_{Fe^{3+} Fe^{3+}}^{Mtss} + \mu_{Fe^{2+} Ti^{4+}}^{Ilmss} = \mu_{Fe^{3+} Fe^{3+}}^{Ilmss} + \mu_{Fe^{2+} Ti^{4+}}^{Mtss} \quad (33)$$

$$K(32) = \frac{(a_{Fe^{3+} Fe^{3+}}^{Ilmss}) (a_{Fe^{2+} Ti^{4+}}^{Mtss})}{(a_{Fe^{3+} Fe^{3+}}^{Mtss}) (a_{Fe^{2+} Ti^{4+}}^{Ilmss})} = \exp \frac{-\Delta G^{\circ}(32)}{RT} \quad (34)$$

Differentiate equation (34) with respect to $1/T$

$$\frac{\partial \ln K(32)}{\partial (1/T)} = \frac{-\Delta H(32)}{R} \quad (35)$$

where ΔH is the enthalpy change of reaction (32). Equation (35) gives the temperature dependence of reaction (32) and indicates that the tie line in Fig. 42 should rotate in response to temperature.

Both minerals contain Fe^{2+} and Fe^{3+} , and the composition of coexisting ilmenite ss and magnetite ss is very much dependent on oxidation-reduction equilibrium. The effect of a change in temperature and a change in the fugacity of oxygen on the location of the tie line, based on observations in nature and experiment (Buddington and Lindsley, 1964, p313), is shown in a general way in Fig. 44.

VANDER BEEK LIBRARY

Figure 43. Exchange of iron and titanium ions between coexisting ilmenite solid solutions (Ilm ss) and magnetite solid solutions (Mt ss).

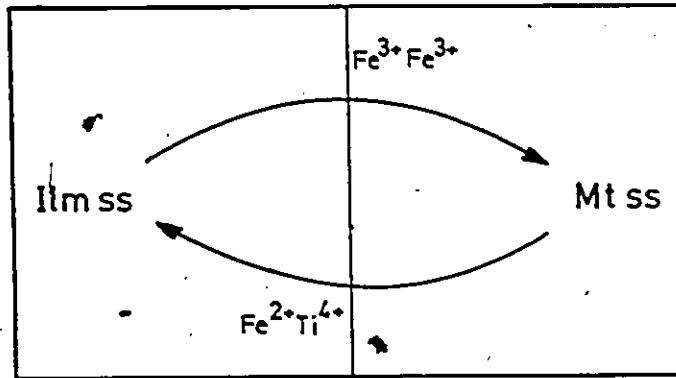


Figure 44. Shift and rotation of the ilmenite-magnetite tie line, in response to a change in temperature (T) and fugacity of oxygen (f_{O_2}), based on natural and experimental data. (Buddington and Lindsley, 1964).

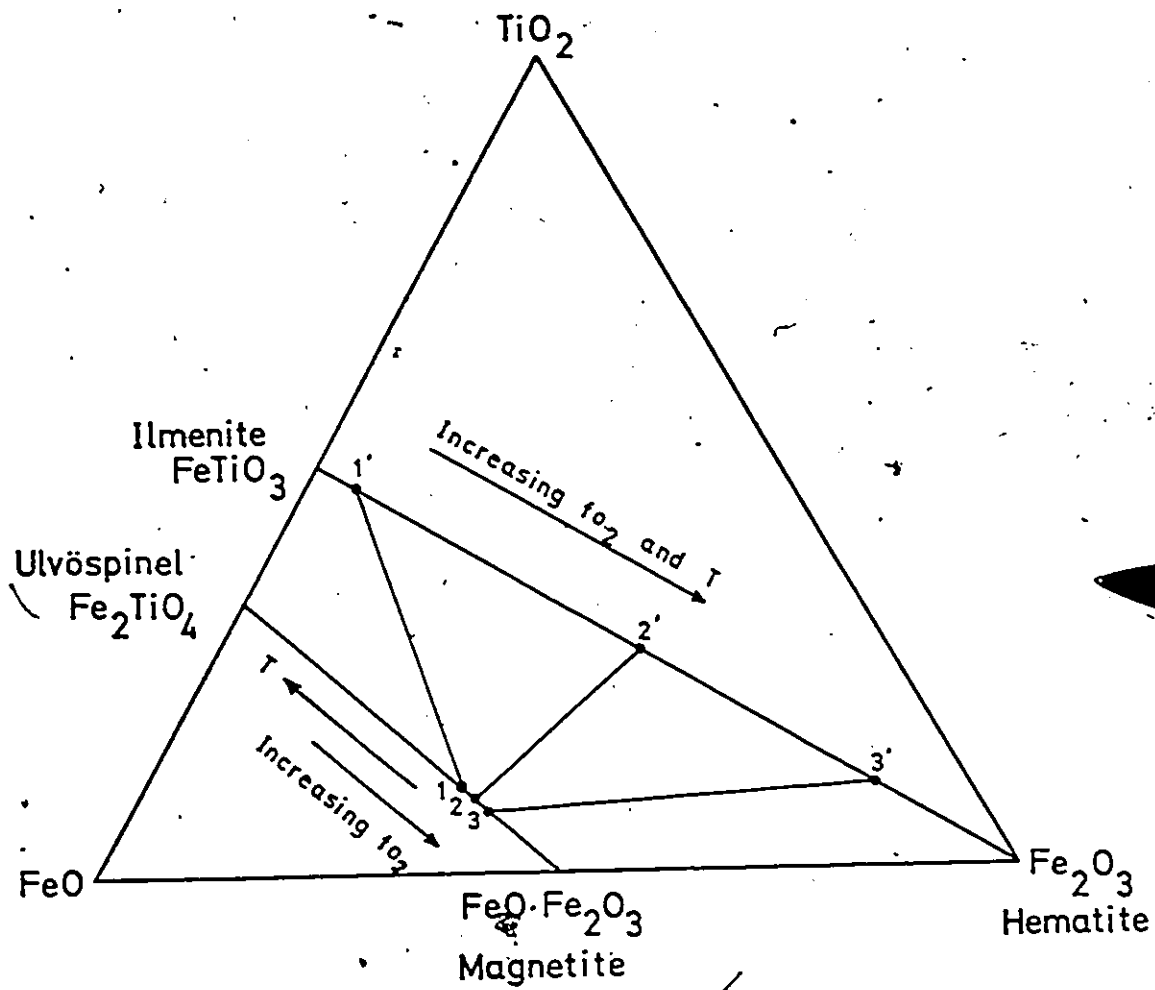


Fig. 45 shows the composition of coexisting ilmenite and magnetite solid solutions from the present charnockitic granulites, together with some published results from igneous and metamorphic rocks. The composition of ilmenite ss and of magnetite ss is very close to pure ilmenite and pure magnetite respectively.

Equilibrium data on the composition of coexisting magnetite and ilmenite were obtained by Buddington and Lindsley (1964) and are presented in Fig. 46. If we assume that an equilibrium between magnetite and ilmenite in the rocks of the present study was attained and retained, then by comparison with the experimental data, the equilibrium temperature was less than 600°C, and the equilibrium oxygen fugacity was less than $10^{-18.5}$ atm. However, it is well known that exsolution reaction involving these minerals occur rather readily, and it is possible that the temperature of metamorphism was higher than that indicated above, and the oxygen fugacity was higher or lower. It is surprising that, in Fig. 45, most of the tie lines do not cross each other, and this is taken as an evidence that an equilibrium or near-equilibrium was established at a temperature below and following the peak of metamorphism.

Data of the present study may be compared with those from Sudbury. Note that tie lines for the south range

Figure 45. Phase diagram showing compositional tie lines of coexisting ilmenite solid solutions (Ilm ss) and magnetite solid solutions (Mt ss) from the charnockitic granulites together with some published results for igneous and metamorphic rocks.

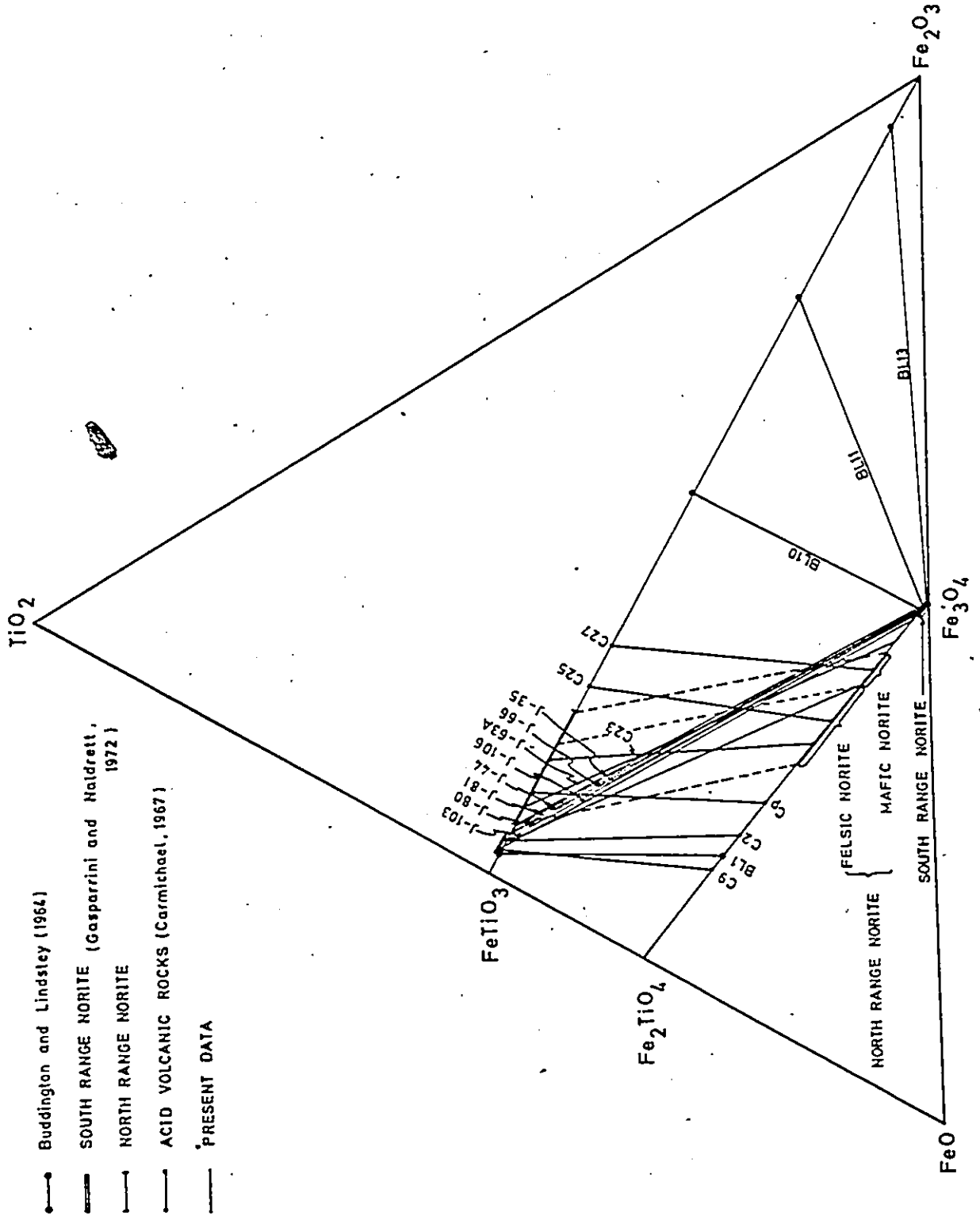
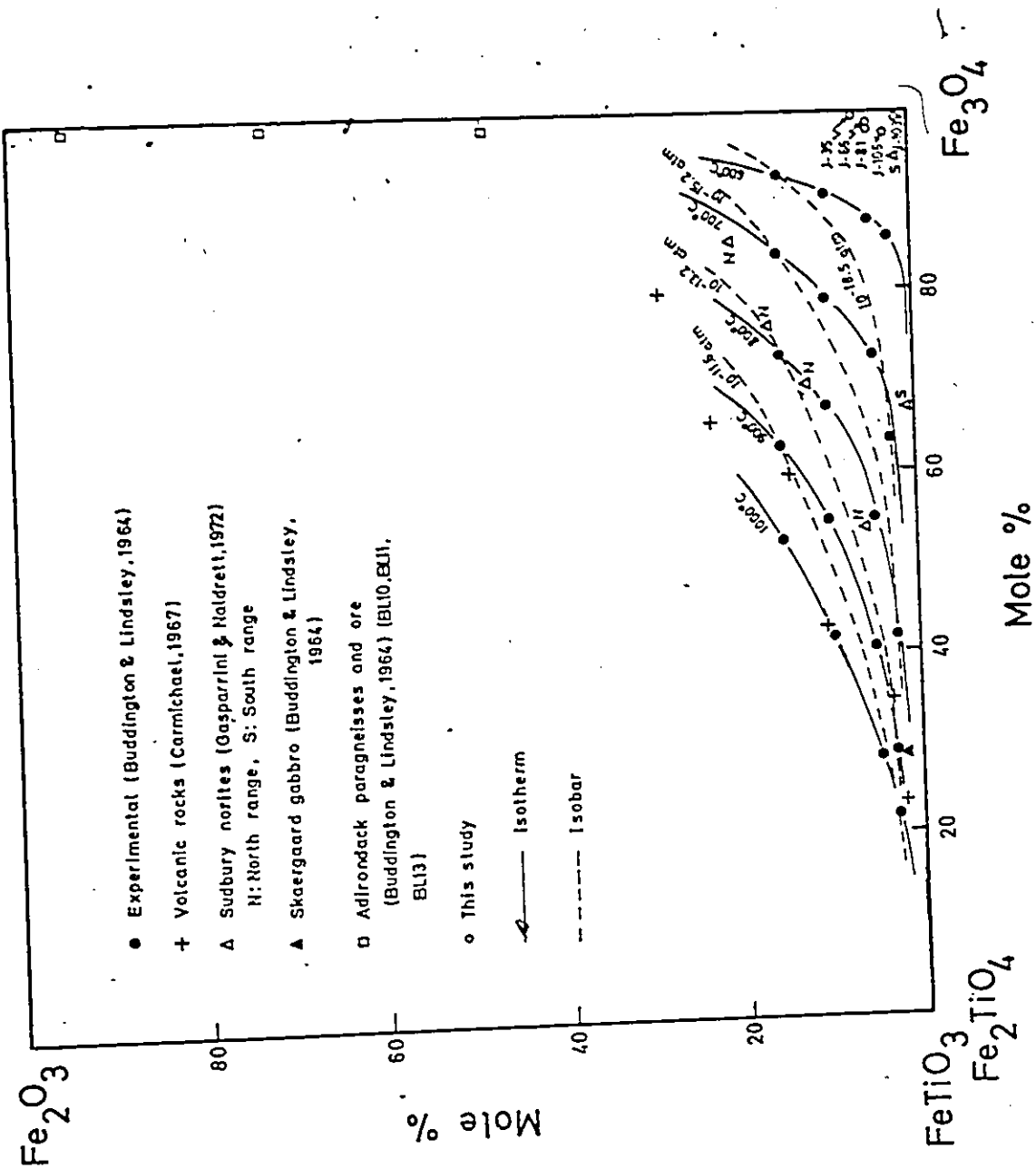


Figure 46. Composition of coexisting ilmenite solid solutions and magnetite solid solutions as determined experimentally by Buddington and Lindsley (1964, p316, 344) at varying temperature and fugacity of oxygen. $P = 1$ atm. Data from present study and other sources are included.



norites from the Sudbury Irruption (Gasparri and Naldrett, 1972) overlap those of the present study while both are crossed diagonally by tie lines of the Sudbury north range norites (Fig. 45). The north range norites were interpreted as being part of a thin periphery which was cooled relatively rapidly with the result that reaction between oxides stopped at a high temperature. The south range, being a deeper and thicker portion of the Irruption, cooled more slowly, thus allowing the oxides to equilibrate to significantly lower temperatures (Gasparri and Naldrett, 1972, p620). If so, the Adirondack charnockitic granulites must have been equilibrated or re-equilibrated under relatively slow cooling conditions, comparable to those of the south range norites.

Sample J-35 of the present study was collected from the same outcrop as No. 133 of Buddington and Lindsley (1964, p337; also Buddington, 1952) who obtained for their specimen a temperature of $650 \pm 50^\circ\text{C}$, compared with $<600^\circ\text{C}$ for J-35. The difference may be attributed to analytical methods employed; probe analysis is more successful in avoiding small amounts of exsolved phase. According to Duchesne (1972) the temperatures determined for Adirondack rocks by Buddington and Lindsley are somewhat low and a temperature of about 700°C or slightly higher may be more realistic for the temperature of metamorphism.

PART 4

PHASE EQUILIBRIUM AND PETROGENESIS

Mineral Abbreviations Used in the Chemical Studies

Ab = albite	Meso-perth = meso-perthite
Alm = almandine	Mt = magnetite
Amph = amphibole	Olig = oligoclase
An = anorthite	Opx = orthopyroxene
Anti-perth = anti-perthite	Or = orthoclase
Bio = biotite	Perth = perthite
Cpx = clinopyroxene	Plag = plagioclase
Gar = garnet	Px = pyroxene
Hb = hornblende	Qtz = quartz
Ilm = ilmenite	2-feld = two-feldspar (plagioclase and K-feldspar)
K-feld = K-feldspar = K feld = K-f	2-px = two-pyroxene (ortho-and clino-pyroxene)

Compositions of Phases Used in Chemical Reactions

Ab = $\text{NaAlSi}_3\text{O}_8$
Alm = $(\text{Fe, Mg})_3 \text{Al}_2\text{Si}_3\text{O}_{12}$ or $\text{Ca}(\text{Fe, Mg})_5 \text{Al}_4\text{Si}_6\text{O}_{24}$
An = $\text{CaAl}_2\text{Si}_2\text{O}_8$
Bio = $\text{K}_2(\text{Fe, Mg})_{5\frac{1}{2}} \text{Al}_3\text{Si}_{5\frac{1}{2}}\text{O}_{20}(\text{OH})_4$
Cpx = $\text{Ca}(\text{Fe, Mg})\text{Si}_2\text{O}_6$
Hb = $\text{NaCa}_2(\text{Fe, Mg})_4 \text{Al}_3\text{Si}_6\text{O}_{22}(\text{OH})_2$
Opx = $(\text{Fe, Mg})\text{SiO}_3$
Or = KAlSi_3O_8
Plag = $\text{NaAlSi}_3\text{O}_8 + \text{CaAl}_2\text{Si}_2\text{O}_8$
Qtz = SiO_2

IX PHASE EQUILIBRIUM, METAMORPHIC GRADE, AND ORIGIN

Phase Equilibrium

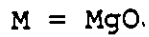
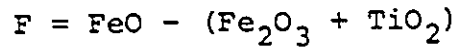
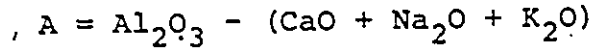
The charnockitic granulites of the present study are characterized by the following silicate mineral assemblages:

1. Plag- Opx- Cpx- Amph- Bio- Gar- Qtz (J-35, J-66, J-80)
2. Plag- K feld- Opx- Cpx- Amph- Bio- Qtz (J-44, J-103, J-106)
3. Plag- K feld- Opx- Cpx- Amph- Bio- Gar- Qtz (J-105B)
4. Plag- K feld- Opx- Cpx- Bio- Gar- Qtz (J-81, J-63A)
5. Plag- K feld- Cpx- Amph- Gar- Bio- Qtz (J-50)
6. Plag- Cpx- Amph- Bio- Gar- Qtz (J-99).

In addition most rocks contain magnetite, ilmenite, and apatite. All are typical granulite facies rocks. In terms of major mafic silicate minerals, four distinct assemblages exist, namely:

7. Opx- Cpx- Amph- Alm- Bio (J-35, J-66, J-80, J-105B)
8. Opx- Cpx- Alm- Bio (J-81, J-63A)
9. Opx- Cpx- Amph- Bio (J-44, J-103, J-106)
10. Cpx- Amph- Alm- Bio (J-50, J-99).

It is possible to represent all assemblages except 1 and 6 (which do not contain K-feldspar) on an AFM diagram using the following definitions of components (Reinhardt, 1968):



This diagram could be regarded as a phase diagram for rocks that contain quartz, K-feldspar, plagioclase (of fixed composition), magnetite and ilmenite, and for constant values of P, T, and $P_{\text{H}_2\text{O}}$. In order to plot the composition of clinopyroxene, it is convenient to employ an orthogonal projection (Thompson, 1957) with the following axes:

Vertical axis $\frac{A}{F+M}$

Horizontal axis $\frac{M}{F+M}$

The compositions of coexisting ferromagnesian silicate phases from the mineral assemblages studied are shown in Figs. 47 to 50. Assemblages in Figs. 47 to 49 represent univariant equilibrium at constant pressure and assemblages in Fig. 50 represent invariant equilibrium at constant pressure. The reason for plotting assemblages that do not apparently contain K-feldspar is because of the existence of trace to minor amounts of anti-perthitic feldspar in them. A systematic shift in phase fields indicate that rocks with the same mineral assemblages represent different equilibrium conditions. Moreover, the fact that all rocks contain 4 or 5 ferromagnesian minerals (including biotite) would, by the above analysis, indicate either non-equilibrium, or variation in metamorphic conditions.






Figure 47. Orthogonal AFM plot showing the phase relations among coexisting clinopyroxene, almandine garnet, and amphibole in the analysed charnockitic granulites along with the bulk rock compositions.



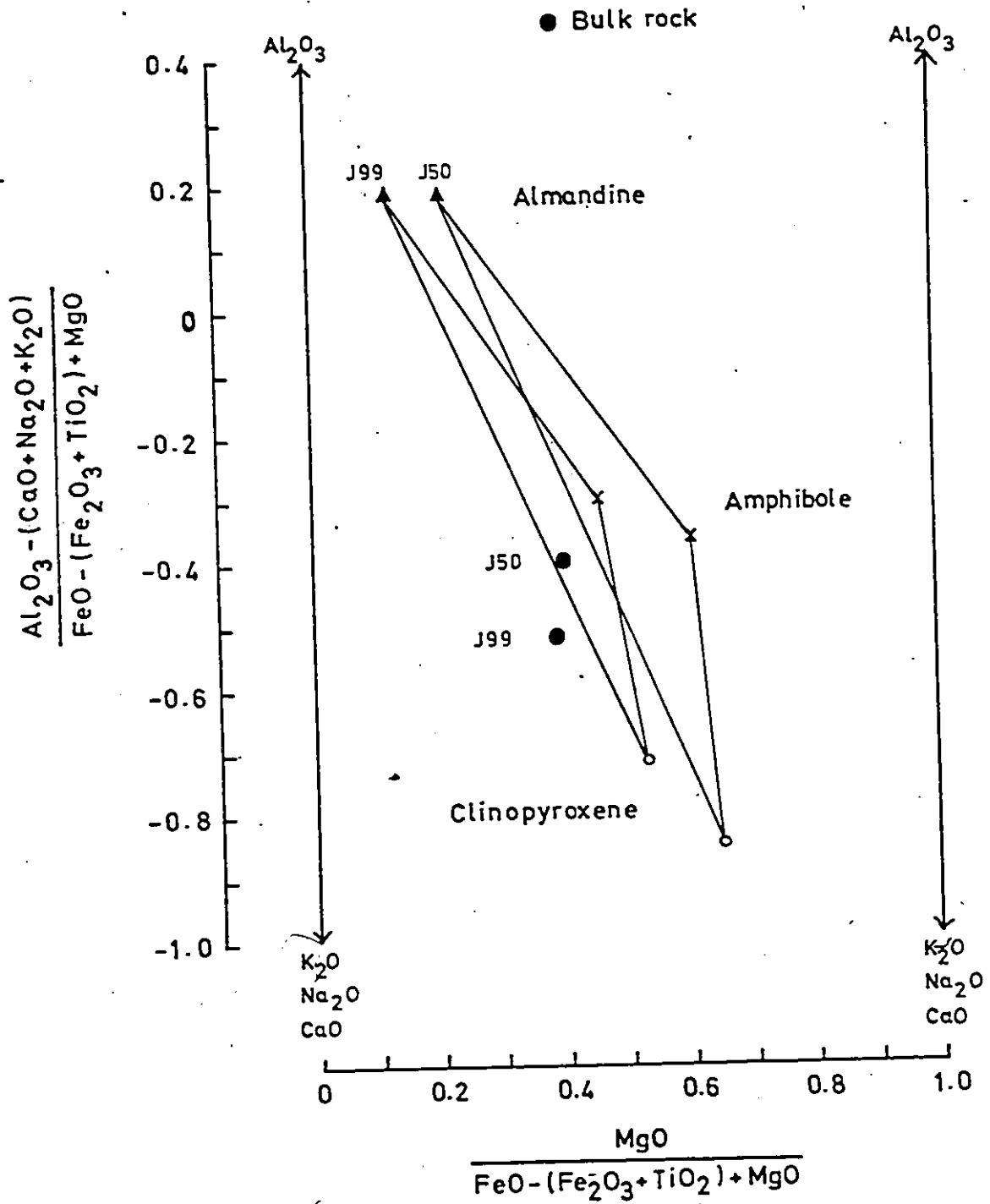


Figure 48. Orthogonal AFM plot showing the phase relations among coexisting orthopyroxene, clinopyroxene, and amphibole in the analysed charnockitic granulites along with the bulk rock compositions.

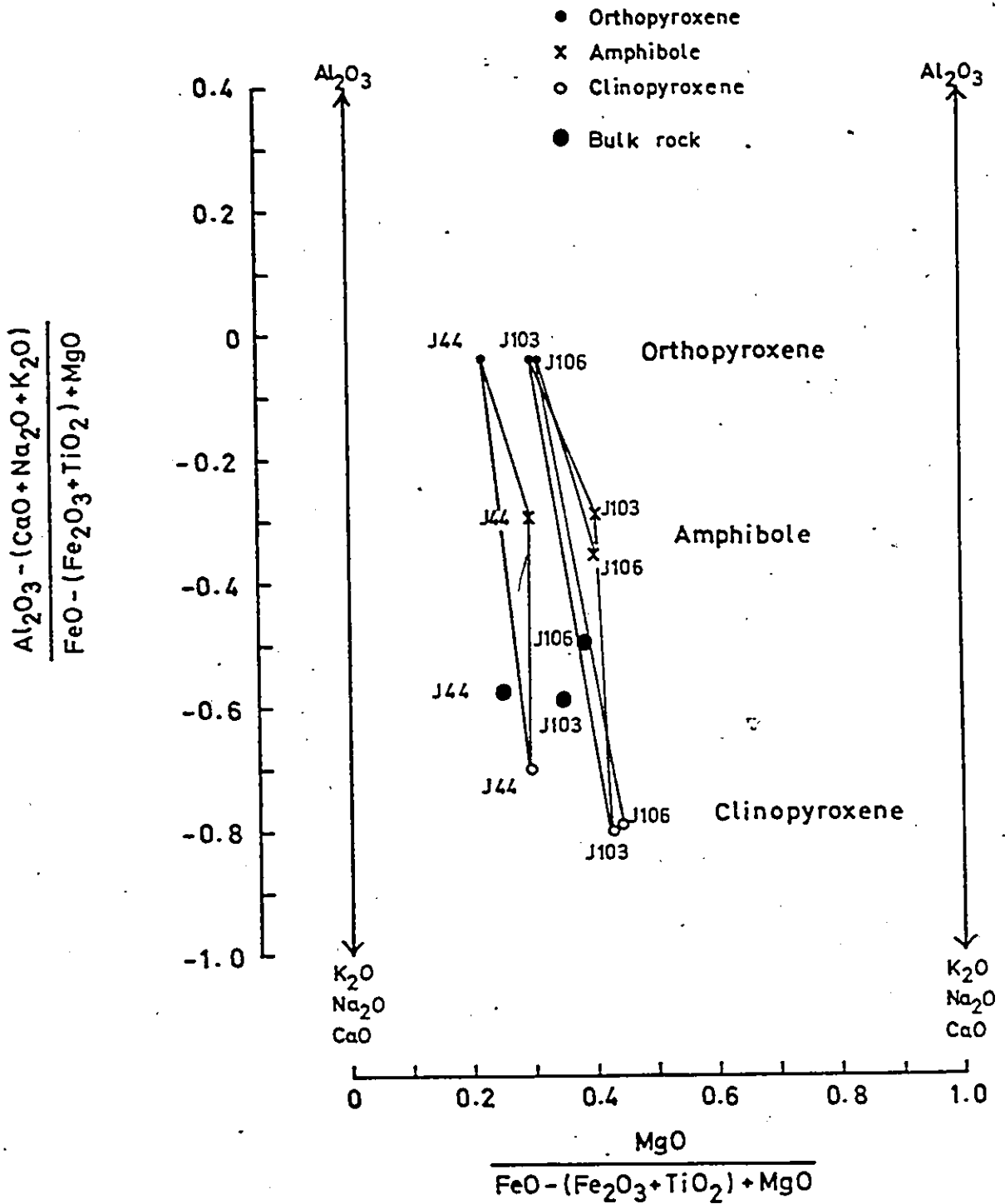
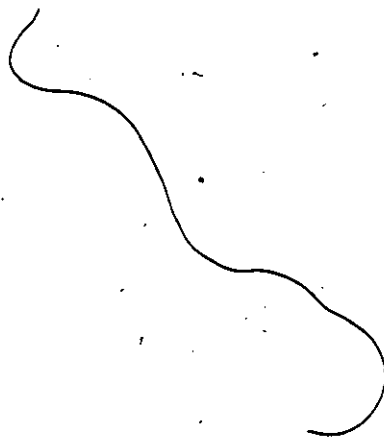


Figure 49. Orthogonal AFM plot showing the phase relations among coexisting orthopyroxene, clinopyroxene, and almandine garnet in the analysed charnockitic granulites along with the bulk rock compositions.



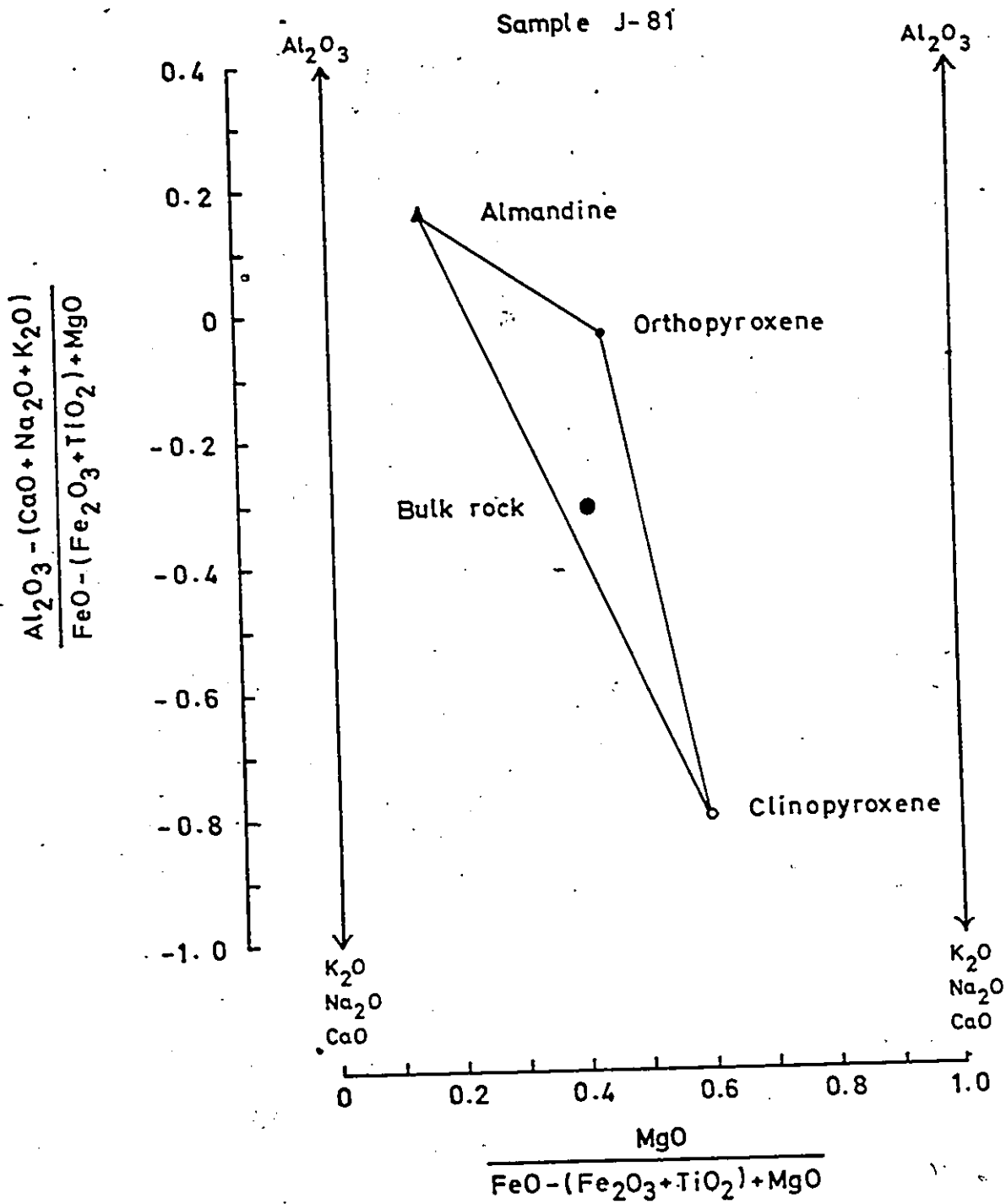
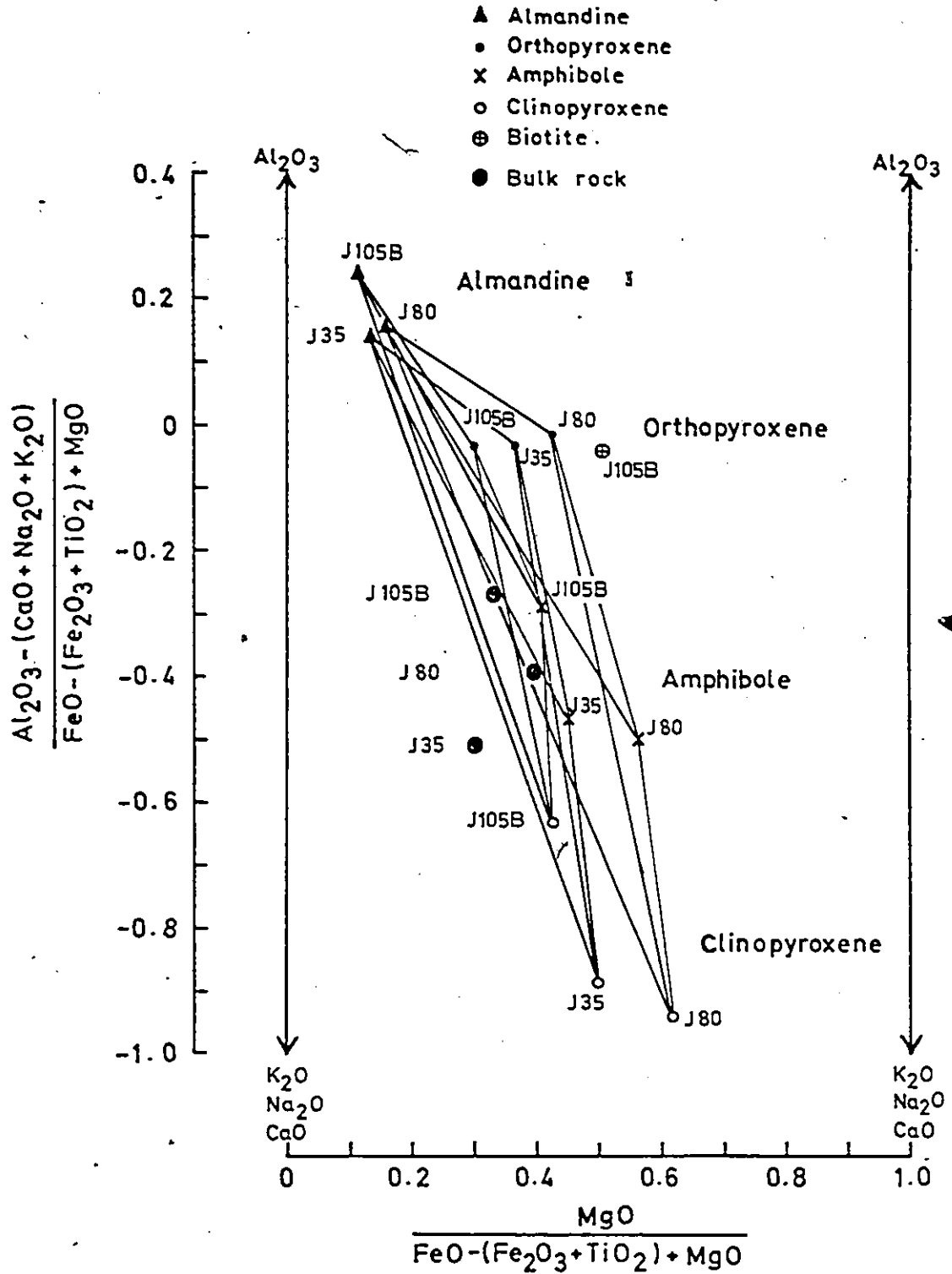


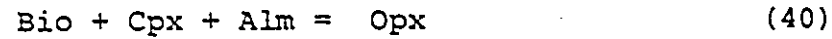
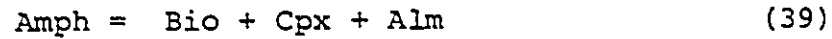
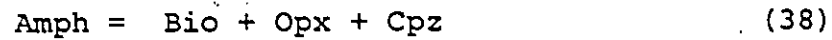
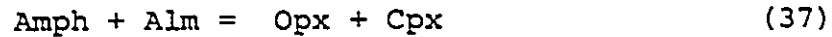
Figure 50. Orthogonal AFM plot showing the phase relations among coexisting orthopyroxene, clinopyroxene, almandine, and amphibole in the analysed charnockitic granulites along with the bulk rock compositions. A fifth phase, biotite, is also shown (rock J-105B). All iron in this mineral is assumed to be ferrous iron. Except for J-105B, these rocks do not contain K-feldspar.



From studies on the partitioning of Mg and Fe^{2+} among coexisting two-pyroxenes, amphibole and garnet, no evidence was found for gross non-equilibrium, nor for a variation in temperature among the study samples. As all of these rocks are closely associated, i.e. they all come from the same field area, large difference in load pressure may also be ruled out. Therefore, a variation in $P_{\text{H}_2\text{O}}$ may be the principal cause for the observed shift in the phase fields; such change would be accompanied by a change in $f\text{O}_2$.

A variation in the composition of plagioclase, perthitic feldspar may be responsible to some extent for the fact that bulk rock compositions plot outside the corresponding phase fields, although the exclusion of some minor components such as P_2O_5 and MnO as well as minor analytical errors may also be contributing factors.

The question of phase equilibrium may also be examined in relation to mineral reactions. The stable co-existence of five ferromagnesian minerals of known composition (J-105B), as shown in Fig. 50, in the presence of quartz, K-feldspar, plagioclase, magnetite and ilmenite, makes it possible to write five mass-balance equations (see Appendix VI), which in simplified form are as follows:



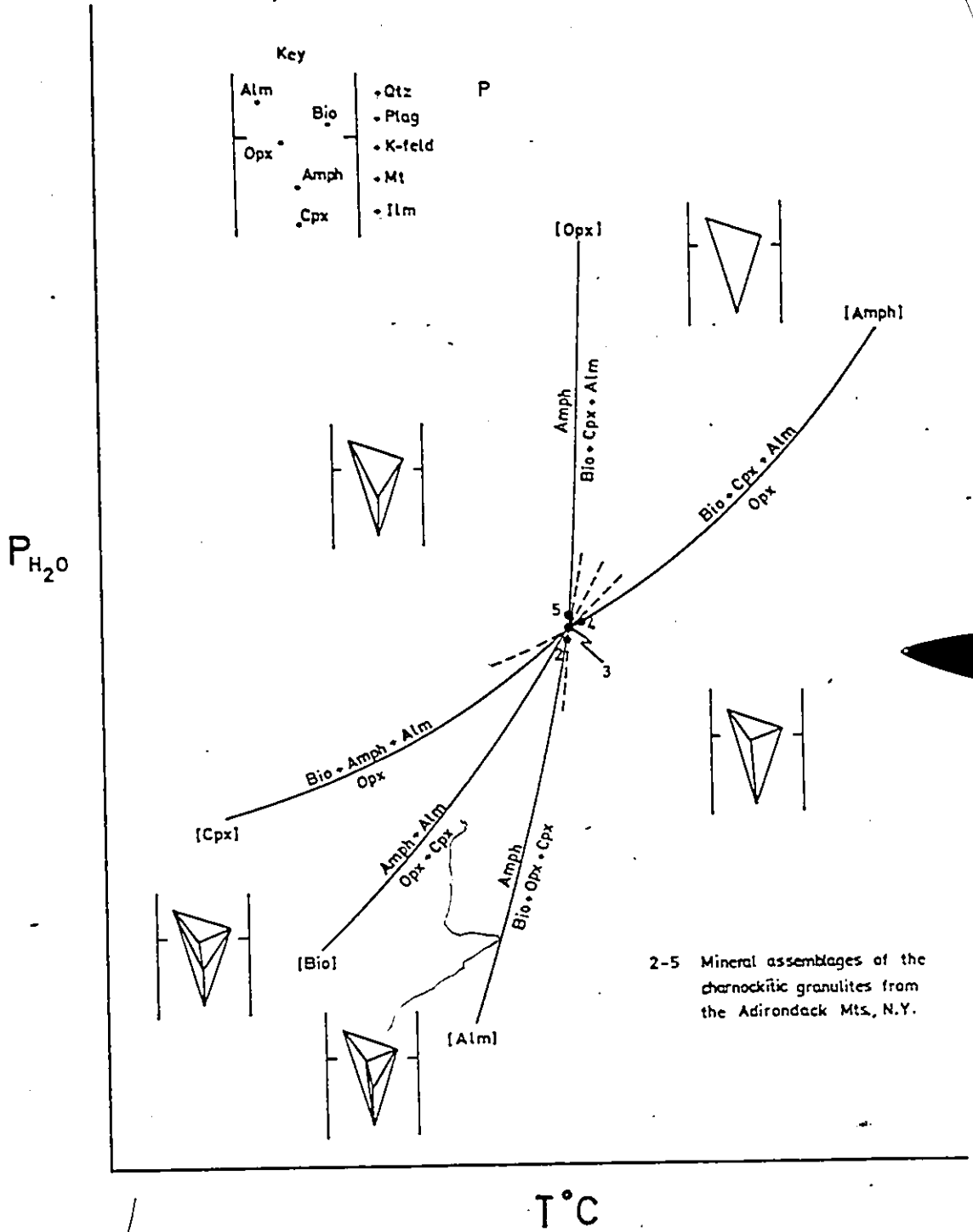
At constant pressure, the five reactions plot as univariant curves on a $P_{\text{H}_2\text{O}}-T$ diagram and meet at an invariant point. These relations are shown schematically in Fig. 51. Assemblages 2, 4, and 5 correspond to three of these relations while assemblage 3 corresponds to the invariant point.

This analysis also suggests that some variation existed in the study area with regard to $P_{\text{H}_2\text{O}}$ and T , probably mainly $P_{\text{H}_2\text{O}}$, to account for the observed differences in mineral assemblage and mineral composition.

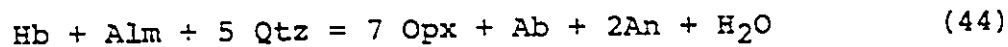
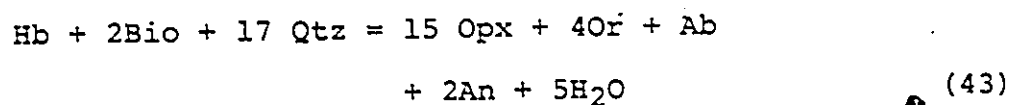
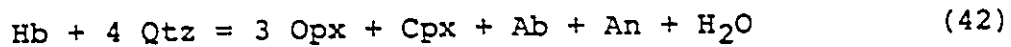
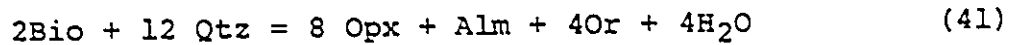
Metamorphic Grade

The boundary between the almandine amphibolite facies and the hornblende granulite facies has been defined by the appearance of orthopyroxene and the boundary between the hornblende granulite facies and the pyroxene granulite facies by the disappearance of biotite and hornblende.

Figure 51. Schematic Schreinemaker's bundle (Zen, 1966) in a P_{H_2O} - T field showing univariant reaction curves for reactions 36 to 40. The supposed relative position of mineral assemblages 2, 3, 4, and 5 are indicated.



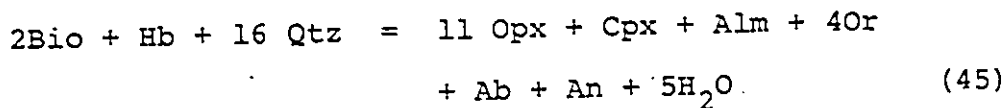
Therefore, de Waard (1965) suggested a set of bivariant equilibria (at constant P), characterized by the coexistence of orthopyroxene with biotite and/or hornblende, as representative of the hornblende granulite facies. The reactions are:



These reactions are represented by three-(ferromagnesian) phase assemblages as compared to the 4- and 5-phase assemblages of the rocks studied. For comparison, the four-phase assemblages of the studied rocks are plotted in Figs. 47, 48 and 49 as three-phase triangles. Although the studied rocks commonly contain four ferromagnesian minerals they satisfy the equilibria suggested by de Waard. Thus the rocks clearly belong to the hornblende granulite facies. The small amount of biotite and amphibole present suggests that the conditions were near the boundary between the hornblende granulite and pyroxene granulite facies. Rocks J-50 and J-99, do not contain orthopyroxene, but because they are associated with the others, they are assigned to the same facies.

From Fig. 51, one other important reaction applicable to the studied rocks is reaction (37) in which two pyroxenes may coexist with amphibole and almandine at univariant equilibrium.

The invariant point in Fig. 51 is represented by the coexisting five mafic silicates biotite, amphibole, orthopyroxine, clinopyroxene and almandine in rock J-105B. From the prograde metamorphism exhibited from the almandine amphibolite facies in the Northwestern Adirondack Lowland to the granulite facies in the Central and Eastern Adirondack Highland, the most likely reaction which lead to this invariant point in Fig. 51 is proposed to be a combination of reactions (41) and (42):



Position of the studied charnockitic
granulites in the metamorphic zones of
the Adirondacks

Five zones of metamorphism ranging between 500°C and 665°C (Engel and Engel, 1960; Buddington, 1963; Buddington and Lindsley, 1964) were recognized in the Adirondacks by Buddington (1966, p331); the mineral assemblages of these rocks were summarized by de Waard (1965, Table 1). The charnockitic, quartz-syenitic, and quartz-bearing syenitic gneisses (Zone E) were formed at the highest temperature level. The temperatures of 635°C to

665°C for the granulites of Zone E, as estimated by Buddington were considered by de Waard (1967, p228-23) to be too low. The present charnockitic granulites belong to this highest zone.

Based on the presence or absence of almandine garnet in charnockitic, metabasic and quartzofeldspathic rocks, Buddington (1963, 1965) delineated three garnet isograds in the Adirondacks which were inferred to represent a general increase in grade of regional metamorphism from the northwest to the southeast and east. This was corroborated by magnetite-ilmenite geothermometry (Buddington and Lindsley, 1964).

The first garnet isograd occurs in the Adirondack lowland in the almandine amphibolite facies terrane, whereas the second and third garnet isograds occur within the region of granulite facies rocks in the Adirondack highlands. The development of garnet in the Adirondacks was considered by Buddington (1965, 1966) to be the result of increasing temperature and pressure, but de Waard (1965a, 1967) thought that the compositional control was more important. de Waard's idea was recently supported by Martignole and Schrijver (1973).

Rejecting Buddington's vaguely defined second garnet isograd in the granulite terrane, de Waard (1964, p308; 1967, p221) proposed an orthopyroxene isograd, to separate the almandine amphibolite facies of the lowland from the hornblende granulite facies in the highland. He

also defined a garnet-clinopyroxene isograd to separate the hornblende granulite facies of the highland into a hornblende-orthopyroxene-plagioclase subfacies to the west, and a hornblende-clinopyroxene-almandine subfacies to the east. The garnet-clinopyroxene isograd, which runs almost north-south, divides the Adirondack highlands into approximately two halves. Although, in the Adirondacks, there is no sizeable regional development of the pyroxene granulite facies, in which hydrous minerals are virtually absent (de Waard, 1967, p210), the pyroxene granulite facies rocks do occur in small amounts throughout the central and eastern Adirondack highlands (de Waard, 1964, p354; Buddington and Lindsley, 1964, p337). The present granulites represent the highest temperature part of the hornblende granulite facies, as noted above. They all occur in the hornblende-clinopyroxene-almandine subfacies terrane of de Waard. The coexistence of the garnet-free and garnetiferous assemblages suggests that the subdivision of the hornblende granulite facies into the hornblende-orthopyroxene-plagioclase and hornblende-clinopyroxene-almandine subfacies in the Adirondacks by de Waard is a rather crude generalization. On the other hand, since all the present rocks represent the narrow 'zone' between hornblende granulite and pyroxene granulite facies, the temperature of formation of these rocks must have been fairly constant. Thus the development of garnet in these rocks must have been controlled

by bulk composition. Based on the breakdown reaction of hornblende (Yoder and Tilley, 1962; Binns, 1964), biotite (Eugster and Wones, 1962) and garnet (Ringwood and Green, 1964; Green and Lambert, 1965), de Waard (1967, p229-230) estimated that the temperature of metamorphism was at least 700°C at the hypersthene isograd and at least 760°C at the garnet-clinopyroxene isograd. He suggested that most of the Adirondack highlands had metamorphic temperatures of at least 800°C and a load pressure as high as 10 Kbs, or a depth of about 35 km. de Waard also pointed out (1967, p228) that the temperature range from 550°C ($\pm 50^\circ\text{C}$) near the hypersthene isograd to 650°C ($\pm 50^\circ\text{C}$) in the Central Adirondacks, as estimated by Buddington and Lindsley (1964) represents a late stage of metamorphism in which the oxide minerals have re-equilibrated upon cooling. Engel and Engel (1962, p37 and 74) estimated the temperature of metamorphism for rocks of the amphibolite facies to be 525°C, and, moving towards the hypersthene isograd of de Waard, their temperature estimates increased to 625°C. Extrapolating upward or eastward into the hornblende granulite and pyroxene granulite boundary of the Central Adirondack highlands, the temperature of metamorphism may well have been around 700°C.

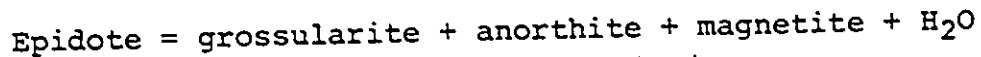
From the distribution of amphibolites in the Northwestern Adirondack lowland, hornblende granulites in the Northwestern and Western to Central highland, to hornblende granulites and pyroxene granulites in the Central to

Eastern highland in the Adirondacks, the grade of metamorphism clearly increases from west to east and reaches its maximum at about the east central main anorthosite massif. The reappearance of hornblende granulites east of Elizabethtown and amphibolites in the eastern margin of the highland near Wilsboro (near Lake Champlain, outside east edge of Fig. 2) indicates a zonal or symmetrical distribution of metamorphic grade across the Adirondacks. Experimental data (Green and Lambert, 1965, p5259) have shown that the mafic assemblage Gar- Cpx forms at a higher pressure than the assemblage Opx- Cpx and Gar- Cpx- Opx. The appearance of the assemblage Opx- Cpx- Alm (present study) and Cpx- Alm (de Waard, 1965a, p189; 1967, p227-228; and present study) in the Eastern and Southeastern Central Adirondacks suggests that not only temperature of metamorphism but also P_{total} have reached their maximum.

Temperature, pressure and partial pressure
of water during metamorphism

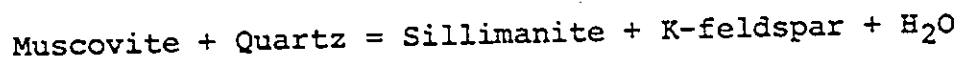
Although several experimental studies have been carried out to delineate fields of stability for minerals that occur in the rocks of the present study, most of the data available refer to pure end members, and as yet, only broad limits may be placed on the temperature and pressure of metamorphism, based on these experiments.

Since epidote was not found in any of the studied rocks, a lower limit to the temperature of metamorphism may be set approximately by the upper limit of the stability field for this mineral as defined by the reaction:



which was determined by Liou (1973) and is shown in Fig. 52, curve 5. The limit is an approximate one because the products of the reaction occur in the studied rocks as components of solid solutions, not as pure minerals.

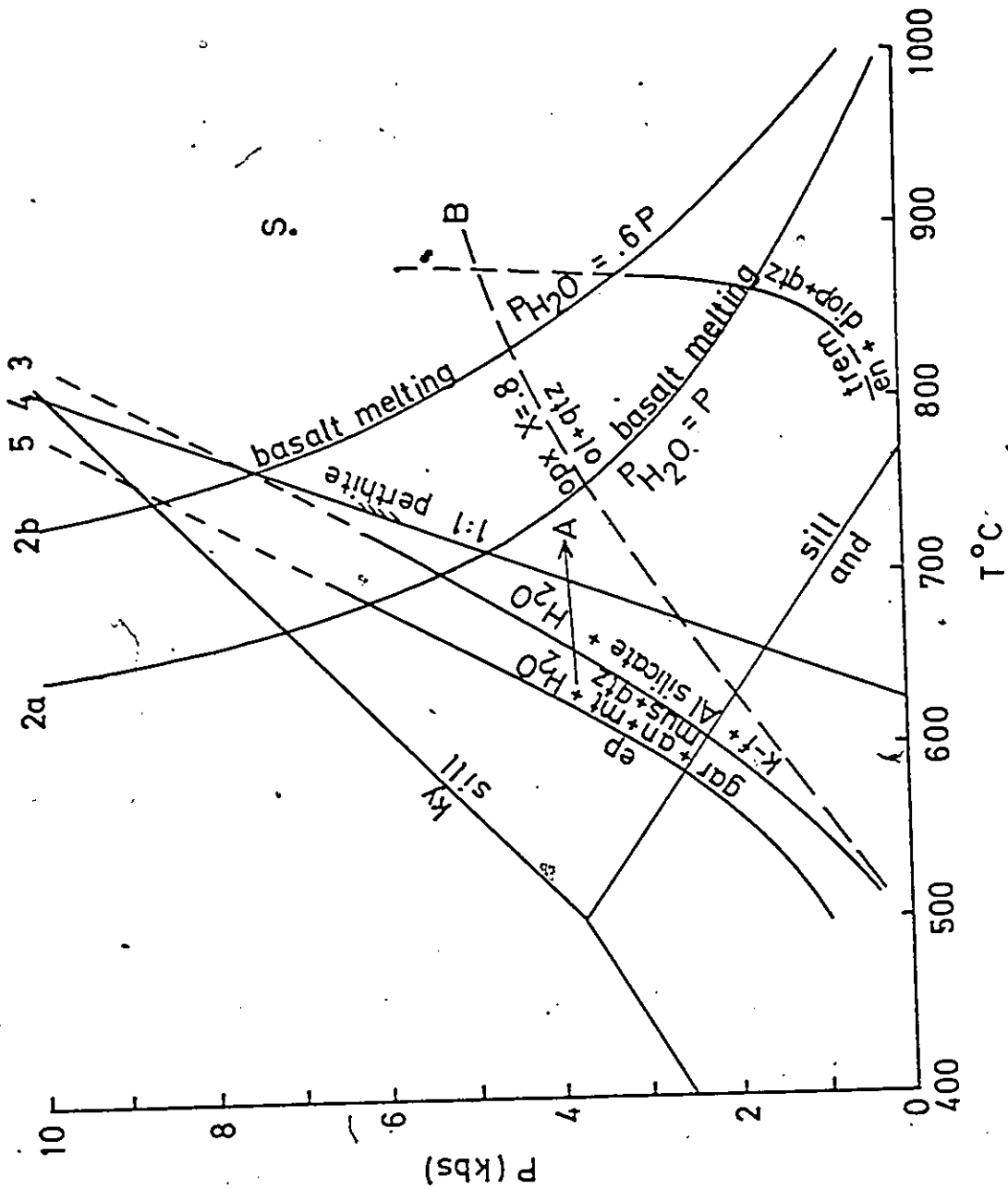
Alternatively, a lower temperature limit may be set by the upper stability field for muscovite and quartz:



determined by Evans (1965) and shown as curve 3 in Fig. 52. Muscovite is generally absent from the rocks of the Adirondack highland while sillimanite + K-feldspar are common (Buddington, 1963; de Waard, 1965a) and the rocks of the present study almost certainly recrystallized within the stability field of sillimanite + K-feldspar.

Since 1:1 perthites are common in the present rocks the temperature corresponding to the top of alkali feldspar solvus would provide another lower limit to temperature. One estimate of this temperature, as obtained by Luth et al. (1974), is shown in Fig. 52. Accordingly, if the pressure was 4 Kbs, the temperature of metamorphism must have exceeded about 700°C.

Figure 52. P-T field of the charnockitic granulites studied in terms of breakdown and chemical reactions of phases. Curve 1 from Boyd (1954); curves 2a and 2b from Holloway and Burnham (1972); curve 3 from Evans (1965); curve 4 from Luth et al. (1974); curve 5 from Liou (1973); arrow A, a P-T gradient of amphibolite-granulite facies rocks of northwestern Adirondacks, from Engel and Engel (1962); curve B from Olsen and Mueller (1966) and Smith (1970); point S shows the stable coexistence of an iron-rich orthopyroxene with $Fe/Fe + Mg = 0.8$, olivine and quartz at 900°C above 7 kbs (Smith, 1970). Shaded area is the proposed P-T field of metamorphism for the study rocks. Abbreviations: an= anorthite, and= andalusite, diop= diopside, en= enstatite, ep= epidote, gar= garnet, ky= kyanite, k-f= K-feldspar, mt= magnetite, mus= muscovite, ol= olivine, opx= orthopyroxene, qtz= quartz, sill= sillimanite, trem= tremolite.



The temperature of intracrystalline equilibrium in orthopyroxene, determined as $700^{\circ} \pm 25^{\circ} \text{C}$ (Chapter VI), provides another estimate of the lower limit of the temperature of metamorphism.

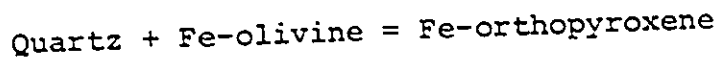
An upper limit to temperature may possibly be taken as the breakdown of amphibole to produce orthopyroxene. For the pure Mg end member, this temperature is high, being about 850°C for a $P_{\text{H}_2\text{O}} = P_{\text{total}}$ of 1 Kbs (Boyd, 1954). The presence of Fe in the amphibole would lower this temperature very considerably. The breakdown of phlogopite to produce orthopyroxene also occurs at a high temperature, about $1,100^{\circ} \text{C}$ for a pressure of 3 Kbs, as determined by Yoder and Eugster (1954) and although various breakdown temperatures for Fe-Mg biotite have been determined by Eugster and Wones (1962) and Wones and Eugster (1965), these are very much dependent on the activity of oxygen. Consequently this reaction, as it occurs in nature is still imperfectly understood, and the field in which this probably takes place is large. According to Turner (1968, Fig. 4-4) the breakdown of biotite in nature, at a pressure of about 5 Kbs may take place within a temperature range of from nearly 500 to 900°C .

In an experiment on a natural rock similar to those of the present study, Binns (1964) showed that the amphibole to orthopyroxene reaction occurred at about 850°C at $P_{\text{H}_2\text{O}}$ of 1 Kbs. He suggested a temperature of

about 800°C for the reaction in the granulite facies rock that he examined.

Finally, by comparing the K_D value of 0.57 for coexisting orthopyroxene and clinopyroxene of the present study with that of 0.69 obtained by Lindsley et al. (1974) for coexisting augite and hypersthene at 810°C, the temperature of metamorphism of the studied granulites could not have exceeded 800°C.

A lower limit to pressure may be set by the reaction



which is displaced to the right with increasing pressure.

Smith (1970) has shown experimentally that an iron-rich orthopyroxene, with $\text{Fe}/\text{Fe} + \text{Mg} = 0.8$, which is the most iron-rich orthopyroxene of the present study is stable relative to olivine and quartz about 7 Kbs pressure, at a temperature of 900°C (point S, Fig. 52). Using the theoretical analysis of Olsen and Mueller (1966), Curve B (Fig. 52) places an approximate lower limit to pressure of metamorphism of the terrane from which the study samples were obtained.

An upper limit to pressure might best be obtained from reasonable estimate of depth of burial, which probably would not exceed 20 km, corresponding to a pressure of 6 Kbs.

Thus the range of temperature of metamorphism is postulated to be between 700° to about 800°C, and the pressure between about 3 and 6 Kbs. The estimates of Engel and Engel (1958, 1962) for the Adirondack region west of the study area, where the highest grade attained was slightly lower, is shown as arrow A in Fig. 52, and the upper part of this arrow falls close within the limits set by the present estimates.

The question of P_{H_2O} relative to P may be examined briefly. The rocks of the present study are similar in composition to that of an alkali basalt (Cf. Yoder and Tilley, 1962) for which the minimum melting curve was determined by Holloway and Burnham (1972) and appears as Curves 2a and 2b in Fig. 52. The curve shifts to right as P_{H_2O} decreases relative to confining pressure, P . Some of the rocks of the present study contain minor feldspar-quartz and garnet-quartz intergrowths, taken as evidence of incipient melting, and hence the P-T point of metamorphism is considered to lie on or slightly to the right of this curve. Since Curve 2a cuts through the field in which the P-T point is estimated to lie, it is possible that P_{H_2O} was somewhat less than P .

A very close estimate of T-P of metamorphism of the studied rocks is difficult as appropriate experimental determinations are lacking. However, on the basis of certain assumptions, estimates may be made, as follows.

Assuming feldspar-quartz and garnet-quartz intergrowths indicate incipient melting and that the presence of mesoperthite in addition to other perthitic and/or anti-perthitic feldspars suggests further homogenization of the feldspar solid solutions as a result of high T-P recrystallization, the T-P of metamorphism of the studied rocks would then be controlled by the intersection of the alkali feldspar 'solvus' curve (4) and the basalt melting curve(s) in Fig. 52. In other words, the temperature must have been above the solvus but near or slightly above the basalt melting curve(s) at different P_{H_2O} conditions. Therefore,

- (1) at $P_{H_2O} = P$, the T-P of metamorphism of the studied rocks would be, allowing for experimental uncertainty, $T = 715^\circ \pm 25^\circ C$, $P_{H_2O} = P = 4.8$ Kbs.
- (2) at $P_{H_2O} = 0.8P$, $T = 735^\circ \pm 25^\circ C$, $P = 6$ Kbs, $P_{H_2O} = 4.8$ Kbs.
- (3) at $P_{H_2O} = 0.6P$, $T = 765^\circ \pm 25^\circ C$, $P = 7.4$ Kbs, $P_{H_2O} = 4.4$ Kbs.

As discussed earlier, P_{H_2O} was likely less than P ; while P was unlikely to exceed 6 Kbs, corresponding to a depth of 20 km. Thus an intermediate condition between cases (1) and (3), i.e. conditions similar to case (2) would seem most likely for the present charnockitic granulites.

Origin

Charnockites and related granulites have been found and studied in many parts of the world, for example in Sweden (Quensel, 1951; Saxena, 1968), Finland (Eskola, 1952; Parras, 1958), Australia (Wilson, 1952, 1954, 1959, 1960a, b; Binns, 1965a, b), British Guiana (Singh, 1966), Uganda (Groves, 1935), India (Holland, 1893, 1900; Howie, 1955; Pichamuthu, 1953; Howie and Subramaniam, 1957; Subramaniam, 1959, 1962; Leelanandam, 1967), Ceylon (Corray, 1962), Canadian Shield (Roach and Duffell, 1968) and the Adirondacks of the United States (Buddington, 1939, 1950, 1952, 1963, 1966, 1969; de Waard, 1964, 1965a, b, 1967, 1969). From these studies it is evident that charnockitic rocks are generally Precambrian in age and occur in the Shield areas. Although some might have been sedimentary rocks prior to metamorphism, a meta-igneous origin is favoured in general.

The charnockitic granulites of the present study are believed to be igneous in origin, and were subsequently metamorphosed to the granulite facies. They occur as dykes and patches of irregularly shaped bodies of gabbroic and syenitic composition in the anorthosite massifs (Buddington, 1939; 1952, 1963, 1965, 1966, 1969, personal communication, 1970; de Waard, 1964, 1965).

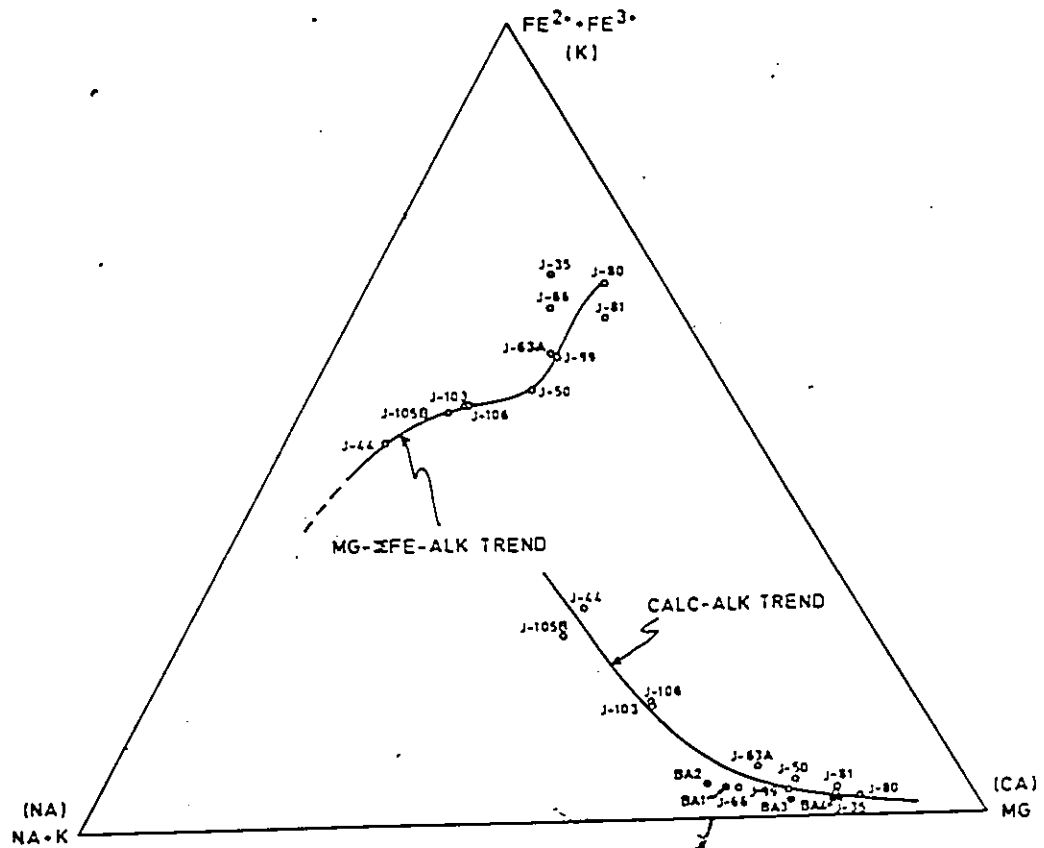
On the variation diagram (Fig. 53), the charnockitic granulites of the present study show a continuous Mg- Fe- Alkali trend and a distinct calc- alkali trend similar to the Madras charnockite series (Howie, 1955, Figs. 1 and 2) and that of the South Savana charnockites (Singh, 1966, p188-90). These smooth curves suggest that the suite of charnockitic granulites was a series of calc-alkali magmatic differentiates rather than a group of sedimentary rocks. Some anorthosite, anorthositic gabbro and gabbroic anorthosite from the Adirondack massifs were also plotted; the analyses were reported by Buddington, (1939, p30, 36 and 235). Assuming that little or no metasomatism took place during metamorphism, some of the rocks studied (e.g. J-35, J-80 and J-81) may represent some of the earliest differentiates separated from the anorthositic or gabbroic anorthosite magma (Bowen, 1927, p89; Bailey, 1928, p173; Buddington, 1939, p235, 1969, p215, 224-230; Yoder, 1955b, p1638-1639, 1969, p13-22; Yoder, Stewart and Smith, 1957, p206-214; Turner and Verhoogen, 1960, p324-328).

From oxygen isotope studies of Adirondack igneous and metamorphic rocks, Taylor (1969, p111, 119-120) concluded that most meta-igneous rock types of the area are enriched in O^{18} relative to their unmetamorphosed counterparts in other localities, so a large fraction of the present Adirondack terrane cannot have been a closed

Figure 53. Variation diagram showing a Mg-Fe-Alk trend and a calc-alkali trend in the charnockitic granulites from the Adirondack Mts., N.Y. Atoms or ions in atomic %.

BA1 to BA4 from Buddington (1939): BA1= gabbroic anorthosite, Adirondack massif (p235, d); BA2= average of 4 analyses of anorthosite from core of Adirondack massif (p30, A); BA3= anorthositic gabbro from sheet in Adirondack massif (p36, no. 25); BA4= pyroxene gabbro facies of coarse anorthositic gabbro, Adirondack massif (p36, no. 27).

1



system during metamorphism. He found only a few relatively unfoliated metagabbros and some granitic plutons have 'normal' O^{18}/O^{16} ratios (for 'normal' basalts and gabbros $\delta = 6.5$ to 6.6). A δ value of 9.2 was obtained for a pyroxene-garnet-oligoclase granulite metagabbro collected near the present samples J-35, J-63A and J-66 and was attributed to reconstitution during metamorphism (Taylor, 1969, p119). In the Adirondacks, the most sodic plagioclase of the unmetamorphosed anorthosite series is An_{40} , and the most calcic plagioclase in the quartz-syenitic series is An_{30} (Buddington, 1969, p221). The above mentioned metagabbroic rocks have clearly undergone reconstitution during metamorphism since garnet also appears (Buddington, 1939, 1952, 1963, 1967). As a result, all rocks of the present study (except J-50) have plagioclase more sodic than An_{35} . Some of the calcium may have been used up to make garnet and calcic pyroxene. These amounts of Ca must be taken from the plagioclase. In addition, some alkalis may have been introduced to produce albite and alkalic feldspars. This is supported by the presence of slightly zoned plagioclase crystals in some rocks (e.g. J-35) with a rim less calcic than the core by an amount of about An_4 to An_5 .

Apart from the possible introduction of a small amount of alkali elements, and the removal of H_2O , the rocks of the present study are considered to have recrystallized under essentially 'closed system' conditions.

From the study of coexisting iron oxides (Chapter VIII) it is evident that the present charnockitic granulites were metamorphosed and perhaps formed initially under conditions of low fO_2 . This and the high iron (in particular Fe^{2+}), low Mg and low free silica nature of the rocks, together with the variation trends suggest that these rocks were early to intermediate differentiates, resulting from the fractional crystallization of a common magma, following the Fenner's trend of crystallization (Osborn, 1959, p609, 618-619). Unlike the Madras charnockites which were due to the emplacement of a charnockitic magma (Subramanian, 1962, p21-36) these rocks were more likely the gabbroic and noritic differentiates of the anorthositic or gabbroic anorthositic magma in the Adirondacks.

References

- Abrahams, S.C., and Geller, S., 1958, Refinement of the crystal structure of a grossularite garnet: Acta Crystallogr., 11, p437-441.
- Agterberg, F.P., 1966, The use of multivariate Markov schemes in petrology: J. Geol., 74, p764-785.
- _____, 1967, Computer techniques in geology: Earth Sci. Rev., 3, p47-77.
- Ahrens, L.H., and Taylor, S.R., 1961, Spectrochemical analysis: Addison-Wesley, Reading, Massachusetts, p116.
- Alff, C., and Wertheim, G.K., 1961, Hyperfine structure of Fe⁵⁷ in yttrium - iron garnet from the Mössbauer Effect: Phys. Rev., 122, p1414-1417.
- Anderson, T.W., and Goodman, L.A., 1957, Statistical inference about Markov chains: Ann. Math. Stat., 28, p89-110.
- Annersten, H., 1974, Mössbauer studies of natural biotites: Am. Min., 59, p143-151.
- Bailey, E.B., 1928, Addendum to N.L. Bowen's 'Ultrabasic types of the Hebrides': in 'The evolution of the igneous rocks' by N.L. Bowen, 1928, Dover, New York, p173.

Bancroft, G.M., Burns, R.G., and Howie, R.A., 1967a, A determination of the cation distribution in the orthopyroxene series by the Mössbauer Effect: *Nature*, 213, p1221-1223.

Bancroft, G.M., Burns, R.G., and Maddock, A.G., 1967b, Determination of cation distribution in the cummingtonite-grunerite series by Mössbauer spectra: *Am. Min.*, 52, p1009-1025.

Bancroft, G.M., Maddock, A.G., and Burns, R.G., 1967c, Applications of the Mössbauer Effect to silicate mineralogy - I. Iron silicates of known crystal structure: *Geochim. Cosmochim. Acta*, 31, p2219-2246.

Bancroft, G.M., Burns, R.G., and Stone, A.J., 1968, Applications of the Mössbauer Effect to silicate mineralogy - II. Iron silicates of unknown and complex crystal structures: *Geochim. Cosmochim. Acta*, 32, p547, 556-558.

Bartholome, P., 1962, Iron-magnesium ratio in associated pyroxenes and olivines: in *Petrological Studies*, Buddington Volume, GSA, p1-12, 19.

Bikerman, J.J., 1959, Discussion, in Johnson, 1959, p1658.

Binns, R.A., 1962, Metamorphic pyroxenes from the Broken Hill district, New South Wales: *Min. Mag.*, 33, p327-334.

_____, 1965a, The mineralogy of metamorphosed basic rocks from the Willyama Complex, Broken Hill District, New South Wales, Part I. Hornblendes: Min. Mag., 35, p325.

_____, 1965b, The mineralogy of metamorphosed basic rocks from the Willyama Complex, Broken Hill District, New South Wales, Part II. Pyroxenes, garnets, plagioclase, and opaque oxides: Min. Mag., 35, p561-587.

Blander, M., 1972, Thermodynamic properties of orthopyroxenes and clinopyroxenes based on the ideal two-site model. Geochim. Cosmochim. Acta, 36, p787-799.

Bonie, R.E., and Derge, G., 1956, Surface structure of non-oxidizing stages containing sulphur: Trans. AIME, J. Metals, 206, p59-64.

Bowen, N.L., 1927, The origin of ultrabasic and related rocks: Am. J. Sci., 14, p89.

Boyd, F.R., 1954, Tremolite: Carnegie Inst. Washington Yearbook, 1954, p109-110.

Broughton, J.G. et al., Compilation, 1961, Geological map of New York, Adirondack Sheet: The University of The State of New York, The State Education Department, N.Y.

Buddington, A.F., 1939, Adirondack igneous rocks and their metamorphism: GSA Memoir 7, p30, A, 36, no. 27, p235d.

_____, 1950, Composition and genesis of pyroxene and garnet related to Adirondack anorthosite and anorthosite-marble contact zones: Am. Min., 35, p659-670.

_____, 1952, Chemical petrology of some metamorphosed Adirondack gabbroic, syenitic and quartz syenitic rocks: Am. J. Sci., Bowen Volume, p37-84.

_____, 1963, Isograds and the role of H₂O in metamorphic facies of orthogneisses of the northwest Adirondack area, New York: Geol. Soc. Amer. Bull., 74, p1155-1182.

_____, 1965, The origin of three garnet isograds in Adirondack gneisses: Min. Mag., 34, Tilley Volume, p71-81.

_____, 1966, The occurrence of garnet in the granulite facies terrane of the Adirondack highlands, a discussion: J. Petrol., 7, p331-335.

_____, 1969, Adirondack anorthositic series: in Origin of anorthosite and related rocks, ed. Y. Isachsen, New York Museum and Science Services Memoir 18, p224-231.

- Buddington, A.F., and Lindsley, D.H., 1964, Iron-titanium oxide minerals and synthetic equivalents: *J. Petrol.*, 5, p310-357.
- Burns, R.G., 1970, Mineralogical applications of crystal field theory: Cambridge University Press, 224p.
- Carmichael, I.S.E., 1967, The iron-titanium oxides of salic volcanic rocks and their associated ferromagnesian silicates: *Contr. Mineral. Petrol.*, 14, p36-64.
- Clark, P.J., and Evans, F.C., 1954, Distance to nearest neighbour as a measure of the spatial relationships in plant populations: *Ecology*, 35, p445-453.
- Cooray, P.G., 1962, Charnockites and their associated gneisses in the Precambrian of Ceylon: *QJGS.*, 118, p239-273.
- Davidson, L.R., 1968, Variation in ferrous iron-magnesium distribution coefficients of metamorphic pyroxenes from Quairading, Western Australia: *Contr. Mineral. Petrol.*, 19, p239-259.
- de Coster, M., Pollak, H., and Amelinckx, S., 1963, A study of Mössbauer absorption in iron silicates: *Phys. Stat. Sol.* 3, p284-285.

Deer, W.A., Howie, R.A., and Zussman, J., 1962, Rock-forming minerals, Vol. I, Ortho - and Ring-silicates: p86-87; Vol. II, Chain-silicates: p19-22, 52-53, 278-281, 288-291; Vol. III Sheet-silicates: p58-60.

_____, 1966, An introduction to the rock forming minerals: Longmans, p171.

DeVore, G.W., 1955, The role of adsorption in the fractionations and distributions of elements: J. Geol., 63, p159-190.

_____, 1956, Surface chemistry as a chemical control on mineral associations: J. Geol., 64, p31-56.

_____, 1959, Role of minimum interfacial free energy in determining the macroscopic features of mineral assemblages. I. The model: J. Geol., 67, p211-227.

de Waard, D., 1964, Mineral assemblages and metamorphic subfacies in the granulites - facies terrane of the Little Moose Mountain Syncline, South-Central Adirondack highlands: Proc. Kon. Ned. Akad. Wetensch., Amsterdam B67, p344-364. 7

_____, 1965a, The occurrence of garnet in the granulite-facies terrane of the Adirondack highlands: J. Petrol., 6, p165-191.

de Waard, D., 1965b, A proposed subdivision of the granulite facies: Am. J. Sci., 263, p455-461.

_____, 1967, The occurrence of garnet in the granulite - facies terrane of the Adirondack highlands and elsewhere, an amplification and a reply: J. Petrol., 8, p210-232.

_____, 1969, The anorthosite problem: The problem of the anorthosite - charnockite suite of rocks: in Origin of anorthosite and related rocks, ed. Y. Isachsen, New York Museum and Sciences Services Memoir 18, p71-91.

Dowty, E., and Lindsley, D.H., 1973, Mössbauer spectra of synthetic hedenbergite-ferrosilite pyroxenes: Am. Min., 58, p850-868.

Dowty, E., Ross, M., and Cuttitta, F., 1972, Fe²⁺-Mg site distribution in Apollo 12021 Clinopyroxenes: Evidence for bias in Mössbauer measurements, and relation of ordering to exsolution: Proc. 3rd Lunar Sci. Conf. (Suppl. 3, Geochim. Cosmochim. Acta, 1), 1, p481-492.

Duchesne, J.-C, 1972, Iron-titanium oxide minerals in the Bjerkrem-Sogndal Massif, Southwestern Norway: J. Petrol., 13, p57-87.

Dundon, R.W., and Walter, L.S., 1967, Ferrous iron order-disorder in meteoritic pyroxenes and the metamorphic history of chondrites: Earth & Plan. Sci. Lett., 2, p372-376.

Engel, A.E.J., and Engel, C.G., 1958, Progressive metamorphism and granitization of the major paragneiss, northwest Adirondack Mountains, New York, Part I. Total rock: Geol. Soc. Am. Bull., 69, p1369-1414.

_____, 1960, Progressive metamorphism and granitization of the major paragneiss, northwest Adirondack Mountains, New York: Geol. Soc. Amer. Bull 71, p1-58.

_____, 1962, Progressive metamorphism of amphibolite, Northwest Adirondack Mountains, New York: Geol. Soc. Amer. Bull., p37, 74.

Eskola, P., 1952, On the granulites of Lapland: A.J.S. Bowen Volume, p133-171.

Eugster, H.P., and Wones, D.R., 1962, Stability relations of the ferruginous biotite, annite: J. Petrol., 3, p82-125.

Evans, B.W., 1965, Application of a reaction-rate method to the breakdown equilibria of muscovite and muscovite plus quartz: Am. J. Sci., 263, p660.

Evans, B.J., Ghose, S., and Hafner, S.S., 1967, Hyperfine splitting of Fe^{57} and Mg-Fe order-disorder in orthopyroxenes (MgSiO_3 - FeSiO_3 solid solutions): J. Geol., 75, p306-322.

Finger, L.W., Hafner, S.S., Schürmann, K., Virgo, D., and Warburton, D., 1972, Distinct cooling histories and reheating of Apollo 14 rocks (abstract): in Lunar Science III (ed. C. Watkin), p259-261, Lunar Sci. Inst. Contr. No. 88.

Fisher, R.A., 1950, The significance of deviations from expectation in Poisson series: Biometrics, 6, p17-24.

Fleet, M.E., 1974, Partition of Mg and Fe^{2+} in coexisting pyroxenes: Contr. Mineral. Petrol., 44, p251-257.

Flinn, D., 1969, Grain contacts in crystalline rocks: Lithos, 2, p361-370.

Froese, E., and Gordon, T.M., 1974, Activity coefficients of coexisting pyroxenes: Am. Min., 59, p204-205.

Gasparrini, E., and Naldrett, A.J., 1972, Magnetite and ilmenite in the Sudbury Nickel Irruptive: Econ. Geol., 67, p605-621.

Gay, P., Bancroft, G.M., and Brown, M.G., 1970, Diffraction and Mössbauer studies of minerals from lunar soils and rocks: Proc. Apollo 11 Lunar Sci. Conf., 1, p481-497.

Gayles, J.B., Lacey, O.L., and Gary, J.H., 1958, Mixing of solids: chi square as a criterion: *Ind. Eng. Chem.*, 50, p1279.

Ghose, S., 1965a, Mg^{2+} - Fe^{2+} order in an orthopyroxene $Mg_{0.91}Fe_{1.07}Si_2O_6$: *Z. Krist.*, 122, p81-99.

_____, 1965b, A scheme of cation distribution in the amphiboles: *Min. Mag.*, 35, p46-54.

Ghose, S., and Hafner, S.S., 1967, Mg^{2+} - Fe^{2+} distribution in metamorphic and volcanic orthopyroxenes: *Z. Krist.*, 125, p157-162.

_____, 1968, Application of Fe^{57} Mössbauer resonance to silicates, in Short Course Lecture Notes on Resonance Spectroscopy in Mineralogy: A.G.I., pGH4-5, 7, 8, 19, 20.

Ghose, S., Ng, G., and Walter, L.S., 1972, Clinopyroxenes from Apollo 12 and 14: Exsolution cation order and domain structure (abstract): in *Lunar Sci. III* (ed. C. Watkins), p300-302, *Lunar Sci. Inst. Contr.* No. 88.

Gibbs, G.V., and Smith, J.V., 1965, Refinement of the crystal structure of synthetic pyrope: *Am. Min.* 50, p2023-2039.

Gleason, H.A., 1920, Some applications of the quadrant method: *Bull. Torrey Bot. Club* 47, p21-33.

- Green, D.H., and Lambert, I.B., 1965, Experimental crystallization of anhydrous granite at high pressures and temperatures, *J. Geophys. Res.*, 70, p5259-5268.
- Greenwood, H.J., Doe, B.R., and Phinney, W.C., 1964, A discussion on: Phase equilibria in the metamorphic rocks of St. Paul Island and Cape North, Nova Scotia: *J. Petrol.*, 4, p189-194.
- Groves, A.W., 1935, The charnockite series of Uganda, *British East Africa, QJGS*, 91, p150-207.
- Gücer, D.E., 1965, A statistical description of distribution of phases: *Bull. Tech. Univ. Istanbul*, 18, p107-125.
- Guggenheim, E.A., 1967, *Thermodynamics*: North-Holland Publishing Co., Amsterdam, p218.
- Gurland, J., 1968, Spatial distribution of discrete particles: in *Quantitative microscopy*, ed. R.T. DeHoff and F.N. Rhines, McGraw-Hill, New York, p278-290.
- Hafner, S.S., 1968, Mössbauer Resonance: in *Short Course Lecture Notes on Resonance Spectroscopy in Mineralogy*, A.G.I. pGH16.
- Hafner, S.S., and Virgo, D., 1970, Temperature-dependent cation distributions in lunar and terrestrial pyroxenes: *Proc. Apollo 11 Lunar Sci. Conf.*, 3, p2183-2198.

Hogarth, D.D., Brown, F.F., and Pritchard, A.M., 1970, Bi-absorption, Mössbauer spectra, and chemical investigation of five phlogopite samples from Quebec: Can. Min., 10, p710, 714-720.

Holdaway, M.J., 1971, Stability of andalusite and the aluminum silicate phase diagram: Am. J. Sci., 271, p97-131.

Holland, T.H., 1893, The petrology of Job Charnock's tombstone: J. Asiatic Soc. Bengal., 62, p162-164.

_____, 1900, The charnockite series, a group of Archaean hypersthenic rocks in peninsula India: Geol. Surv. India Memoir, 28, p119-249.

Holloway, J.R., and Burnham, C.W., 1972, Melting relations of basalt with equilibrium water pressure less than total pressure: J. Petrol., 13, p1-29.

Howie, R.A., 1955, The geochemistry of the charnockite series of Madras, India, Trans. Royal Soc. Edinburgh, 62, pt. 3, p727-768.

_____, 1965, The pyroxenes of metamorphic rocks: in Controls of metamorphism, ed. W.S. Pitcher and G.W. Flinn, p319-326.

Howie, R.A., and Subramaniam, A.P., 1957, The paragenesis of garnet in charnockite, enderbite and related granulites: Min. Mag., 31, p565-586.

Jen, L.S., 1973, The determination of iron (II) in silicate rocks and minerals: Anal. Chim. Acta, 66, p315-318.

Johnson, R.E., 1959, Conflicts between Gibbsian thermodynamics and recent treatments of interfacial energies in solid-liquid-vapour systems: J. Phys. Chem. Ithaca, 63, p1655-1658.

Jura, G., and Garland, C.W., 1952, The experimental determination of the surface tension of magnesium oxide: J. Am. Chem. Soc., 74, p6033-6044.

Kalvius, G.M., and Hafner, S.S., 1968, Paramagnetic hyperfine splittings in pyroxenes: Bull. Am. Phys. Soc., 13, p29.

Kemey, J.G., and Snell, J.L., 1960, Finite Markov chains: D. Van Nostrand, New York, p123-125.

Kendall, M.G., and Moran, P.A.P., 1963, Geometric probability: Griffin & Co. Ltd., London, p37-38.

Kitayama, K., 1970, Activity measurements in orthosilicate and metasilicate solid solutions. II. MgSiO_3 - FeSiO_3 at 1154, 1204, and 1250°C: Bull. Chem. Soc. Japan, 43, p1390-1393.

Kitayama, K., and Katsura, T., 1968, Activity measurements in orthosilicate and metasilicate solid solutions. I. Mg_2SiO_4 - Fe_2SiO_4 and MgSiO_3 - FeSiO_3 at 1204°C: Bull. Chem. Soc. Japan, 41, p1146-1151.

- Korzhinskii, D.S., 1959, Physicochemical basis of the analysis of the paragenesis of minerals (translation): N.Y. Consultants Bureau Inc., p71, 142.
- Kullback, S., 1959, Information theory and statistics: John Wiley & Sons, New York, p119.
- Kretz, R., 1959, Chemical study of garnet, biotite, and hornblende from gneiss of southwest Quebec, with emphasis on distribution of elements in coexisting minerals: J. Geol., 67, p371-402.
- _____, 1961, Some applications of thermodynamics to coexisting minerals of various compositions. Example: orthopyroxene-clinopyroxene and orthopyroxene-garnet: J. Geol., 69, p361-387.
- _____, 1963, Distribution of magnesium and iron between orthopyroxene and calcic pyroxene in natural mineral assemblages: J. Geol. 71, p373-385.
- _____, 1964, Analysis of equilibrium in garnet-biotite-sillimanite gneisses from Quebec: J. Petrol., 5, p1-20.
- _____, 1966a, Grain size distribution for certain metamorphic minerals in relation to nucleation and growth: J. Geol., 74, p147-173.

Kretz, R., 1966b, Interpretation of the shape of mineral grains in metamorphic rocks: J. Petrol.; 7, p68-94.

_____, 1969, On the spatial distribution of crystals in rocks: Lithos, 2, p39-65.

_____, 1970, Variation in the composition of muscovite and albite in a pegmatite dike near Yellowknife: Can. J. Earth Sci., 7, p1219-1235.

Krumbein, W.C., 1967, Fortran IV computer programs for Markov chain experiments in geology: Computer Contribution 13, State Geological Survey, The University of Kansas, Lawrence, p8.

Lafeber, D., 1963, On the spatial distribution of fabric elements in rocks and soil fabrics: Proc. Austr. New Zealand Conf. Soil Mech. Found. Eng. 4th, Adelaide, p185-199.

_____, 1966, Soil structural concept: Eng. Geol., 1, p261-290.

Laffitte, P., 1957, Introduction à l'étude des roches métamorphiques et des gites métallifères: Paris, p328, in Flinn, 1969.

- Leelanandam, C., 1967, Chemical study of pyroxenes from the charnockitic rocks of Kondapalli (Andhra Pradesh), India, with emphasis on the distribution of elements in coexisting pyroxenes: *Min. Mag.*, 37, p153-179.
- Liou, J.G., 1973, Synthesis and stability relations of epidote, $\text{Ca}_2\text{Al}_2\text{FeSi}_3\text{O}_{12}(\text{OH})$: *J. Petrol.*, 14, p381-413.
- Lindsley, D.H., King, Jr., H.E., and Turnock, A.C., 1974, Compositions of synthetic augite and hypersthene coexisting at 810°C: Application to pyroxenes from lunar highlands rocks: *Geoph. Res. Letts.*, 1, No. 3, p134-136.
- Luth, W.C., Martin, R.F., and Fenn, P.M., 1974, Peralkaline alkali feldspar solvi: in *The Feldspars*. Edited by W.S. Mackenzie and J. Zussman. Crane, Russak & Company, Inc., New York, p297-312.
- Mahan, S.M., and Rogers, J.J.W., 1968, A study of grain contacts in some high grade metamorphic rocks: *Am. Min.*, 53, p323-327.
- Martignole, J., and Schrijver, K., 1973, Effect of rock composition on appearance of garnet in anorthosite-charnockite suites: *Can. J. Earth Sci.*, 10, p1132-1139.

Maxey, L.R., and Vogel, T.A., 1974, Compositional dependence of the coexisting pyroxene iron-magnesium distribution coefficient: *Contr. Mineral. Petrol.* 43, p295-306.

Moore, P.G., 1954, Spacing in plant population: *Ecology*, 35, p222-227.

Muan, A., Nafziger, R.H., and Roeder, P.L., 1964, A method for determining the instability of ferrosilite: *Nature*, 202, p688-689.

Mueller, R.F., 1960, Compositional characteristics of equilibrium relations in mineral assemblages of a metamorphosed iron formation: *Am. J. Sci.*, 258, p449-497.

_____, 1961, Analysis of relations among Mg, Fe and Mn in certain metamorphic minerals: *Geochim. Cosmochim. Acta*, 25, p267-296.

_____, 1962, Energetics of certain silicate solid solutions: *Geochim. Cosmochim. Acta*, 26, p581-598.

_____, 1964, Theory of immiscibility in mineral systems: *Min. Mag.*, 33, p1015-1023.

_____, 1967, Model of order-disorder kinetics in certain quasi-binary crystals of continuously variable compositions: *J. Phys. Chem. Solids*, 28, p2239-2243.

Mueller, R.F., 1969, Kinetics and thermodynamics of intracrystalline distributions: Mineral. Soc. Amer. Spec. Pap. 2, p83-93.

_____, 1970, Two-step mechanism for order-disorder kinetics in silicates: Am. Min., 55, p1210-1218.

Mueller, R.F., Ghose, S., and Saxena, S.K., 1970, Partitioning of cations between coexisting single- and multi-site phases: A discussion: Geochim. Cosmochim. Acta, 34, p1356-1360.

Neyman, J., 1939, On a new class of contagious distributions applicable in entomology and bacteriology: Ann. Math. Statist., 10, p35-57.

Nicholson, W.J., and Burns, R.G., 1964, Quadruple coupling constant eqQ/h , of Fe^{3+} in several rare-earth iron garnets: Phys. Rev.; 133, pA1568-A1570.

Olsen, E., and Bunch, T.E., 1970, Empirical derivation of activity coefficients for the magnesium rich portion of the olivine solid solution: Am. Min., 55, p1829-1842.

Olsen, E., and Mueller, R.F., 1966, Stability of orthopyroxene with respect to pressure, temperature and composition: J. Geol., 74, p620-625.

- Orville, P.M., 1963, Alkali ion exchange between vapour and feldspar phases: *Am. J. Sci.*, 261, p301-337.
- Osborn, E.F., 1959, Role of oxygen pressure in the crystallization and differentiation of basaltic magma: *Am. J. Sci.*, 257, p609-619.
- Owen, D.B., 1962, *Handbook of statistical tables*: Addison-Wesley, Reading, Mass.
- Parras, K., 1958, On the charnockites in the light of a highly metamorphic rock complex in southwestern Finland: *Bull. Comm. Geol. Finland*, no. 181, pl-137.
- Parzen, E., 1962, *Stochastic processes*: Holden-Day, San Francisco, Calif., 324p.
- Perchuk, L.L., 1968, Pyroxene-garnet equilibria and the depth facies concept of eclogite: *Internat. Geol. Rev.*, 10, no. 3, p284.
- Philpotts, A.R., 1966, Origin of the anorthosite-mangerite rocks in Southern Quebec: *J. Petrol.*, 7, pl-64.
- Phinney, W.C., 1963, Phase equilibria in the metamorphic rocks of St. Paul Island and Cape North, Nova Scotia: *J. Petrol.* 4, p90-130.
- Pichamuthu, C.S., 1953, *The charnockite problem*: Mysore Geologists Assoc., Bangalore, India.

- Pielou, E.C., 1959, The use of point-to-point distances in the study of the pattern of plant populations: J. Ecol., 47, p607-613.
- Quensel, P., 1951, The charnockite series of the Varberg district on the southwestern coast of Sweden: Arkiv. Mineral. Geol., 1, p227-322.
- Ramberg, H., 1952, The origin of metamorphic and metasomatic rocks: The University of Chicago Press, p220-225.
- Ramberg, H., and DeVore, G.W., 1951, The distribution of Mg^{2+} and of Fe^{2+} ions in coexisting olivines and pyroxenes: J. Geol., 59, p193-210.
- Ray, S., and Sen, S.K., 1970, Partitioning of major exchangeable cations among orthopyroxene, calcic pyroxene and hornblende in basic granulites from Madras: N. Jb. Miner. Abh., 114, p61-88.
- Reinhardt, E.W., 1968, Phase relations in cordierite-bearing gneisses from the Gananoque area, Ontario: Can. J. Earth Sci., 5, p465-467.
- Ringwood, A.E., and Green, D.H., 1964, Experimental investigations bearing on the nature of the Mohorovicic discontinuity: Nature, 201, p566-567.
- Roach, R.A., and Duffell, S., 1968, The pyroxene granulites of the Mount Wright Map-Area, Quebec-Newfoundland: Geol. Soc. Can. Bull., 162, 83p.

- Rogers, J.J.W., and Bogy, D.B., 1958, A study of grain contacts in granitic rocks: *Science*, 127, p470-471.
- Romanova, M.A., 1972, The influence of greisenization on the markovian properties of grain sequences in granitic rocks: Abstract, 24th IGC in Montreal, p517.
- Rucklidge, J., and Gasparrini, E.L., 1969, Electron microprobe analytical data reduction - EMPADR VII: Dept. of Geology, University of Toronto.
- Saxena, S.K., 1968, Chemical study of phase equilibria in charnockites, Varberg, Sweden: *Am. Min.* 53, p1674-1694.
- _____, 1969b, Silicate solid solutions and geothermometry, 1. Use of the regular solution model: *Contr. Mineral. Petrol.*, 21, p338-345.
- _____, 1971, $Mg^{2+}-Fe^{2+}$ order-disorder in orthopyroxene and the $Mg^{2+}-Fe^{2+}$ distribution between coexisting minerals: *Lithos.* 4, p345-354.
- _____, 1973, Thermodynamics of rock-forming crystal-line solutions. Springer-Verlag New York, p39-40.
- Saxena, S., and Ghose, S., 1970, Order-disorder and the activity composition relation in a binary crystal-line solution I. Metamorphic orthopyroxene: *Am. Min.*, 55, p1219-1225.

Saxena, S.K., and Ghose, S., 1971, Mg²⁺-Fe²⁺ order-disorder and the thermodynamics of the orthopyroxene crystalline solutions: Am. Min., 56, p532-559.

Sen, S.K., and Saha, J.R., 1970, Phase relations in three charnockites from Pallavaram-Tambaram: Contr. Mineral. Petrol., 27, p239-243.

Singh, S., 1966, Orthopyroxene-bearing rocks of charnockitic affinities in the South Savana-Kanuku Complex of British Guiana: J. Petrol., 7, p171-192.

Sinnott, M.J., 1958, The solid state for engineers: John Wiley & Sons, New York, p272-273.

Smith, C.S., 1948, Grains, phases and interfaces: an interpretation of microstructure: Trans. AIME, 175, p15-51.

_____, 1952, Interphase interfaces: in Imperfections in Nearly Perfect Crystals, ed. W. Shockley, John Wiley & Sons, New York, p377-401.

Smith, D., 1970, Iron-rich pyroxenes: Carnegie Inst. Washington Yearbook 1970, p286.

Spry, A., 1969, Metamorphic textures: Pergamon Press, New York, p25-29.

Stockwell, C.H., 1972, Revised Precambrian time scale for the Canadian Shield: Geol. Surv. Can. Paper 72-52, p1-4.

Subramaniam, A.P., 1959, Charnockites of the type area near Madras -- A reinterpretation: *Am. J. Sci.*, 257, p321-353.

_____, 1962, Pyroxenes and garnets from charnockites and associated granulites: *Petrological Studies, Buddington Volume*, p21-36.

Swalin, R.A., 1962, *Thermodynamics of solids*: John Wiley & Sons, New York, Chapter 12, p180-213.

Taylor, H.P., Jr., 1969, Oxygen isotope studies of anorthosites with particular reference to the origin of bodies in the Adirondack Mts., New York: in *Origin of Anorthosite and Related Rocks*, ed. Y.W. Isachsen, New York State Museum and Science Service Memoir 18.

Thompson, J.B., Jr., 1957, The graphic analysis of mineral assemblages in pelitic schists: *Am. Min.*, 42, p842-859.

Turner, F.J., 1968, *Metamorphic petrology*: McGraw-Hill Book Company, New York, p359.

Turner, F.J., and Verhoogen, J., 1960, *Igneous and metamorphic petrology*: McGraw-Hill, New York, p324-328.

Vincent, E.A., and Phillips, R., 1954, Iron-titanium oxide minerals in layered gabbros of the Skaergaard Intrusion, East Greenland: *Geochim. Cosmochim. Acta*, 6, p1-26.

Virgo, D., and Hafner; S.S., 1968, Re-evaluation of the cation distribution in orthopyroxenes by the Mössbauer effect: Earth Planet. Sci. Lett., 4, p265-269.

_____, 1969, Fe²⁺, Mg order-disorder in heated orthopyroxenes: Min. Soc. Amer. Spec. Pap. 2, p67-81.

_____, 1970, Fe²⁺, Mg order-disorder in natural orthopyroxenes: Am. Min., 55, p201-223.

Vistelius, A.B., 1966, Genesis of the Mt. Belaya granodiorite, Kamchatka (an experiment in stochastic modelling): Doklady Acad. Sci., U.S.S.R., Earth Sci. Sec., 167, p48-50.

_____, 1972, Ideal granites and their metasomatic transformation: Stochastic model, statistical description of natural rocks: Abstract, 24th IGC in Montreal, p518-519.

Warren, B.E., and Bragg, W.L., 1929, The structure of diopside CaMg(SiO₃)₂: Z. Krist., 69, p168.

Wertheim, G.R., 1964, Mössbauer effect, principles and applications: Academic Press, New York.

Williams, R.J., 1971, Reaction constants in the system Fe-MgO-SiO₂-O₂ at 1 atm between 900° and 1300°C: Experimental results: Am. J. Sci., 270, p334-360.

Wilson, A.F., 1952, The charnockite problem, Australia: Univ. of Adelaide Sir Douglas Mawson Volume, p203-224.

_____, 1954, The charnockite and associated rocks of northwestern South Australia: J. Dolentes from the Musgrave and Everard Ranges, Roy. Soc. South Australia Tr. v72.

_____, 1959, The charnockite rocks of Australia: Geol. Rundschau, 47, p491-510.

_____, 1960a, The charnockite granites and associated granites of Central Australia: Trans. Roy. Soc. South Australia, 83, p37-75.

_____, 1960b, Coexisting pyroxenes: Some causes of variation and anomalies in the optically derived compositional tie-lines, with particular reference to charnockitic rocks: Geol. Mag., 97, pl-17.

Wones, D.R., and Eugster, H.P., 1965, Stability of biotite: experiment, theory, and application: Am. Min., 50, p1228-1272.

Yoder, H.S., Jr., 1955a, Almandine garnet stability range (Abs): Am. Min., 40, p342.

_____, 1955b, Dipside-anorthite-water system at 5000 bars: Geol. Soc. Amer. Bull., 68, p1638-1639.

Yoder, H.S., Jr., 1967, Anorthite-akermanite and albite-soda melilite reaction relations: Carnegie Inst. Washington Yearbook 1967-1968, p106.

_____, 1969, Experimental studies bearing on the origin of anorthosite, in Origin of Anorthosite and Related Rocks: Ed. Y. Isachsen, New York Museum and Science Services Memoir 18, p13-22.

Yoder, H.S., Jr., and Eugster, H.P., 1954, Phlogopite synthesis and stability range: Geochim. Cosmochim. Acta, 6, p157-185.

_____, 1955, Synthetic and natural muscovites: Geochim. Cosmochim. Acta, 8, p225-280.

Yoder, H.S., Jr., Stewart, D.B., and Smith, J.R., 1957, Ternary feldspars: Carnegie Inst. Washington Yearbook 1956, p206-214.

Yoder, H.S., Jr., Tilley, C.E., 1962, Origin of basalt magma: An experimental study of natural and synthetic rock systems: J. Petrol., 3, p342-532.

Zen, E-An, 1963, Components, phases, and criteria of chemical equilibrium in rocks: Am. J. Sci., 261, p929-942.

Zen, E-An, 1966, Construction of pressure-temperature diagram for multicomponent systems after the method of Schreinemakers - A geometric approach: U.S. Geol. Survey Bull., 1225, 56p.

Zverev, N.D., Val'ter, A.A., Romanov, V.P., and Gorogótskaya, L.I., 1971, Character of Fe^{2+} ion distribution in pyroxenes from eulysite: Lithos, 4, p17-21.

Additional references

Binns, R.A., 1964, Zones of progressive regional metamorphism in New South Wales: J. Geol. Soc. Aust., 11, p283-330.

Flanagan, F.J., 1967, U.S. Geological Survey silicate rock standards: Geochim. Cosmochim. Acta, 31, p289-308.

_____, 1973, 1972 values for international geochemical reference samples: Geochim. Cosmochim. Acta, 37, p1189-1200.

Saxena, S.K., 1969a, Distribution of elements in coexisting mineral and the problem of chemical disequilibrium in metamorphosed basic rocks: Contr. Mineral. Petrol., 20, p177-197.

APPENDIX I

A Fortran IV computer program to perform calculations from
chemical analyses of pyroxenes, garnets, amphiboles and micas

1 A
2 A
3 A
4 A
5 A
6 A
7 A
8 A
9 A
10 A
11 A
12 A
13 A
14 A
15 A
16 A
17 A
18 A
19 A
20 A
21 A
22 A
23 A
24 A
25 A
26 A
27 A
28 A
29 A
30 A
31 A
32 A
33 A
34 A
35 A
36 A
37 A
38 A
39 A
40 A
41 A
42 A

```

C A FORTRAN PROGRAM TO RECALCULATE CHEMICAL ANALYSES OF PYROXENES,
C AMPHIBOLES, MICAS, AND GARNETS-----L. S. JEN
C THIS PROGRAM IS DESIGNED TO RUN JOB ON IBM360/65 COMPUTER
C (1) CALCULATION OF TOTAL WT%, MOLECULAR PROPORTION, ATOMIC
C PROPORTION
C (2) CALCULATION OF NUMBERS OF IONS ON THE BASIS OF 6 OXYGENS FOR
C PYROXFNS,24(O,OH,F,CL) OR 22(O,OH,F,CL) IF H2O IS NOT ANALYSED
C FOR AMPHIBOLES AND MICAS, AND 24 OXYGENS FOR GARNETS
C (3) CALCULATION OF VARIOUS ATOMIC RATIOS
C EXPLANATION OF ABBREVIATIONS IN OUTPUT RESULTS
C APSIAL=ATOMIC PROPORTION OF SI+AL, APALT=ATOMIC PROPORTION OF
C TETRAHEDRAL AL
C APALO=ATOMIC PROPORTION OF OCTAHEDRAL AL, APTIT=ATOMIC PROPORTION
C OF
C TETRAHEDRAL TI, APTIO=ATOMIC PROPORTION OF OCTAHEDRAL TI,
C APFE3=ATOMIC PROPORTION OF TETRAHEDRAL FERRIC IRON,APFE3O=
C ATOMIC PROPORTION OF OCTAHEDRAL FERRIC IRON
C ALT=TETRAHEDRAL AL, ALO=OCTAHEDRAL AL, TIT=TETRAHEDRAL TI,
C TIO=OCTAHEDRAL TI, FE3T=TETRAHEDRAL FERRIC IRON, FE3O=OCTAHEDRAL
C FERRIC IRON
C Z=TETRAHEDRAL LATTICE SITE(OCCUPANCY)
C XY=OCTAHEDRAL LATTICE SITE(OCCUPANCY) EXCEPT IN GARNETS X=CUBIC
C SITE
C TOLERANCE OF PROGRAM ON INPUT DATA IN % OXIDES---SI02,AL203,FE203,
C CR203,FFO,MGO,MNO,NIO,CAO,NA20,K20,LI20,SRO,BAO,RB20,H20,F,CL
C DIMENSION R(4)
C REAL W(20),MW(20),MP(20),APO(20),APC(20),X(20,2),XX(20),YY(20)
C DOUBLE PRECISION SI,ALT,ALO,TIT,TIO,FE3T,FE3O,CR,FE2,MG,MN,CA,NA,K
C 1,LI,TI,FE3,MGMG,SRO,SR,BAO,BA,RB20,RR,H,F,CL
C READ (1,2) MO
C DO 1 I=1,MO
C READ (1,3) NSUB
C IF (NSUB.EQ.1) CALL PYROX
C IF (NSUB.EQ.2) CALL AMICA
C IF (NSUB.EQ.3) CALL GARNET
C CONTINUE
C STOP
C
C 1
C 2
C 3
C 4
C 12
C 13
C 14
C 15
C 16
C 17
C 18
C 19
C 20
C 21
C 22
C 23
C 24
C 25
C 26
C 27
C 28
C 29
C 30
C 31
C 32
C 33
C 34
C 35
C 36
C 37
C 38
C 39
C 40
C 41
C 42

```

FORTRAN IV G LEVEL 21

```

0001 SUBROUTINE PYROX
0002 A FORTRAN PROGRAM TO RECALCULATE CHEMICAL ANALYSES OF
0003 PYROXENES-----
0004 --L. S. JEN
0005 DIMENSION B(4)
0006 REAL W(20),MW(20),MP(20),APO(20),X(20,2),XX(20),YY(20)
0007 DOUBLE PRECISION SI,AL,ALO,TIT,TIO,FE3T,FE3O,CR,FE2,MG,MN,CA,NA,K
0008 1,LI,TI,FE3,MG*MG
0009 READ (1,45) N,L
0010 DO 1 I=1,N
0011 READ (1,46) (X(I,J),J=1,2)
0012 CONTINUE
0013 DO 2 I=1,L
0014 READ (1,47) XX(I)
0015 CONTINUE
0016 READ (1,48) (MW(I),I=1,N)
0017 READ (1,49) NO
0018 DO 44 NM=1,NO
0019 READ (1,50) M,(B(I),I=1,4)
0020 WRITE (3,51) M,(B(I),I=1,4)
0021 READ (1,52) (W(I),I=1,N)
0022 SW=0.0
0023 DO 3 I=1,N
0024 SW=SW+W(I)
0025 CONTINUE
0026 IF (MW(I).EQ.0.0) GO TO 5
0027 MP(I)=W(I)/MW(I)
0028 CONTINUE
0029 CONTINUE
0030 APO(1)=2.0*MP(1)
0031 APO(2)=3.0*MP(2)
0032 APO(3)=2.0*MP(3)
0033 APO(4)=3.0*MP(4)
0034 APO(5)=3.0*MP(5)
0035 APO(6)=MP(6)
0036 APO(7)=MP(7)
0037 APO(8)=MP(8)
0038 APO(9)=MP(9)
0039 APO(10)=MP(10)
0040 APO(11)=MP(11)
0041 APO(12)=MP(12)
0042 APO(13)=MP(13)
0043

```

1 B
2 B
3 B
4 B
5 B
6 B
7 B
8 B
9 B
10 B
11 B
12 B
13 B
14 B
15 B
16 B
17 B
18 B
19 B
20 B
21 B
22 B
23 B
24 B
25 B
26 B
27 B
28 B
29 B
30 B
31 B
32 B
33 B
34 B
35 B
36 B
37 B
38 B
39 B
40 B
41 B
42 B
43 B

R 44
 B 45
 B 46
 B 47
 B 48
 B 49
 B 50
 B 51
 B 52
 B 53
 B 54
 B 55
 B 56
 B 57
 B 58
 B 59
 B 60
 B 61
 B 62
 B 63
 B 64
 B 65
 B 66
 B 67
 B 68
 B 69
 B 70
 B 71
 B 72
 B 73
 B 74
 B 75
 B 76
 B 77
 B 78
 B 79
 B 80
 B 81
 B 82
 B 83
 B 84
 B 85
 B 86

```

0000 SUMAPO=0.0
0001 DO 6 I=1,N
0002 SUMAPO=SUMAPO+APO(I)
0003 CONTINUE
0004 FACT1=SUMAPO/6.0
0005 APC(1)=MP(1)
0006 APC(2)=2.0*MP(2)
0007 APC(3)=MP(3)
0008 APC(4)=2.0*MP(4)
0009 APC(5)=2.0*MP(5)
0010 APC(6)=MP(6)
0011 APC(7)=MP(7)
0012 APC(8)=MP(8)
0013 APC(9)=MP(9)
0014 APC(10)=MP(10)
0015 APC(11)=2.0*MP(11)
0016 APC(12)=2.0*MP(12)
0017 APC(13)=2.0*MP(13)
0018 IF (APC(1).GE.2.0*FACT1) GO TO 13
0019 FACT2=2.0
0020 APSIAL=FACT2*FACT1
0021 APALT=APSTAL-APC(1)
0022 APALO=APC(2)-APALT
0023 IF (APALO.GT.0.0) GO TO 12
0024 APALO=0.0
0025 APALT=APC(2)
0026 APTIT=APSIAL-APC(1)-APC(2)
0027 APTIO=APC(3)-APTIT
0028 IF (APTIO.GT.0.0) GO TO 10
0029 APALT=APC(2)
0030 APALO=0.0
0031 APTIT=APC(3)
0032 APTIO=0.0
0033 APFE31=APSIAL-APC(1)-APC(2)-APC(3)
0034 APFE30=APC(4)-APFE31
0035 IF (APFE30.GT.0.0) GO TO 8
0036 APFE30=0.0
0037 APFE31=APC(4)
0038 SUMK=0.0
0039 DO 7 J=5,N
0040 SUMK=SUMK+APC(J)
0041 CONTINUE
0042 SUM=SUMK+APFE3T
  
```

16/53/03

DATE = 73169

PYROX

FORTRAN IV G LEVEL 21

```

0083      GO TO 17
0084      SUMF=0.0
0085      DO 9 I=5,N
0086      SUMF=SUMF+APC(I)
0087      CONTINUE
0088      SUM=SUMF+APFE30
0089      GO TO 17
0090      APFE3T=0.0
0091      APFE30=APC(4)
0092      SUMG=0.0
0093      DO 11 I=4,N
0094      SUMG=SUMG+APC(I)
0095      CONTINUE
0096      SUM=SUMG+APTIO
0097      GO TO 17
0098      APTIT=0.0
0099      APTIO=APC(3)
0100      APFE3T=0.0
0101      APFE30=APC(4)
0102      GO TO 15
0103      APALT=0.0
0104      APAL0=APC(2)
0105      APTIT=0.0
0106      APTIO=APC(3)
0107      APFE3T=0.0
0108      APFE30=APC(4)
0109      APSIAL=APC(1)
0110      FACT2=APSIAL/FACT1
0111      SUM=0.0
0112      DO 14 I=2,N
0113      SUM=SUM+APC(I)
0114      CONTINUE
0115      SUMA=0.0
0116      DO 16 I=3,N
0117      SUMA=SUMA+APC(I)
0118      CONTINUE
0119      SUM=APAL0+SUMA
0120      CONTINUE
0121      FACT3=SUM/FACT1
0122      ST=FACT2*APC(1)/APSIAL
0123      ALT=FACT2*APALT/APSIAL
0124      AL0=FACT3*APAL0/SUM
0125
0126
0127
0128
0129

```

```

B 87
B 88
B 89
B 90
B 91
B 92
B 93
B 94
B 95
B 96
B 97
B 98
B 99
B 100
B 101
B 102
B 103
B 104
B 105
B 106
B 107
B 108
B 109
B 110
B 111
B 112
B 113
B 114
B 115
B 116
B 117
B 118
B 119
B 120
B 121
B 122
B 123
B 124
B 125
B 126
B 127
B 128
B 129

```

B 130
 B 131
 B 132
 B 133
 B 134
 B 135
 B 136
 B 137
 B 138
 B 139
 B 140
 B 141
 B 142
 B 143
 B 144
 B 145
 B 146
 B 147
 B 148
 B 149
 B 150
 B 151
 B 152
 B 153
 B 154
 B 155
 B 156
 B 157
 B 158
 B 159
 B 160
 B 161
 B 162
 B 163
 B 164
 B 165
 B 166
 B 167
 B 168
 B 169
 B 170
 B 171
 B 172

```

0126 TIT=FACT2*APTIT/APSIAL
0127 TIO=FACT3*APTIO/SUM
0128 TI=FACT3*APC(3)/SUM
0129 FE3T=FACT2*APFE3T/APSIAL
0130 FE3O=FACT3*APFE3O/SUM
0131 FE3=FACT3*APC(4)/SUM
0132 CR=FACT3*APC(5)/SUM
0133 FE2=FACT3*APC(6)/SUM
0134 MG=FACT3*APC(7)/SUM
0135 MN=FACT3*APC(8)/SUM
0136 NI=FACT3*APC(9)/SUM
0137 CA=FACT3*APC(10)/SUM
0138 NA=FACT3*APC(11)/SUM
0139 K=FACT3*APC(12)/SUM
0140 LI=FACT3*APC(13)/SUM
0141 YY(1)=SI
0142 YY(2)=ALT
0143 YY(3)=AL0
0144 YY(4)=TIT
0145 YY(5)=TIO
0146 YY(6)=FE3T
0147 YY(7)=FE3O
0148 YY(8)=CR
0149 YY(9)=FE2
0150 YY(10)=MG
0151 YY(11)=MN
0152 YY(12)=NI
0153 YY(13)=CA
0154 YY(14)=NA
0155 YY(15)=K
0156 YY(16)=LI
0157 IF (ALT.GT.0.0) GO TO 19
0158 Z=SI
0159 XY=0.0
0160 DO 18 I=2,L
0161 XY=XY+YY(I)
0162 CONTINUE
0163 GO TO 37
0164 Z=SI+ALT
0165 XY=0.0
0166 DO 20 I=3,L
0167 XY=XY+YY(I)
0168 CONTINUE
0169
0170
0171
0172
  
```

20

18
19
20

16/53/03

DATE = 73169

PYROX

FORTRAN IV G LEVEL 21

```

2169 IF (ALO.LE.0.0) GO TO 22
0170 Z=SI+ALT
0171 XY=0.0
0172 DO 21 I=3,L
0173 XY=XY+YY(I)
0174 CONTINUE
21 GO TO 37
0175 Z=SI+ALT+ALO
0176 XY=0.0
0177 DO 23 I=4,L
0178 XY=XY+YY(I)
0179 CONTINUE
23 IF (TI.EQ.0.0) GO TO 31
IF (TIT.GT.0.0) GO TO 25
0180 Z=SI+ALT+ALO
0181 XY=0.0
0182 DO 24 I=4,L
0183 XY=XY+YY(I)
0184 CONTINUE
24 GO TO 37
0185 Z=SI+ALT+ALO+TIT
0186 XY=0.0
0187 DO 26 I=5,L
0188 XY=XY+YY(I)
0189 CONTINUE
26 IF (TIO.LF.0.0) GO TO 28
Z=SI+ALT+ALO+TIT
0190 XY=0.0
0191 DO 27 I=5,L
0192 XY=XY+YY(I)
0193 CONTINUE
27 GO TO 37
0194 Z=SI+ALT+ALO+TIT+TIO
0195 XY=0.0
0196 DO 29 I=6,L
0197 XY=XY+YY(I)
0198 CONTINUE
29 IF (FF3T.GT.0.0) GO TO 31
Z=SI+ALT+ALO+TIT+TIO
0199 XY=0.0
0200 DO 30 I=6,L
0201 XY=XY+YY(I)
0202 CONTINUE
30
0203
0204
0205
0206
0207
0208
0209
0210
0211

```

```

B 173
B 174
B 175
B 176
B 177
B 178
B 179
B 180
B 181
B 182
B 183
B 184
B 185
B 186
B 187
B 188
B 189
B 190
B 191
B 192
B 193
B 194
B 195
B 196
B 197
B 198
B 199
B 200
B 201
B 202
B 203
B 204
B 205
B 206
B 207
B 208
B 209
B 210
B 211
B 212
B 213
B 214
B 215

```

16/53/03

DATE = 73169

PYROX

21

FORTRAN IV G LEVEL

```

0212 GO TO 37
0213 Z=SI+ALT+ALO+TIT+TIO+FE3T
0214 XY=0.0
0215 DO 32 I=7,L
0216 XY=XY+YY(I)
0217 CONTINUE
0218 IF (FE30.LE.0.0) GO TO 34
0219 Z=SI+ALT+ALO+TIT+TIO+FE3T
0220 XY=0.0
0221 DO 33 I=7,L
0222 XY=XY+YY(I)
0223 CONTINUE
0224 GO TO 37
0225 Z=0.0
0226 DO 35 I=1,7
0227 Z=7+YY(J)
0228 CONTINUE
0229 XY=0.0
0230 DO 36 I=8,L
0231 XY=XY+YY(I)
0232 CONTINUE
0233 WRITE (3,53)
0234 DO 38 I=1,N
0235 WRITE (3,54) (X(I,J),J=1,2),W(I),HW(I),MP(I),APO(I),APC(I)
0236 CONTINUE
0237 WRITE (3,55) SW
0238 WRITE (3,56) SUMAPO
0239 WRITE (3,57) FACT1,FACT2,FACT3
0240 WRITE (3,58) APSIAL,APALT,APALO
0241 WRITE (3,59) APTIT,APTIO
0242 WRITE (3,60) APFE3T,APFE30,SUM
0243 WRITE (3,61)
0244 DO 39 I=1,L
0245 WRITE (3,62) XX(I),YY(I)
0246 CONTINUE
0247 WRITE (3,63) Z,XY
0248 AL=ALT+ALO
0249 A=AL/ST
0250 IF (AL.NE.0.0) GO TO 40
0251 PR=0.0
0252 BR=ALT/AL
0253 C=SI/Z
0254 D=ALT/Z

```

B 216
 B 217
 B 218
 B 219
 B 220
 B 221
 B 222
 B 223
 B 224
 B 225
 B 226
 B 227
 B 228
 B 229
 B 230
 B 231
 B 232
 B 233
 B 234
 B 235
 B 236
 B 237
 B 238
 B 239
 B 240
 B 241
 B 242
 B 243
 B 244
 B 245
 B 246
 B 247
 B 248
 B 249
 B 250
 B 251
 B 252
 B 253
 B 254
 B 255
 B 256
 B 257
 B 258

16/53/03

DATE = 73169

PYROX

21

FORTRAN IV G LEVEL

IF (FE2.NE.0.0) GO TO 41

E=0.0

E=MG/FE2

G=MG/XY

H=FE3/XY

P=MN/XY

Q=CA/XY

R=K/XY

S=NA/XY

TT=K+NA

IF (TT.NE.0.0) GO TO 42

T=0.0

GO TO 43

T=K/(K+NA)

XMG=MG/(MG+FE2)

XFF2=FE2/(FE2+MG)

XXMG=MG/(MG+FE2+FE3)

XXFE2=FE2/(FE2+FE3+MG)

XFE=(FE2+FE3)/(FE2+FE3+MG)

F=XMG/(1-XMG)

FF=XFE2/(1-XFE2)

U=XFF2/XMG

V=XMG/XFE2

CC=MN/(MG+FE2+MN)

FEMN=FF2+FE3+MN

DD=CA+MG+FE2+FE3

MGMG=MG/DD*100.0

FFFE=(FE2+FE3)/DD*100.0

CACA=CA/DD*100.0

WRITE (3,64) A,BB

WRITE (3,65) C

WRITE (3,66) D,E

WRITE (3,67) G,H

WRITE (3,68) P,Q

WRITE (3,69) R,S

WRITE (3,70) T,XMG

WRITE (3,71) XFE2

WRITE (3,72) XXMG

WRITE (3,73) XXFE2

WRITE (3,74) XFE

WRITE (3,75) F,FF

WRITE (3,76) U,V

WRITE (3,77) CC

0255

0256

0257

0258

0259

0260

0261

0262

0263

0264

0265

0266

0267

0268

0269

0270

0271

0272

0273

0274

0275

0276

0277

0278

0279

0280

0281

0282

0283

0284

0285

0286

0287

0288

0289

0290

0291

0292

0293

0294

0295

0296

0297

0298

0299

0300

0301

B 259

B 260

B 261

B 262

B 263

B 264

B 265

B 266

B 267

B 268

B 269

B 270

B 271

B 272

B 273

B 274

B 275

B 276

B 277

B 278

B 279

B 280

B 281

B 282

B 283

B 284

B 285

B 286

B 287

B 288

B 289

B 290

B 291

B 292

B 293

B 294

B 295

B 296

B 297

B 298

B 299

B 300

B 301

DATE = 73169

PYROX

FORTRAN IV 6 LEVEL 21

```

0208 WRITE (3,78) FEMN
0209 WRITE (3,79)
0300 WRITE (3,80) MIMG,FEFF,CACA
0301 CONTINUE
0302 RETURN

C
45 FORMAT (2I3)
46 FORMAT (2A3)
47 FORMAT (A4)
48 FORMAT (13F6.2)
49 FORMAT (I2)
50 FORMAT (A4,4A4)
51 FORMAT ('1',0',2X,'SAMPLE J-',A4,5X,4A4)
52 FORMAT (13F6.2)
53 FORMAT ('0',5X,'OXIDES',12X,'WT %',10X,'MOL WT',8X,'MOL PROP',6X,'
1 ATOMIC PROP OXYGEN',2X,'ATOMIC PROP CATIONS')
54 FORMAT ('0',5X,2A3,8X,3(F10.5,5X),5X,F10.5,12X,F10.5)
55 FORMAT ('0',5X,'TOTAL WT %',1X,F10.5)
56 FORMAT ('0',5X,'TOTAL ATOMIC PROPORTION OF OXYGEN=',1X,F10.5)
57 FORMAT ('0',5X,'FACT1=',1X,F10.5,10X,'FACT2=',1X,F10.5,10X,'FACT3=
1',1X,F10.5)
58 FORMAT ('0',5X,'APSIAL=',1X,F10.5,5X,'APALT=',1X,F10.5,5X,'APALO=',
1,1X,F10.5)
59 FORMAT ('0',5X,'APTIT=',1X,F10.5,5X,'APTIO=',1X,F10.5)
60 FORMAT ('0',5X,'APFE3T=',1X,F10.5,5X,'APFE3O=',1X,F10.5,5X,'SUM=',
1X,F10.5)
61 FORMAT ('0',/,5X,'NUMBERS OF IONS ON THE BASIS OF 6 OXYGENS')
62 FORMAT ('0',15X,A4,5X,F10.5)
63 FORMAT ('0',15X,'Z=',1X,F10.5,10X,'XY=',1X,F10.5)
64 FORMAT ('0',1X,'AL/SI=',1X,F10.5,10X,'ALT/AL=',1X,F10.5)
65 FORMAT ('0',1X,'SI/Z=',1X,F10.5)
66 FORMAT ('0',1X,'ALT/Z=',1X,F10.5,10X,'MG/FE2=',1X,F10.5)
67 FORMAT ('0',1X,'MG/XY=',1X,F10.5,10X,'FE3/XY=',1X,F10.5)
68 FORMAT ('0',1X,'MN/XY=',1X,F10.5,10X,'CA/XY=',1X,F10.5)
69 FORMAT ('0',1X,'K/XY=',1X,F10.5,10X,'NA/XY=',1X,F10.5)
70 FORMAT ('0',1X,'K/(K+NA)=',1X,F10.5,10X,'XMG=MG/(MG+FE2)=',1X,F10.5)
71 FORMAT ('0',1X,'XFF2=FE2/(FE2+MG)=',1X,F10.5)
72 FORMAT ('0',1X,'XIMG=MG/(MG+FE2+FE3)=',1X,F10.5)
73 FORMAT ('0',1X,'XFFF2=FE2/(FE2+FE3+MG)=',1X,F10.5)
74 FORMAT ('0',1X,'XFFF=(FE2+FE3)/(FE2+FE3+MG)=',1X,F10.5)
75 FORMAT ('0',1X,'XMG/(1-XMG)=',1X,F10.5,10X,'XFE2/(1-XFE2)=',1X,F10.5)

```

```

B 302
B 303
B 304
B 305
B 306
B 307
B 308
B 309
B 310
B 311
B 312
B 313
B 314
B 315
B 316
B 317
B 318
B 319
B 320
B 321
B 322
B 323
B 324
B 325
B 326
B 327
B 328
B 329
B 330
B 331
B 332
B 333
B 334
B 335
B 336
B 337
B 338
B 339
B 340
B 341
B 342
B 343
B 344

```

```

FORTRAN IV G LEVEL 21          PYROX          DATE = 73169          16/53/03
0334      76      FORMAT ('0',1X,'XFE2/XMG=1,1X,F10.5'/(2X,'XMG/XFE2=',1X,F10.5))      0 345
0335      77      FORMAT ('0',1X,'MN/(MG+FE2+MN)=' ,1X,F10.5)      0 346
0336      78      FORMAT ('0',1X,'FE2+FE3+MN=' ,1X,F10.5)      0 347
0337      79      FORMAT ('0',/,5X,'RECALCULATION OF MG,FE AND CA TO 100 %')      0 348
0338      80      FORMAT ('0',14X,'MG=' ,1X,F10.5'/(15X,'FE=' ,1X,F10.5'/(15X,'CA=' ,1,      0 349
                1X,F10.5))      0 350
0339      END      B 351

```

16/53/03

DATE = 73169

AMICA

FORTRAN IV G LEVEL 21.

```

0001      SURROUTINE AMICA
0002      A FORTRAN PROGRAM TO RECALCULATE CHEIEMICAL ANALYSES OF AMPHIBOLES
0003      AND MICAS-----L. S. JEN
0004      DIMENSION B(4)
0005      REAL W(20),MW(20),MP(20),APO(20),APC(20),X(20,2),XX(20),YY(20)
0006      DOUBLE PRECISION SI,Al,T,AL0,TIT,TIO,FE3T,FE30,CR,FE2,HG,MN,CA,NA,K
0007      I,LI,TI,FE3,MGMG
0008      READ (1,23) N,L
0009      DO 1 I=1,N
0010      READ (1,24) (X(I,J),J=1,2)
0011      CONTINUE
0012      DO 2 I=1,L
0013      READ (1,25) XX(I)
0014      CONTINUE
0015      READ (1,26) (MW(I),I=1,N)
0016      READ (1,27) NO
0017      DO 22 NH=1,NO
0018      READ (1,28) M,(B(I),I=1,4)
0019      WRITE (3,29) M,(B(I),I=1,4)
0020      READ (1,30) (W(I),I=1,N)
0021      SW=0.0
0022      DO 3 I=1,N
0023      SW=SW+W(I)
0024      CONTINUE
0025      WF=W(12)*16.0/(2.0*19.0)
0026      WCL=W(13)*16.0/(2.0*35.457)
0027      TOTALW=SW-WF-WCL
0028      DO 4 I=1,N
0029      IF (MW(I).EQ.0.0) GO TO 5
0030      MP(I)=W(I)/MW(I)
0031      CONTINUE
0032      CONTINUE
0033      APO(1)=2.0*MP(1)
0034      APO(2)=3.0*MP(2)
0035      APO(3)=2.0*MP(3)
0036      APO(4)=3.0*MP(4)
0037      APO(5)=MP(5)
0038      APO(6)=MP(6)
0039      APO(7)=MP(7)
0040      APO(8)=MP(8)
0041      APO(9)=MP(9)
0042      APO(10)=MP(10)
0043      APO(11)=MP(11)
0044
0045
0046
0047
0048
0049
0050
0051
0052
0053
0054
0055
0056
0057
0058
0059
0060
0061
0062
0063
0064
0065
0066
0067
0068
0069
0070
0071
0072
0073
0074
0075
0076
0077
0078
0079
0080
0081
0082
0083
0084
0085
0086
0087
0088
0089
0090
0091
0092
0093
0094
0095
0096
0097
0098
0099
0100

```



16/53/03

DATE = 73169

AMICA

FORTRAN IV G LEVEL 21

```

0001 APO(12)=MP(12)
0002 APO(13)=MP(13)
0003 APO(14)=MP(14)
0004 SUMAPO=0.0
0005 DO 6 I=1,N
0006 SUMAPO=SUMAPO+APO(I)
0007 CONTINUE
0008 APF=MP(13)/2.0
0009 APCL=MP(14)/2.0
0010 TOTAL0=SUMAPO-APF-APCL
0011 DO 7 I=1,N
0012 IF (APO(12).NE.0.0) GO TO 8
0013 APC(I)=22.0/TOTAL0*APO(I)
0014 CONTINUE
0015 GO TO 10
0016 DO 9 I=1,N
0017 APC(I)=24.0/TOTAL0*APO(I)
0018 CONTINUE
0019 SJ=APC(1)/2.0
0020 AL=APC(2)*2.0/3.0
0021 TI=APC(3)/2.0
0022 FF3=APC(4)*2.0/3.0
0023 FF2=APC(5)
0024 NG=APC(6)
0025 LI=APC(7)*2.0
0026 MN=APC(8)
0027 CA=APC(9)
0028 NA=APC(10)*2.0
0029 KE=APC(11)*2.0
0030 HE=APC(12)*2.0
0031 FE=APC(13)
0032 CL=APC(14)
0033 IF (SI.GE.A.0) GO TO 11
0034 ALTY=R.0-SI
0035 ALN=AL-ALT
0036 GO TO 12
0037 ALT=0.0
0038 AL0=AL
0039 IF (AL0.GT.0.0) GO TO 13
0040 ALT=AL
0041 AL0=0.0
0042 YY(1)=SI
0043 YY(2)=ALT

```

```

C 44
C 45
C 46
C 47
C 48
C 49
C 50
C 51
C 52
C 53
C 54
C 55
C 56
C 57
C 58
C 59
C 60
C 61
C 62
C 63
C 64
C 65
C 66
C 67
C 68
C 69
C 70
C 71
C 72
C 73
C 74
C 75
C 76
C 77
C 78
C 79
C 80
C 81
C 82
C 83
C 84
C 85
C 86

```

16/53/03

DATE = 73169

AMICA

FORTRAN IV G LEVEL 21

```

0004      YY(3)=AL0
0005      YY(4)=TI
0006      YY(5)=FE3
0007      YY(6)=FE2
0008      YY(7)=MG
0009      YY(8)=LI
0010      YY(9)=MN
0011      YY(10)=CA
0012      YY(11)=NA
0013      YY(12)=K
0014      YY(13)=H
0015      YY(14)=F
0016      YY(15)=CL
0017      IF (ALT.NE.0.0) GO TO 14
0018      Z=SI
0019      XY=ALT+AL0+TI+FE3+FE2+MG+MN+LI
0020      GO TO 15
0021
0022      Z=SI+ALT
0023      XY=AL0+TI+FE3+FE2+MG+MN+LI
0024      WW=CA+NA+K
0025      OHFCL=H+F+CL
0026      WRITE (3,31)
0027      DO 16 I=1,N
0028      WRITE (3,32) (X(I),J,J=1,2),W(I),MW(I),MP(I),APO(I),APC(I)
0029      CONTINUE
0030      WRITE (3,33) SW,TOTALW
0031      WRITE (3,34)
0032      DO 17 I=1,L
0033      WRITE (3,35) XX(I),YY(I)
0034      CONTINUE
0035      WRITE (3,36).Z,XY,MW,OHFCL
0036      AL=ALT+AL0
0037      A=AL/SI
0038      IF (AL.NE.0.0) GO TO 18
0039      BR=0.0
0040      RR=ALT/AL
0041      C=SI/Z
0042      D=ALT/Z
0043      IF (FE2.NE.0.0) GO TO 19
0044      E=0.0
0045      F=MG/FE2
0046      G=MG/XY
0047      H=FE3/XY
0048
0049
0050
0051
0052
0053
0054
0055
0056
0057
0058
0059
0060
0061
0062
0063
0064
0065
0066
0067
0068
0069
0070
0071
0072
0073
0074
0075
0076
0077
0078
0079
0080
0081
0082
0083
0084
0085
0086
0087
0088
0089
0090
0091
0092
0093
0094
0095
0096
0097
0098
0099
0100
0101
0102
0103
0104
0105
0106
0107
0108
0109
0110
0111
0112
0113
0114
0115
0116
0117
0118
0119
0120
0121
0122
0123
0124
0125
0126
0127
0128
0129

```

C 87
C 88
C 89
C 90
C 91
C 92
C 93
C 94
C 95
C 96
C 97
C 98
C 99
C 100
C 101
C 102
C 103
C 104
C 105
C 106
C 107
C 108
C 109
C 110
C 111
C 112
C 113
C 114
C 115
C 116
C 117
C 118
C 119
C 120
C 121
C 122
C 123
C 124
C 125
C 126
C 127
C 128
C 129

16/53/03

DATE = 73169

AMICA

FORTRAN IV G LEVEL 21

```

0127 P=MN/XY
0128 O=CA/XY
0129 R=K/XY
0130 S=NA/XY
0131 TT=K+NA
0132 IF (TT.NE.0.0) GO TO 20
0133 T=0.0
0134 GO TO 21
0135 T=K/(K+NA)
0136 XMG=MG/(MG+FE2)
0137 XFF2=FF2/(FE2+MG)
0138 XXMG=MG/(MG+FE2+FE3)
0139 XXFE2=FF2/(FE2+FE3+MG)
0140 XFE=(FE2+FF3)/(FE2+FE3+MG)
0141 F=XMG/(1-XMG)
0142 FF=XFE2/(1-XFE2)
0143 U=XFE2/XMG
0144 V=XMG/XFE2
0145 CC=NN/(MG+FE2+MN)
0146 GG=LI/XY
0147 PP=100*MG/(MG+FE2+FE3+MN)
0148 WRITE (3,37) A,BB
0149 WRITE (3,38) C
0150 WRITE (3,39) D,E
0151 WRITE (3,40) G,H
0152 WRITE (3,41) P,Q
0153 WRITE (3,42) R,S
0154 WRITE (3,43) T,XMG
0155 WRITE (3,44) XFE2
0156 WRITE (3,45) XXMG
0157 WRITE (3,46) XXFE2
0158 WRITE (3,47) XFE
0159 WRITE (3,48) F,FF
0160 WRITE (3,49) U,V
0161 WRITE (3,50) CC,GG
0162 WRITE (3,51) PP
0163 CONTINUE
0164 RETURN
0165
0166 FORMAT (2I3)
0167 FORMAT (2A3)
0168 FORMAT (A4)
0169 FORMAT (13F6.2,2X)

```

C 130
C 131
C 132
C 133
C 134
C 135
C 136
C 137
C 138
C 139
C 140
C 141
C 142
C 143
C 144
C 145
C 146
C 147
C 148
C 149
C 150
C 151
C 152
C 153
C 154
C 155
C 156
C 157
C 158
C 159
C 160
C 161
C 162
C 163
C 164
C 165
C 166
C 167
C 168
C 169
C 170
C 171
C 172

```

0169 FORMAT (I2)
0170 FORMAT (A4,4A4)
0171 FORMAT (11,10,2X,1SAMPLE J-1,A4,5X,4A4)
0172 FORMAT (13F6.2)
0173 FORMAT (10,5X,OXIDES,12X,WT %,10X,MOL WT,6X,MOL PROP,6X,
1ATOMIC PROP OXYGEN,4X,ATOMIC PROP CATIONS)
0174 FORMAT (10,5X,2A3,8X,3(F10.5,5X),5X,F10.5,12X,F10.5) TOTA
0175 FORMAT (10,2X,(SUM OF WT %=1,1X,F10.5)/(2X,CORRECTED
1L WT %=1,1X,F10.5))
0176 FORMAT (10,/,5X,NUMBERS OF IONS ON THE BASIS OF 24(O,OH,F,CL) OR
1, ON THE BASIS OF 22(O,OH,F,CL) IF H2O IS NOT ANALYZED)
0177 FORMAT (10,15X,A4,5X,F10.5)
0178 FORMAT (10,15X,Z=1,1X,F10.5,10X,XY=1,1X,F10.5,10X,MW=1,1X,F10.
15,10X,OHFCL=1,1X,F10.5)
0179 FORMAT (10,1X,AL/SI=1,1X,F10.5/(2X,ALT/AL=1,1X,F10.5)).
0180 FORMAT (10,1X,SI/Z=1,1X,F10.5)
0181 FORMAT (10,1X,ALT/Z=1,1X,F10.5/(2X,MG/FE2=1,1X,F10.5))
0182 FORMAT (10,1X,MG/XY=1,1X,F10.5/(2X,FE3/XY=1,1X,F10.5))
0183 FORMAT (10,1X,MN/XY=1,1X,F10.5/(2X,CA/XY=1,1X,F10.5))
0184 FORMAT (10,1X,K/XY=1,1X,F10.5/(2X,NA/XY=1,1X,F10.5))
0185 FORMAT (10,1X,K/(K+NA)=1,1X,F10.5/(2X,XMG=(MG+FE2)=1,1X,F10.5)
1)
0186 FORMAT (10,1X,XFE2=FE2/(FE2+MG)=1,1X,F10.5)
0187 FORMAT (10,1X,XXMG=MG/(MG+FE2+FE3)=1,1X,F10.5)
0188 FORMAT (10,1X,XXFE2=FE2/(FE2+FE3+MG)=1,1X,F10.5)
0189 FORMAT (10,1X,XFE=(FE2+FE3)/(FE2+FE3+MG)=1,1X,F10.5)
0190 FORMAT (10,1X,XMG/(1-XMG)=1,1X,F10.5/(2X,XFE2/(1-XFE2)=1,1X,F1
10.5))
0191 FORMAT (10,1X,XFE2/XMG=1,1X,F10.5/(2X,XMG/XFE2=1,1X,F10.5))
0192 FORMAT (10,1X,MN/(MG+FE2+MN)=1,1X,F10.5/(2X,LI/XY=1,1X,F10.5))
0193 FORMAT (10,1X,100MG/(MG+FE2+FE3+MN)=1,1X,F10.5)
0194 END
C 173
C 174
C 175
C 176
C 177
C 178
C 179
C 180
C 181
C 182
C 183
C 184
C 185
C 186
C 187
C 188
C 189
C 190
C 191
C 192
C 193
C 194
C 195
C 196
C 197
C 198
C 199
C 200
C 201
C 202
C 203
C 204-

```

DATE = 73169

GARNET

FORTRAN IV G LEVEL 21

```

SUBROUTINE GARNET
A FORTRAN PROGRAM TO RECALCULATE CHEMICAL ANALYSES OF
GARNETS-----
--L. S. JEN
DIMENSION R(4)
REAL W(20), MW(20), MP(20), APO(20), APC(20), X(20,2), XX(20), YY(20)
DOUBLE PRECISION SI, ALI, ALO, TIT, TIO, FE3T, FE3O, CR, FE2, HG, MN, CA, NA, K
1, LI, TI, FE3, MG, MG
READ (1,20) N, L
DO 1 I=1, N
READ (1,21) (X(I,J), J=1,2)
CONTINUE
DO 2 I=1, L
READ (1,22) XX(I)
CONTINUE
READ (1,23) (MW(I), I=1, N)
READ (1,24) NO
DO 19 NM=1, NO
READ (1,25) M, (R(I), I=1, 4)
WRITE (3,26) M, (R(I), I=1, 4)
READ (1,27) (W(I), I=1, N)
SW=0.0
DO 3 I=1, N
SW=SW+W(I)
CONTINUE
DO 4 I=1, N
IF (MW(I).EQ.0.0) GO TO 5
MP(I)=W(I)/MW(I)
CONTINUE
CONTINUE
APO(1)=2.0*MP(1)
APO(2)=3.0*MP(2)
APO(3)=2.0*MP(3)
APO(4)=3.0*MP(4)
APO(5)=3.0*MP(5)
APO(6)=MP(6)
APO(7)=MP(7)
APO(8)=MP(8)
APO(9)=MP(9)
APO(10)=MP(10)
APO(11)=MP(11)
APO(12)=MP(12)
APO(13)=MP(13)

```

1 D
2 D
3 D
4 D
5 D
6 D
7 D
8 D
9 D
10 D
11 D
12 D
13 D
14 D
15 D
16 D
17 D
18 D
19 D
20 D
21 D
22 D
23 D
24 D
25 D
26 D
27 D
28 D
29 D
30 D
31 D
32 D
33 D
34 D
35 D
36 D
37 D
38 D
39 D
40 D
41 D
42 D
43 D

FORTRAN IV G LEVEL 21

0040
0041
0042
0043
0044
0045
0046
0047
0048
0049
0050
0051
0052
0053
0054
0055
0056
0057
0058
0059
0060
0061
0062
0063
0064
0065
0066
0067
0068
0069
0070
0071
0072
0073
0074
0075
0076
0077
0078
0079
0080
0081
0082

APC(14)=MP(14)
APC(15)=MP(15)
SUMAPO=0.0
DO 6 I=1,N
SUMAPO=SUMAPO+APC(I)
CONTINUE
DO 7 I=1,N
APC(I)=24.0/SUMAPO*APC(I)
CONTINUE
SI=APC(1)/2.0
AL=APC(2)*2.0/3.0
TI=APC(3)/2.0
CR=APC(4)*2.0/3.0
FE3=APC(5)*2.0/3.0
FE2=APC(6)
MN=APC(7)
MG=APC(8)
LI=APC(9)*2.0
CA=APC(10)
NA=APC(11)*2.0
K=APC(12)*2.0
SR=APC(13)
BA=APC(14)
RB=APC(15)*2.0
IF (SI.GE.6.0) GO TO 8
ALT=6.0-SI
ALO=AL-ALT
GO TO 9
ALT=0.0
IF (ALO.GT.0.0) GO TO 10
ALT=AL
ALO=0.0
YY(1)=SI
YY(2)=ALT
YY(3)=ALO
YY(4)=TI
YY(5)=CR
YY(6)=FE3
YY(7)=FE2
YY(8)=MN
YY(9)=MG
YY(10)=LT
YY(11)=CA

8
9
10

D 44
D 45
D 46
D 47
D 48
D 49
D 50
D 51
D 52
D 53
D 54
D 55
D 56
D 57
D 58
D 59
D 60
D 61
D 62
D 63
D 64
D 65
D 66
D 67
D 68
D 69
D 70
D 71
D 72
D 74
D 75
D 76
D 77
D 78
D 79
D 80
D 81
D 82
D 83
D 84
D 85
D 86
D 87

J/A

16/53/03

DATE = 73169

GARNET

FORTRAN IV G LEVEL 21

```

0003 YY(12)=NA
0004 YY(13)=K
0005 YY(14)=SR
0006 YY(15)=BA
0007 YY(16)=RH
0008 IF (AL0.NE.0.0) GO TO 11
0009 Z=SI
0010 Y=ALT+ALO+TI+CR+FE3
0011 XSITEF=MN+FE2+MG+CA+NA+K+LI
0012 GO TO 12
0013 Z=SI+ALT
0014 Y=ALO+TI+FE3+CR
0015 XSITEF=MN+FE2+MG+CA+NA+K+LI
0016 XY=XSITE+Y
0017 WRITE (3,28)
0018 DO 13 I=1,N
0019 WRITE (3,29) (X(I,J),J=1,2),W(I),MH(I),MP(I),APO(I),APC(I)
0020 CONTINUE
0021 WRITE (3,30) SW
0022 WRITE (3,31)
0023 DO 14 J=1,L
0024 WRITE (3,32) XX(I),YY(I)
0025 CONTINUE
0026 WRITE (3,33) Z,Y,XSITE
0027 AL=ALT+ALO
0028 A=AL/SI
0029 IF (AL.NE.0.0) GO TO 15
0030 BR=0.0
0031 BR=ALT/AL
0032 C=SI/Z
0033 D=ALT/Z
0034 IF (FF2.NE.0.0) GO TO 16
0035 E=0.0
0036 E=MG/FE2
0037 G=MG/XSITE
0038 H=FE3/Y
0039 P=MN/XSITE
0040 Q=CA/XSITE
0041 R=K/XSITE
0042 S=NA/XSITE
0043 TT=K+NA
0044 IF (TT.NE.0.0) GO TO 17
0045 T=M.0

```



16/53/03

DATE = 73169

GARNET

FORTRAN IV. G LEVEL 21

```

0126 GO TO 18
0127 T=K/(K+NA)
0128 XMG=MG/(MG+FE2)
0129 XFE2=FE2/(FE2+MG)
0130 XXMG=MG/(MG+FE2+FE3)
0131 XXFE2=FE2/(FE2+FE3+MG)
0132 XFE=(FE2+FE3)/(FE2+FE3+MG)
0133 F=XMG/(1-XMG)
0134 FF=XFEP/(1-XFE2)
0135 U=XFF2/XMG
0136 V=XMG/XFE2
0137 CC=MN/(MG+FE2+MN)
0138 GG=LI/XY
0139 WRITE (3,34) A,BB
0140 WRITE (3,35) C
0141 WRITE (3,36) D,E
0142 WRITE (3,37) G,H
0143 WRITE (3,38) P,Q
0144 WRITE (3,39) R,S
0145 WRITE (3,40) T,XMG
0146 WRITE (3,41) XFE2
0147 WRITE (3,42) XXMG
0148 WRITE (3,43) XFE2
0149 WRITE (3,44) XFE
0150 WRITE (3,45) F,FF
0151 WRITE (3,46) U,V
0152 WRITE (3,47) CC,GG
0153 CONTINUE
0154 RETURN
C
0155 FORMAT (2I3)
0156 FORMAT (2A3)
0157 FORMAT (A4)
0158 FORMAT (13F6.2,2X)
0159 FORMAT (I2)
0160 FORMAT (A4,4A4)
0161 FORMAT ('1',10',2X,'SAMPLE J',A4,5X,4A4)
0162 FORMAT (13F6.2)
0163 FORMAT ('10',5X,'OXIDES',12X,'WT %',10X,'MOL WT',8X,'MOL PROP',6X,'
0164 1 ATOMIC PROP OXYGEN',4X,'ATOMIC PROP CATIONS')
0165 FORMAT ('10',5X,2A3,8X,3(F10.5,5X),5X,F10.5,12X,F10.5)
0166 FORMAT ('10',2X,'TOTAL WT %',1X,F10.5)
0167 FORMAT ('10',5X,'NUMBERS OF IONS ON THE BASIS OF 24(O)')
0168
0169
0170
0171
0172
0173

```

16/53/03

DATE = 73169

GARNET

FORTRAN IV G LEVEL 21

```

0167   FORMAT ('0',15X,A4,5X,F10.5)
0168   FORMAT ('0',15X,'Z=',1X,F10.5,10X,'Y =',1X,F10.5,10X,'X =',1X,F10.5)
0169   15)  FORMAT ('0',1X,'AL/SI=',1X,F10.5// (2X,'ALT/AL=',1X,F10.5))
0170   FORMAT ('0',1X,'SI/Z=',1X,F10.5)
0171   FORMAT ('0',1X,'ALT/Z=',1X,F10.5// (2X,'MG/FE2=',1X,F10.5))
0172   FORMAT ('0',1X,'MG/X =',1X,F10.5// (2X,'FE3/Y =',1X,F10.5))
0173   FORMAT ('0',1X,'MN/X =',1X,F10.5// (2X,'CA/X =',1X,F10.5))
0174   FORMAT ('0',1X,'K/X =',1X,F10.5// (2X,'NA/X =',1X,F10.5))
0175   FORMAT ('0',1X,'K/(K+NA)=' ,1X,F10.5// (2X,'XMG=(MG+FE2)=' ,1X,F10.5)
1)
0176   FORMAT ('0',1X,'XFE2=FE2/(FE2+MG)=' ,1X,F10.5)
0177   FORMAT ('0',1X,'XXMG=MG/(MG+FE2+FE3)=' ,1X,F10.5)
0178   FORMAT ('0',1X,'XFE2=FE2/(FE2+FE3+MG)=' ,1X,F10.5)
0179   FORMAT ('0',1X,'XFE=(FE2+FE3)/(FE2+FE3+MG)=' ,1X,F10.5)
0180   FORMAT ('0',1X,'XMG/(1-XMG)=' ,1X,F10.5// (2X,'XFE2/(1-XFE2)=' ,1X,F1
10.5))
0181   FORMAT ('0',1X,'XFE2/XMG=' ,1X,F10.5// (2X,'XMG/XFE2=' ,1X,F10.5))
0182   FORMAT ('0',1X,'MN/(MG+FE2+MN)=' ,1X,F10.5// (2X,'LI/X =',1X,F10.5))
0183   END
0184
0185
0186
0187
0188
0189
0190
0191
0192
0193

```

APPENDIX II

A Fortran IV computer program for analyses of
grain transitions (randomness test) based on chi square test

```

C A FORTRAN PROGRAM TO CALCULATE CRYSTAL SPATIAL DISTRIBUTION DATA-----00000000
00000010
00000020
00000030
00000040
00000050
00000060
00000070
00000080
00000090
00000100
00000110
00000120
00000130
00000140
00000150
00000160
00000170
00000180
00000190
00000200
00000210
00000220
00000230
00000240
00000250
00000260
00000270
00000280
00000290
00000300
00000310
00000320
00000330
00000340
00000350
00000360
00000370
00000380
00000390
00000400
00000410
00000420

-----L. S. JEN
--- PART (I) RANDOMNESS DATA
(1) CALCULATION OF SUMS OF INDIVIDUAL ROWS AND COLUMNS
AND THE TOTAL SUM OF THE TRANSITION TABLE A(I,J)
(2) CALCULATION OF THE TRANSITION MATRIX T
AND PRINT OUT THE VALUES IN MATRIX FORM
(3) CALCULATION OF THE FIXED VECTOR PI
AND PRINT OUT THE VALUES IN VECTOR FORM
(4) CALCULATION OF THE EXPECTED MATRIX E
AND PRINT OUT THE VALUES IN MATRIX FORM
(5) CALCULATION OF THE INDIVIDUAL AND TOTAL CRYSTAL OR
MINERAL CHI SQUARE
(6) PRINTING OUT OF A(I,J) AND E(I,J)
FOR COMPARISON OF THESE TWO MATRICES
(7) LISTING OF THEORETICAL CHI SQUARE VALUES AT THE 95%
AND 99% SIGNIFICANCE LEVELS FOR COMPARISON WITH
THE CALCULATED OBSERVED CRYSTAL CHI SQUARES
IMPLICIT REAL*(A-H,O-Z)
DIMENSION A(10,10), SX(10), SY(10), T(10,10), PI(10),
1F(10,10), CHISQR(10,10), X(10), Y(10)
READ (1,130) (X(I), Y(I), I=2,10)
130 FORMAT (2(F7.3, 6X))
WRITE (3,340)
340 FORMAT (20X, 'THEORETICAL CHI SQUARES AT THE 95X AND 99X SIGNIFICA
INCF LEVELS WITH DEGREES OF FREEDOM=1,4,9,16,25,36,49,64, AND 81
2 RESPECTIVELY')
I=2
33 NEXT I
M=1
WRITE (3,230) M, X(I), M, Y(I)
230 FORMAT (10I, 19X, 'X**2, 95X(1, 13, 1)=1, 1X, F8.3, 20X, 'X**2, 99
1X(1, 13, 1)=1, 1X, F8.3)
I=I+1
IF(I.GT.10) GO TO 44
GO TO 33
44 CONTINUE
111 READ (1,210,END=6000) M
210 FORMAT (A4)
WRITE (3,220) M
220 FORMAT (11I, 10I, 4X, 'SAMPLE J=1, A4)
1000 READ (1,10) N
1000 FORMAT (15)

```

20/33/48

DATE = 73171

MAIN

FORTAN IV 6 LEVEL 21

```

0022 DO 222 I=1,10
0023 DO 222 J=1,10
0024 A(I,J)=0.0
0025 DO 11 I=1,N
0026 11 READ (1,20) (A(I,J), J=1,N)
0027 20 FORMAT (10F6.0)
0028 DO 25 I=1,N
0029 SX(I)=0.0
0030 25 SY(I)=0.0
0031 DO 35 I=1,N
0032 DO 35 J=1,N
0033 35 SX(I)=SX(I)+A(I,J)
0034 WRITE (3,30)
0035 30 FORMAT (10I, 6X, 'THE VALUES OF SX(I) ARE')
0036 DO 37 I=1, N
0037 WRITE (3,40) I, SX(I)
0038 40 FORMAT (10I, 7X, 'SX(I), I3, ')=1, 1X, 10(F6.1, 3X))
0039 37 CONTINUE
0040 DO 49 I=1,N
0041 DO 49 J=1,N
0042 49 SY(J)=SY(J)+A(I,J)
0043 WRITE (3,40)
0044 40 FORMAT (10I, 6X, 'THE VALUES OF SY(J) ARE')
0045 DO 47 J=1,N
0046 WRITE (3, 50) J, SY(J)
0047 50 FORMAT (10I, 7X, 'SY(I, I3, ')=1, 1X, 10(F6.1, 3X))
0048 47 CONTINUE
0049 SUMSX=0.0
0050 SUMSY=0.0
0051 DO 55 I=1,N
0052 55 SUMSX=SUMSX+SX(I)
0053 DO 57 J=1,N
0054 57 SUMSY=SUMSY+SY(J)
0055 TOTAL1=SUMSX
0056 TOTAL2=SUMSY
0057 WRITE (3,50) SUMSX, SUMSY, TOTAL1, TOTAL2
0058 50 FORMAT (10I, 6X, ('SUMSX=1, 1X, F6.1), 6X, ('SUMSY=1, 1X, F6.1),
16X, ('TOTAL1=1, 1X, F6.1), 6X, ('TOTAL2=1, 1X, F6.1))
0059 DO 333 I=1,10
0060 DO 333 J=1,10
0061 T(I,J)=0.0
0062 DO 75 I=1,N
0063 DO 75 J=1,N

```

```

000000430
000000440
000000450
000000460
000000470
000000480
000000490
000000500
000000510
000000520
000000530
000000540
000000550
000000560
000000570
000000580
000000590
000000600
000000610
000000620
000000630
000000640
000000650
000000660
000000670
000000680
000000690
000000700
000000710
000000720
000000730
000000740
000000750
000000760
000000770
000000780
000000790
000000800
000000810
000000820
000000830
000000840
000000850

```

00000860
 00000870
 00000880
 00000890
 00000900
 00000910
 00000920
 00000930
 00000940
 00000950
 00000960
 00000970
 00000980
 00000990
 00001000
 00001010
 00001020
 00001030
 00001040
 00001050
 00001060
 00001070
 00001080
 00001090
 00001100
 00001110
 00001120
 00001130
 00001140
 00001150
 00001160
 00001170
 00001180
 00001190
 00001200
 00001210
 00001220
 00001230
 00001240
 00001250
 00001260
 00001270
 00001280

```

0064 T(I,J)=A(I,J)/SX(I)
0065 75 CONTINUE
0066 WRITE (3,60)
0067 60 FORMAT (10I, 6X, ITRANSITION MATRIX T=I)
0068 DO 61 I=1,N
0069 61 WRITE (3,900) (T(I,J), J=1,N)
0070 900 FORMAT (10I, 6X, 10(F7.3, 2X))
0071 DO 444 J=1,10
0072 444 PI(J)=0.0
0073 DO 85 J=1,N
0074 85 PI(J)=SY(J)/SUMSY
0075 WRITE (3,70) (PI(J), J=1,N)
0076 70 FORMAT (10I, 6X, IFIXED VECTOR PI=I, 2X, 10(F7.3, 2X))
0077 DO 555 I=1,10
0078 DO 555 J=1,10
0079 555 E(I,J)=0.0
0080 DO 95 I=1,N
0081 DO 95 J=1,N
0082 E(I,J)=SX(I)*PI(J)
0083 95 CONTINUE
0084 WRITE (3,8)
0085 80 FORMAT (10I, 6X, IEXPECTED MATRIX E=I)
0086 DO 81 I=1,N
0087 81 WRITE (3,700) (E(I,J), J=1,N)
0088 700 FORMAT (10I, 6X, 10(F7.3, 2X))
0089 CHISQR(I,J)=0.0
0090 DO 105 I=1,N
0091 DO 105 J=1,N
0092 CHISQR(I,J)=(E(I,J)-A(I,J))*2/E(I,J)
0093 105 CONTINUE
0094 WRITE (3,500)
0095 500 FORMAT (10I, 6X, IINDIVIDUAL CHI SQUARE IS CHISQR=I)
0096 DO 91 I=1,N
0097 91 WRITE (3,90) (CHISQR(I,J), J=1,N)
0098 90 FORMAT (10I, 6X, 10(F7.3))
0099 SUMCHI=0.0
0100 DO 110 I=1,N
0101 DO 110 J=1,N
0102 110 SUMCHI=SUMCHI+CHISQR(I,J)
0103 300 WRITE (3,300) SUMCHI
0104 300 FORMAT (10I, 6X, ISUMCHI=I, 2X, F8.3)
0105 WRITE (3,1000)
0106 1000 FORMAT (10I, 15X, IA(T,J) VS E(I,J)I)

```

20/33/48

DATE = 73171

MAIN

FORTRAN IV G LEVEL 21

```

0107 WRITE (3, 4000)
0108 FORMAT (10I, 6X, 1THE OBSERVED TRANSITION AS TRANSITION TABLE A(I,
00001290
00001300
00001310
00001320
00001330
00001340
00001350
00001360
00001370
00001380
00001390
00001400
00001410
00001420
0109 DO 125 I=1,N
0110 WRITE (3,2000) (A(I,J), J=1,N)
0111 FORMAT (10I, 6X, 10(F7.3, 2X))
0112 WRITE (3, 5000)
0113 FORMAT (10I, 6X, 1THE EXPECTED TRANSITION MATRIX E(I,J)=')
0114 DO 135 I=1,N
0115 WRITE (3,3000) (E(I,J), J=1,N)
0116 FORMAT (10I, 6X, 10(F7.3, 2X))
0117 GO TO 111
0118 6000 STOP
0119 END

```

APPENDIX III

A sample calculation of
test for randomness of crystals in a rock

A sample calculation of test for randomness of
crystals in a rock:

SAMPLE J- 35

THE OBSERVED TRANSITION AS TRANSITION MATRIX A (I, J)=

	F	H	C	A	D	O
F	51.000	6.000	39.000	14.000	26.000	23.000
H	4.000	1.000	4.000	1.000	0.0	2.000
C	42.000	3.000	12.000	1.000	21.000	26.000
A	12.000	0.0	1.000	4.000	6.000	5.000
D	21.000	2.000	24.000	5.000	0.0	25.000
O	25.000	0.0	27.000	5.000	24.000	38.000

THE VALUES OF SX(I) ARE

SX(1)= 159.0
SX(2)= 12.0
SX(3)= 105.0
SX(4)= 28.0
SX(5)= 77.0
SX(6)= 119.0

THE VALUES OF SY(J) ARE

SY(1)= 155.0
SY(2)= 42.0
SY(3)= 107.0
SY(4)= 30.0
SY(5)= 77.0
SY(6)= 119.0

SUMSX= 500.0

SUMSY= 500.0

TOTAL1= 500.0

TOTAL2= 500.0

PROBABILITY TRANSITION MATRIX T=

	F	H	C	A	D	O
F	0.321	0.038	0.245	0.088	0.164	0.145
H	0.333	0.083	0.333	0.083	0.0	0.167
C	0.400	0.029	0.114	0.010	0.200	0.248
A	0.429	0.0	0.036	0.143	0.214	0.179
D	0.273	0.026	0.312	0.065	0.0	0.325
O	0.210	0.0	0.227	0.042	0.202	0.319

FIXED VECTOR PI= 0.310 0.024 0.214 0.060 0.154 0.238

EXPECTED MATRIX E=

F	49.290	3.816	34.026	9.540	24.486	37.842
H	3.720	0.288	2.568	0.720	1.848	2.856
C	32.550	2.520	22.470	6.300	16.170	24.990
A	8.680	0.672	5.992	1.680	4.312	6.664
D	23.870	1.848	16.478	4.620	11.858	18.326
O	36.890	2.856	25.466	7.140	18.326	28.322

INDIVIDUAL CHI SQUARE IS CHISQR=

F	0.059	1.250	0.727	2.085	0.094	5.821
H	0.021	1.760	0.799	0.109	1.848	0.257
C	2.744	0.091	4.879	4.459	1.443	0.041
A	1.270	0.672	4.159	3.204	0.661	0.416
D	0.345	0.013	3.434	0.031	11.858	2.431
O	3.832	2.856	0.092	0.641	1.757	3.307

SUMCHI = $\sum X_M^2 = 69.463$

The distribution of crystals in this rock is not random since:

$$\left[\sum X_M^2 = 69.463 \right] > \left[\chi_{0.95}^2 (v=25) = 37.652 \right]$$

APPENDIX IV

Observed and expected transition matrices for
charnockitic granulites from the Adirondack Mts., New York

The observed and expected transition matrices for rock sample J-35. F--feldspar, H--orthopyroxene, C--clino-pyroxene, A--amphibole, G--garnet, D--opaque minerals, O--others.

THE OBSERVED TRANSITION AS TRANSITION TABLE A(I,J)=

	F	H	C	A	G	D	O
F	51.000	6.000	39.000	14.000	7.000	26.000	16.000
H	4.000	1.000	4.000	1.000	0.0	0.0	2.000
C	42.000	3.000	12.000	1.000	16.000	21.000	10.000
A	12.000	0.0	1.000	4.000	2.000	6.000	3.000
G	9.000	0.0	15.000	2.000	0.0	16.000	15.000
D	21.000	2.000	24.000	5.000	16.000	0.0	9.000
O	16.000	0.0	12.000	3.000	18.000	8.000	5.000

THE EXPECTED TRANSITION MATRIX E(I,J)=

F	49.290	3.816	34.026	9.540	18.762	24.486	19.380
H	3.720	0.288	2.568	0.720	1.416	1.848	1.440
C	32.550	2.520	22.470	6.300	12.390	16.170	12.600
A	8.640	0.672	5.992	1.680	3.304	4.312	3.360
G	17.670	1.368	12.198	3.420	6.726	8.778	6.840
D	23.870	1.848	16.478	4.620	9.086	11.858	9.240
O	19.220	1.488	13.268	3.720	7.316	9.548	7.440

The observed and expected transition matrices for rock sample J-44.

THE OBSERVED TRANSITION AS TRANSITION TABLE A(I,J)=

	F	H	C	A	D	O
F	358.000	29.000	20.000	20.000	14.000	20.000
H	32.000	6.000	7.000	5.000	4.000	9.000
C	19.000	6.000	4.000	3.000	6.000	7.000
A	18.000	3.000	4.000	1.000	5.000	7.000
D	13.000	8.000	3.000	3.000	0.0	7.000
O	18.000	11.000	7.000	7.000	5.000	2.000

THE EXPECTED TRANSITION MATRIX E(I,J)=

F	241.311	43.178	30.841	26.729	23.302	35.639
H	42.919	5.420	3.878	3.361	2.930	4.482
C	30.657	3.878	2.770	2.401	2.093	3.201
A	25.888	3.275	2.229	2.027	1.767	2.703
D	23.163	2.930	2.093	1.814	1.581	2.419
O	34.063	4.305	3.078	2.668	2.326	3.557

The observed and expected transition matrices
for rock sample J-50.

THE OBSERVED TRANSITION AS TRANSITION TABLE $A(I,J) =$

	P	H	C	A	G	D	O
P	247.000	6.000	40.000	12.000	26.000	13.000	9.000
H	5.000	0.0	3.0	2.300	2.300	1.000	1.000
C	40.000	1.000	12.000	6.000	8.000	4.000	8.000
A	14.000	2.000	4.000	4.000	5.000	7.000	3.000
G	21.000	1.000	13.000	2.000	0.0	6.000	6.000
D	16.000	1.000	6.000	7.000	5.000	0.0	4.000
O	7.000	1.000	4.000	6.000	5.000	8.000	1.000

THE EXPECTED TRANSITION MATRIX $E(I,J) =$

P	204.652	7.025	46.247	22.831	29.856	23.416	18.733
H	6.385	0.219	1.441	0.711	0.930	0.730	0.584
C	45.854	1.572	10.350	5.109	6.682	5.240	4.192
A	22.637	3.776	5.109	2.522	3.299	2.587	2.370
G	28.441	0.975	6.420	3.169	4.144	3.250	2.600
D	23.217	0.796	5.240	2.587	3.383	2.653	2.123
O	18.574	0.637	4.152	2.070	2.706	2.123	1.698

The observed and expected transition matrices
for rock sample J-63A.

THE OBSERVED TRANSITION AS TRANSITION TABLE $A(I,J) =$

	P	H	C	G	D	O
P	180.000	7.000	39.000	94.000	20.000	36.000
H	8.000	2.000	6.000	6.000	3.000	4.000
C	50.000	7.000	21.000	21.000	10.000	12.000
G	87.000	7.000	32.000	0.0	20.000	20.000
D	14.000	2.000	15.000	22.000	0.0	10.000
O	34.000	4.000	13.000	21.000	13.000	6.000

THE EXPECTED TRANSITION MATRIX $E(I,J) =$

P	165.778	12.889	56.000	72.889	29.333	39.111
H	12.786	0.994	4.319	5.622	2.262	3.017
C	53.349	4.148	18.021	23.456	9.440	12.586
G	73.189	5.690	24.723	32.180	12.950	17.267
D	27.777	2.160	9.383	12.213	4.915	6.553
O	40.122	3.119	13.553	17.641	7.099	9.466

The observed and expected transition matrices
for rock sample J-66.

THE OBSERVED TRANSITION AS TRANSITION TABLE A(I,J)=

	F	H	C	G	D	O
F	180.000	23.000	51.000	72.000	31.000	43.000
H	25.000	7.000	12.000	2.000	13.000	13.000
C	44.000	15.000	22.000	11.000	16.000	18.000
G	71.000	2.000	11.000	0.0	34.000	14.000
D	37.000	7.000	16.000	27.000	0.0	18.000
O	47.000	17.000	11.000	20.000	14.000	23.000

THE EXPECTED TRANSITION MATRIX E(I,J)=

F	167.115	29.269	50.279	54.622	44.674	53.361
H	30.081	5.266	9.158	9.828	8.041	9.605
C	52.641	9.251	16.027	17.200	14.372	16.839
G	55.148	9.692	16.790	18.019	14.743	17.609
D	43.868	7.709	13.356	14.333	11.727	14.007
O	55.148	9.692	16.790	18.019	14.743	17.609

The observed and expected transition matrices
for rock sample J-80.

THE OBSERVED TRANSITION AS TRANSITION TABLE A(I,J)=

	F	H	C	A	G	D	O
F	60.000	23.000	8.000	15.000	13.000	22.000	26.000
H	26.000	67.000	44.000	18.000	2.000	35.000	26.000
C	18.000	38.000	13.000	5.000	7.000	21.000	17.000
A	12.000	21.000	9.000	9.000	3.000	11.000	7.000
G	9.000	8.000	4.000	7.000	0.0	5.000	4.000
D	24.000	42.000	11.000	8.000	10.000	0.0	26.000
O	16.000	23.000	24.000	9.000	6.000	28.000	10.000

THE EXPECTED TRANSITION MATRIX E(I,J)=

F	32.138	42.656	22.010	13.829	7.012	23.762	22.594
H	42.720	56.701	25.257	18.362	9.321	31.587	30.333
C	22.340	29.651	15.299	9.613	4.874	16.518	15.705
A	14.109	18.727	9.663	6.071	3.078	10.432	9.919
G	7.251	9.624	4.566	3.120	1.582	5.361	5.097
D	23.711	31.471	16.739	10.203	5.173	17.532	16.670
O	22.732	30.171	15.568	9.781	4.960	16.808	15.951

The observed and expected transition matrices
for rock sample J-81.

THE OBSERVED TRANSITION AS TRANSITION TABLE A(I,J)=

	P	H	C	G	D	O
P	148.000	34.000	33.000	31.000	21.000	20.000
H	36.000	29.000	26.000	25.000	27.000	15.000
C	30.000	49.000	35.000	12.000	23.000	23.000
G	27.000	15.000	23.000	0.0	22.000	9.000
D	21.000	28.000	17.000	19.000	0.0	18.000
O	20.000	15.000	26.000	9.000	13.000	6.000

THE EXPECTED TRANSITION MATRIX E(I,J)=

P	89.430	53.912	50.740	30.444	33.615	28.859
H	49.233	26.680	27.534	16.760	18.506	15.887
C	53.556	32.309	30.409	18.245	20.146	17.295
G	29.914	18.033	16.572	10.183	11.244	9.653
D	32.055	19.348	18.210	10.526	12.064	10.357
O	27.733	16.710	15.735	9.441	10.424	8.949

The observed and expected transition matrices
for rock sample J-92.

THE OBSERVED TRANSITION AS TRANSITION TABLE A(I,J)=

	P	H	C	A	D	O
P	333.000	38.000	13.000	3.000	12.000	44.000
H	35.000	3.000	3.000	1.000	7.000	11.000
C	11.000	4.000	1.000	1.000	1.000	0.0
A	4.000	1.000	1.000	0.0	1.000	0.0
D	13.000	8.000	3.0	1.000	3.0	2.000
O	45.000	8.000	0.0	1.000	2.000	13.000

THE EXPECTED TRANSITION MATRIX E(I,J)=

P	214.594	44.229	12.841	4.994	16.407	49.936
H	42.609	5.590	1.739	0.676	2.222	6.763
C	12.783	1.787	0.522	0.203	0.667	2.029
A	4.971	0.659	0.203	0.079	0.259	0.789
D	17.043	2.396	0.696	0.271	0.889	2.705
O	49.000	6.889	2.000	0.778	2.556	7.778

The observed and expected transition matrices
for rock sample J-99.

THE OBSERVED TRANSITION AS TRANSITION TABLE A(I,J)*

	P	C	A	G	D	O
P	117.000	66.000	47.000	39.000	29.000	23.000
C	58.000	33.000	35.000	40.000	19.000	23.000
A	59.000	32.000	14.000	4.000	21.000	11.000
G	39.000	34.000	10.000	1.000	23.000	19.000
D	23.000	23.000	15.000	22.000	0.0	15.000
O	24.000	22.000	13.000	20.000	11.000	2.000

THE EXPECTED TRANSITION MATRIX E(I,J)*

P	105.374	67.322	43.521	40.679	33.498	30.246
C	68.280	43.623	28.239	26.553	21.706	19.595
A	44.216	28.313	19.228	17.234	14.098	12.720
G	41.362	26.426	17.106	16.055	13.149	11.877
D	34.468	22.021	14.255	13.404	10.957	9.894
O	30.201	19.295	12.450	11.745	9.601	8.669

The observed and expected transition matrices
for rock sample J-103.

THE OBSERVED TRANSITION AS TRANSITION TABLE A(I,J)*

	P	H	C	A	D	O
P	250.000	30.000	45.000	17.000	27.000	24.000
H	36.000	11.000	11.000	2.000	6.000	9.000
C	41.000	11.000	8.000	4.000	6.000	10.000
A	17.000	4.000	2.000	3.000	1.000	0.0
D	24.000	9.000	7.000	1.000	0.0	2.000
O	24.000	10.000	9.000	0.0	4.000	3.000

THE EXPECTED TRANSITION MATRIX E(I,J)*

P	230.623	44.124	48.243	15.885	25.586	28.240
H	44.012	8.421	5.207	3.031	4.940	5.389
C	46.546	9.982	5.820	3.234	5.269	5.759
A	15.844	3.031	3.314	1.091	1.778	1.940
D	25.234	4.828	5.278	1.738	2.832	3.090
O	29.341	5.614	6.128	2.021	3.293	3.593

The observed and expected transition matrices
for rock sample J-106.

THE OBSERVED TRANSITION AS TRANSITION TABLE A(I,J)=

	P	H	C	A	D	O
T	286.200	55.000	38.000	31.000	29.000	29.000
H	47.000	5.000	8.000	1.000	10.000	9.000
C	48.000	3.000	6.000	5.000	8.000	3.000
A	24.000	3.000	6.000	1.000	7.000	7.000
D	35.000	7.000	11.000	4.000	0.0	3.000
O	28.000	7.000	5.000	5.000	5.000	1.000

THE EXPECTED TRANSITION MATRIX F(I,J)=

T	279.724	47.816	46.023	28.092	35.264	31.080
H	47.816	8.174	7.867	4.802	6.028	5.313
C	43.632	7.458	7.179	4.382	5.501	4.848
A	28.690	4.504	4.720	2.781	3.617	3.188
D	35.862	6.130	5.900	3.602	4.521	3.985
O	22.276	5.517	5.310	3.241	4.069	3.586

APPENDIX V

Transition series for
charnockitic granulites from the Adirondack Mts., New York

Abbreviations used in Appendix V

1. Mineral

F = feldspar

H = orthopyroxene

C = clinopyroxene

A = amphibole

G = garnet

D = opaque minerals

O = all other minerals, e.g. biotite + apatite + zircon

2. Spatial distribution

NR = not random

R = random

Rg = regular

ARg = anti-regular

C = clustered

AC = anti-clustered

3. Uncertainty of spatial distribution indicated by

(s) = similar values of chi squares and/or similar values of observed and expected transitions

(l) = very low values of observed and expected transitions, e.g. less than 4 or 5

Transition matrices of transition series I for
rock sample J-35. Total transitions measured = 500

Transition Series I (in matrix form)	Degrees of freedom	ΣX_M^2	$X_{.95}^2$	Distribution
FHCAGDO	36	113.126	50.998	NR
FHCADO	25	69.463	37.652	"
FHCAO	16	42.224	26.296	"
FHCO	9	20.005	16.919	"
FHAO	"	17.746	"	"
FCAO	"	32.657	"	"
HCAO	"	28.588	"	"
FHO	4	4.567	9.488	R
FCO	"	11.606	"	NR
FAO	"	12.217	"	"
HCO	"	10.641	"	"
HAO	"	6.202	"	R
CAO	"	25.037	"	NR
HO	1	1.848	3.841	R
AO	"	3.610	"	" (s)
CO	"	7.857	"	NR
FO	"	0.126	"	R

Transition matrices of
transition series II for rock sample J-35

Transition series II	ΣX_M^2	$\Sigma X_{.95}^2$	Observed	Expected	Distribution	
Two-phase						
Transition matrices						
AA			4	1.680	R (1)	
CC			12	22.470	AC	
HH			1	0.288	R (1)	
FF			51	49.290	"	
FH			FH	6	3.720	"
			HF	4	3.720	"
FC			FC	39	34.036	Rg
			CF	42	32.550	
FA			FA	14	9.540	"
			AF	12	8.680	
HC			HC	4	2.568	" (1)
			CH	3	2.520	
HA			HA	1	0.720	R (1)
			AH	0	0.672	"
CA			CA	1	6.300	ARg(1)
			AC	1	5.992	"
HO	1.848	3.841	HO	11	11.712	R (s)
			OH	11	11.712	
AO	3.610	"	AO	24	26.320	" (s)
			OA	26	28.320	
CO	7.857	"	CO	93	82.530	Rg
			OC	95	84.530	
FO	0.126	"	FO	108	109.710	R
			OF	104	105.710	

Transition matrices of transition series I
for rock J-44. Total transition measurements = 731

Transition series I	Degrees of freedom	ΣX_M^2	$\chi_{.95}^2$	Distribution
FHCADO	25	134.620	37.652	NR
FHCAO	16	118.950	26.296	"
FHCO	9	99.532	16.919	"
FHAO	"	108.667	"	"
FCAO	"	99.964	"	"
HCAO	"	9.319	"	R
FHO	4	97.644	9.488	NR
FCO	"	94.486	"	"
FAO	"	97.831	"	"
HCO	"	5.549	"	R
HAO	"	1.559	"	"
CAO	"	2.716	"	"
HO	1	0.072	3.841	"
AO	"	0.580	"	"
CO	"	0.620	"	"
FO	"	93.887	"	NR

Transition matrices of transition series II for
rock sample J-44

Transition series II Two-phase Transition matrices	Σx_M^2	$\Sigma x_{.95}^2$	Observed	Expected	Distribution
AA			1	2.027	R (1)
CC			4	2.770	" (1)
HH			6	5.436	"
FF			398	341.310	C
FB			29	43.178	ARg
			32	42.919	
FC			20	30.841	"
			19	30.657	
FA			20	26.729	"
			18	25.888	
HC			7	3.878	R
			6	3.878	
HA			5	3.361	" (1)
			3	3.275	
CA			3	2.401	" (1)
			4	2.339	
HO	0.072	3.841	57	57.570	" (s)
			57	57.570	
AO	0.580	"	37	35.973	" (s)
			38	36.973	
CO	0.620	"	41	42.230	" (s)
			41	42.230	
FO	93.887	"	103	159.689	ARg
			100	159.689	

Transition matrices of transition series I for
rock sample J-50. Total transition measurements = 603

Transition	Series I	Degrees of freedom	χ^2_{M}	$\chi^2_{.95}$	Distribution
FHCAGDO		36	118.266	50.998	NR
FHCAGO		25	97.766	37.652	"
FHCAO		16	68.271	26.296	"
FHCO		9	62.679	16.919	"
FHAO		"	55.843	"	"
FCAO		"	62.927	"	"
HCAO		"	8.315	"	R
FHO		4	50.467	9.488	NR
FCO		"	58.403	"	"
FAO		"	52.790	"	"
HCO		"	2.506	"	R
HAO		"	6.000	"	"
CAO		"	1.836	"	"
HO		1	0.228	3.841	"
AO		"	0.989	"	"
CO		"	0.348	"	"
FO		"	49.748	"	NR

Transition matrices of transition series II for
rock sample J-50

Transition Series II Two-phase Transition matrices	Σx_M^2	$\Sigma x_{.95}^2$	Observed	Expected ^a	Distribution
AA			4	2.522	R
CC			12	10.350	"
HH			0	0.219	" (1)
FF			247	204.892	C
FH			6	7.025	ARg (s)
			5	6.385	
FC			40	46.247	"
			40	45.854	
FA			12	22.831	"
			14	22.637	
HC			0	1.441	R (1)
			1	1.572	
HA			2	0.711	" (1)
			2	0.776	
CA			6	5.109	" (s)
			4	5.109	
HO		0.228	11	10.781	"
			12	11.781	
			35	36.478	
AO		0.989	35	36.478	"
			67	68.650	
CO		0.348	67	68.650	"
			106	148.108	
FO		49.748	103	145.108	ARg

Transition matrices of transition series I for
rock sample J-63A. Total transition measurements = 846

Transition Series I	Degrees of freedom	χ^2_M	$\chi^2_{.95}$	Distribution
FHCGDO	25	99.730	37.652	NR
FHCGO	16	77.686	26.296	"
FHCO	9	20.674	16.919	"
FHO	4	10.136	9.488	"
FCO	"	11.756	"	"
HCO	"	5.735	"	R
HO	1	1.091	3.841	"
CO	"	0.675	"	"
FO	"	3.928	"	NR (s)

Transition matrices of transition series II for
rock sample J-63A

Transition Series II Two-phase Transition matrices	χ^2_M	$\chi^2_{.95}$	Observed	Expected	Distribution
CC			21	18.021	R
HH			2	0.994	" (1)
FF			180	165.778	C (s)
FH			7	12.889	ARg
			8	12.786	
FC			39	56.000	"
			50	53.349	
HC			6	4.319	R
			7	4.148	
HO	1.091	3.841	27	28.006	"
			27	28.006	
CO	0.675	"	100	102.979	"
			105	107.979	
FO	3.928	"	196	210.222	ARg (s)
			193	207.222	

Transition matrices of transition series I for
rock sample J-66. Total transition measurements = 967

Transition Series I	Degrees of freedom	χ^2_{M}	$\chi^2_{.95}$	Distribution
FHCGDO	25	129.616	37.652	NR
FHCGO	16	86.213	26.296	"
FHCO	9	14.733	16.919	R
FHO	4	5.237	9.488	"
FCO	"	6.984	"	"
HCO	"	11.172	"	NR
HO	1	0.648	3.841	R
CO	"	2.933	"	"
FO	"	2.911	"	"

Transition matrices for transition series II for
rock sample J-66

Transition Series II Two-phases Transition matrices	ΣX_M^2	$\Sigma X_{.95}^2$	Observed	Expected	Distribution
CC			22	16.027	R
HH			7	5.286	"
FF			180	167.115	"
FH			23	29.369	"
			25	30.081	
FC			51	50.879	" (s)
			44	52.641	
HC			12	9.158	Rg
			15	9.251	
HO	0.648	3.841	65	66.714	R
			64	65.714	
CO	2.933	"	104	109.973	"
			101	106.973	
FO	2.911	"	220	232.885	"
			224	236.885	

Transition matrices of transition series I for
rock sample J-80. Total transition measurements = 842

Transition Series I	Degrees of freedom	ΣX_M^2	$\Sigma X_{.95}^2$	Distribution
FHCAGDO	36	143.926	50.998	NR
FHCAGO	25	95.660	37.652	"
FHCAO	16	71.942	26.296	"
FHCO	9	67.405	16.919	"
FHAO	"	50.548	"	"
FCAO	"	51.773	"	"
HCAO	"	32.316	"	"
FHO	4	47.914	9.488	NR
FCO	"	45.243	"	"
FAO	"	41.094	"	"
HCO	"	25.291	"	"
HAO	"	6.701	"	R
CAO	"	4.838	"	"
HO	1	3.412	3.841	"
AO	"	1.687	"	"
CO	"	0.462	"	"
FO	"	37.310	"	NR

Transition matrices of
transition series II for rock sample J-80

Transition Series II Two-phase Transition matrices	ΣX_M^2	$X_{.95}^2$	Observed	Expected	Distribution	
AA			9	6.071	R	
CC			13	15.299	"	
HH			67	56.701	"	
FF			60	32.138	C	
FH			FH	20	42.656	ARg
			HF	26	42.720	
FC			FC	8	22.009	"
			CF	18	22.340	
FA			FA	15	13.829	" (s)
			AF	12	14.109	
HC			HC	44	29.257	Rg
			CH	38	29.651	
HA			HA	18	18.382	R (s)
			AH	21	18.727	
CA			CA	5	9.613	"
			AC	9	9.663	
HO	3.412	3.841	HO	151	161.299	"
			OH	152	162.299	
AO	1.687	"	AO	63	65.929	"
			OA	62	64.929	
CO	0.462	"	CO	101	98.701	"
			OC	100	97.701	
FO	37.310	"	FO	104	131.862	ARg
			OF	105	132.862	

Transition matrices of transition series I for
rock sample J-81. Total transition measurements=905

Transition Series I	Degrees of freedom	ΣX_M^2	$X_{.95}^2$	Distribution
FHCGDO	25	160.777	37.652	NR
FHCGO	16	123.631	26.296	"
FHCO	9	95.138	16.919	"
FHO	4	89.122	9.488	"
FCO	"	84.350	"	"
HCO	"	17.074	"	"
HO	1	13.108	3.841	"
CO	"	0.197	"	R
FO	"	81.600	"	NR

Transition matrices of
transition series II of rock samples J-81

Transition Series II Two-phase Transition matrices	ΣX_M^2	$X_{.95}^2$	Observed	Expected	Distribution	
CC			26	27.934	R	
HH			49	32.309	C	
FF			148	89.430	C	
FH			{ FH	34	53.912	ARg
			{ HF	30	53.596	
FC			{ FC	33	50.740	"
			{ CF	36	49.233	
HC			{ HC	35	30.409	Rg
			{ CH	29	29.680	
HO	13.108	3.841	{ HO	123	139.691	ARg
			{ OH	121	137.691	
CO	0.197	"	{ CO	132	130.066	R
			{ OC	134	132.066	
FO	81.600	"	{ FO	139	197.570	ARg
			{ OF	134	192.570	

Transition matrices of transition series I for
rock sample J-92. Total transition measurements=621

Transition Series I	Degrees of freedom	Σx_M^2	$x_{.95}^2$	Distribution
FHCADO	25	60.634	37.652	NR
FHCAO	16	38.519	26.296	"
FHCO	9	28.808	16.919	"
FHAO	"	28.638	"	"
FCAO	"	21.880	"	"
HCAO	"	13.784	"	R
FHO	4	25.137	9.488	NR
FCO	"	14.768	"	"
FAO	"	14.575	"	"
HCO	"	6.267	"	R
HAO	"	2.150	"	"
CAO	"	7.129	"	"
HO	1	1.836	3.841	"
AO	"	0.081	"	"
CO	"	0.465	"	"
FO	"	12.961	"	NR

Transition matrices of
transition series II for rock sample J-92

Transition Series II Two-phase Transition matrices	ΣX_M^2	$X_{.95}^2$	Observed	Expected	Distribution
AA			0	0.079	R
CC			1	0.522	"
HH			3	5.990	"
FF			333	314.594	C
FH			38	44.229	ARg
			35	42.609	
FC			13	12.841	" (s)
			11	12.783	
FA			3	4.994	" (1)
			4	4.971	
HC			3	1.739	R (1)
			4	1.797	
HA			1	0.676	" (1)
			1	0.699	
CA			1	0.203	" (1)
			1	0.203	
HO	1.836	3.841	57	54.010	"
			59	56.010	
AO	0.081	"	7	6.921	"
			7	6.921	
CO	0.465	"	17	17.478	"
			17	17.478	
FO	12.961	"	110	128.406	ARg
			108	126.406	

Transition matrices of transition series I for
rock sample J-99. Total transition measurements=987

Transition Series I	Degrees of freedom	Σx_M^2	$X_{.95}^2$	Distribution
FCAGDO	25	97.760	37.652	NR
FCAGO	16	77.141	26.296	"
FCAO	9	20.037	16.919	"
FCO	4	12.734	9.488	"
FAO	"	9.553	"	"
CAO	"	6.295	"	R
AO	1	1.370	3.841	"
CO	"	4.148	"	NR
FO	"	2.830	"	R



Transition matrices of
transition series II for rock sample J-99.

Transition Series II Two-phase Transition matrices	ΣX_M^2	$X_{.95}^2$	Observed	Expected	Distribution
AA			14	18.328	R
CC			33	43.623	AC
FF			117	105.374	R
FC			66	67.322	ARg
			58	68.280	
FA			47	43.581	Rg
			53	44.316	
CA			35	28.239	R
			32	28.313	
AO	1.370	3.841	121	116.672	ARg
			120	115.672	
CO	4.148	"	175	164.377	Rg
			174	163.377	
FO	2.830	"	204	215.626	R
			207	218.626	

Transition matrices of transition series I for
rock sample J-103. Total transition measurements=668

Transition Series I	Degrees of freedom	χ^2_{M}	$\chi^2_{.95}$	Distribution
FECADO	25	39.993	37.652	NR
FHCAO	16	34.711	26.296	"
FECO	9	24.302	16.919	"
FHAO	"	25.622	"	"
FCAO	"	22.747	"	"
HCAO	"	7.811	"	R
FHO	4	16.976	9.488	NR
FCO	"	11.697	"	"
FAO	"	18.741	"	"
HCO	"	2.684	"	R
HAO	"	5.461	"	"
CAO	"	4.870	"	"
HO	1	0.994	3.841	"
AO	"	3.625	"	" (s)
CO	"	0.437	"	"
PO	"	9.572	"	NR

Transition matrices of
transition series II for rock sample J-103

Transition Series II Two-phase Transition matrices	ΣX_{ij}^2	$X_{.95}^2$	Observed	Expected	Distribution	
AA			3	1.091	R (1)	
CC			8	9.820	"	
HH			11	8.421	"	
FF			250	230.623	C	
FH			{ FH	30	44.124	ARg
			{ HF	36	44.012	
FC			{ FC	45	48.242	"
			{ CF	41	46.946	
FA			{ FA	17	15.885	Rg
			{ AF	17	15.844	
HC			{ HC	11	9.207	R
			{ CH	11	8.982	
HA			{ HA	2	3.031	" (1)
			{ AH	4	3.031	
CA			{ CA	4	3.234	" (1)
			{ AC	2	3.314	
HO	0.994	3.841	{ HO	64	66.569	"
			{ OH	64	66.569	
AO	3.625	"	{ AO	24	25.909	"
			{ OA	24	25.909	
CO	0.437	"	{ CO	72	70.180	"
			{ OC	74	72.180	
FO	9.57	"	{ FO	143	162.377	ARg
			{ OF	142	161.377	

Transition matrices of transition series I for
rock sample J-106. Total transition measurements=783

Transition Series I	Degrees of freedom	χ^2_{M}	$\chi^2_{.95}$	Distribution
FHCADO	25	44.354	37.652	NR
FHCAO	16	37.642	26.296	"
FHCO	9	14.682	16.919	R
FHAO	"	21.213	"	NR
FCAO	"	11.947	"	R
HCAO	"	13.685	"	"
FHO	4	6.573	9.488	"
FCO	"	7.019	"	"
FAO	"	5.748	"	"
HCO	"	5.854	"	"
HAO	"	8.710	"	"
CAO	"	1.913	"	"
H ^o O	1	1.529	3.841	"
AO	"	1.392	"	"
CO	"	0.237 ^l	"	"
FO	"	0.870	"	"

Transition matrices of
transition series of rock sample J-106

Transition Series II Two-phase Transition matrices	$\Sigma \chi^2_M$	$\chi^2_{.95}$	Observed	Expected	Distribution
AA			1	2.881	R (1)
CC			6	7.179	" (s)
HH			5	8.174	"
FF			286	279.724	"
FH			55	47.816	"
			47	47.816	
FC			38	46.023	"
			48	43.632	
FA			31	28.092	"
			24	28.690	
HC			8	7.867	"
			3	7.458	
HA			1	4.802	" (1)
			3	4.904	
CA			5	4.382	"
			6	4.720	
HO	1.529	3.841	75	71.826	"
			75	71.826	
AO	1.392	"	47	45.119	"
			46	44.119	
CO	0.237	"	67	65.821	"
			71	69.821	
FO	0.870	"	182	188.276	"
			182	188.276	

APPENDIX VI

Mass-balance of chemical reactions

36-40

Mass-balance of chemical reactions

Short form

Bio + Amph + Gar = Opx
Amph = Cpx + Gar + Bio
Amph = Opx + Cpx + Bio
Bio + Gar + Cpx = Opx
Amph + Gar = Opx + Cpx

Mass-balanced form

1.0 Qtz + 0.04671 Bio + 0.24333 Amph + 0.16942 Gar = 0.98212 Opx + 0.17574 Kf + 0.49233 An + 0.13157 Ab + 0.02761 Mt + 0.09272 Ilm + 0.33675 H₂O
0.53937 Amph + 0.61956 Qtz + 0.05387 Kf = 1.0 Cpx + 0.0696 Gar + 0.12965 Bio + 0.14688 An + 0.23387 Ab + 0.11013 Mt + 0.08176 Ilm + 0.28067 H₂O
0.63 Amph + 0.99121 Qtz = 0.365 Opx + 1.0 Cpx + 0.11209 Bio + 0.32985 An + 0.28276 Ab + 0.01145 Kf + 0.12039 Mt + 0.11621 Ilm + 0.40582 H₂O
0.107 Bio + 0.20142 Gar + 0.45918 Cpx + 0.73372 Qtz + 0.02246 Mt = 1.0 Opx + 0.43385 An + 0.02658 Ab + 0.20368 Kf + 0.05686 Ilm + 0.214 H₂O
0.358 Amph + 0.11989 Gar + 1.0 Qtz = 0.80267 Opx + 0.29492 Cpx + 0.44569 An + 0.1765 Ab + 0.12774 Kf + 0.05505 Mt + 0.09989 Ilm + 0.358 H₂O

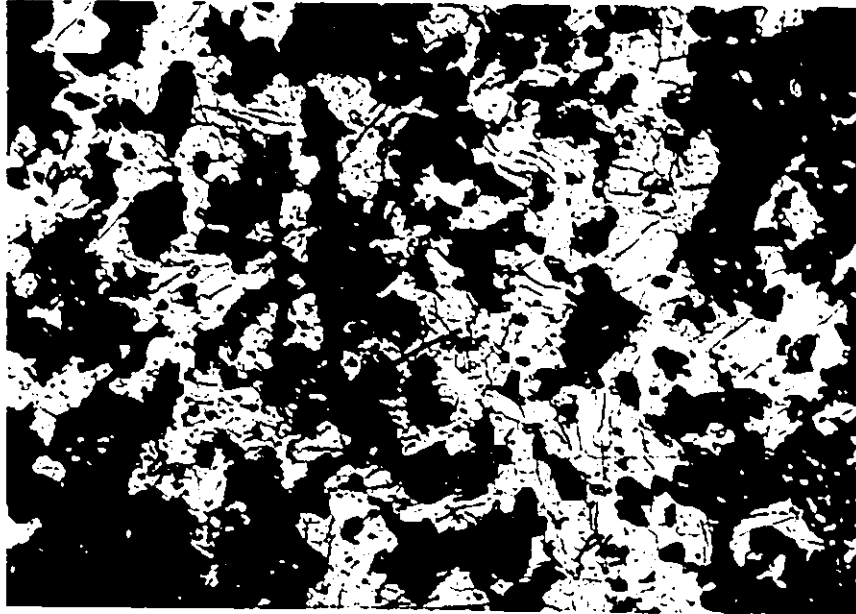
PLATES



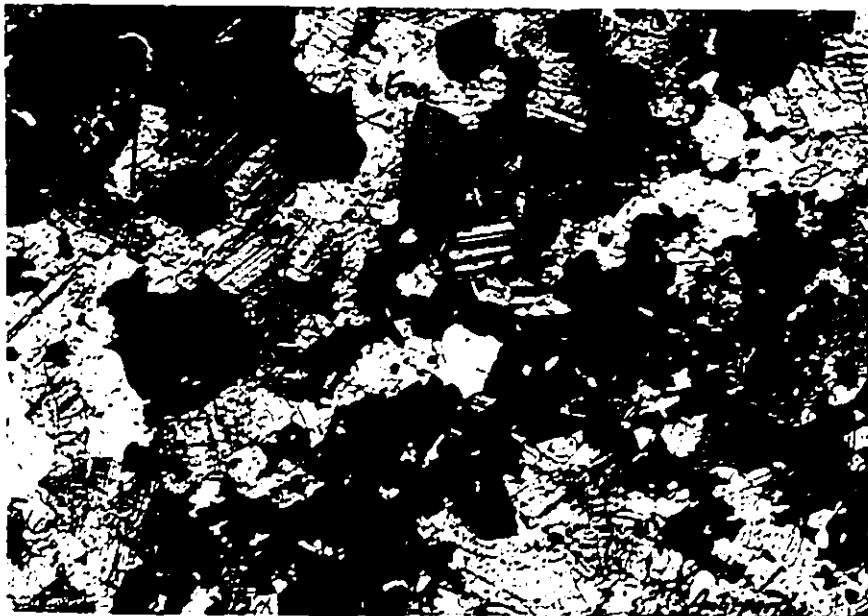
J-35 Representative of the plagioclase-two pyroxene-garnet-amphibole-biotite-quartz-iron oxide mafic granulites (noritic to gabbroic) showing fine grained, granoblastic texture. Certain mafic minerals appear to associate preferentially. (Plane polarized light)

J-50 Fine to medium grained two feldspar-clinopyroxene-amphibole-garnet-biotite-quartz-iron oxide mafic granulite showing slight porphyroblastic texture. Also note the euhedral or idiomorphic garnet, antiperthite, and ilmenite rimmed by quartz. Feldspars appear to be clustered. (Partial polarized light)





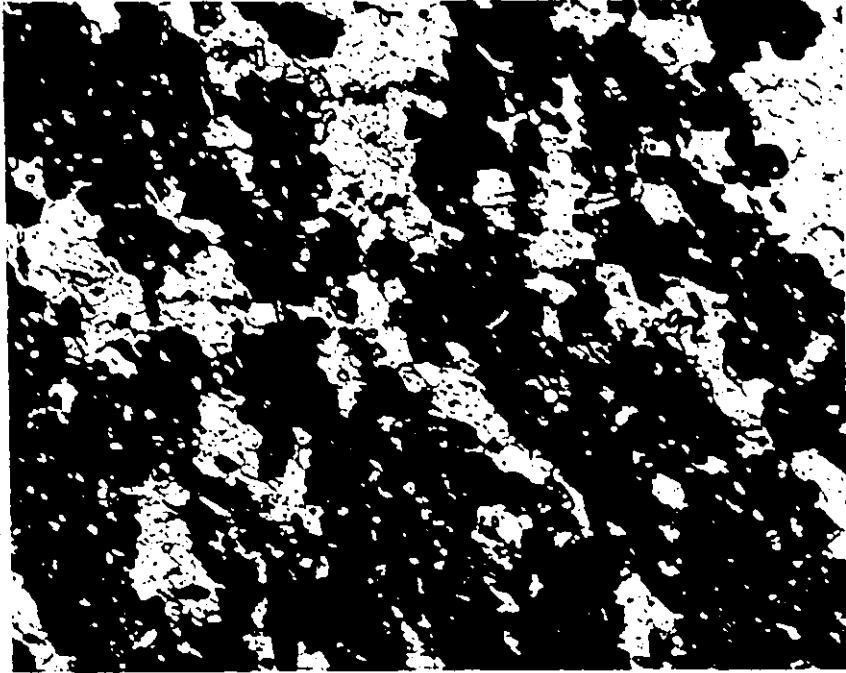
100μ



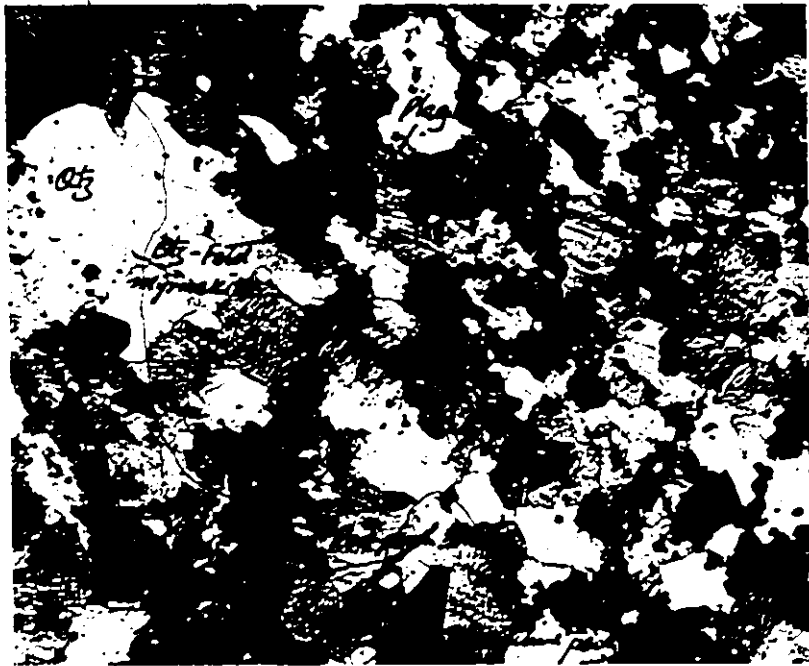
100μ

J-81 Fine grained two feldspar-two pyroxene-garnet-biotite-quartz-iron oxide mafic granulite (noritic to gabbroic) showing granoblastic-foliated texture. Mafic minerals appear to be clustered. (Plane polarized light)

J-92 Fine to medium grained, intermediate, K-feldspar-rich two feldspar-two pyroxene-garnet-biotite-quartz-iron oxide farsundite showing serial porphyroblastic texture. Also note the feldspar-quartz myrmekite and the coexistence of rod perthite, mesoperthite, and microcline perthite. Preferred mineral association is not obvious here. (Partial polarized light)



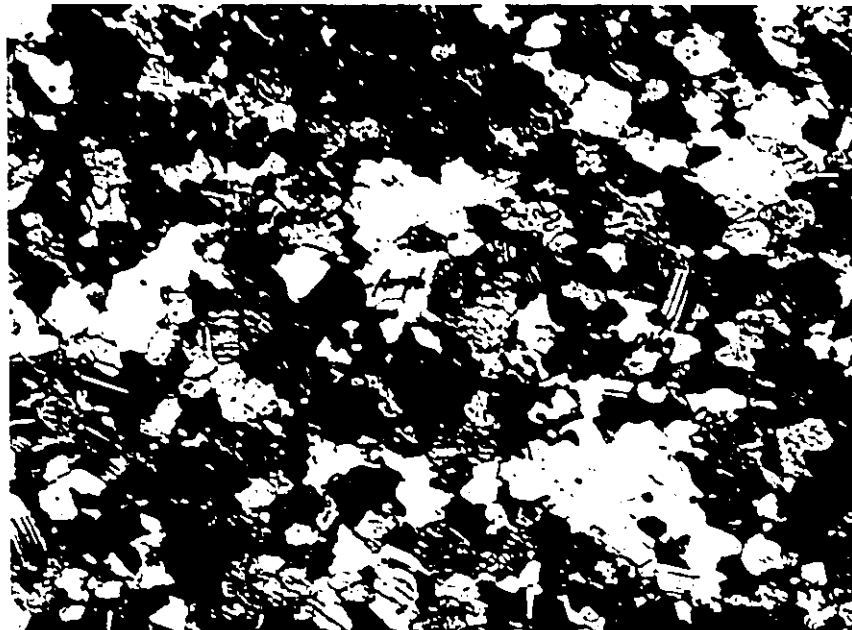
Lamin



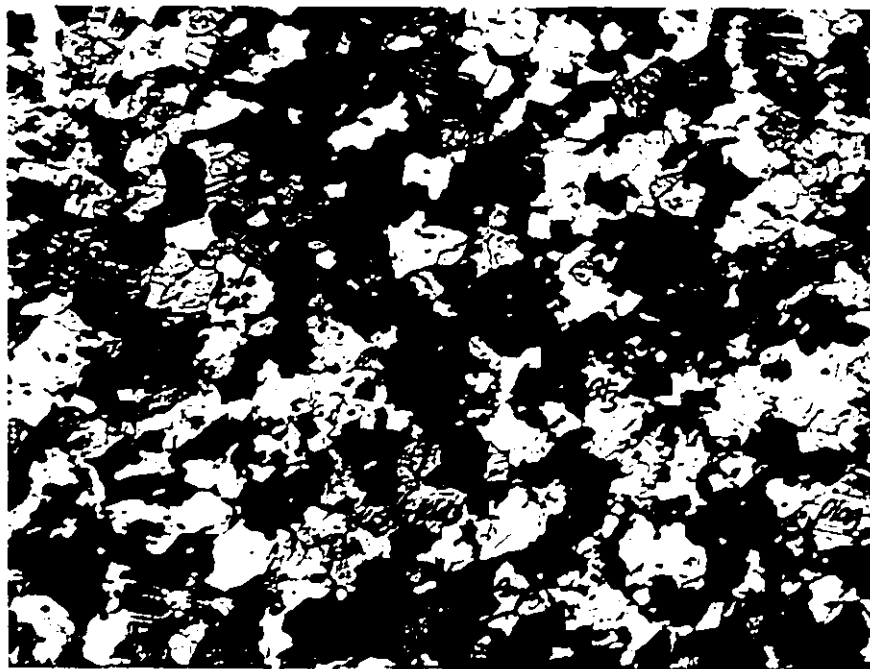
Lamin

J-99 Fine grained equigranoblastic plagioclase-clinopyroxene-amphibole-garnet-biotite-quartz-iron oxide mafic granulite (anorthositic to gabbroic). Garnet symplektite with quartz, iron oxide and plagioclase are shown. Most minerals appear to be randomly distributed. (Polarized light)

J-106 Fine grained equigranoblastic two feldspar-two pyroxene-amphibole-biotite-quartz-iron oxide mafic granulite (gabbroic to noritic). Minerals appear to be randomly distributed. (Partial polarized light)



1000



1000

